Parker

REPORT NO. MA-06-0025-73

ANALYSES OF RAIL VEHICLE DYNAMICS IN SUPPORT OF DEVELOPMENT OF THE WHEEL RAIL DYNAMICS RESEARCH FACILITY

Herbert Weinstock

JUNE 1973
INTERIM REPORT

Prepared for

DEPARTMENT OF TRANSPORTATION
URBAN MASS TRANSPORTATION ADMINISTRATION
Office of Research Development and Demonstrations
Washington, D.C. 20590

TECHNICAL REPORT STANDARD TITLE PAGE

1. Report No.	2. Government Accession No.	3. Recipient's Catalog No.
MA-06-0025-73		

4. Title and Subtitle ANALYSES OF RAIL VEHICLE DYNAMICS IN SUPPORT OF DEVELOPMENT OF THE WHEEL RAIL DYNAMICS RESEARCH FACILITY	5. Report Date June 1973 6. Performing Organization Code
7. Author(s) Herbert Weinstock	8. Performing Organization Report No. DOT-TSC-UMTA-72-10
9. Performing Organization Name and Address Department of Transportation Transportation Systems Center Kendall Square Cambridge, Ma. 02142	10. Work Unit No. UM204 11. Contract or Grant No.
12. Sponsoring Agency Name and Address Department of Transportation Urban Mass Transportation Administration Office of Research Dev. and Dem. Washington, D.C. 20590	13. Type of Report and Period Covered Interim Report Nov. 1971 - May 1972 14. Sponsoring Agency Code

15. Supplementary Notes

16. Abstract

The development of experimental facilities for rail vehicle testing at the DOT High Speed Ground Test Center is being complemented by analytical studies conducted by Transportation System Center under the UM204 Rail Supporting Technology Program to the Urban Mass Transportation Administrations Office of Research, Development, and Demonstrations. The purpose of this effort has been to gain insight into the dynamics of rail vehicles to guide the equipment development and to establish an analytic framework for the design and interpretation of tests to be conducted at the facility. The mechanics of rail vehicle lateral guidance are reviewed on the basis of linearized models. Computer programs are developed for predicting stability and general lateral response characteristics. Computer programs for predicting vertical and pitch vehicle response to track irregularities are included. Implications of non-linear effects are discussed. The report describes the status of work currently in progress and subject to revision. Publication is intended primarily to stimulate the exchange of information.

17. Key Words	18. Distribution Statement
Rail Vehicle Dynamics	DOCUMENT IS AVAILABLE TO THE PUBLIC THROUGH THE NATIONAL TECHNICAL INFORMATION SERVICE, SPRINGFIELD, VIRGINIA 22151.

19. Security Classif. (of this report)	20. Security Classif. (of this page)	21. No. of Pages	22. Price
Unclassified	Unclassified	230	

Form DOT F 1700.7 (8-69)

PREFACE

The development of experimental facilities for rail vehicle testing at the DOT High Speed Ground Test Center is being complemented by analytic studies being conducted by Transportation Systems Center under the UM204 UMTA Rail Supporting Technology Program for the Urban Mass Transportation Administration, Office of Research, Development, & Demonstrations. The purpose of this effort has been to gain insight into the dynamics of rail vehicles in order to guide the development of the wheel/rail simulators and to establish an analytic framework for the design and interpretation of tests to be conducted at these facilities. Continuation of these efforts are expected to result in definition of the interrelations between track construction and maintenance requirements and the vehicle design parameters, required for meeting ride vibrations and noise transmission standards at minimum costs.

The work described here represents an initial effort towards meeting these objectives. This report describes work currently in progress and subject to revision. It is intended primarily to provide information on the current status of in-house TSC analytic efforts conducted from November 1971 to May 1972.

CONTENTS

LIST OF ILLUSTRATIONS

LIST OF ILLUSTRATIONS (CONT.)

LIST OF ILLUSTRATIONS (CONT.)

1.0 INTRODUCTION

A major limitation on rail transportation is the tracking error produced by the lateral vibrations of rail vehicles and wheel assemblies in response to track irregularities. In addition to producing undesirable vibration in the passenger compartment, these vibrations are capable of producing severe wear of both the rails and vehicle wheels. Under extreme conditions, these oscillations may result in derailment.

The most dramatic effect of the lateral dynamics of rail vehicles is the hunting phenomenon. At low speeds (25 to 50 mph) in vehicles with lightly damped secondary suspensions the phenomenon is observed as a large (possibly violent) oscillation of the vehicle body which occurs at a characteristic speed. At speeds above and below this characteristic speed the oscillations are reduced. This low speed body hunting normally does not result in a catastrophic situation but does contribute to excessive wheel and rail wear and passenger discomfort. At very high speeds (above 100 mph) the hunting phenomenon appears as a violent oscillation of the wheel assemblies which is limited only by flange impact and eventual derailment. This oscillation begins at a critical vehicle speed and the motion is unstable at all velocities above the critical velocity.

Although the hunting instabilities have been observed for many years, the mechanism of the instability was first fully understood only in the past decade. Analytical and experimental studies conducted by Wickens at British Railways (Ref. 1) and Matsuidaira at Japanese National Railways (Ref. 2) resulted in the development of linearized analytic models which could be applied to determine the stability of two axled rail vehicles operating on straight track. These studies also resulted in the development of roller rigs which were employed to simulate straight track for full scale stability investigations of prototype truck and vehicle designs.

Although stability is a necessary condition for a new rail vehicle design it is not sufficient to assure safe and reliable performance on less than a perfectly straight track. In order to assure safety, limit wheel and rail wear and provide satisfactory ride vibration characteristics it is necessary to evaluate the response of the vehicle and wheel assemblies to rail irregularities. The U.S. Department of Transportation is currently designing and fabricating a Wheel/Rail Dynamics Research facility which will include a dynamic track simulator capable of full scale vehicle tests to fully evaluate the coupled response of rail vehicles to track irregularities and limiting rail conditions.

This development of experimental facilities for rail vehicle testing is being complemented by analytic studies being conducted by the Transportation Systems Center (TSC) on behalf of the Urban

Mass Transportation Administration, Office of Research, Development, & Deomonstrations.

The analytic models developed as a result of these studies will provide a framework for interpretation of the results of experimental investigations of the dynamics of rail vehicles and permit extrapolation of the test results to new vehicle design concepts and to prediction of the dynamic performance of vehicles under real track conditions. The analytic efforts will also support the design of the simulation equipment by providing a comparison of vehicle performance on track with that expected in the simulation. The analyses will also identify the range of test parameters required for vehicle performance evaluation and identification of critical test conditions that might approach limits of the simulation capabilities. The results obtained from simulator and track tests will be used to validate and improve the analytic models to permit their application to new vehicle and component designs and provide improved specifications for track alignment.

This document is intended to provide a summary of the work currently in progress at TSC towards establishing analytic models of the lateral response of rail vehicles to track irregularities and preliminary results of these analyses. Section 2 develops the mechanism of the hunting instability through the use of simplified wheelset, truck and vehicle models to develop an intuitive understanding of the hunting phenomenon. It is shown that at low speeds the energy associated with the lateral vibrations of rail vehicles is dissipated by a complex interaction between the creep forces developed by the different axles of the vehicle through the compliance of the vehicle suspension and wheel assembly structures. The linearized models of rail vehicle lateral dynamics for two axled vehicles developed by Wickens (Ref. 1) and Cooperrider (Ref. 3) are extended to include track irregularities. It is shown that by appropriate substitutions this model can also be applied to four axled vehicles for the important special cases of a rigid truck frame and of flexible truck frames with either very low lateral stiffness or low torsional stiffnesses between axles. A heuristic formulation is presented for calculating the critical speeds of rail vehicles. This argument predicts low speed hunting will occur when the kinematic frequency associated with the geometry and compliance of the wheel assembly is in the neighborhood of a vehicle body lateral, yaw or roll natural frequency. High speed hunting will occur when the kinematic frequency approaches the larger of the wheel assembly yaw and lateral natural frequencies. This heuristic argument yields similar results for the critical speed to those obtained from the "resonance" theory but is based upon stability arguments rather than treatment of the kinematic oscillations of the wheelset as a forcing sinusoid. The basis of the "resonance" theory of lateral motions and the limitations associated with this theory are discussed in Reference 4. This result is essentially in agreement with the numerical results obtained by Wickens and Cooperrider and those obtained for a

Mass Transportation Administration, Office of Research, Development, & Deomonstrations.

The analytic models developed as a result of these studies will provide a framework for interpretation of the results of experimental investigations of the dynamics of rail vehicles and permit extrapolation of the test results to new vehicle design concepts and to prediction of the dynamic performance of vehicles under real track conditions. The analytic efforts will also support the design of the simulation equipment by providing a comparison of vehicle performance on track with that expected in the simulation. The analyses will also identify the range of test parameters required for vehicle performance evaluation and identification of critical test conditions that might approach limits of the simulation capabilities. The results obtained from simulator and track tests will be used to validate and improve the analytic models to permit their application to new vehicle and component designs and provide improved specifications for track alignment.

This document is intended to provide a summary of the work currently in progress at TSC towards establishing analytic models of the lateral response of rail vehicles to track irregularities and preliminary results of these analyses. Section 2 develops the mechanism of the hunting instability through the use of simplified wheelset, truck and vehicle models to develop an intuitive understanding of the hunting phenomenon. It is shown that at low speeds the energy associated with the lateral vibrations of rail vehicles is dissipated by a complex interaction between the creep forces developed by the different axles of the vehicle through the compliance of the vehicle suspension and wheel assembly structures. The linearized models of rail vehicle lateral dynamics for two axled vehicles developed by Wickens (Ref. 1) and Cooperrider (Ref. 3) are extended to include track irregularities. It is shown that by appropriate substitutions this model can also be applied to four axled vehicles for the important special cases of a rigid truck frame and of flexible truck frames with either very low lateral stiffness or low torsional stiffnesses between axles. A heuristic formulation is presented for calculating the critical speeds of rail vehicles. This argument predicts low speed hunting will occur when the kinematic frequency associated with the geometry and compliance of the wheel assembly is in the neighborhood of a vehicle body lateral, yaw or roll natural frequency. High speed hunting will occur when the kinematic frequency approaches the larger of the wheel assembly yaw and lateral natural frequencies. This heuristic argument yields similar results for the critical speed to those obtained from the "resonance" theory but is based upon stability arguments rather than treatment of the kinematic oscillations of the wheelset as a forcing sinusoid. The basis of the "resonance" theory of lateral motions and the limitations associated with this theory are discussed in Reference 4. This result is essentially in agreement with the numerical results obtained by Wickens and Cooperrider and those obtained for a typical rapid transit vehicle in Section 2.

In Section 3 the linear models developed in Section 2 are extended to include the non-linearities included by Cooperrider in Ref. 3 of flange impact, wheel slip and suspension friction and those implied by profiled wheels. The model is extended to include track irregularities and a simulation program is being planned for exercising this model. Section 3 also discusses the extension of the analyses to include the coupling of forward, vertical and lateral oscillations which are believed to limit wheel adhesion at high speeds.

2.0 LINEARIZED MODELS OF LATERAL RAIL VEHICLE DYNAMICS

2.1 SUMMARY

The mechanism of lateral guidance of rail vehicles by the wheel conicity is reviewed based on linearized models. These models are developed towards demonstration of the mechanics of the hunting instability and the influence of the compliance between axles and secondary suspension damping on controlling this instability. The equations of motion for predicting the characteristic roots describing transient performance and for predicting lateral response to track irregularities are described. The requirements of a relatively stiff compliance between axles is in conflict with the guidance requirements in negotiating curves. The relationships between compliance between axles and curve negotiations are developed.

Approximate relationships are developed for predicting wheel slip in curve negotiation. The lateral dynamics programs are checked against published results. The implications of these results are applied for the parameters of a typical transit car. Section 3 discusses the extension of these models to include the non-linearities associated with the wheel/rail interaction and real suspension system designs.

2.2 ISOLATED WHEELSET

Rail vehicles are guided along a track by the creep forces developed by the interaction of the conicity of the wheels with the rail for small tracking errors and by the forces developed by the contact of the flange and the rail for large lateral displacement relative to the track centerline.

As shown in Figure 2-1, when the wheel set is given a lateral displacement y the radius r_1 of the right wheel increases by αy_1 where α is the cone angle, and the radius of the left wheel decreases by αy

$$r_1 = r_o + \alpha y \tag{2-1}$$

$$r_2 = r_o - \alpha_y \tag{2-2}$$

so that the velocities of points a and b on the axles are

$$V_a = \frac{V}{r_o} (r_o + \alpha y) \tag{2-3}$$

$$V_b = \frac{V}{r} (r_o - \alpha y) \tag{2-4}$$

This implies an angular velocity,

$$\dot{\psi} = - \frac{Va - Vb}{2\ell} = \frac{2V \alpha y}{2r_o\ell} = - \frac{V \alpha y}{r_o\ell} \tag{2-5}$$

If the vehicle is turning around a constant radius curve, R, and is in a steady state condition, with no oscillations this angular velocity is:

$$\dot{\psi} = \frac{-V}{R} \tag{2-6}$$

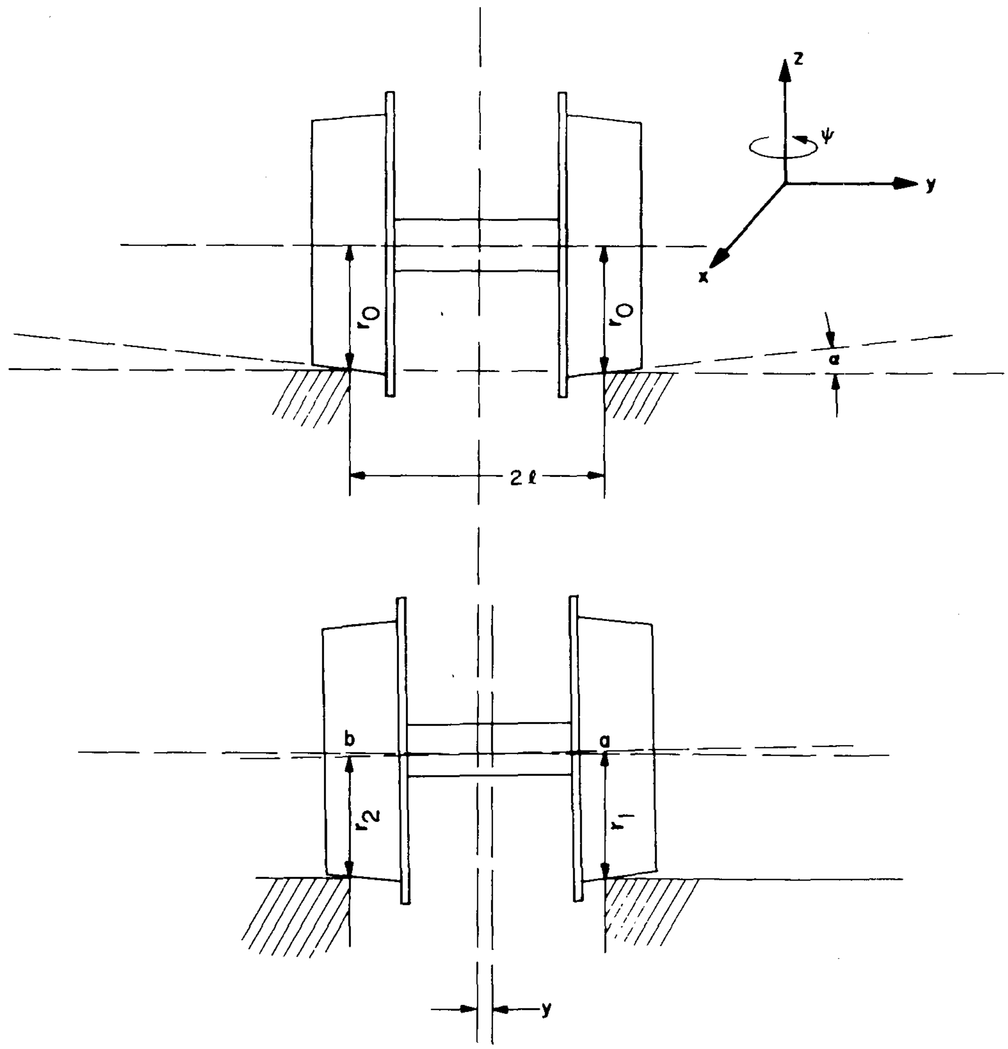

Figure 2-1. Steering Action of Wheelset with Coned Wheels

so that in rounding a curve the lateral tracking error is

$$y = \frac{+r_o \ell}{\alpha R} \tag{2-7}$$

For a wheelset with a radius of 17" a cone angle of 0.05 and flange clearance of 13/16" on a track with a gauge of 56.5" the minimum curve radius that can be negotiated without flange contact is:

$$R = \frac{r_o \ell}{\alpha y} = \frac{17 \times 28.25}{0.05 \times 13/32} = 23{,}600''$$

So that the sharpest curve that can be negotiated without flange contact is 1970 feet which is about 3/8 of a mile.

On straight track the wheel set corrects for a lateral position error by turning according to Equation 2-5 to produce a lateral velocity component:

$$\dot{y} = V \psi \tag{2-8}$$

Combining Equations 2-5 and 2-8 we obtain:

$$\ddot{y} + \frac{V^2 \alpha}{r_o \ell} y = 0 \tag{2-9}$$

This is the equation of motion of an undamped second order system with a sinusoidal solution. The frequency of oscillation is:

$$f_k = \frac{V}{2\pi} \sqrt{\frac{\alpha}{r_o \ell}} \tag{2-10}$$

Noting that dx = Vdt, Equation 2-9 can be rewritten as

$$y'' + \frac{\alpha}{r_o \ell} y = 0 \tag{2-11}$$

The solution of this equation is a sinusoid in space with a characteristic wavelength

$$\lambda_k = 2\pi \sqrt{\frac{r_o \ell}{\alpha}} \qquad (2\text{-}12)$$

This undamped oscillation of a single unrestrained wheelset is known as "kinematic hunting" since the wheelset traces the same path independent of velocity. f_k and λ_k are known as the kinematic frequency and kinematic wavelength respectively. For $r_o = 17"$. $\ell = 28.25"$, $\alpha = 0.05$, the kinematic wavelength is:

$$\lambda_k = 2\pi \sqrt{\frac{r_o \ell}{\alpha}} = 615" = 51.3 \text{ ft.}$$

for a speed of 60 mph, this wavelength corresponds to a kinematic frequency of 1.71 Hz.

When the wheelset travels along an irregular track as shown in Figure 2-2 the velocities of points a and b for a pure rolling condition on the axles are:

$$V_a = \frac{V}{r_o}\left(r_o + \alpha \ (y-\delta_1)\right) \qquad (2\text{-}14a)$$

$$V_b = \frac{V}{r_o}\left(r_o - \alpha \ (y-\delta_2)\right) \qquad (2\text{-}14b)$$

This implies an angular velocity

$$\dot{\psi} = \frac{-(V_a - V_b)}{2\ell} = \frac{-V\alpha\left(y-\frac{\delta_1 + \delta_2}{2}\right)}{r_o \ell} \qquad (2\text{-}15)$$

For pure rolling of the wheelset on the track

$$\dot{y} = V \ \psi \qquad (2\text{-}16)$$

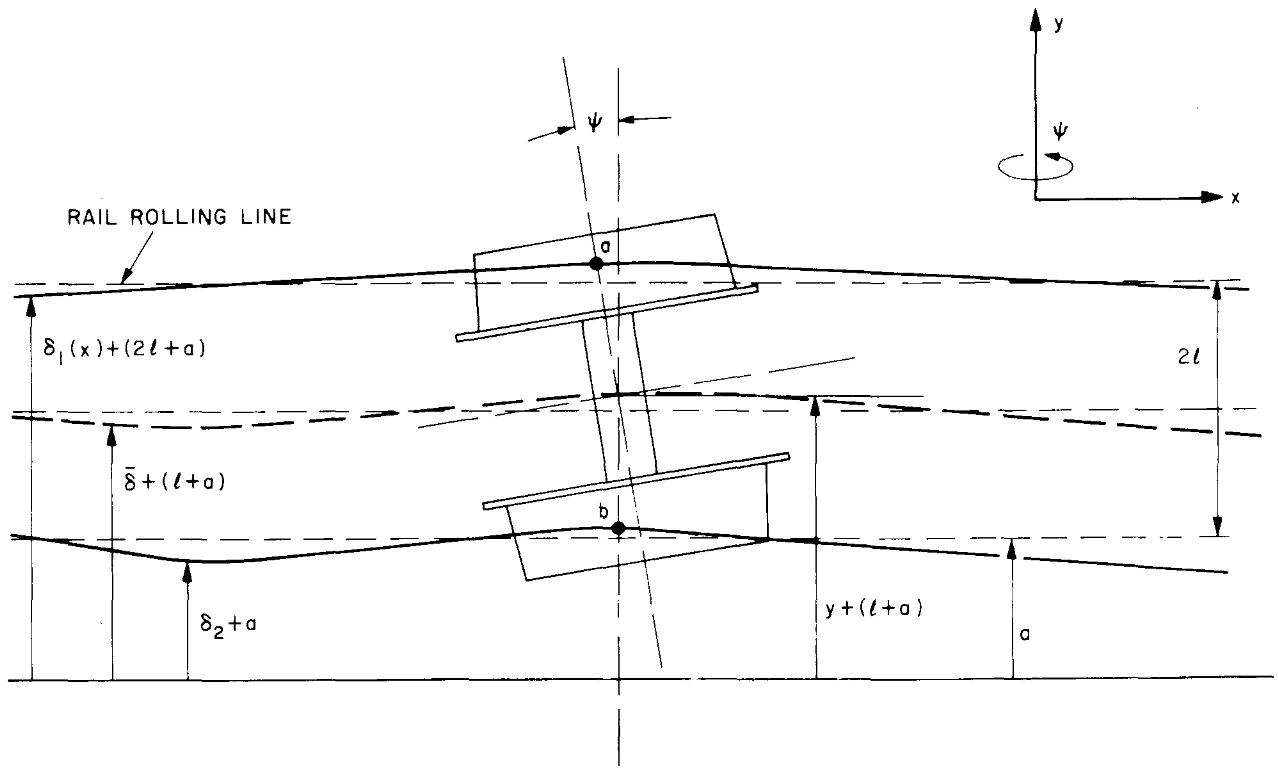

Figure 2-2. Wheelset Travelling on Irregular Track

We define the location of the track centerline as

$$\bar{\delta} = \frac{\delta_1 + \delta_2}{2} \tag{2-17}$$

and Equation 2-15 becomes

$$y + \frac{r_o \ell}{\alpha V} \dot{\psi} = \bar{\delta} \tag{2-18}$$

Combining Equations 2-16 and 2-18 yields:

$$y + \frac{\beta_k^{\,2} \ddot{y}}{V^2} = \bar{\delta} \tag{2-19}$$

Noting that dx = Vdt equation 2-19 can be rewritten as

$$y + \beta_k^{\,2} y'' = \bar{\delta} \tag{2-20}$$

where

$$\beta_k^{\,2} = \left(\frac{\lambda k}{2\pi}\right)^2 = \frac{r_o \ell}{\alpha} \tag{2-21}$$

For straight track, $\bar{\delta}$ = constant, the solution is an oscillation at the kinematic frequency centered about $y = \bar{\delta}$ as obtained above.

For a vehicle travelling on curved track of constant radius R,

$$\bar{\delta} = R\left(1 - \frac{x^2}{R^2}\right)^{1/2} \tag{2-22}$$

For small angles,

$$\bar{\delta} \approx R - \frac{x^2}{2R} \tag{2-23}$$

The solution to Equation 2-20 for this input is:

$$y = \left(R + \beta_k^{\,2}\right) - \frac{x^2}{2R} \tag{2-24}$$

so that

$$(y - \bar{\delta}) = \frac{\beta_k{}^2}{R} = \frac{r_o \ell}{\alpha R} \tag{2-25}$$

as obtained in Equation 2-7.

For sinusoidal track irregularities the steady state solution to Equation 2-20 is

$$y = \frac{\bar{\delta}}{1 - \left(\frac{\lambda k}{\lambda}\right)^2} = \frac{\bar{\delta}}{1 - \left(\frac{f}{f_k}\right)^2} \tag{2-26}$$

where λ is the wavelength of the irregularity and $f = V/\lambda$ is the frequency corresponding to that wavelength. For wavelengths of 39 feet and $\lambda_k = 51.3$ ft. the center of the wheelset will trace a path that has an amplitude of about 135% of the amplitude of the irregularity. For irregularity wavelengths of 78 ft. the response amplitude will be 1.77 times the irregularity amplitude. The tracking error in following irregularities is

$$(y - \bar{\delta}) = \frac{\bar{\delta}\left(\frac{\lambda k}{\lambda}\right)^2}{1 - \left(\frac{\lambda k}{\lambda}\right)^2} = \frac{\bar{\delta} \cdot \left(\frac{f}{f_k}\right)^2}{1-\left(\frac{f}{f_k}\right)^2} \tag{2-27}$$

For wavelengths of 39 feet the tracking error is 235% of the irregularity amplitude and for wavelengths of 78 ft. the error is 77% of the irregularity amplitude. Therefore with a flange clearance of 13/16 inch, the maximum irregularity in the track centerline that can be accommodated without flange impact at a 39 foot wavelength is 0.346 inch peak to peak.

Forces and torques applied to the wheelset are resisted by forces generated at the wheel rail contact which are approximately proportional to the relative velocities between wheel and rail at the contact for relative velocities which are small (less than 0.1%) compared to the forward vehicle velocity. For the wheelset shown in Figure 2-2, the difference between the actual velocities and those predicted for pure rolling contact in the forward and lateral directions are:

$$v_{aT} = (V - \ell\dot{\psi}) - \frac{V}{r_o}\left(r_o + \alpha(y-\delta_1)\right) \tag{2-28}$$

$$v_{bT} = (V + \ell\dot{\psi}) - \frac{V}{r_o}\left(r_o - \alpha(y-\delta_2)\right) \tag{2-29}$$

$$v_{aL} = \dot{y} - V\psi \tag{2-30a}$$

$$v_{bL} = \dot{y} - V\psi \tag{2-30b}$$

The corresponding creep forces are:

$$F_{aT} = -f_T \frac{v_{aT}}{V} = - f_T \left(\frac{\alpha\ (y_1 - \delta_1)}{r_o} + \frac{\ell\dot{\psi}}{V}\right) \tag{2-31}$$

$$F_{bT} = -f_T \frac{v_{bT}}{V} = + f_T \left(\frac{\alpha\ (y - \delta_2)}{r_o} \quad \frac{\ell\psi}{V}\right) \tag{2-32}$$

$$F_{aL} = F_{bL} = f_L \frac{v_{aL}}{V} = f_L\left(\frac{\dot{y}}{V} - \psi\right) \tag{2-33}$$

The net force in the y direction is:

$$F_y = -2f_L\left(\frac{\dot{y}}{V} - \psi\right) \tag{2-34}$$

The net torque in the ψ direction is:

$$M = -2F_T\left(\frac{\alpha\ell}{r_o}y + \frac{\ell^2\dot{\psi}}{V}\right) + 2f_T\left(\frac{\alpha\ell\bar{\delta}}{r_o}\right) \tag{2-35}$$

which for zero force and moment yield Equations 2-16 and 2-18. If the wheelset is given mass and inertia,

$$Fy = m\ddot{y} \tag{2-36}$$

$$M = C\ddot{\psi} \tag{2-37}$$

Equations 2-34 and 2-35 become

$$m\ddot{y} + 2f_L\left(\frac{\dot{y}}{V} - \psi\right) = 0 \tag{2-38}$$

$$c\ddot{\psi} + 2f_T\left(\frac{\alpha\ell}{r_o}y + \frac{\ell^2\dot{\psi}}{V}\right) = 2f_T\frac{\alpha\ell\bar{\delta}}{r_o} \tag{2-39a}$$

Equations 2-38 and 2-39 can be written as

$$\begin{bmatrix} \left(Ms^2 + \frac{2f_L S}{V}\right) & -2f_L \\ 2f_T\frac{\alpha\ell}{r_o} & \left(CS^2 + \frac{2f_T\ell^2 S}{V}\right) \end{bmatrix} \begin{bmatrix} y(S) \\ \psi(S) \end{bmatrix} = \begin{bmatrix} 0 \\ 2f_T\frac{\alpha\ell\bar{\delta}(S)}{r_o} \end{bmatrix} \tag{2-39b}$$

where S is the laplace transform variable. The transient solution is defined by the roots of the determinant of the coefficient matrix. This determinant is:

$$D = 4f_Lf_T\frac{\alpha\ell}{r_o} + \frac{4f_Tf_L\ell^2}{V^2}S^2 + \left(\frac{2Mf_T\ell^2}{V} + \frac{2Cf_L}{V}\right)S^3 + MCS^4 \tag{2-40}$$

The roots of this equation lie in the right half plane for all values of velocity indicating that the simple wheelset is unstable under all conditions unless some additional restraint is provided.

2.3 ISOLATED RIGID TRUCK

For the rigid two axle assembly shown in Figure 2-3, the lateral velocity of the leading wheelset is

$$\dot{y}_1 = \dot{y} + h\ell\dot{\psi} \tag{2-41}$$

and for the trailing wheetset

$$\dot{y}_2 = \dot{y} - h\ell\dot{\psi} \tag{2-42}$$

The lateral creep forces are from Equation 2-34.

$$Fy_1 = -2f_L\left(\frac{\dot{y}}{V} - \psi\right) -2f_L h\ell\,\frac{\dot{\psi}}{V} \tag{2-43}$$

$$Fy_2 = -2f_L\left(\frac{\dot{y}}{V} - \psi\right) +2f_L h\ell\,\frac{\dot{\psi}}{V} \tag{2-44}$$

The moments generated at each axle are

$$M_1 = -2f_T\left(\frac{\alpha\ell(y + h\ell\psi)}{r_o} + \frac{\ell^2\psi}{V}\right) + \frac{2f_T\alpha\ell\bar{\delta}_1}{r_o} \tag{2-45}$$

$$M_2 = -2f_T\left(\frac{\alpha\ell(y - h\ell\psi)}{r_o} + \frac{\ell^2\psi}{V}\right) + \frac{2f_T\alpha\ell\bar{\delta}_2}{r_o} \tag{2-46}$$

The net lateral force is

$$Fy = 4f_L\left(\frac{\dot{y}}{V} - \psi\right) \tag{2-47}$$

The net moment acting on the truck is:

$$M = M_1 + M_2 + \left(F_1 - F_2\right) h\ell \tag{2-48}$$

$$M = \left(- 4f_T\left(\frac{\alpha\ell}{r_o}\,y + \frac{\ell^2\dot{\psi}}{V}\right) + 4f_L\,\frac{h^2\ell^2\dot{\psi}}{V}\right) + 4f_T\,\frac{\alpha\ell}{r_o}\left(\frac{\bar{\delta}_1 + \bar{\delta}_2}{2}\right) \tag{2-49}$$

For no applied net force or moment these equations reduce to:

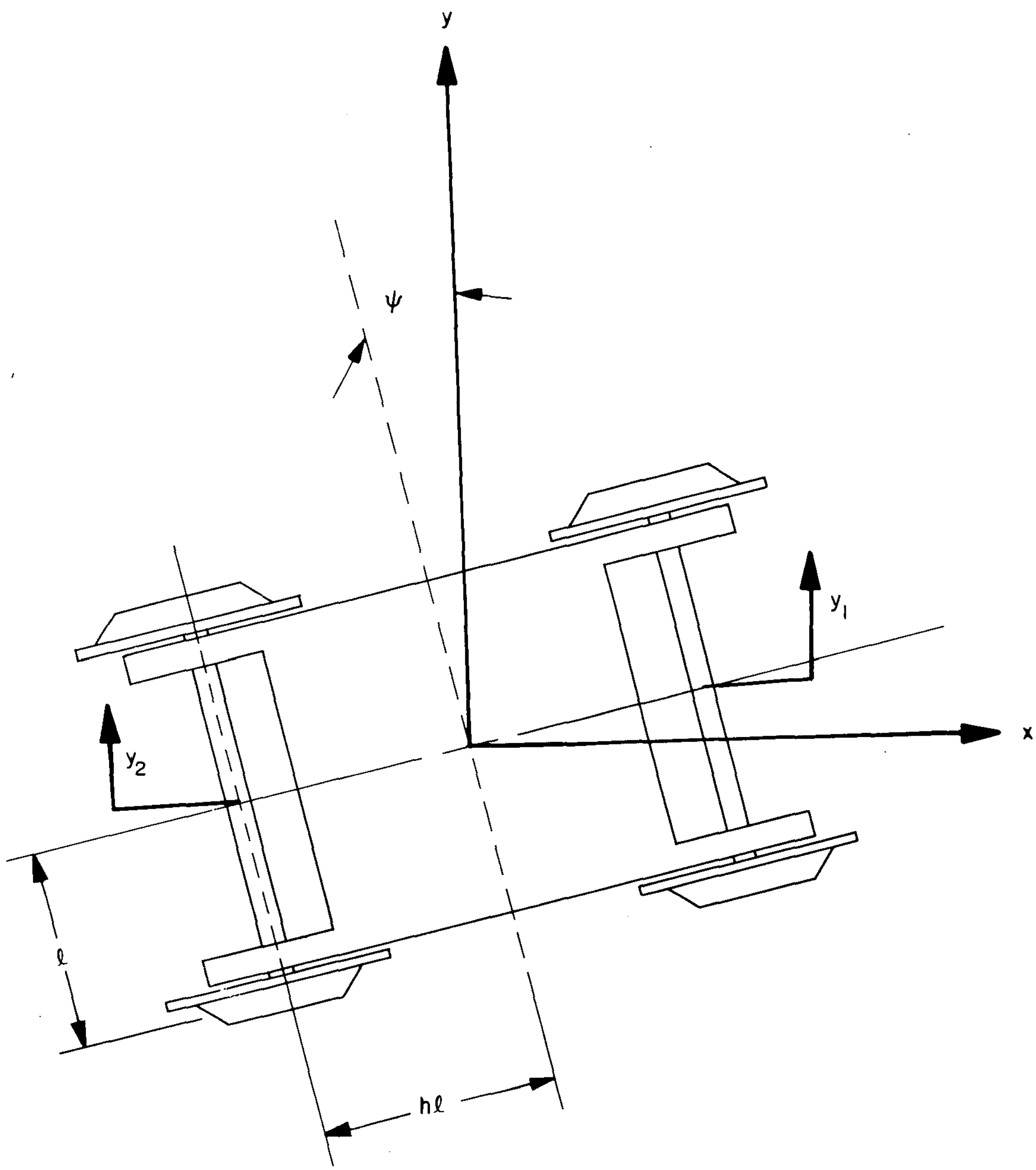

Figure 2-3. Two Axle Rigid Truck Assembly

$$\frac{\dot{y}}{V} - \psi = 0 \tag{2-50}$$

$$y + \frac{r_o \ell}{\alpha V}\left(1 + h^2 \frac{f_L}{f_T}\right)\dot{\psi} = \frac{\bar{\delta}_1 + \bar{\delta}_2}{2} \tag{2-51}$$

If we define

$$\beta_{KT}^2 = \left(1 + h^2 \frac{f_L}{f_T}\right)\beta_K^2 \tag{2-52}$$

Equations 2-50 and 2-51 are identical to equation 2-16 and 2-18 from a single wheelset. The equation of lateral motion of the rigid truck is:

$$\ddot{y} + \beta_{KT}^2\, y = \frac{\bar{\delta}_1 + \bar{\delta}_2}{2} \tag{2-53}$$

This results in a kinematic wavelength

$$\lambda_{KT} = \left(1 + h^2 \frac{f_L}{f_T}\right)^{1/2} \lambda_K \tag{2-54}$$

for $h = 1.41$ and $\lambda_K = 51.3$ ft, the kinematic wavelength for a rigid truck is 88.8 feet. The sharpest curve that can be negotiated without flange contact for the wheelset used as an example in Section 2.3 is 5,910 ft.

Since the rigid truck does not provide any dissipation forces to damp the kinematic oscillation and has the same equation form as the single wheelset, the addition of either mass or inertia will result in unstable behavior. This apparent instability of a rigid truck was noted by Langer in Reference 5 and caused him to conclude that guidance through the action of the wheel conicity is impossible and that only flange guidance acted to keep a truck on a track. Fortunately, as shown below, most truck designs have finite stiffnesses between axles which results in an energy dissipation that permits stable behavior. The response of the rigid truck to irregularities can be obtained from Equation 2-26 by substituting λ_{KT} for λ_K and the average of $\bar{\delta}_1$ and $\bar{\delta}_2$ for $\bar{\delta}$.

2.4 FLEXIBLE TRUCK

The simplified models given in the previous sections do not provide any means of dissipation of the kinematic hunting oscillation. As shown in the following paragraphs, a real truck does provide dissipation forces for the hunting mechanism by a complex interaction between the truck axles through the elastic members connecting the two axles. The rigid truck and simple wheelset represent the limiting cases where the compliance of these elastic members is extremely small or extremely large.

For the model shown in Figure 2-4, the creep forces and moments generated by each wheelset motion are:

$$F_1 = -2f_L\left(\frac{\dot{y}_1}{V} - \psi_1\right) \tag{2-55}$$

$$F_2 = -2f_L\left(\frac{\dot{y}_2}{V} - \psi_2\right) \tag{2-56}$$

$$M_1 = -2f_T\left(\frac{\alpha\ell}{r_o}\,y_1 + \frac{\ell^2\dot{\psi}_1}{V}\right) + 2f_T\,\frac{\alpha\ell}{r_o}\,\bar{\delta}_1 \tag{2-57}$$

$$M_2 = -2f_T\left(\frac{\alpha\ell}{r_o}\,y_2 + \frac{\ell^2\dot{\psi}_2}{V}\right) + 2f_T\,\frac{\alpha\ell}{r_o}\,\bar{\delta}_2 \tag{2-58}$$

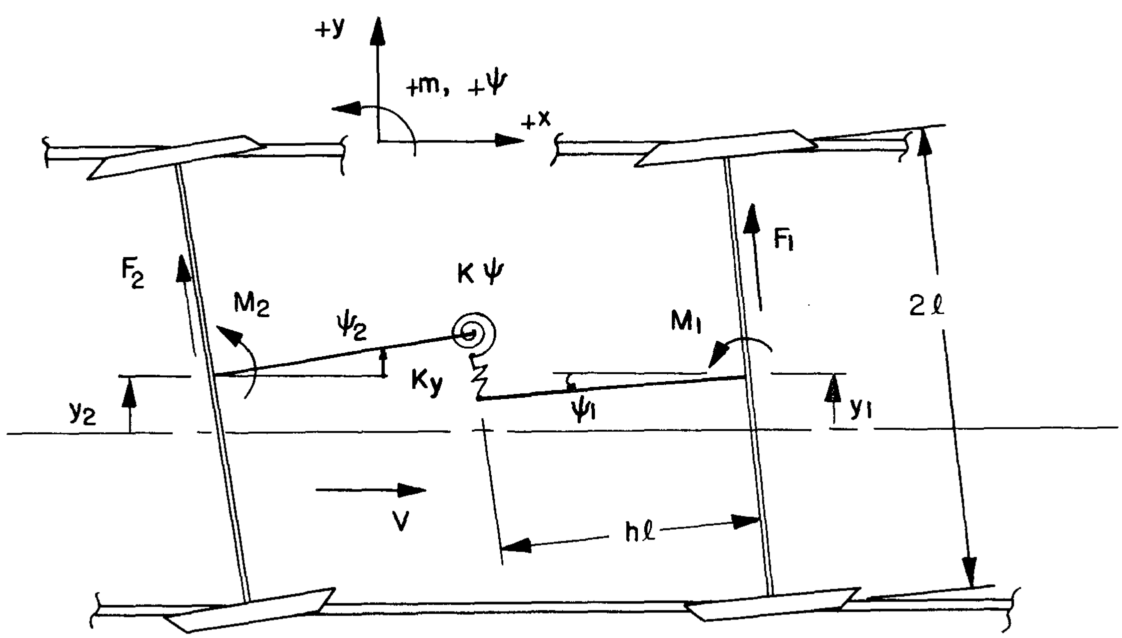

Figure 2-4. Flexible Two Axle Truck Assembly

If no external forces are applied, the requirements of equilibrium are:

$$F_1 + F_2 = 0 \tag{2-59}$$

$$M_1 + M_2 + h\ell(F_1 - F_2) = 0 \tag{2-60}$$

$$y_1 - y_2 = h\ell(\psi_1 + \psi_2) + \frac{F_1}{K_y} \tag{2-61}$$

$$K_\psi(\psi_1 - \psi_2) = F_1 h\ell + M_1 \tag{2-62}$$

The substitutions:

$$y\Delta = \frac{y_1 - y_2}{2} \quad , \ \bar{y} = \frac{y_1 + y_2}{2} \tag{2-63}$$

$$\psi\Delta = \frac{\psi_1 - \psi_2}{2} \quad , \ \bar{\psi} = \frac{\psi_1 + \psi_2}{2} \tag{2-64}$$

and some algebraic manipulations permit these requirements to be rewritten as:

$$\frac{\dot{\bar{y}}}{V} - \bar{\psi} = 0 \tag{2-65}$$

$$\frac{\alpha\ell}{r_o}\,\bar{y} + \frac{h\ell f_L}{f_T}\,\frac{\dot{y}\Delta}{V} - \frac{h\ell f_L}{f_T}\,\psi\Delta + \frac{\ell^2}{V}\,\dot{\bar{\psi}} = \frac{\alpha\ell}{r_o}\left(\frac{\bar{\delta}_1 + \bar{\delta}_2}{2}\right) \tag{2-66}$$

$$y\Delta + \frac{f_L}{K_y V}\,\dot{y}\Delta\ \frac{f_L}{K_y}\,\psi\Delta - h\ell\bar{\psi} = 0 \tag{2-67}$$

$$\frac{f_T\alpha\ell}{K_\psi r_o}\,y\Delta + \psi\Delta + \frac{f_T\ell^2}{K_\psi V}\,\psi\Delta = \frac{f_T\alpha\ell}{K_\psi r_o}\left(\frac{\bar{\delta}_1 - \bar{\delta}_2}{2}\right) \tag{2-68}$$

For large values of K_y, $y\Delta = hl\bar{\psi}$. For large values of K_ψ, $\psi\Delta = 0$ so that Equations 2-65 and 2-66 for a rigid truck reduce to:

$$\frac{\dot{\bar{y}}}{V} - \bar{\psi} = 0 \tag{2-65}$$

$$\bar{y} + \frac{r_o \ell}{\alpha V}\left(1 + h^2 \frac{f_L}{f_T}\right)\dot{\bar{\psi}} = \frac{\bar{\delta}_1 + \bar{\delta}_2}{2} \tag{2-69}$$

which agree with Equations 2-50 and 2-51 derived for a rigid truck. If $K_Y \to 0$, from Equation 2-67

$$\frac{\dot{y}\Delta}{V} - \psi\Delta = 0 \tag{2-70}$$

If $K_\psi \to o$ from Equation 2-68,

$$\frac{\alpha\ell}{r_o} y\Delta + \frac{\ell^2}{V}\dot{\psi}\Delta = \frac{\alpha\ell}{r_o}\left(\frac{\bar{\delta}_1 - \bar{\delta}_2}{2}\right) \tag{2-71}$$

Substitution of Equation 2-70 into Equation 2-66) yields

$$\frac{\alpha\ell}{r_o}\bar{y} + \frac{1^2}{V}\dot{\bar{\psi}} = \frac{\alpha\ell}{r_o}\left(\frac{\bar{\delta}_1 + \bar{\delta}_2}{2}\right) \tag{2-72}$$

addition and subtraction of Equations 2-65 and 2-70 and of 2-71 and 2-72 yield the simple wheelset equations obtained in Section 2.2.

The transient response of the flexible truck described by Equations 2-65 through 2-68 is defined by the roots of the determinant:

$$D = \begin{vmatrix} \frac{S}{V} & 0 & 0 & -1 \\ \frac{\alpha}{r_o} & h\frac{f_L}{f_T}\frac{S}{V} & -h\frac{f_L}{f_T} & \frac{\ell}{V}S \\ 0 & \left(1 + \frac{f_L S}{K_Y V}\right) & -\frac{f_L}{K_Y} & -h\ell \\ 0 & \frac{f_T \alpha\ell}{K\psi r_o} & \left(1 + \frac{f_T \ell^2 S}{K\psi V}\right) & 0 \end{vmatrix} \tag{2-73}$$

which provides the characteristic Equation:

$$D = 1 + \left(\frac{\alpha \ell}{r_o}\right)\left(\frac{f_L}{K_y}\right)\left(\frac{f_T}{K_\psi}\right)$$

$$+ \frac{f_T \ell^2}{K_\psi V}\left[1 + h^2 \frac{f_L}{f_T} + \frac{f_L}{f_T}\left(\frac{K_\psi}{K_y \ell^2}\right)\right] \quad s$$

$$+ \frac{r_o \ell}{\alpha V^2}\left[1 + h^2 \frac{f_L}{f_T} + 2\left(\frac{f_L}{K_y \ell}\right)\left(\frac{f_T \ell}{K_\psi}\right) \frac{\alpha \ell}{r_o}\right] \quad s^2$$

$$+\left(\frac{r_o \ell}{\alpha V^2}\right)\left(\frac{\ell}{V}\right)\left(\frac{f_T \ell}{K\psi}\right)\left[1 + h^2 \frac{f_L}{f_T} + \frac{f_L}{f_T}\left(\frac{K\psi}{K_y \ell^2}\right)\right] \quad s^3$$

$$+\left(\frac{r_o \ell^3}{\alpha V^4}\right)\left(\frac{f_T \ell}{K\psi}\right)\left(\frac{f_L}{Ky\ell}\right) \quad s^4 = 0 \tag{2-74}$$

Some simplification results from defining

$$s = \frac{V}{\beta_K} s_1 \tag{2-75}$$

and regrouping terms to obtain:

$$\left[1 + \left(1 + h^2 \frac{f_L}{f_T}\right) s_1^2\right] + \left(\frac{f_T \beta_K}{K_\psi}\right)\left(\frac{\ell}{\beta_K}\right)^2 \left[1 + h^2 \frac{f_L}{f_T}\right]\left(s_1 + s_1^3\right)$$

$$+ \frac{f_L}{K_y \beta_K}\left(s_1 + s_1^3\right)$$

$$+ \left(\frac{f_T \beta_K}{K\psi}\right)\left(\frac{f_L}{K_y \beta_K}\right)\left(\frac{\ell}{\beta_K}\right)^2 \left(1 + 2s_1^2 + s_1^4\right) = 0 \tag{2-76}$$

For the limiting cases of $K_y \to \infty$, $K_\psi \to \infty$, the characteristic equation predicts the rigid truck kinematic hunting. For $K_\psi \to 0$, $K_y \to 0$, the equation reduces to the pair of single wheelset kinematic hunting equations. We also obtain the result that for small values of either the lateral or rotational stiffness, the solution is the kinematic oscillation of a single wheelset.

Equation 2-76 may also be written in the form:

$$\left(S_1^2 + 2\beta_a w_a S_1 + w_a^2\right)\left(S_1^2 + 2\beta_b w_b S_1 + w_b^2\right) = 0 \qquad (2\text{-}76a)$$

where for oscillatory solutions of the equations of motion w_a and w_b are the natural frequencies of the equivalent second order system. β_a and β_b are the associated damping ratios. The roots of the characteristic equation (Eq. 2-76) have been calculated as functions of the dimensionless stiffnesses for axle distances of h = 1.41 times the gauge distance (2ℓ) which is typical of truck designs and for axle distances of h = 10 which is typical of truck center separations. These results are plotted in Figures 2-5 through 2-10.

It is seen that the interaction between the two axles through the elastic members does result in a dissipation of energy and that flexible trucks can be designed with a damping ratio of 0.35 for the kinematic truck oscillation. The kinematic wavelength of the damped truck would be about midway between the wavelength calculated for the rigid truck and that calculated for a simple wheelset. A change in the creep coefficient can result in a dramatic change in truck behavior. An increase in the creep coefficient will increase the kinematic frequency at a given speed. Depending on the truck design a change in

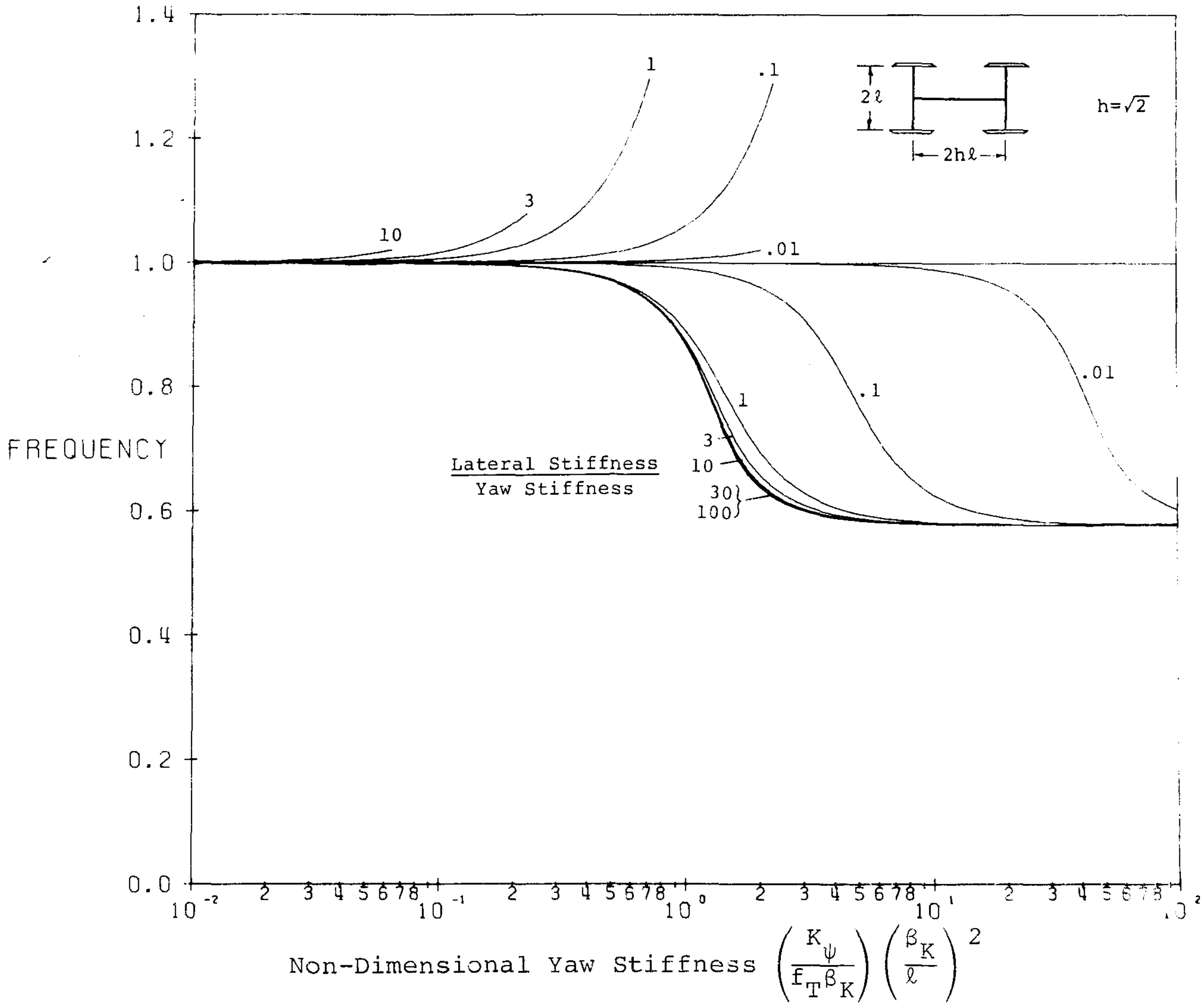

Figure 2-5. Kinematic Frequency of Two Axled Vehicle Vs. Non-Dimensional Yaw Stiffness (h=1.4)

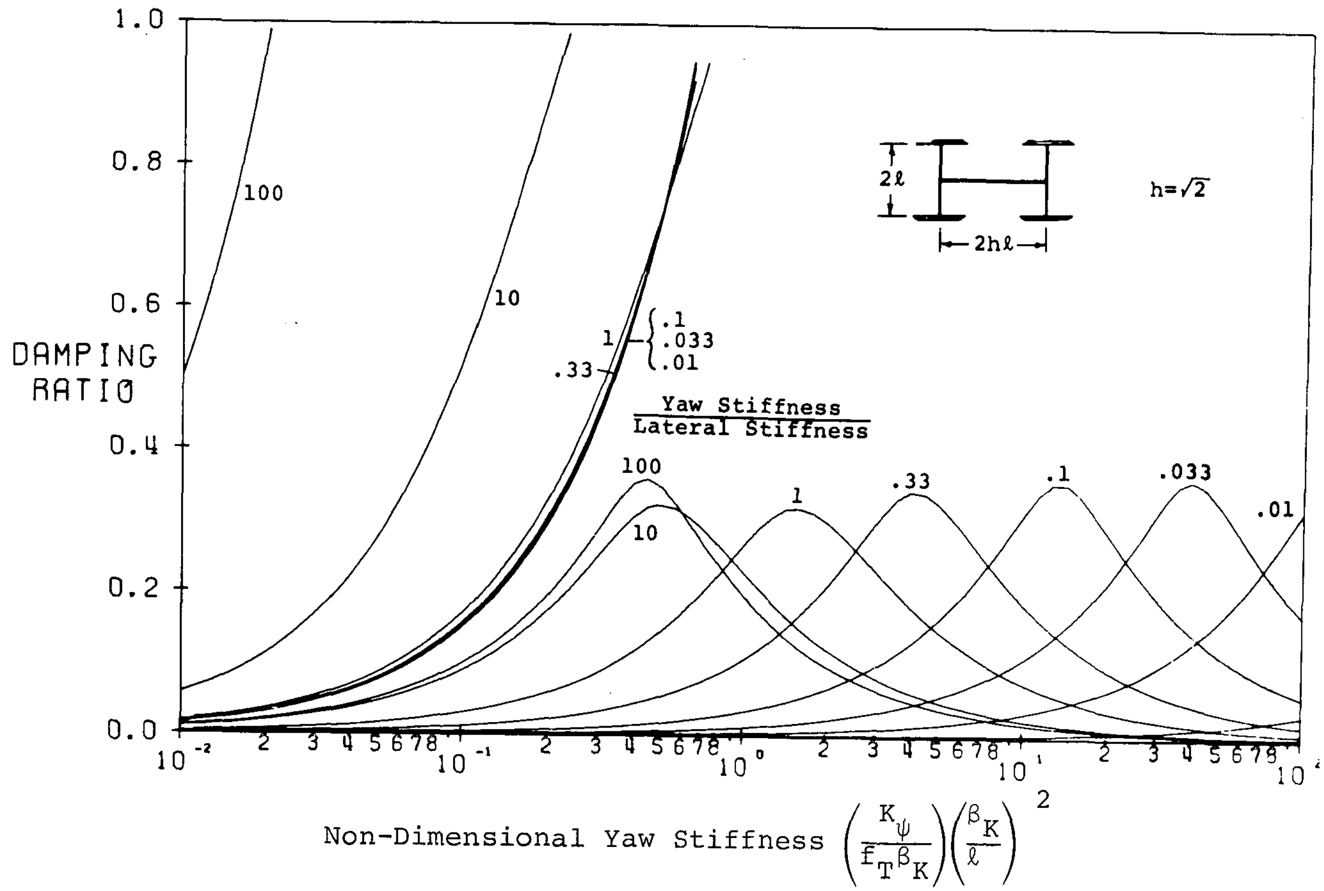

Figure 2-6. Damping of Kinematic Modes of Two Axled Vehicle Vs. Non-Dimensional Yaw Stiffness (h=1.4)

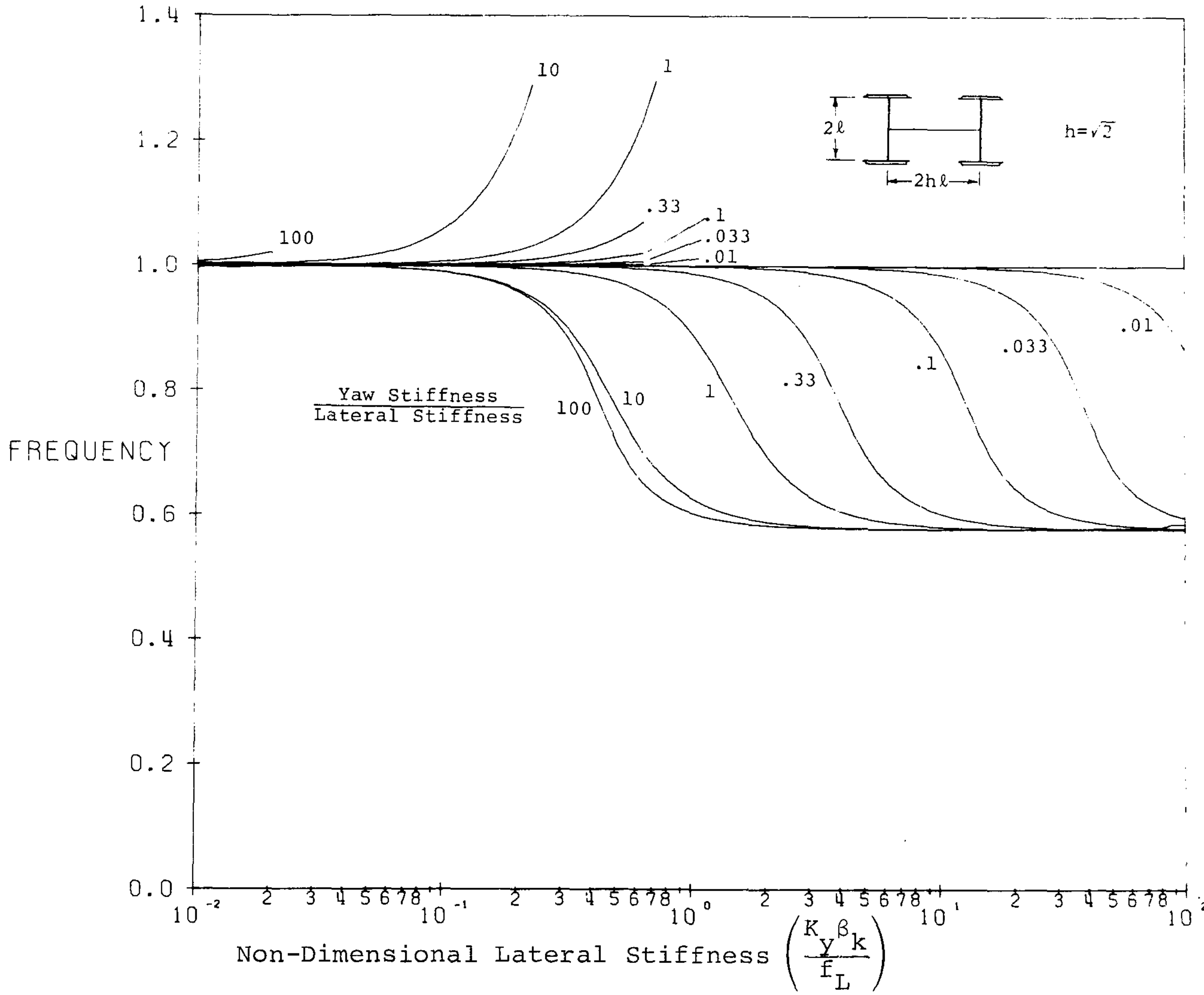

Figure 2-7. Kinematic Frequencies of two Axled Vehicles Vs. Lateral Stiffness (h=1.4)

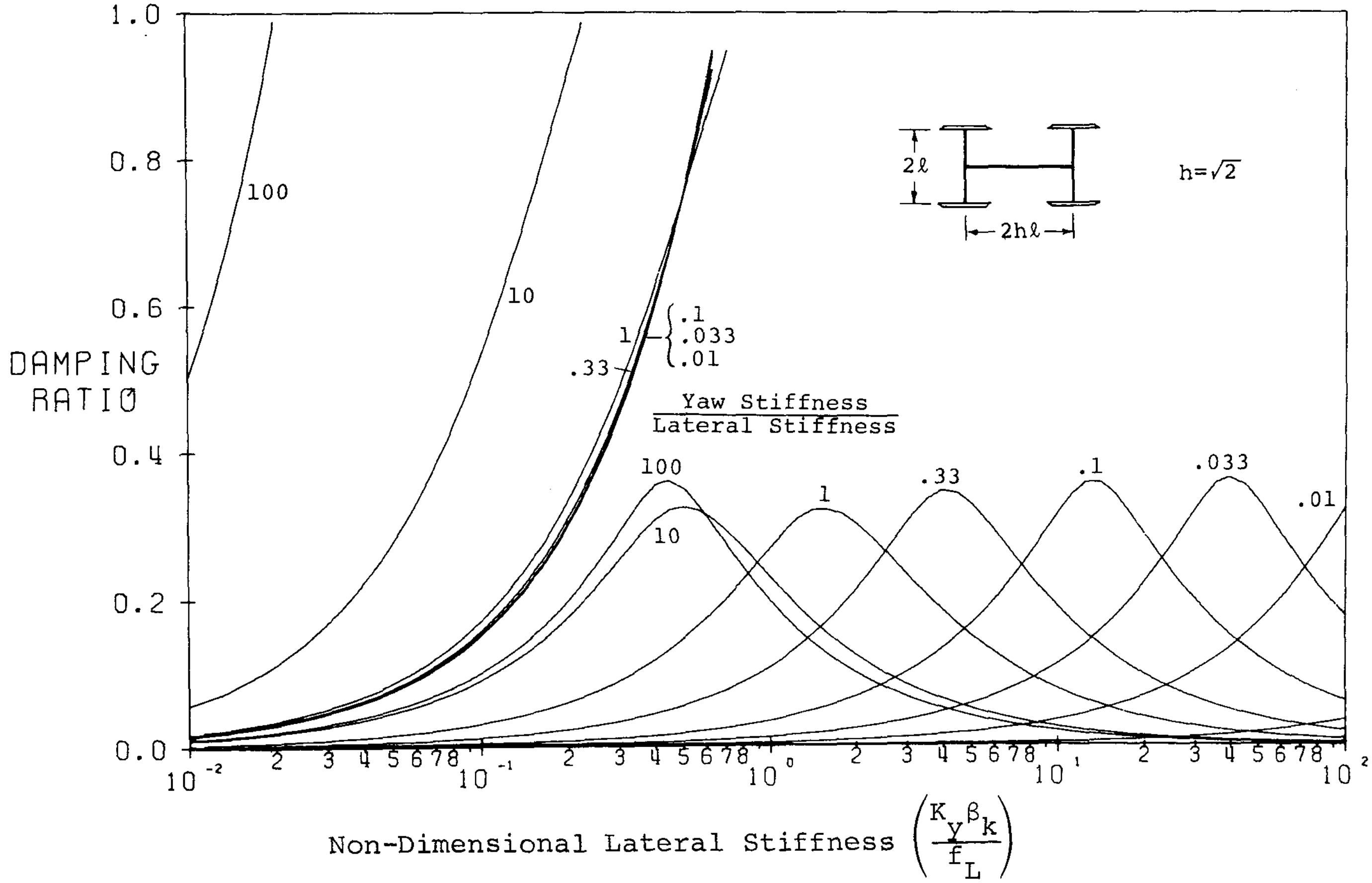

Figure 2-8. Damping of Kinematic Modes of Two Axled Vehicle Vs. Lateral Stiffness (h=1.4)

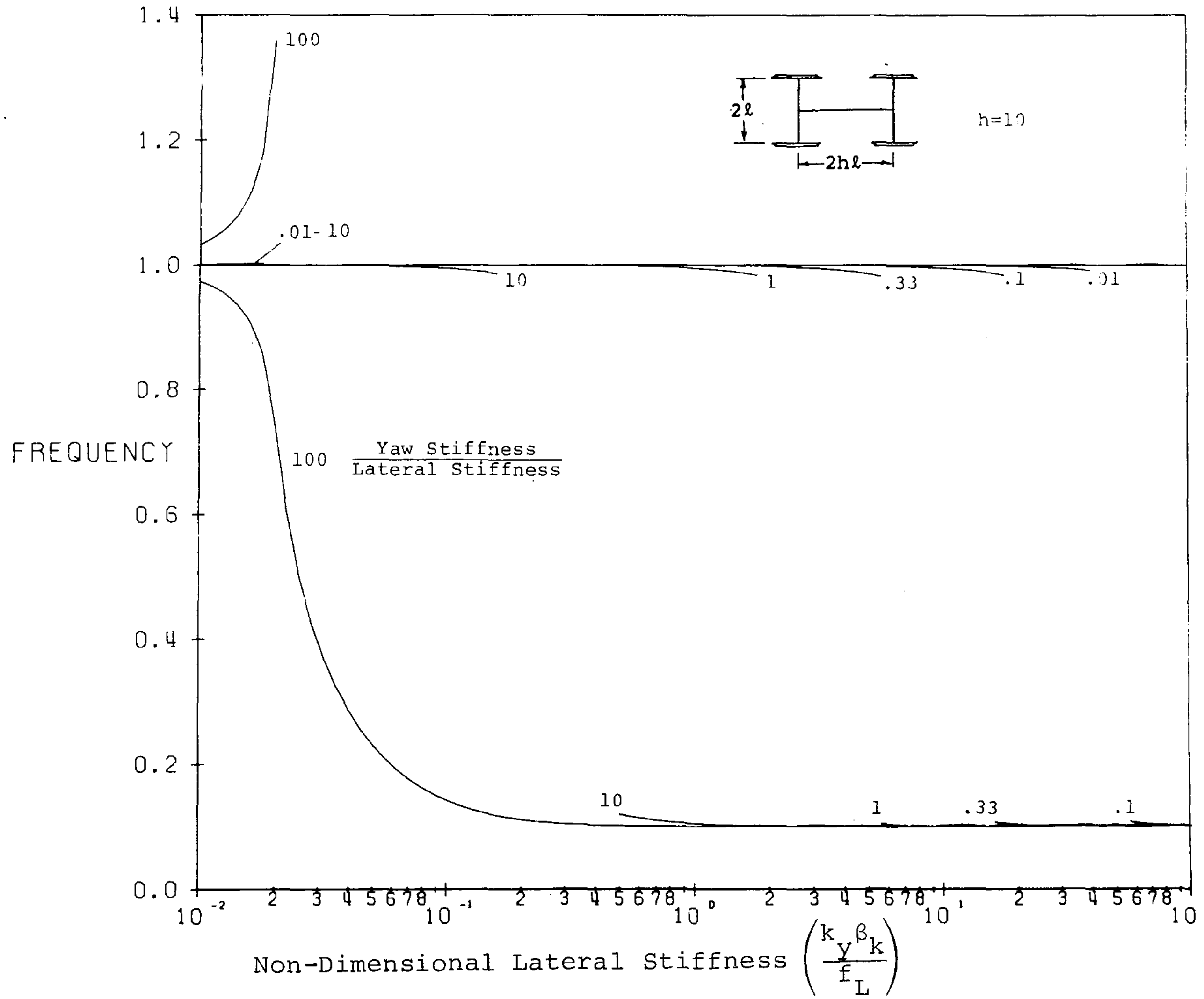

Figure 2-9. Kinematic Frequencies of Two Axled Vehicle Vs. Non-Dimensional Lateral Stiffness (h=10)

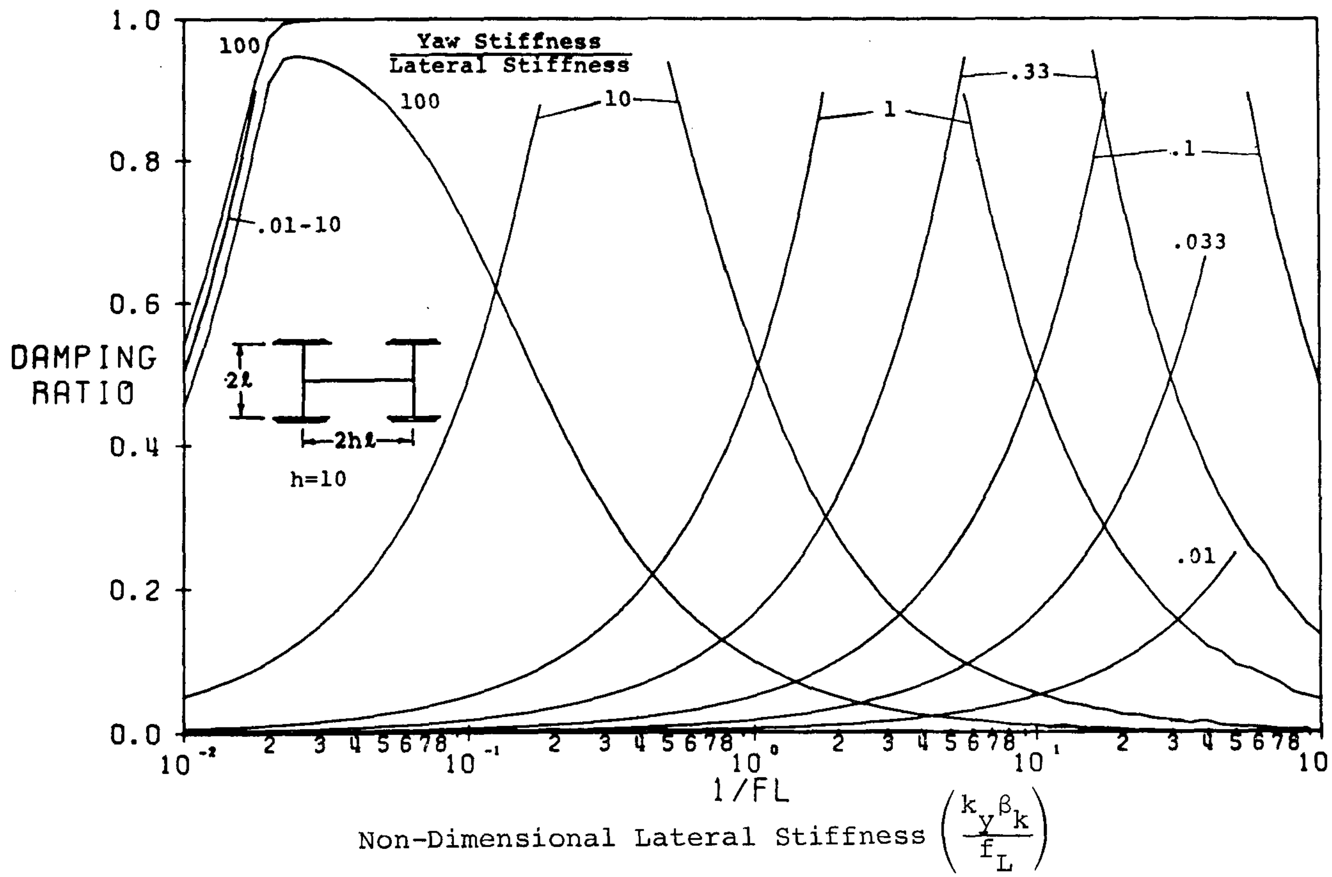

Figure 2-10. Damping Ratio of Kinematic Modes of Two Axled Vehicle Vs. Lateral Stiffness (h=10)

creep coefficient can result in either an increase or a decrease in the effective damping of the transient oscillations.

As seen by comparison of Figures 2-6 and 2-10 the dissipation available for damping transient oscillations increase with vehicle length. However, a high stiffness between axles for a long vehicle results in a limitation on the ability of the vehicle to negotiate curves. For truck designs where the axle suspensions are connected to a rigid truck body as shown in Figure 2-11, the effective stiffnesses between axles are:

$$K_\psi = \frac{k_\psi}{2}$$

$$K_y = \frac{k_y}{2}\left(\frac{k_\psi}{k_\psi + k_y h^2 \ell^2}\right)$$

For the stiffest primary suspension designs of LIM motor test vehicle:

$$k_y = 52{,}000 \text{ lb/in}$$

$$k_\psi = 20 \times 10^6 \text{ lb-in/rad}$$

resulting in effective stiffnesses for 102" distance between axles of $K_\psi = 10 \times 10^6 \ \frac{\text{lb-in}}{\text{rad}}$ and $K_y = 3{,}350 \ \frac{\text{lb}}{\text{in}}$. The dimensionless stiffnesses for a creep coefficient of 10^6 lb and a cone angle of 0.05 are:

$$K_y' = \frac{K_y \beta_K}{f_L} \approx \frac{3{,}350 \times 100}{10^6} = 0.335$$

$$K_\psi' = \left(\frac{\beta_K}{\ell}\right)^2 \frac{K_\psi}{f_T \beta_K} = \left(\frac{100}{28.5}\right)^2 \frac{10 \times 10^6}{10^6 \times 100} = 1.23$$

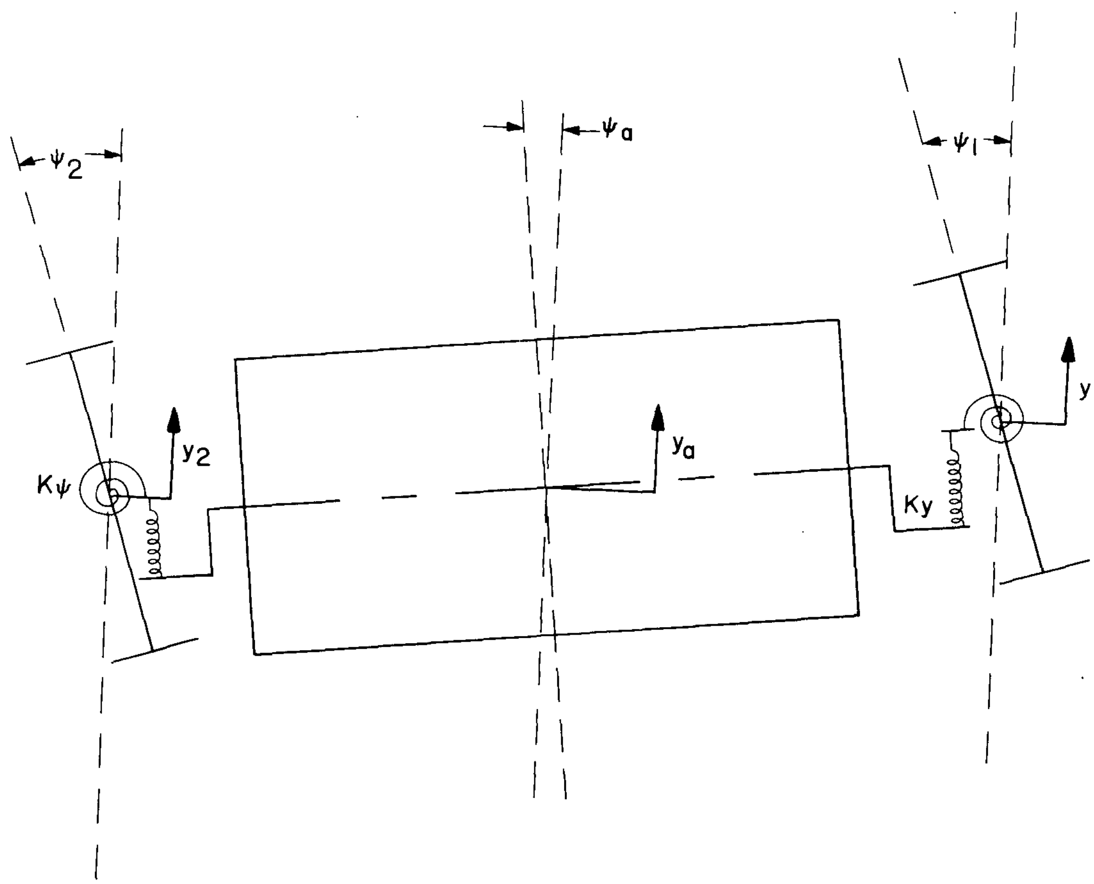

Figure 2-11. Model of Two Axle Flexible Truck Including Truck Body

For a cone angle of 0.025 these non-dimensionless stiffnesses would be 0.475 and 1.75.

For a flexible truck travelling in a constant radius curve the Equations 2-65 to 2-68 can be simplified by the substitutions

$$\dot{\psi}\Delta = 0, \quad \dot{\bar{\psi}} = -\frac{V}{R}$$

$$\dot{\bar{y}}\ (t_1) = 0 = \bar{\psi}\ (t_1)$$

$$\dot{y}\Delta = -h\ell\dot{\bar{\psi}}$$

$$\delta_1(t_1) - \delta_2(t_1) = 0$$

yield a tracking error

$$\bar{y} = \frac{r_o \ell}{\alpha R} \left[1 + \frac{h^2 \frac{f_L}{f_T}}{1 + \left(\frac{\alpha \ell}{r_o}\right) \frac{f_L f_T}{K y K \psi}} \right] \tag{2-77}$$

$$\psi\Delta = \frac{-\frac{h\ell}{R}}{1 + \frac{KyK_\psi}{f_L f_T}\left(\frac{r_o}{\alpha \ell}\right)} \tag{2-78}$$

$$y\Delta = \frac{\frac{f_L}{Ky}\left(\frac{h\ell}{R}\right)}{1 + \frac{\alpha \ell}{r_o} \frac{f_L f_T}{K y K \psi}} \tag{2-79}$$

The tracking error of the forward wheelset is

$$y_1 = \bar{y} + y\Delta = \frac{r_o \ell}{\alpha R} \left[1 + \frac{h^2 \frac{f_L}{f_T} \left(1 + \frac{\alpha \ell}{r_o} \frac{f_T}{Kyh\ell} \right)}{1 + \frac{\alpha \ell}{r_o} \frac{f_L f_T}{KyK\psi}} \right] \tag{2-80}$$

for the case of a rigid truck frame the tracking error is

$$\bar{y} = \frac{r_o \ell}{\alpha R} \left[1 + h^2 \frac{f_L}{f_T} \right] \tag{2-81}$$

as obtained in Section 2.3 and for an infinitely flexible truck frame we obtain the simple wheelset solution of Section 2.2. For low values of yaw stiffness the tracking error for the leading wheelset decreases with decreasing lateral stiffness. However, for large values of yaw stiffness, a decrease in lateral compliance results in a larger tracking error than that for a rigid truck.

The above result has also been obtained by Newland in Reference 6 from the static case of the model shown in Figure 2-11, with the substitutions:

$$K_\psi = \frac{k_\psi}{2}$$

$$K_y = \frac{k_y}{2} \left(\frac{k_\psi}{k\psi + kyh^2 \ell^2} \right)$$

Newland also obtains the tracking error due to application of a lateral force P as

$$y_1 = \frac{r_o \ell}{\alpha R}\left[1 + \frac{h^2 \frac{f_L}{f_T}\left(1 + \frac{\alpha \ell}{r_o}\frac{f_T}{Ky h \ell}\right)}{1 + \frac{\alpha \ell}{r_o}\frac{f_L f_T}{Ky K\psi}}\right] + \frac{P h \ell}{4f}\left[\frac{\frac{f h \ell}{K\psi} - 1}{1 + \frac{\alpha \ell}{r_o}\frac{f_L f_T}{Ky K\psi}}\right] \tag{2-82}$$

Slip of the wheels will occur when the creep forces, required to maintain the geometric relations of the axles implied by the elastic restraint of the assemblies, exceeds a critical value. This force is defined by the coefficient of sliding friction μ as $\mu W/2$ where W is the axle load. This results in a minimum radius curve that can be negotiated by the flexible truck without wheel slip. This radius is obtained by Newland as:

$$R \leq \frac{2 f_T h \ell}{\mu W}\frac{\left[1 + h^2 \frac{f_L}{f_T}\left[1 + \frac{\alpha \ell}{r_o}\left(\frac{f_T}{Ky h \ell}\right)\right]^2\right]^{1/2}}{1 + \frac{\alpha \ell}{r_o}\frac{f_L f_T}{Ky K\psi}} \tag{2-83}$$

For an infinitely rigid truck this minimum radius is

$$R = \frac{2 f_L h \ell}{\mu W}\left[1 + h^2\right]^{1/2} \tag{2-84}$$

Measurements of the limiting adhesion coefficient range from $\mu = 0.15$ to $\mu = 0.3$. The creep coefficient is of the order of 150 times the normal contact force. For a rigid truck with $\ell = 28.25$ inch, $h = 1.41$, the minimum radius that can be negotiated without wheel slip is 2,870 feet for $\mu = 0.3$ and 5,740 feet for $\mu = 0.15$. As obtained above, flange contact for this rigid truck will occur at a radius of 3,410 feet. Sharper curve radii may be negotiated by flexible trucks without slipping. For the case of zero yaw stiffness any curve can be negotiated. For zero lateral stiffness the minimum curve radius that can be negotiated without slipping is:

$$R = \left(\frac{2f_L h\ell}{\mu W}\right)\left(\frac{K\psi}{f_T h\ell}\right) \approx \frac{2K\psi}{\mu W} \qquad (2\text{-}85)$$

For a yaw stiffness of 10×10^6 lb-in/rad. and an axle load of 20,000 lb this minimum radius is 565 feet which is considerably sharper than the 1970 foot radius at which flange contact will begin for a single isolated wheelset. The above equations assume that the vehicle is travelling at zero speed around a curve with no superelevation. When the vehicle is travelling at speed, a centrifugal force will be generated that may or may not be compensated by the superelevation of the track. If there is no slip, the tracking error can be calculated from Equation 2-82 by substituting for P the difference between the centrifugal force and the lateral gravity force component produced by the superelevation. The minimum radius that can be negotiated without slip is calculated by reducing the effective adhesion force μW by the same quantity. This is equivalent to reducing μ by the lateral acceleration sensed by a passenger in g units. Therefore, the smallest radius curve that can be negotiated without slip for the rigid truck example above with lateral accelerations of 0.1g is 4,300 feet for $\mu = 0.3$ and 17,300 feet for $\mu = 0.15$.

Misalignments between axles will cause tracking errors and loss of adhesion on straight track similar to those that would occur if the vehicle was travelling around a curve whose center was located at the intersection of the center lines of the two axles. For a truck having an 80 inch wheelbase and an axle misalignment of one milliradian, this equivalent radius would be 6,670 feet or 1.27 miles. A misalignment of 0.1° would be equivalent to travelling around a curve having a radius of 3,830 feet.

2.5 PARALLELOGRAM WHEELSET ASSEMBLY

In practice, many rail vehicle trucks are designed so that the journal boxes of the wheel axles are connected by rigid structural members, (which serve to equalize the load between axles) which rest on a rubber type pad mounted on the journal boxes as shown in Figure 2-12. The truck frame which houses the drive motors and provides suspension for the vehicle body is connected to these equalizing members through the primary suspension springs. This type of assembly suggests the model shown in Figure 2-13. For a hard rubber pad (about 70 durometer) having a shear modulus of about 150 psi, an effective diameter of 3.6 inch and a 1/8 inch thickness, the stiffnesses of the journal box connection to the equalizer bar on side frame are about:

$$k_x = k_y = 12{,}000 \text{ lb/in.}$$

$$k_\alpha = 37{,}000 \text{ lb-in/rad.}$$

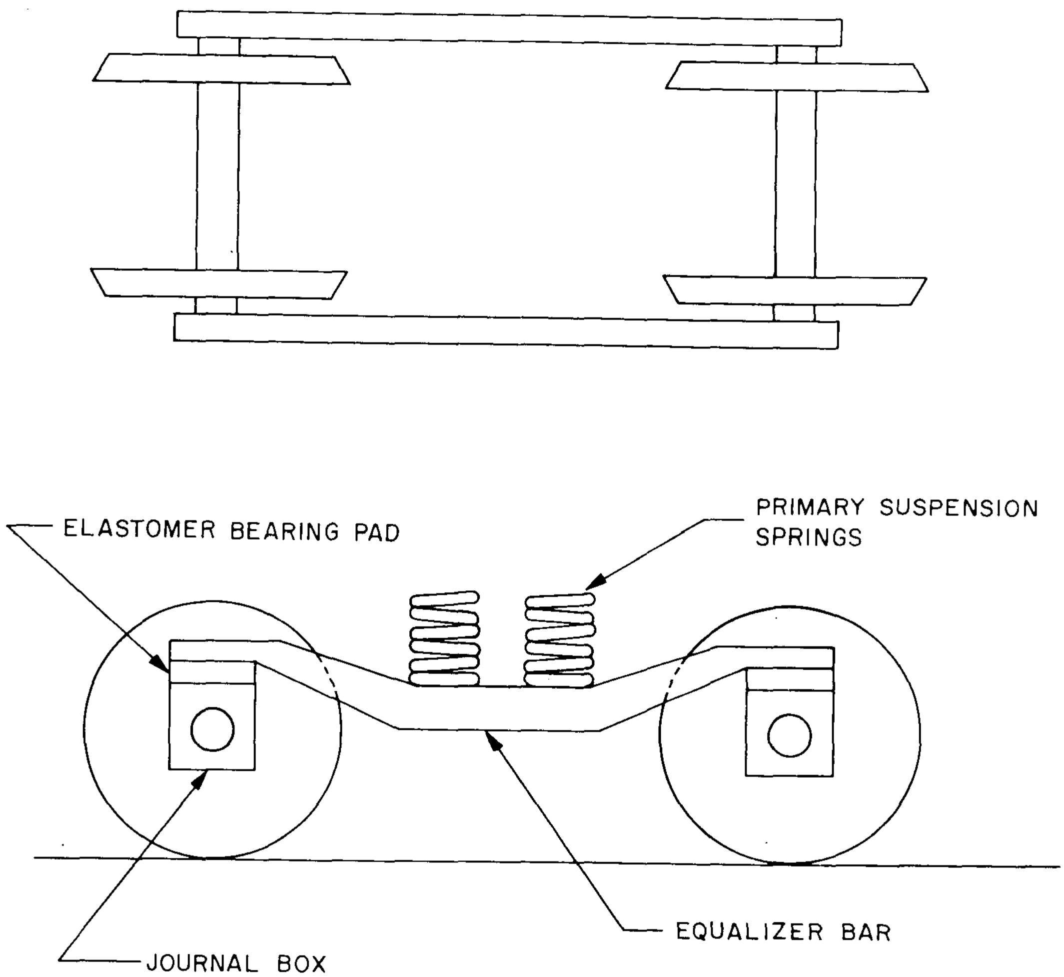

Figure 2-12. Typical Assembly of Wheel Axles and Equalizer Bars in Transit Truck Designs

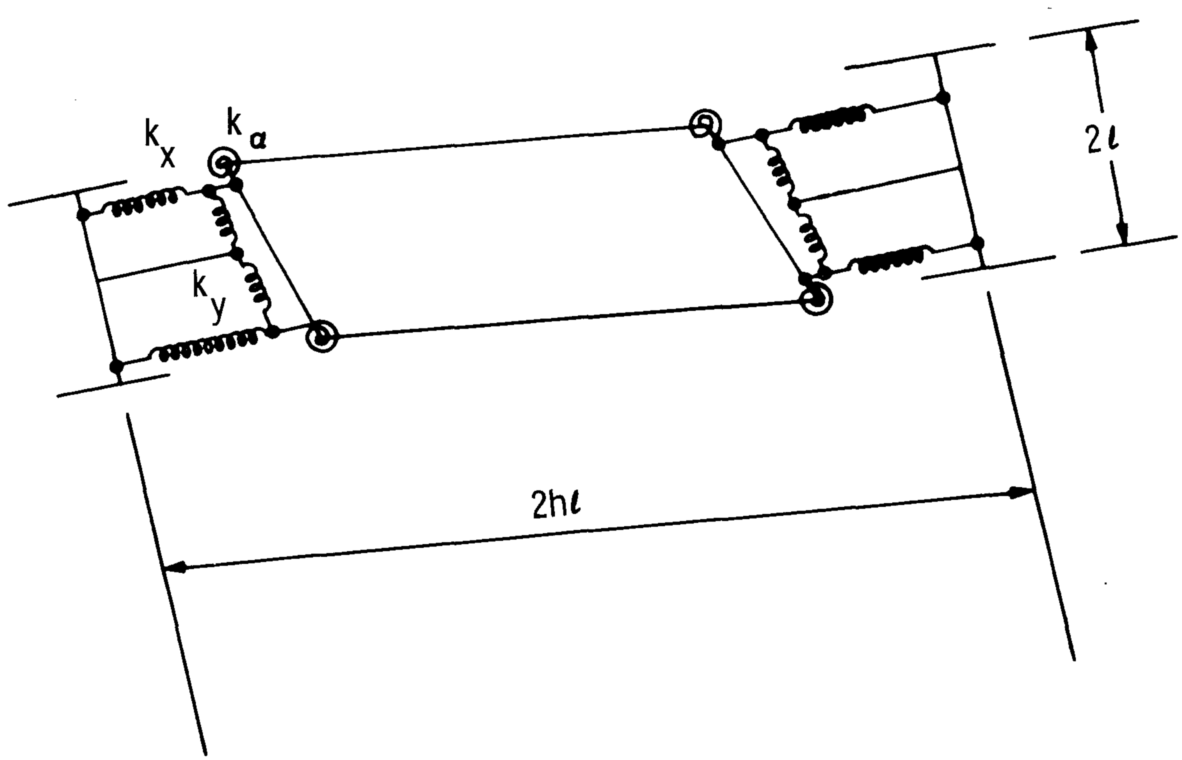

Figure 2-13. Model of Equalizer Bar-Wheel Axle Assembly

This results in effective stiffness between axles referring to model of Figure 2-4, of:

$$Ky \approx \frac{k_\alpha}{h^2 \ell^2} = \frac{37,000}{(40)^2} = 22.5 \text{ lb/in}$$

$$K\psi = k_x \ell^2 = 12,000 \times 28^2 = 9.4 \times 10^6 \text{ lb-in/rad.}$$

The very small effective lateral stiffness of this type of design permits the model of Figure 2-13 to be redrawn as shown in Figure 2-14. Since no moments can be resisted at the link connections of the parallelogram,

$$M = M_1 + M_2$$

$$M_1 = M_2$$

The equations of motion of the wheelset assembly are

$$P = F_1 + F_2 = -2f_L\left(\frac{\dot{y}_1}{V} - \psi_1\right) - 2f_L\left(\frac{\dot{y}_2}{V} - \psi_2\right) \tag{2-86}$$

$$M = M_1 + M_2 = -2f_T\left(\frac{\alpha \ell y_1}{r_o} + \frac{\ell^2 \dot{\psi}_1}{V}\right) - 2f_T\left(\frac{\alpha \ell y_2}{r_o} + \frac{\ell^2 \dot{\psi}_2}{V}\right) + 2f_T\left(\frac{\alpha \ell}{r_o}(\delta_1 + \delta_2)\right) \tag{2-87}$$

$$M = -2K_\psi(2\psi_a - \psi_1 - \psi_2) \tag{2-88}$$

which may be rewritten as:

$$M = -4K\psi(\psi a - \bar{\psi}) \tag{2-89}$$

$$M = -4f_T\left(\frac{\alpha \ell}{r_o}\,\bar{y} + \frac{\ell^2 \dot{\bar{\psi}}_1}{V}\right) + 4f_T\,\frac{\alpha \ell}{r_o}\left(\frac{\delta_1 + \delta_2}{2}\right) \tag{2-90}$$

$$P = -4f_L\left(\frac{\dot{\bar{y}}}{V} - \bar{\psi}\right) \tag{2-91}$$

These equations are recognized as having exactly the same form as those of a simple wheelset suspended from a frame having a yaw stiffness of $4K\psi$ as indicated in Figure 2-15.

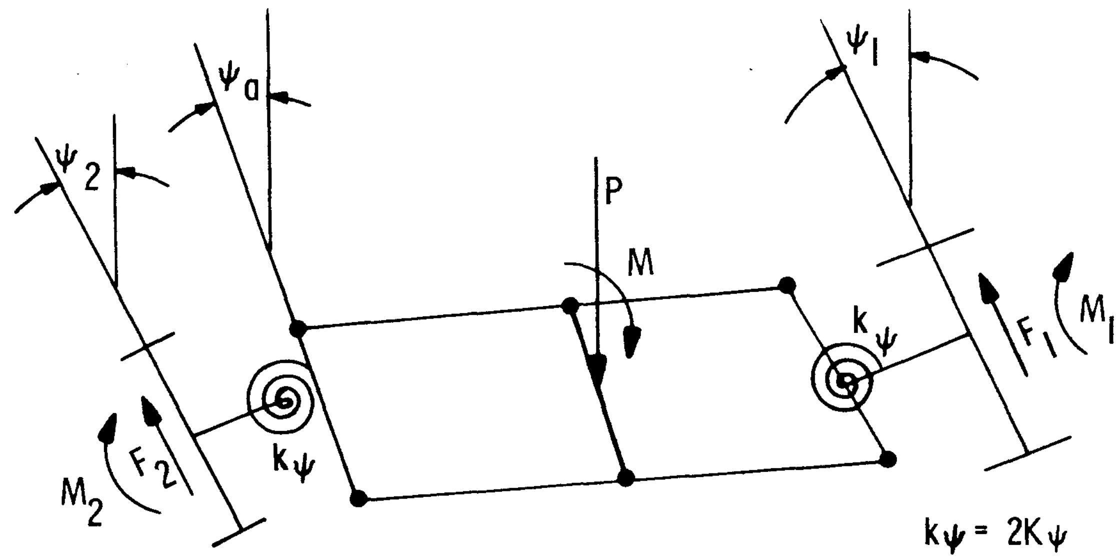

Figure 2-14. Parallelogram Model of Equalizer Bar-Wheelset Assembly

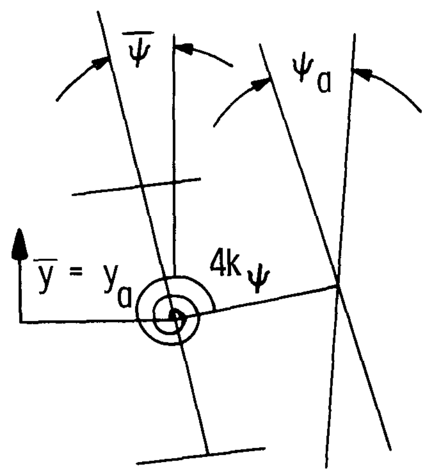

Figure 2-15. Equivalent Single Axle Model of Equalizer Bar-Wheelset Assembly for Small Yaw Stiffness Between Equalizer Bar and Journal Box

2.6 SPRING SUSPENDED WHEELSET

For high frequency vibrations, the suspension system acts to isolate the vehicle body from motions of the truck assemblies. As a result of this isolation the vehicle body appears to be a rigid frame moving at a constant forward velocity along the track for vibrations at frequencies well above the car body suspension natural frequency. Under these conditions the truck and suspension can be modelled as shown in Figure 2-16. For truck designs in which the wheelset assembly can be modelled as a single wheelset, the equations of motion are:

$$M\ddot{\bar{y}} + 2f_L\left(\frac{\dot{\bar{y}}}{V} - \bar{\psi}\right) + ky(\bar{y} - y_a) = 0 \qquad (2\text{-}92)$$

$$C\ddot{\bar{\psi}} + 2f_T\ell\left(\frac{\alpha\bar{y}}{r} + \frac{\ell\dot{\bar{\psi}}}{V}\right) + k_\psi(\bar{\psi} - \psi_a) = 2f_T\,\frac{\alpha\ell\bar{\delta}}{r} \qquad (2\text{-}93)$$

For high frequency motions the car body displacements y_a and ψ_a approach zero. The characteristic equation governing the transient response of this system is:

$$S^4 + 2S^3\left(\frac{f_T\ell^2}{VC} + \frac{f_L}{mV}\right) + S^2\left(w_y{}^2 + w_\psi{}^2 + \frac{4f_Lf_T\ell^2}{mCV^2}\right)$$
$$+ 2S\left(w_\psi{}^2\,\frac{f_L}{mV} + w_y{}^2\,\frac{f_Tb^2}{CV}\right) + \left(w_y{}^2w_\theta{}^2 + \frac{4f_Tf_L}{mC}\,\frac{\alpha\ell}{r}\right) = 0 \qquad (2\text{-}94)$$

The substitutions:

$$\beta_k{}^2 = \frac{r_o\ell}{2}\quad,\quad w_k = \frac{V}{\beta_k}$$

$$w_T{}^2 = \frac{2f_T\ell^2}{C\beta}\quad,\quad w_L{}^2 = \frac{2f_L}{m\beta}$$

$$S = w_kS_1$$

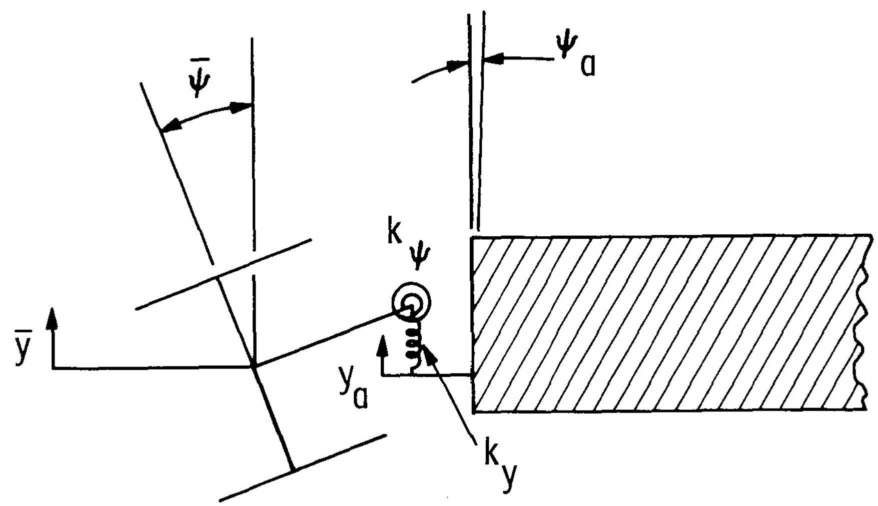

Figure 2-16. Wheelset Suspended from Vehicle by Simple Suspension

permit rewriting this equation as:

$$1 + \left(\frac{w_\psi^2\ w_L^2 + w_y^2\ w_T^2}{w_y^2\ w_\psi^2 + w_T^2\ w_L^2}\right)s_1 + \left[\frac{w_k^2(w_y^2 + w_\psi^2) + w_L^2\ w_T^2}{w_y^2\ w_\psi^2 + w_T^2\ w_L^2}\right]s_1^2$$
$$+ \left(\frac{w_k^2(w_T^2 + w_L^2)}{w_y^2\ w_\psi^2 + w_T^2\ w_L^2}\right)s_1^3 + \left(\frac{w_k^4}{w_T^2\ w_L^2 + w_y^2\ w_\psi^2}\right)s_1^4 = 0 \qquad (2\text{-}95)$$

Rouths criteria gives the kinematic frequency at which hunting instability will occur as:

$$w_k^2 = \frac{w_\psi^2 + \frac{w_T^2}{w_L^2}\ w_y^2}{\left(1 + \frac{w_T^2}{w_L^2}\right)\left(1 - \frac{(w_\psi^2 - w_y^2)^2}{(w_L^2 + w_\psi^2)^2}\right)} \qquad (2\text{-}96)$$

The above criteria can be simplified by noting that

$$\frac{w_T^2}{w_L^2} = \left(\frac{f_T}{f_L}\right)\left(\frac{m\ell^2}{C}\right) \approx 1$$

$$\frac{w_y^2}{w_L^2} = \frac{K_y\beta}{2f_L}$$

$$\frac{w_\psi^2}{w_T^2} = \frac{K_\psi\beta}{2f_T\ell^2}$$

and that the creep coefficient is about 150 times the normal force,

$$\frac{w_y^2}{w_L^2} \approx \frac{K_y\beta}{150W}$$

and that the lateral vehicle natural frequency is:

$$f_1 \approx \frac{1}{2\pi}\sqrt{\frac{Ky\ g}{W}}$$

$$\frac{w_y^2}{w_L^2} = \frac{(2\pi)^2 f_1{}^2 \beta}{386 \times 150} \approx \frac{f_1{}^2 \beta}{1500}$$

and $\beta \approx 100$ inch

and $\beta \approx 100$ inch

$$\frac{w_y^2}{w_L^2} = \frac{f_1^2}{15}$$

f_1 is normally less than 2 HZ and w_y and w_ψ are normally of similar magnitudes. The magnitude of the term

$$A = \left(\frac{w_\psi^2 - w_y^2}{w_L^2 + w_\psi^2}\right)^2$$

is of the order

$$A < \frac{f_1^4}{225} < \frac{2^4}{225} = .07$$

This term can, for many designs, therefore be neglected in Equation 2-96 and the critical kinematic frequency is given by:

$$w_k^2 \approx \frac{w_\psi^2 + \left(\frac{f_T}{f_L}\right)\left(\frac{m\ell^2}{C}\right)w_y^2}{1 + \frac{f_T}{f_L}\left(\frac{m\ell^2}{C}\right)} \tag{2-97}$$

$$w_k^2 \approx \frac{w_\psi^2 + w_y^2}{2} \tag{2-97a}$$

The high speed hunting instability is therefore expected to occur when the kinematic frequency of the wheelset is 70% of the larger natural frequency of the wheelset on the vehicle suspension, if the two natural frequencies are different. The instability will occur at the natural frequency when the two natural frequencies are equal. At low frequencies the terms $k_y(\bar{y} - y_a)$, $k_\psi(\bar{\psi} - \psi_a)$ represent the inertia forces associated with the car body and a portion of the creep forces associated with the other axles. If there is no damping, these inertia forces tend to destabilize the lateral guidance of the vehicle. These destabilizing forces are reacted by the dissipation provided by the interaction between vehicle axles. The effective inertia forces are a maximum at the vehicle body natural frequencies. It is therefore expected that lateral vibrations will increase with speed until these natural frequencies are reached by the kinematic frequency. At speeds well above the natural frequencies the simplifications used above are valid and the suspension acts to stabilize the vehicle. A characteristic speed whose kinematic frequency is at the vehicle natural frequency evidenced by large body oscillations is therefore not unlikely.

Predictions of the critical speeds based upon the above arguments yield results which are similar to those that would be obtained from the "resonance" theory described in Reference 4. This theory considered the kinematic oscillation as a forcing function to the vehicle suspension. The "resonance" theory, however, does not account for the unstable nature of the hunting problem and can in some cases result in grossly incorrect results. However, for many vehicle designs, these approximations permit a good first estimate of the critical speeds. In order to fully describe the vehicle behavior a more complete model is required. The simplest credible model for predicting vehicle response and critical speeds is the seven degree of freedom two-axle vehicle model described below.

2.7 TWO AXLE VEHICLE MODEL

The two axle vehicle discussed by Wickens (Reference 1) and Cooperrider (Reference 3) shown in Figure 2-17 can be used to model vehicles with either rigid trucks or flexible trucks whose behavior is equivalent to the single axle as discussed above. This model can also be applied directly to study of more complex trucks when the natural frequencies associated with the truck assembly are much larger than natural frequencies of the car body mounted on the secondary suspension system. For more complex vehicle assemblies, the model of Figure 2-17 serves as a basic building block for construction of the more complete model.

The equations of motion of this model are:

$$\begin{aligned} m\ddot{y}_1 &+ c_y\left[\dot{y}_1 - \left(\dot{y}_a + e\dot{\theta} + h\ell\dot{\psi}_a\right)\right] \\ &+ k_y\left[y_1 - \left(y_a + e\theta + h\ell\psi_a\right)\right] = \\ &- 2f_L\left(\frac{\dot{y}_1}{V} - \psi_1\right) - k_g\left(y_1 - \bar{\delta}\right) = F_1 \end{aligned} \qquad (2\text{-}98)$$

$$\begin{aligned} C\ddot{\psi}_1 &+ c_\psi\left(\dot{\psi}_1 - \dot{\psi}_a\right) + k_\psi\left(\psi_1 - \psi_a\right) = \\ &- 2f_T\left(\frac{\alpha\ell}{r_o}\,y_1 + \frac{\ell^2\dot{\psi}_1}{V}\right) + K_a\psi_1 + 2f_T\,\frac{\alpha\ell}{r_o}\,\bar{\delta}_1 = M_1 \end{aligned} \qquad (2\text{-}99)$$

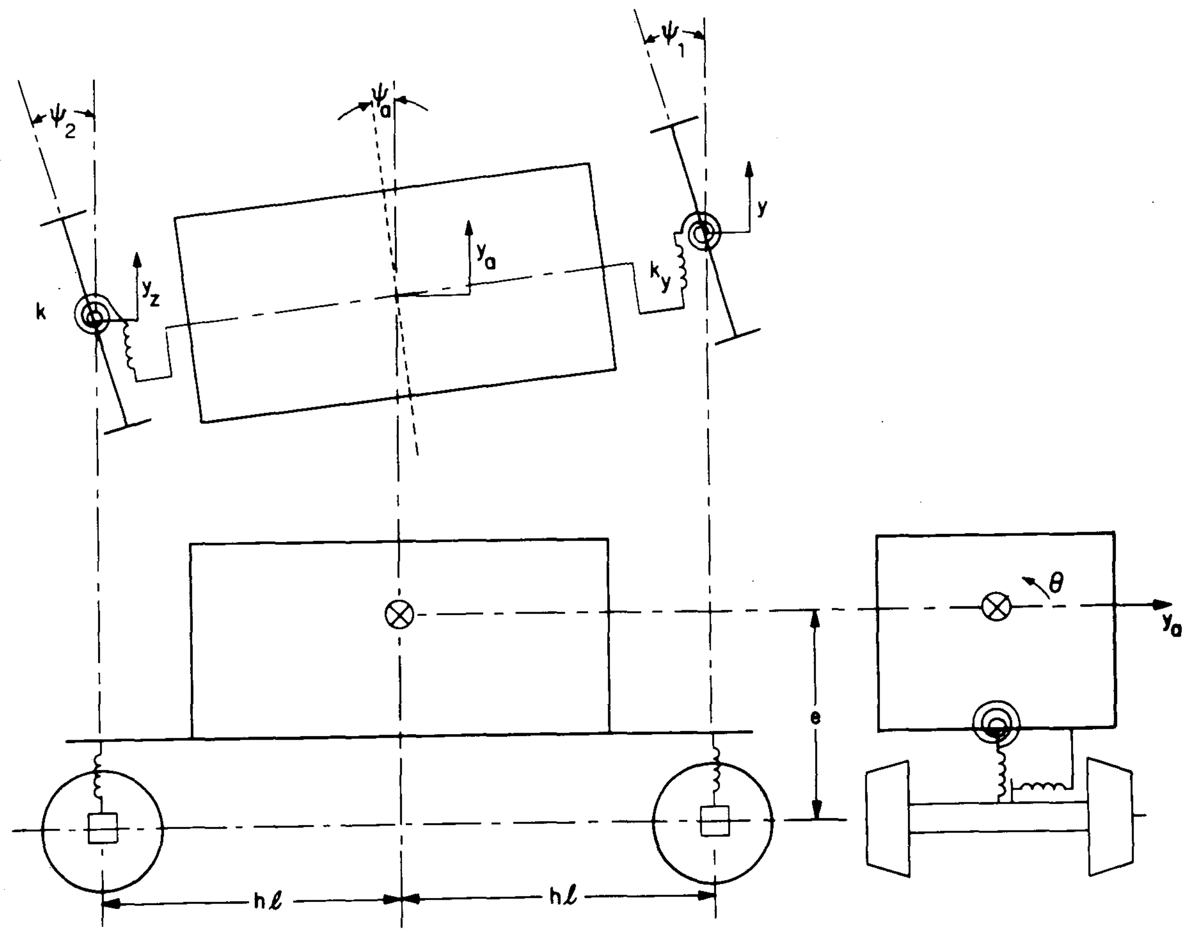

Figure 2-17. Lateral Dynamics Model for Two Axled Vehicle

$$M\ddot{y}_a + 2ky\left[y_a + e\theta - \left(\frac{y_1 + y_2}{2}\right)\right] + 2cy\left[\dot{y}_a + e\dot{\theta} - \left(\frac{\dot{y}_1 + \dot{y}_2}{2}\right)\right] = 0 \tag{2-100}$$

$$J\ddot{\psi}_a + c\psi_a\,\dot{\psi}_a + K_\psi\psi_a - k_\psi\left(\psi_1 + \psi_2\right) - c_\psi\left(\dot{\psi}_1 + \dot{\psi}_2\right)$$

$$- 2kyh\ell\left(\frac{y_1 - y_2}{2}\right) - 2cyh\ell\left(\frac{\dot{y}_1 - \dot{y}_2}{2}\right) = 0 \tag{2-101}$$

$$I\ddot{\theta} + c_\theta(\dot{\theta}) + K_\theta\theta + 2ky\left[y_a - \frac{y_1 + y_2}{2}\right]e$$

$$+ 2cy\left[\dot{y}_a - \frac{\left(\dot{y}_1 + \dot{y}_2\right)}{2}\right] e = K_\theta\bar{\theta}_o + c_\theta\dot{\bar{\theta}}_o \tag{2-102}$$

$$m\ddot{y}_2 + c_y\left[\dot{y}_2 - \left(\dot{y}_a + e\dot{\theta} - h\ell\psi_a\right)\right]$$

$$+ky\left[y_2 - \left(y_a + e\theta - h\ell\psi_a\right)\right] = -2f_L\left(\frac{\dot{y}_2}{V} - \psi_2\right)$$

$$- kg\left(y_2 - \bar{\delta}_2\right) = F_2 \tag{2-103}$$

$$C\ddot{\psi}_2 + c\psi\left(\dot{\psi}_2 - \dot{\psi}_a\right) + k_\psi\left(\psi_2 - \psi_a\right) = -\, 2f_T\left(\frac{\alpha\ell}{r_o}\, y_2 + \frac{\ell^2\dot{\psi}_2}{V}\right)$$

$$+ K_a\psi_2 + 2f_T\,\frac{\alpha\ell}{r_o}\,\bar{\delta}_2 = M_2 \tag{2-104}$$

where:

$Ky = 2ky$

$cy = 2cy$

$K\psi = 2k\psi + Kyh^2\ell^2$

$c\psi a = 2c\psi + cyh^2\ell^2$

$K_\theta \doteq Kye^2 + K_z b^2 = Kye^2 + 2k_\theta$

$c_\theta = cye^2 + c_z b^2 = Cye^2 + 2c_{\theta 1}$

kg = Gravitational stiffness resulting from wheel/rail normal forces (discussed in more detail in Section 3).

These equations can be non-dimensionalized and cast into a simpler form by the substitutions:

$$\beta_K^2 = \frac{r_o \ell}{\alpha}, \qquad w_K = \frac{V}{\beta_K}, \qquad T = w_K t$$

$$w_L^2 = \frac{2f_L}{m\beta_K}, \qquad w_T^2 = \frac{2f_T \ell^2}{C\beta_K}$$

$$w_1^2 = \frac{Ky}{2m}, \qquad w_2^2 = \frac{k\psi}{C}$$

$$\beta_1 - \frac{cy}{4mw_1}, \qquad \beta_2 = \frac{c\psi_1}{2cw_2}$$

$$w_\psi^2 = \frac{K_\psi}{J}, \qquad \beta_\psi = \frac{c_{\psi a}}{2Jw_\psi}$$

$$w_\theta^2 = \frac{K_\theta}{I}, \qquad \beta_\theta = \frac{c_\theta}{2Iw_\theta}$$

$$w_3^2 = \frac{Kye^2}{I}, \qquad \beta_3 = \frac{cye^2}{2Iw_3}$$

$$w_4^2 = \frac{2k_\psi}{J}, \qquad \beta_4 = \frac{c_{\psi 1}}{Jw_4}$$

$$w_5^2 = \frac{Kyh^2\ell^2}{J}, \qquad \beta_5 = \frac{cyh^2\ell^2}{2Jw_5}$$

$$w_g^2 = \frac{kg}{m}, \qquad w_a^2 = \frac{ka}{C}$$

$$e' = \frac{e}{\beta_K}, \qquad \ell' = \frac{\ell}{\beta_K}, \qquad r_o = \frac{y_a}{\beta_K}$$

$$\bar{r} = \frac{y_1 + y_2}{2\beta_K}, \qquad r_o = \frac{y_1 - y_2}{2\beta_K}$$

$$R_t^2 = \frac{w_1^2}{w_L^2} = \frac{Ky\beta_K}{4f_L} \quad , \qquad R_T^2 = \frac{w_2^2}{w_T^2} = \left(\frac{\beta_K}{\ell}\right)^2 \left(\frac{k_\psi}{2f_T\beta_K}\right)$$

With these substitutions Equations 2-98 through 2-104 are reduced to:

$$\frac{w_K^2}{w_L^2}\ddot{\bar{r}} + \left[1 + 2\beta_1 R_L \frac{w_K}{w_L}\right]\dot{\bar{r}} + \left(R_L^2 + \left(\frac{w_g}{w_L}\right)^2\right)\bar{r}$$

$$- R_L^2\left(r_a + e'\theta\right) - 2\beta_1 R_L \frac{w_K}{w_L}\left(\dot{r}_a + e'\dot{\theta}\right)$$

$$- \bar{\psi} = \frac{w_g^2}{w_L^2}\frac{\left(\bar{\delta}_1 + \bar{\delta}_2\right)}{2\beta_K} \qquad (2\text{-}105)$$

$$\frac{w_K^2}{w_L^2}\ddot{r}_\Delta + \left[1 + 2\beta_1 R_L \frac{w_K}{w_L}\right]\dot{r}_\Delta + \left(R_L^2 + \left(\frac{w_g}{w_L}\right)^2\right) r_\Delta - \psi_\Delta$$

$$- R_L^2\, h\ell'\psi_a - 2\beta_1 R_L \frac{w_K}{w_L} h\ell'\dot{\psi}_a = \frac{w_g^2}{w_L^2}\frac{\left(\bar{\delta}_1 - \bar{\delta}_2\right)}{2\beta_K} \qquad (2\text{-}106)$$

$$\frac{w_K^2}{w_T^2}\ddot{\bar{\psi}} + \left[1 + 2\beta_2 R_T \frac{w_K}{w_T}\right]\dot{\bar{\psi}} + \left(R_T^2 - \frac{w_a^2}{w_T^2}\right)\bar{\psi}$$

$$- 2\beta_2 R_T \frac{w_K}{w_T}\dot{\psi}_a - R_T^2\,\psi_a + \bar{r} = \frac{\delta_1 + \delta_2}{2\beta_K} \qquad (2\text{-}107)$$

$$\frac{w_K^2}{w_T^2}\ddot{\psi}_\Delta + \left[1 + 2\beta_2 R_T \frac{w_K}{w_T}\right]\dot{\psi}_\Delta + \left(R_T^2 - \frac{w_a^2}{w_T^2}\right)\psi\Delta + r_\Delta = \frac{\bar{\delta}_1 - \bar{\delta}_2}{2\beta_K} \qquad (2\text{-}108)$$

$$\frac{w_K^2}{w_y^2}\,\ddot{r}_a + 2\beta_y \frac{w_K}{w_y}\,\dot{r}_a + r_a - (\bar{r} - e'\theta)$$

$$- 2\beta_y \frac{w_K}{w_y}\,(\bar{r} - e'\dot{\theta}) = 0 \tag{2-109}$$

$$\frac{w_K^2}{w_\psi^2}\,\ddot{\psi}_a + 2\beta_{\psi a} \frac{w_K}{w_\psi}\,\dot{\psi}_a + \psi_a$$

$$- \frac{w_4^2}{w_\psi^2}\,\bar{\psi} - 2\beta_4 \frac{w_K}{w_\psi}\left(\frac{w_4}{w_\psi}\right)\dot{\bar{\psi}}$$

$$- \frac{w_5^2}{w_\psi^2}\left(\frac{r_\Delta}{h\ell'}\right) - 2\beta_5 \left(\frac{w_5}{w_\psi}\right)\left(\frac{w_K}{w_\psi}\right)\left(\frac{\dot{r}_\Delta}{h_\ell}\right) = 0 \tag{2-110}$$

$$\frac{w_K^2}{w_\theta^2}\,\ddot{\theta} + 2\beta_2 \frac{w_K}{w_\theta}\,\dot{\theta} + \theta\;\frac{w_3^2}{w_\theta^2}\left(\frac{\bar{r}}{e'}\right)\; 2\beta_3\left(\frac{w_3}{w_\theta}\right)\left(\frac{w_K}{w_\theta}\right)\left(\frac{\bar{r}}{e'}\right)$$

$$+ \frac{w_3^2}{w_\theta^2}\left(\frac{r_a}{e'}\right) + 2\beta_3\left(\frac{w_3}{w_\theta}\right)\left(\frac{w_K}{w_\theta}\right)\left(\frac{r_a}{e'}\right) = -\,\bar{\theta}_o + 2\beta_\theta \frac{w_K}{w_\theta}\,\dot{\bar{\theta}}_o \tag{2-111}$$

where the dot represents differentiation with respect to dimensionless time (τ).

This normalized form serves to reduce the magnitude of the coefficients in the equations of motion with a resulting simplification in the computation requirements to obtain characteristic roots and frequency response characteristics. Numerical solutions of the equations of motion indicate that stability problems normally represent motions at the wheelset kinematic frequency.

In the normalized set of equations, displacements and their derivatives (e.g., ψ, $\dot{\psi}$, $\ddot{\psi}$) at the kinematic frequency have the same magnitude. This permits a rapid qualitative evaluation of the significance of the various design parameters in the determination of critical speeds. The normalized form also defines the scaling laws required for an experimental scale model of rail vehicle behavior. That is, for conducting a scaled experiment, the coefficients of Equations 2-105 through 2-111 must be the same for both the model and the full sized vehicle.

Computer programs are being prepared to obtain the characteristic roots of the above equations in order to describe the vehicle transient response and stability. A program is also being prepared to calculate the response of the vehicle to sinusoidal track irregularities and stationary random track irregularities.

In order to check the results, the programs are being applied to the example vehicle used by Wickens in Reference 1 with the following parameters.

$m = 90$ slug (2,810 lb)	$K_Y = 2 \times 10^4$ lb/ft
$M = 400$ slug (12,900 lb)	$K_\psi = 7.11 \times 10^6$ lb-ft/rad
$C = 360$ lb-ft-sec^2	$K_\theta = 2.43 \times 10^6$ lb-ft/rad
$J = 12{,}000$ lb-ft-sec^2	$k_g = 9.5 \times 10^4$ lb/ft

$I = 4{,}000$ lb-ft-sec^2 $\qquad e = 4.0$ ft

$f_T = 3 \times 10^6$ lb $\qquad \ell = 2.5$ ft

$f_L = 3 \times 10^6$ lb $\qquad h = 2.0$

$\alpha = 0.4$ $\qquad k_\psi = 1.06 \times 10^5$

$\ell = 2.5$ ft $\qquad \beta_K = 3.31$ ft

The results of the calculations for this vehicle are in agreement with those obtained by Wickens. The oscillatory components of the solution are represented as the natural frequency and damping ratio of an equivalent second order system. Negative damping ratios represent unstable occillations.

The results of the computations for a vehicle with no damping are shown in Figures 2-18 and 2-19. As shown in Figure 2-18 the frequencies of oscillation are the vehicle lateral natural frequencies and the frequency corresponding to the wheelset motion. At very low speeds, damping of the wheelset motion exists due to the restraint provided by the gravitational stiffness and the stiffness between axles. When the wheelset frequency approaches the lateral natural frequency there are large changes in the damping ratio associated with that frequency. If there is no damping in the secondary suspension, the oscillations become unstable as shown in Figure 2-19. The introduction of a small amount of damping (as shown in Figure 2-20) into the suspension (3%) results in the suppression of the unstable oscillations at speeds that do not coincide with the character-

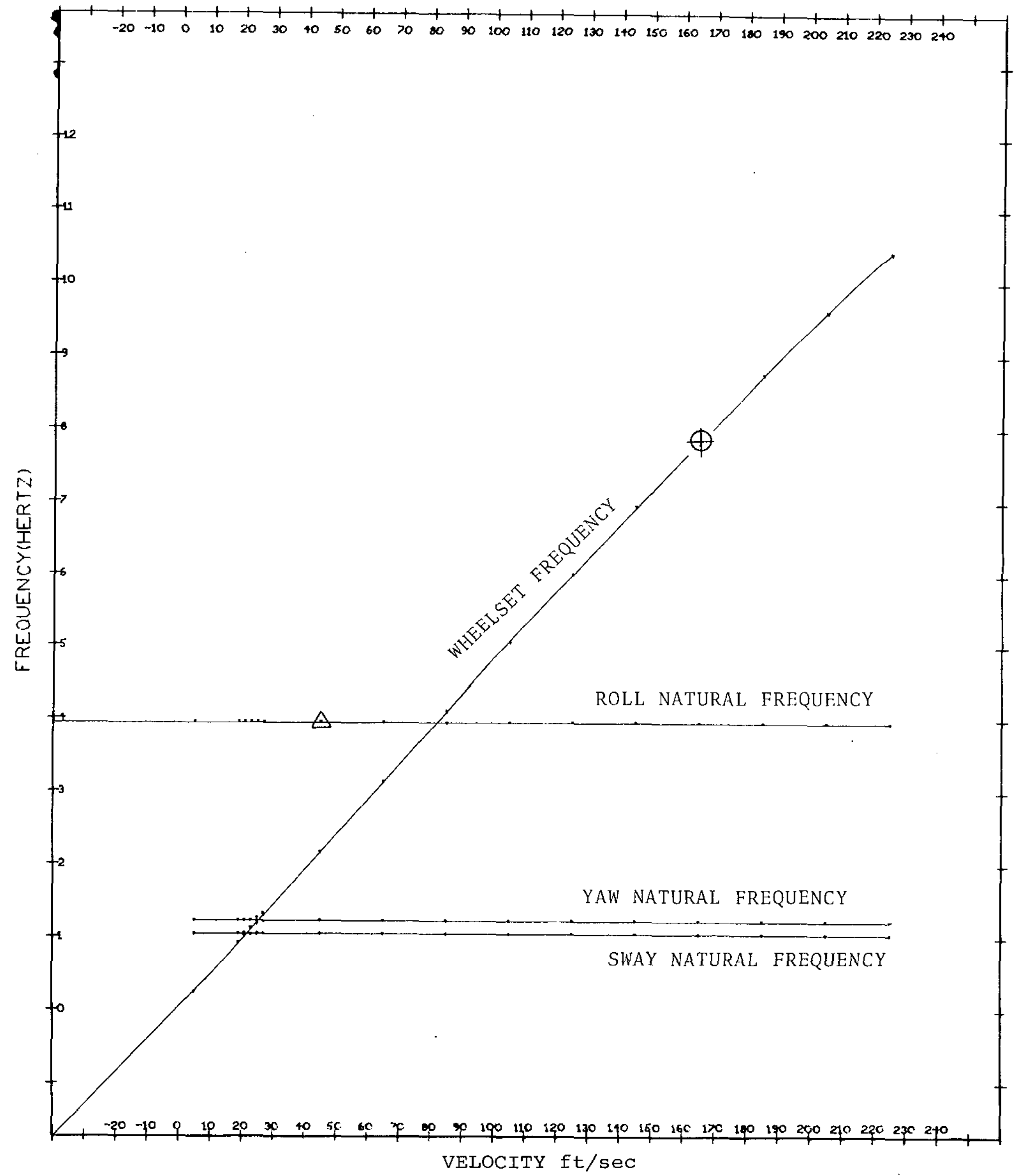

Figure 2-18. Characteristic Frequencies of Two-Axled Vehicle

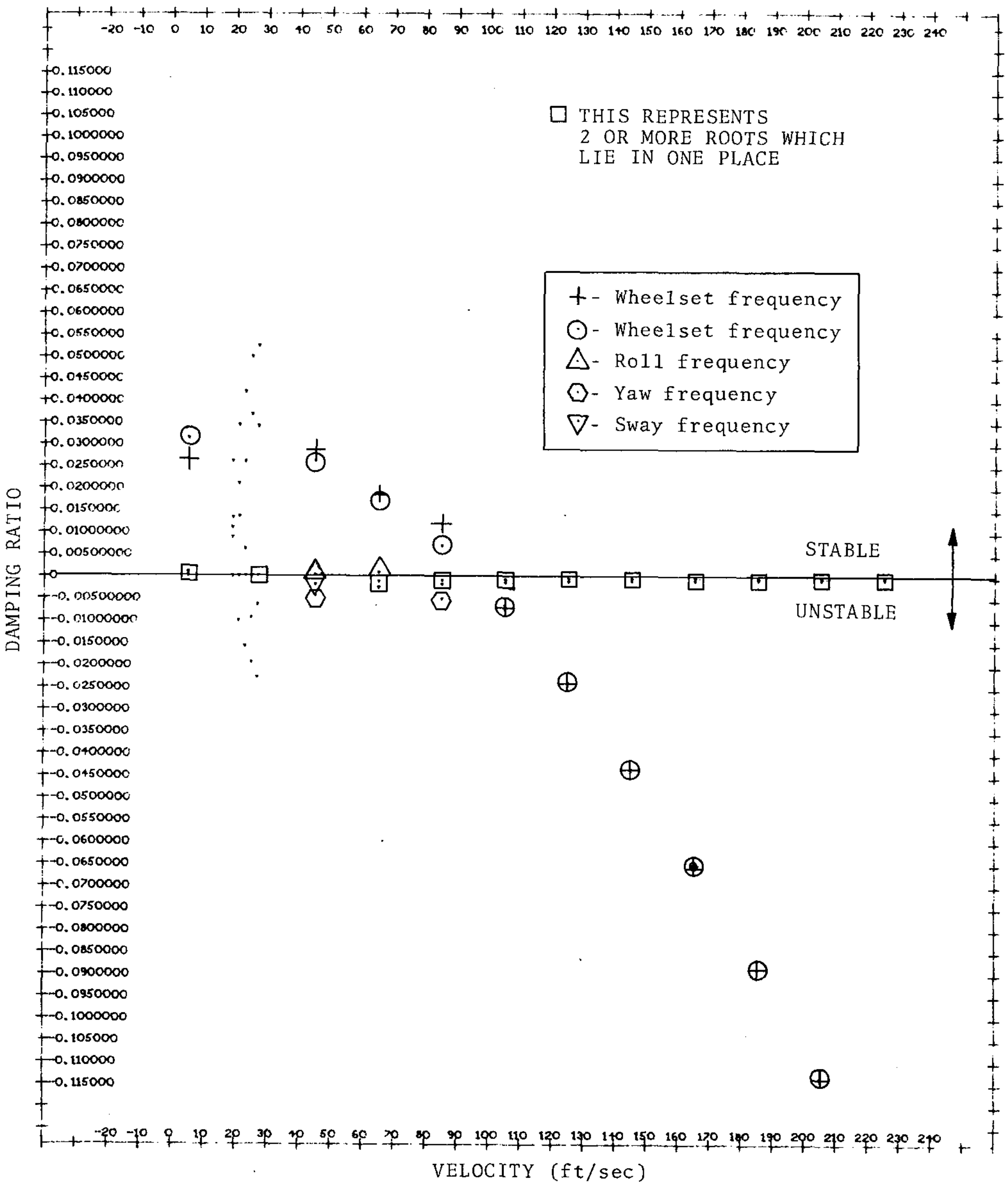

Figure 2-19. Damping Ratio of Undamped Two-Axled Vehicle Oscillations

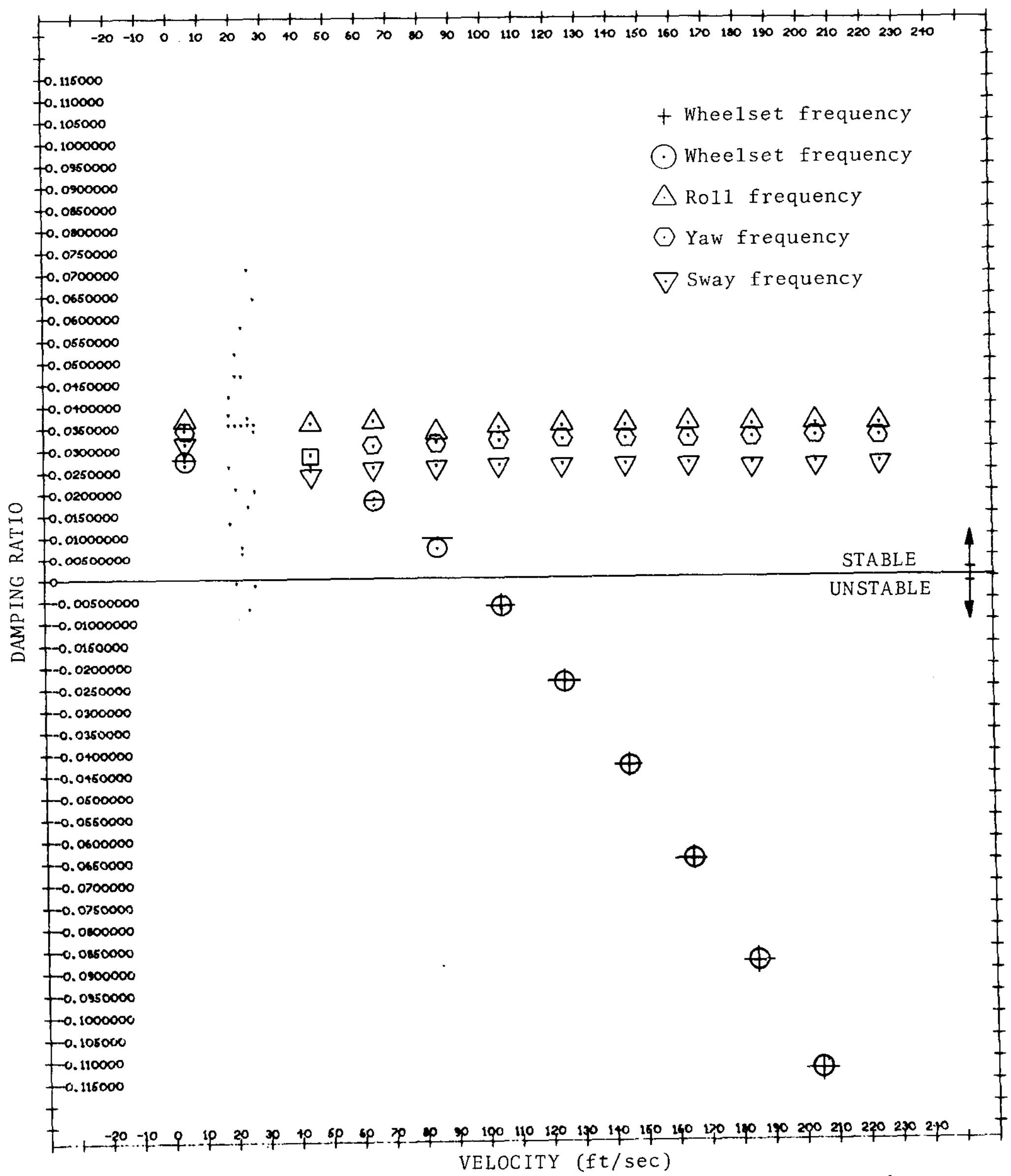

Figure 2-20. Damping Ratio of Lightly Damped Two-Axled Vehicle Oscillations

istic speeds at which the wheelset frequency is equal to a body lateral natural frequency. As shown in Figure 2-21 the low speed unstable behaviour can be completely eliminated by the introduction of additional damping. However, we still note a characteristic speed at which there is a sharp reduction in the effective damping ratio which occurs when the wheelset frequency is equal to the lower body mode natural frequencies. This is evidenced by an increase in the lateral oscillations of the vehicle until the characteristic speed is exceeded. Once this speed is passed, however, the lateral oscillations decrease and the damping is about the same as that under crawl conditions. At very high speeds, the vehicle behaves according to the behaviour predicted in Section 2.5 for the spring suspended wheelset. If the gravitational stiffness is included in the lateral natural frequency w_y Equation 2-96 correctly predicts unstable motion of the wheelsets at all speeds above 95.1 ft/sec.

The low speed hunting phenomenon has been observed during tests of two R-42 cars borrowed from the New York City Transit Authority at the DOT High Speed Ground Test Center. Figure 2-23 shows the lateral accelerations of the wheelset at speeds of 15, 30 and 50 mph, maximum accelerations of both the wheelsets and the car body lateral motions were observed at about 30 mph at a frequency of about 0.9 Hz. The dominant frequency of car body vibration at all speeds was about 0.9 Hz. This would imply a kinematic wavelength of about 50 feet which agrees with the 51.3 feet predicted for conical wheels with a conicity of 0.05

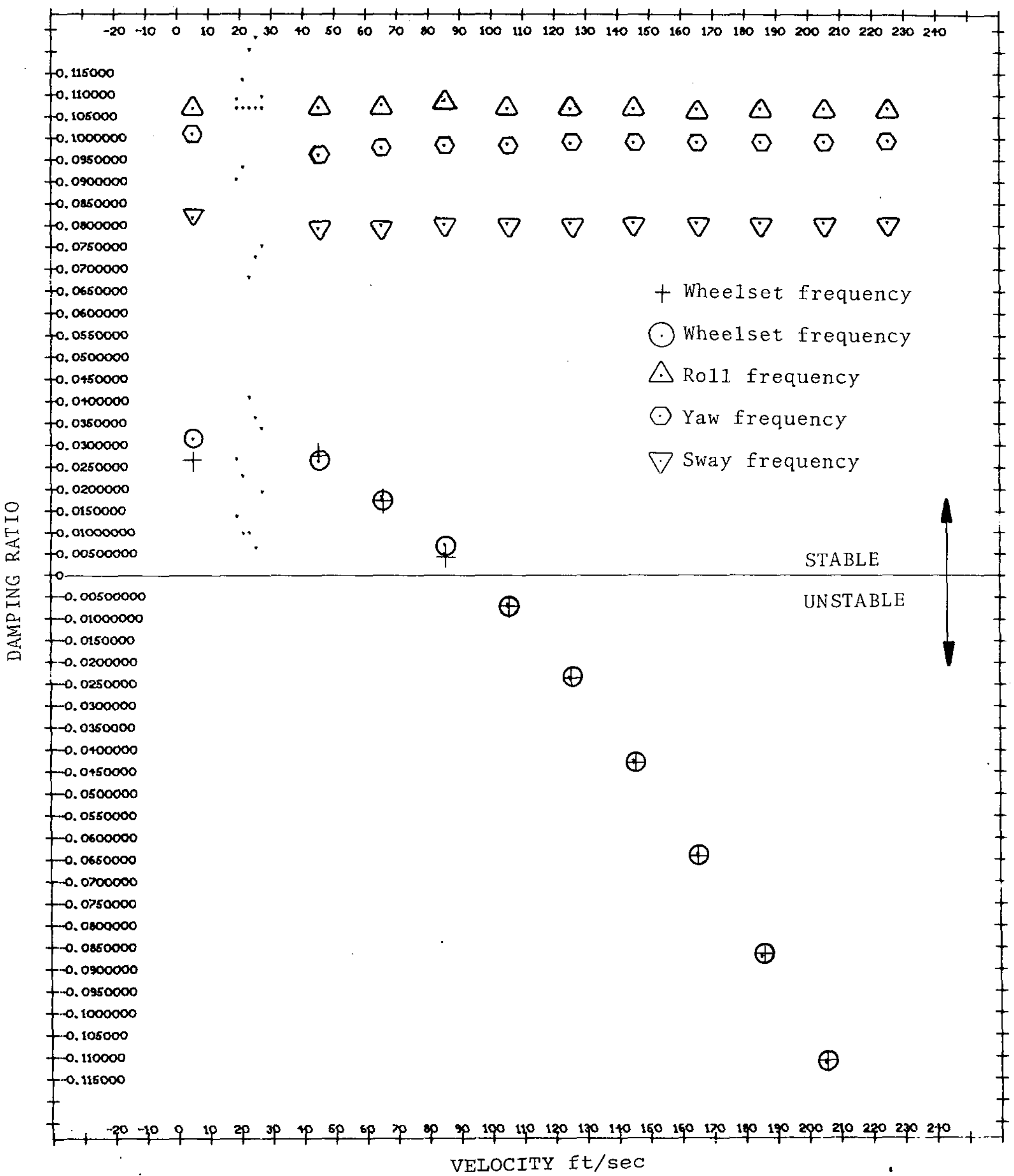

Figure 2-21. Damping Ratio of Damped Two-Axle Vehicle Oscillations

above. The measurements of lateral displacements of the truck body indicate a dominant wavelength of about 50 feet as shown in Figure 2-22 (plots have common time scale) at all speeds. The large wheelset accelerations at 30 mph imply that there is an increase in the lateral wear forces at the wheel/rail interface at this speed. A reduction in wheel and rail maintenance costs could probably be achieved if this characteristic speed could be avoided.

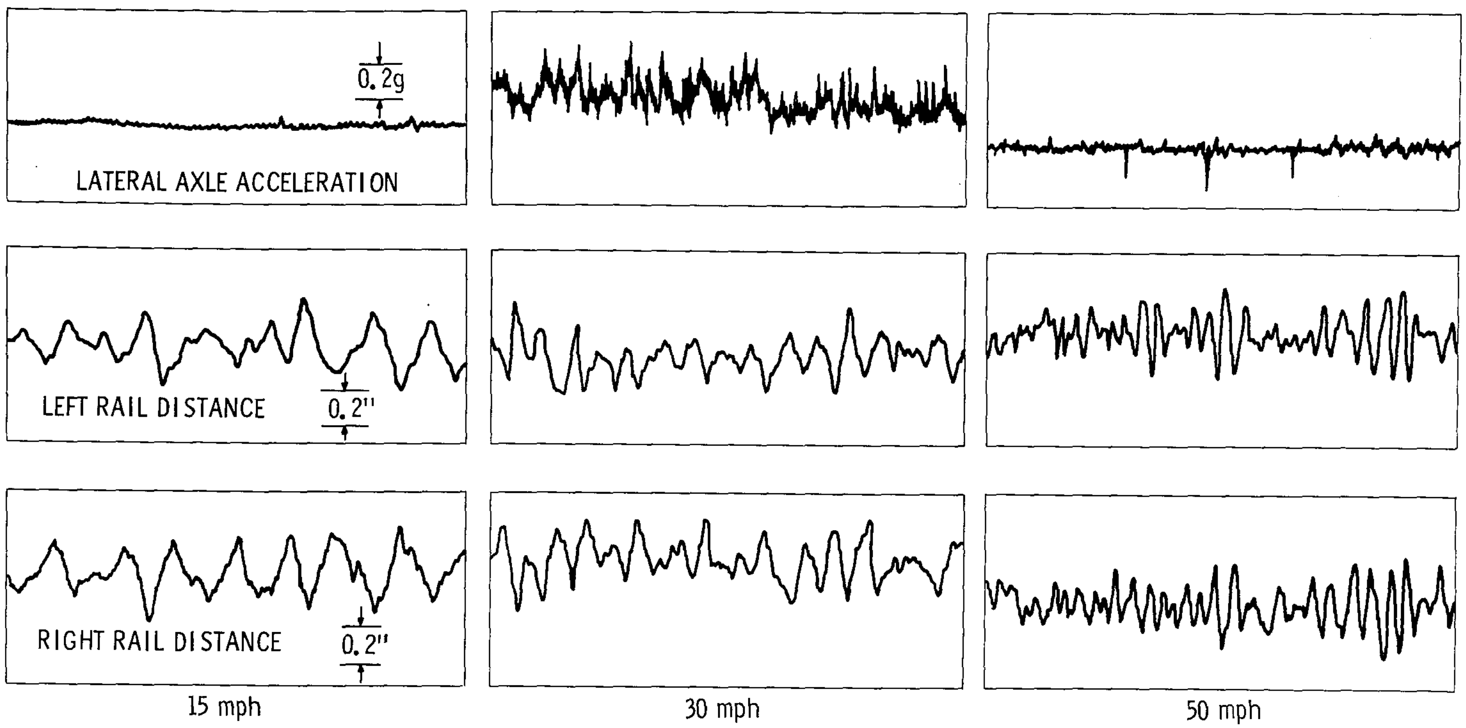

Figure 2-22. Measurements of Lateral Journal Box Acceleration and Truck to Rail Displacements on R-42 Cars on Pueblo Test Track, Nov. 1971

3.0 EFFECTS OF NON-LINEARITIES ON LATERAL RAIL VEHICLE DYNAMICS

3.1 SUMMARY

Section 2 develops the mechanics of lateral guidance and lateral oscillations of rail vehicles based on linearized models of the vehicle. These analyses provide good results for well maintained vehicles and roadbeds on straight routes. However, for rail vehicles travelling on track with large lateral and vertical irregularities and negotiating sharp curves, the non-linearities that result from flange contact, wheelslip, suspension friction and mechanical stops must be taken into account. In addition it is necessary to consider the effects of vertical wheel motions which may result in a decrease in creep coefficient and a loss of adhesion. The mechanics of these non-linearities and the modifications in the equations of motion resulting from them are discussed in the following paragraphs.

3.2 PROFILED WHEELSET

In Section 2 it was assumed that the wheels were perfectly conical so that the rolling radius was linearly proportional to the wheelset lateral displacement. Although this may be approximately accurate for newly ground wheels, wear of the wheel surface will act to hollow out the wheels to produce curvature. New rail vehicle designs have been using profiled wheels in order to take advantage of the increase in gravitational stiffness that results from the action of the normal forces at the wheel/rail contact. The gravitational stiffness is defined as the force per unit lateral displacement that is required to move a loaded wheelset laterally in the absence of friction.

If a horizontal force Fyg is applied to the wheelset shown in Figure 3-1. the wheelset will translate laterally a distance y, and tilt through an angle θ_1. This will result in raising the axle load W against gravity through a vertical distance δ_z. This height change is:

$$\delta_z = y_1\theta_1 + \left(\frac{r_1 + r_2}{2} - r_o\right) \tag{3-1}$$

$$\theta_1 = \frac{r_1 - r_2}{2\ell} \tag{3-2}$$

The work performed by the force F_{yg} to produce a virtual displacement δy_1 is equal to the change in potential energy of the system

$$P.E. = Wy_1 \left(\frac{r_1 - r_2}{2\ell}\right) + W\left[\frac{r_1 + r_2}{2} - r_o\right] \qquad (3\text{-}3$$

δy_1 is equal to the change in potential energy of the system

$$Fyg\,\delta y_1 = \frac{\partial P.E.}{\partial y_1}\,\delta y_1 \tag{3-4}$$

so that

$$Fyg = \frac{\partial (P.E.)}{\partial y_1} = W\frac{(r_1 - r_2)}{2\ell} + Wy_1\left(\frac{r_1' - r_2'}{2\ell}\right) + \frac{W}{2}\left(r_1' + r_2'\right) \tag{3-5}$$

The gravitational stiffness may be defined as:

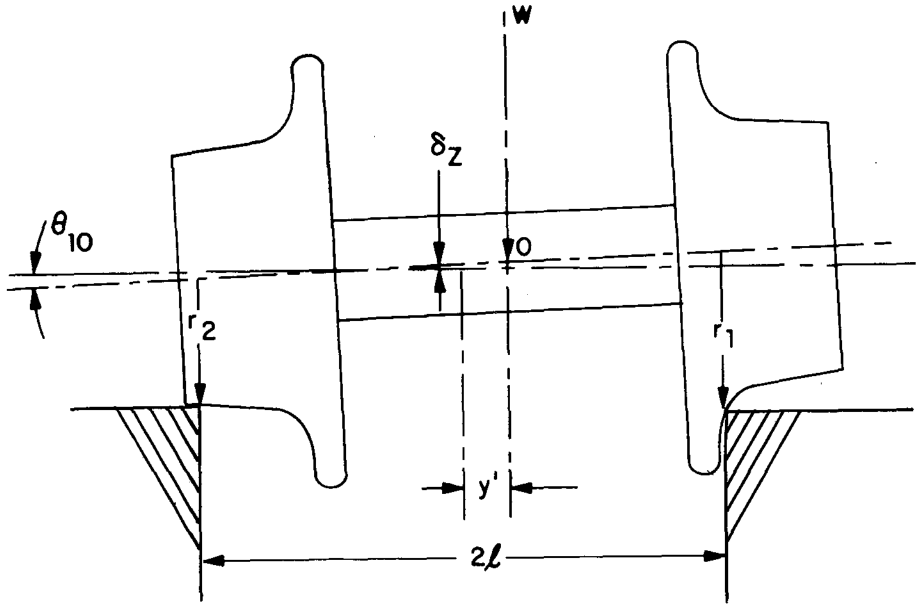

$$\delta_z = y'\theta_{10} + \Delta\bar{r} = y'\left(\frac{r_1 - r_2}{2\ell}\right) + \left(\frac{r_1 + r_2}{2} - r_o\right)$$

$$P.E. = W(y - \bar{\delta})\left(\frac{r_1 - r_2}{2\ell}\right) + W\left[\frac{r_1 + r_2}{2} - r_o\right]$$

$$F_y = \frac{\partial(P.E.)}{\partial y} = \frac{W\left(r_1 - r_2\right)}{2\ell} + W(y - \bar{\delta})\left(\frac{r_1' - r_2'}{2\ell}\right) + \frac{W}{2}\left(r_1' + r_2'\right)$$

$$K_g = \frac{\partial Fy}{\partial y} = \frac{W\left(r_1' - r_2'\right)}{\ell} + W(y - \bar{\delta})\left(\frac{r_1'' - r_2''}{2\ell}\right) + \frac{W}{2}\left(r_1'' + r_2''\right)$$

Figure 3-1. Gravitational Stiffness Produced by Lateral Curvature

$$Kg = \frac{\partial Fyg}{\partial y_1} = W\left(\frac{r_1' - r_2'}{\ell}\right) + Wy_1\left(\frac{r_1'' - r_2''}{2\ell}\right)$$

$$+ \frac{W}{2}\left(r_1'' + r_2''\right) \tag{3-6}$$

For conical wheels

$$r_1 = r_o + \alpha y_1 \tag{3-7a}$$

$$r_2 = r_o - \alpha y_1 \tag{3-7b}$$

we obtain:

$$Kg = \frac{2\alpha W}{\ell} \tag{3-8}$$

For profiled wheels

$$r_1 = r_o + g\ (y_1 + \delta_o) - g\ \delta_o \tag{3-9a}$$

$$r_2 = r_o + g\ (\delta_o - y_1) - g\ \delta_o \tag{3-9b}$$

if

$$g(v) = a_, v + a_n v^n \tag{3-10}$$

$$r_1' = a_1 + a_N(n)(y_1 + \delta_o)^{n-1} \tag{3-11a}$$

$$r_2' = -a_1 - a_N(n)(\delta_o - y_1)^{n-1} \tag{3-11b}$$

$$r_1'' = a_N(n)(n-1)(y_1 + \delta_o)^{n-2} \tag{3-12a}$$

$$r_2'' = a_n(n)(n-1)(\delta_o - y_1)^{n-2} \tag{3-12b}$$

The gravitational stiffness is then for small displacements

$$Kg = \frac{W}{\ell}\left[2a_1 + 2na_N\delta_o^{\,n-1} + n(n-1)\ell\ \delta_o^{\,n-2}\right] \tag{3-13}$$

For large displacements the lateral force is given by:

$$Fyg = \frac{2Wa_1}{\ell} y_1 + \frac{Wa_N}{2\ell}\left[\left(y_1 + \delta_o\right)^n - \left(\delta_o - y_1\right)^n\right]$$
$$+ \frac{W}{2\ell} na_N \left[\left(y_1 + \delta_o\right)^{n-1} + \left(\delta_o - y_1\right)^{n-1}\right] y_1$$
$$+ \frac{W}{2} na_N \left[\left(y_1 + \delta_o\right)^{n-1} - \left(\delta_o - y_1\right)^{n-1}\right] \quad (3\text{-}14)$$

It is seen from Equation 3-13 that the effective gravitational stiffness can be made quite large without affecting the norminal conicity. This gravitational stiffness adds to the lateral suspension system stiffness in the analysis of Section 2.6 to produce an increase in the vehicle and wheelset critical speeds. Profiled wheel designs are currently being employed by the British and the Swiss to take advantage of this effect. The total force applied by the rails on the wheelsets in the lateral direction is

$$F_y = -2f_L\left[\frac{\dot{y}}{V} - \psi\right] - \frac{W}{2\ell}\left[\left[g\left(y_1+\delta_o\right) - g\left(\delta_o-y_1\right)\right]\right.$$
$$+ y_1\left[g'\left(y_1+\delta_o\right) - g'\left(\delta_o-y_1\right)\right]$$
$$\left.+ \ell\left[g'\left(y_1+\delta_o\right) - g'\left(\delta_o-y_1\right)\right]\right] \quad (3\text{-}15)$$

where $y_1 = y - \bar{\delta}$ = displacement from track centerline

δ_o is defined by the wheel gauge, track gauge and the wheel rail profiles. Changes in track gauge will produce corresponding changes in δ_o.

The moment applied by the rails on the wheelset due to creep forces is

$$M_c = -2f_T \left(\frac{\ell\dot{\psi}}{V} + \frac{r_1 - r_2}{r_1 + r_2}\right) \tag{3-16}$$

The normal forces also produce a destabilizing torque that is given approximately by

$$M_N = \frac{W}{2}\left[g'\left(y_1+\delta_o\right) - g'\left(\delta_o-y_1\right)\right] \ell\psi \tag{3-17}$$

The net torque acting on the wheelset is:

$$M = -2f_T \left(\frac{\ell\dot{\psi}}{V} + \frac{r_1 - r_2}{r_1 + r_2}\right) + \frac{W\ell}{2}\left[g'\left(y_1+\delta_o\right) - g'\left(\delta_o-y_1\right)\right] \tag{3-18}$$

For a profile that can be represented by Equation 3-10, Equation 3-18 becomes

$$M = -2f_T\left[\frac{\ell\dot{\psi}}{V} + \frac{a_1y_1 + a_N\left[\left(y_1+\delta_o\right)^n - \left(\delta_o-y_1\right)^n\right]}{r_o + a_N\left[\left(y_1+\delta_o\right)^{n-1} + \left(\delta_o-y_1\right)^n\right]}\right.$$

$$\left. + \frac{W\ell}{2}\left[2a_1 + na_N\left[\left(y_1+\delta_o\right)^{n-1} + \left(\delta_o-y_1\right)^{n-1}\right]\right]\right] \tag{3-19}$$

3.3 TRACK COMPLIANCE

The analyses given above have assumed that the rails and roadbed are infinitely stiff compared to the gravitational stiffness and have negligible deflection as a result of the creep forces. These assumptions are essentially correct for small displacements from the track centerline. However, for large displacements where the flanges do come into contact, the gravitational stiffness becomes quite large and significient track deflections may take place Assuming the track has a linear load deflection characteristic, the deflection of the track centerline is given by

$$\bar{\delta} - \bar{\delta}_i = - \frac{Fy}{K_{TC}} \tag{3-20}$$

the change in track gauge is given approximately by:

$$2\left(\delta_o - \delta_{oi}\right) = - \frac{\frac{W}{2}\left[g'\left(y_1+\delta_o\right) - g'\left(\delta_o - y_1\right)\right]}{K_{TG}} \tag{3-21}$$

where K_{TC} is the overall track lateral stiffness and K_{TG} is the stiffness between opposite rails to a gauge spreading force. Since the track is now capable of an instantaneous velocity, Equation 3-15 must be modified to include the track velocity in the creep forces. The creep force in the lateral direction is now given by:

$$Fy_c = - 2f_L \left[\frac{\dot{y}}{V} - \psi - \frac{\partial \bar{\delta}}{V\partial t}\right] \tag{3-22}$$

making note of

$$\dot{\delta} = \frac{\partial \delta}{\partial t} + V \frac{\partial \delta}{\partial x}$$

and assuming the track deflects parallel to its initial geometry

$$\frac{\partial \bar{\delta}}{\partial x} \approx \frac{d\bar{\delta}_i}{dx} = \bar{\delta}_i'$$

we obtain

$$Fy_c = - 2f_L \left[\frac{\dot{y}}{V} - \psi - \frac{\dot{\bar{\delta}}}{V} + \bar{\delta}_i'\right] \tag{3-23}$$

The form of Equation 3-23 permits interchanging the space variable x and the time variable Vt in the computation. Otherwise it would be necessary in computations to maintain the variables as functions of both x and t.

3.4 CREEP FORCES

The formulations given above have assumed linear relations between the creep velocities and the creep forces. The Johnson and Vermuellen Analysis (Reference 5) which is in good agreement with laboratory data gives the following relations between creep velocities and creep forces:

$$\frac{v_x}{V} = \frac{3\mu N}{G\pi ab}\,\phi\,\frac{F_x}{F_R}\left[1 - \left(1 - \frac{F_R}{\mu N}\right)^{1/3}\right] \tag{3-24}$$

$$\frac{v_y}{V} = \frac{3\mu N}{G\pi ab}\,\psi_1\,\frac{F_y}{F_R}\left[1 - \left(1 - \frac{F_R}{\mu N}\right)^{1/3}\right] \tag{3-25}$$

$$F_R = \sqrt{F_x^2 + F_y^2} \tag{3-26}$$

for $F_R < \mu N$

where:

μ = adhesion constant (coefficient of friction)

ψ_1 = constant depending on wheel/rail curvatures

ϕ = constant depending on wheel/rail curvatures

a,b = major and minor semi-axes of contact ellipse (proportional to $N_{1/3}$)

G = Shear modulus of material

F_x = longitudinal creep force

F_y = lateral creep force

v_x = longitudinal creep velocity

v_y = lateral creep velocity

V = forward velocity

N = Normal force.

Equations 3-24 and 3-25 can be rewritten as

$$\frac{v_x}{V} = C_1 \; N^{1/3} \; \frac{F_x}{F_R} \left[1 - \left(1 - \frac{F_R}{\mu N} \right)^{1/3} \right] \qquad (3\text{-}27)$$

$$\frac{v_y}{V} = C_2 \; N^{1/3} \; \frac{F_y}{F_R} \left[1 - \left(1 - \frac{F_R}{\mu N} \right)^{1/3} \right] \qquad (3\text{-}28)$$

for $F_R < \mu N$

where C_1 and C_2 are functions of the geometry and material of the wheel and rail.

The analyses of Section 2 have assumed a constant ratio between creep force and creep velocity until the adhesion limit. This approximation is valid only for very small values of the creep forces and creep velocities. Use of a constant creep coefficient results in the prediction of larger creep forces than those which will actually exist. For designs having low primary suspension stiffness, the actual value of the creep coefficient has little influence on the dynamic characteristics of the vehicle as long as the dimensionless stiffness is small. When the dimensionless stiffnesses are of the order of one, however, the actual magnitude of the creep coefficient is significant.

The existence of lateral creep forces resulting from axle - misalignment on rigid truck designs results in a decrease in the creep coefficients in both the lateral and longitudinal directions.

Field experiments on the adhesion coefficients as a function of speed indicate a decrease in adhesion and creep coefficients as a function of speed. Recent work by Paul (Reference 5) indicates that this decrease in apparent adhesion is due to oscillations in the magnitude of the contact stresses resulting from wheel/rail vibrations. This effect can be approximated by setting

$$N = N_o \left(1 + a \sin wt\right)$$

where N_o is the nominal normal load and "a" is the ratio of the oscillatory component of the normal load to the nominal normal load. Equations 3-27 and 3-28 become:

$$\frac{v_x}{V} = C_1 N_o^{1/3} \frac{F_x}{F_R} \left(1 + a \sin wt\right)^{1/3} \left[1 - \left(1 - \frac{F_R}{\mu N_o\left(1 + a \sin wt\right)}\right)^{1/3}\right] \tag{3-29}$$

$$\frac{v_y}{V} = C_1 N_o^{1/3} \frac{F_x}{F_R} \left(1 + a \sin wt\right)^{1/3} \left[1 - \left(1 - \frac{F_R}{\mu N_o\left(1 + a \sin wt\right)}\right)^{1/3}\right] \tag{3-30}$$

Since the vibrations associated with variations of the normal load will be at high frequency (above 40 Hz) compared to those of interest for the investigation of lateral dynamics (below 10 Hz), an approximate relationship between creep force and average creep velocity is obtained by:

$$\frac{\bar{v}_x}{V} = \frac{1}{2\pi} \int_o^{2\pi} \frac{v_x}{V} (\theta) d\theta \tag{3-31}$$

$$\frac{\bar{v}_y}{V} = \frac{1}{2\pi}\int_0^{2\pi} \frac{v_y}{V}(\theta)d\theta \tag{3-32}$$

The creep force, creep velocity relations implied by the above expressions resulting from variations in normal force are shown in Figure 3-2.

The fluctuations in normal force result from the vertical interaction of the rails and vehicle wheels in response to track and wheel and wheel irregularities. A computer program has been prepared for calculation of the response of rail vehicles and prediction of track deflection due to vertical rail irregularities. This program is described in Appendix B. The program assumes the half car model shown in Figure 3-3 which is a valid approximation at short wavelengths. Typical results of the calculations are shown in Figures 3-4 and 3-5. at relatively short wavelengths corresponding to irregularity frequencies in the neighborhood of the wheel/rail natural frequencies large amplifications of the irregularity motions occur. The accelerations associated with these motions result in fluctuations of the contact stress which produce a decrease in both the adhesion limit and the effective creep coefficient as discussed above. Under some conditions these changes may actually act to stabilizing the hunting behaviors of the vehicle which under other conditions the adhesion may increase the likehood of derailment.

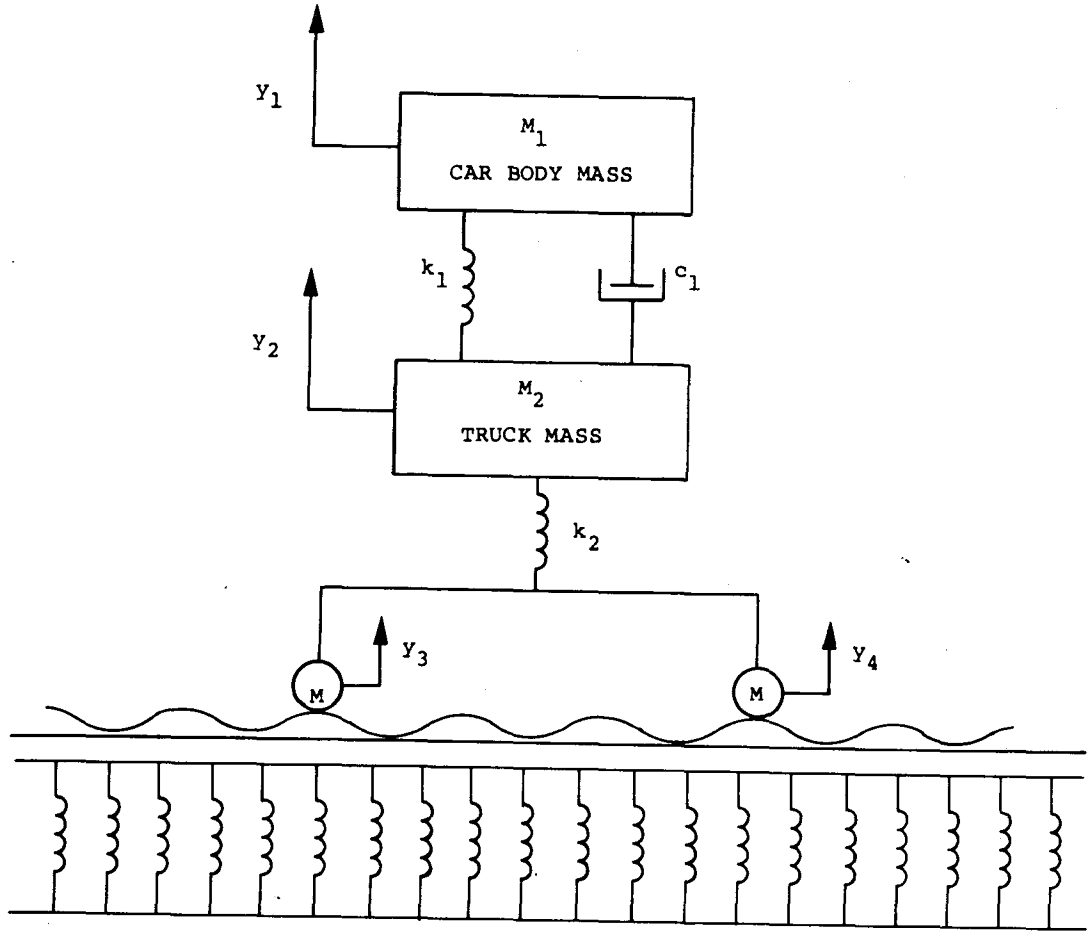

Figure 3-2. Half-Car Model to Evaluate Influence of Track Compliance

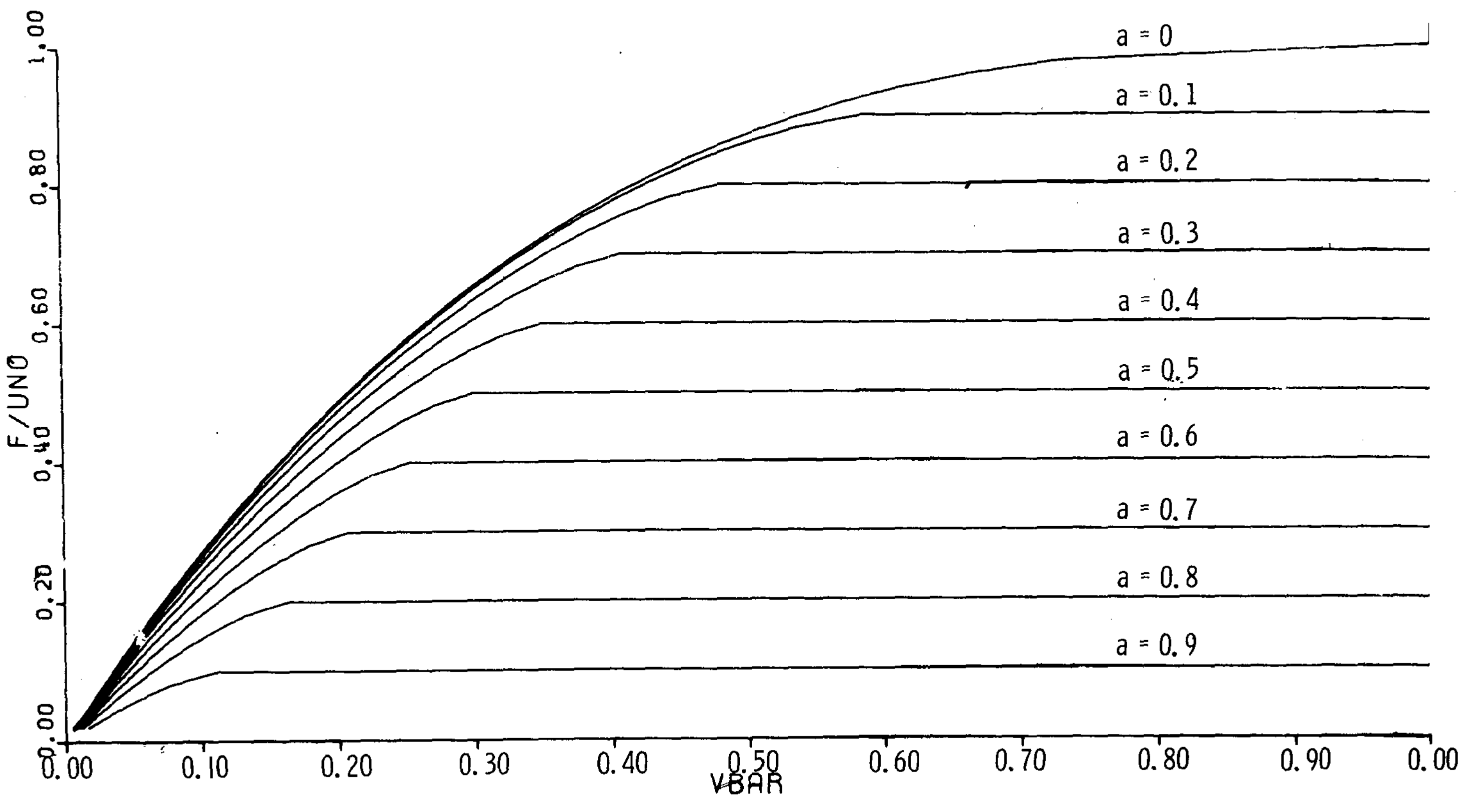

Figure 3-3. Creep Force Vs Creep Velocity in the Presence of Normal Load Oscillations.

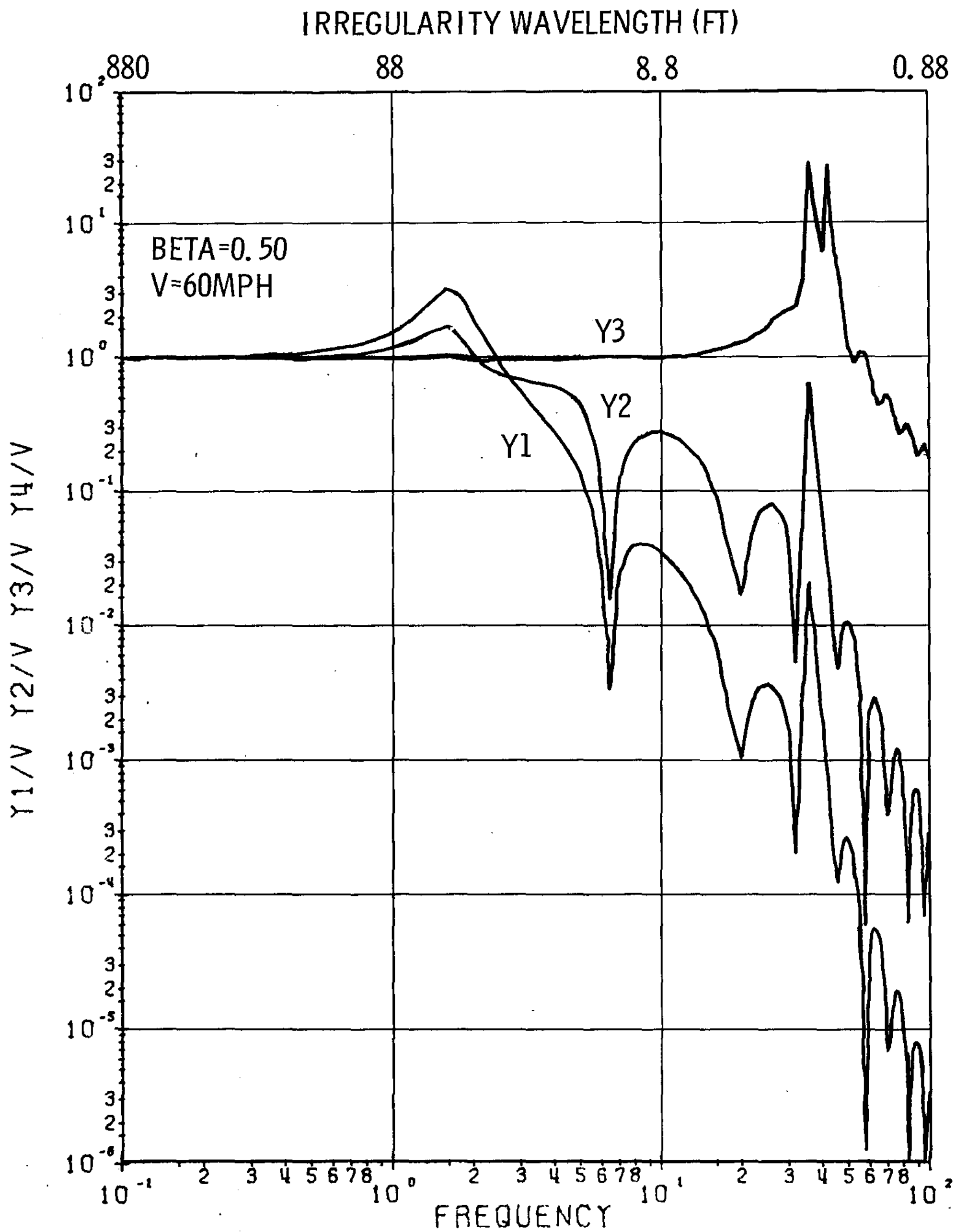

Figure 3-4. Displacements of Car Body (y_1), Truck Body (y_2) and Wheels (y_3, y_4) of a Rail Vehicle Travelling Over Track with Vertical Irregularities

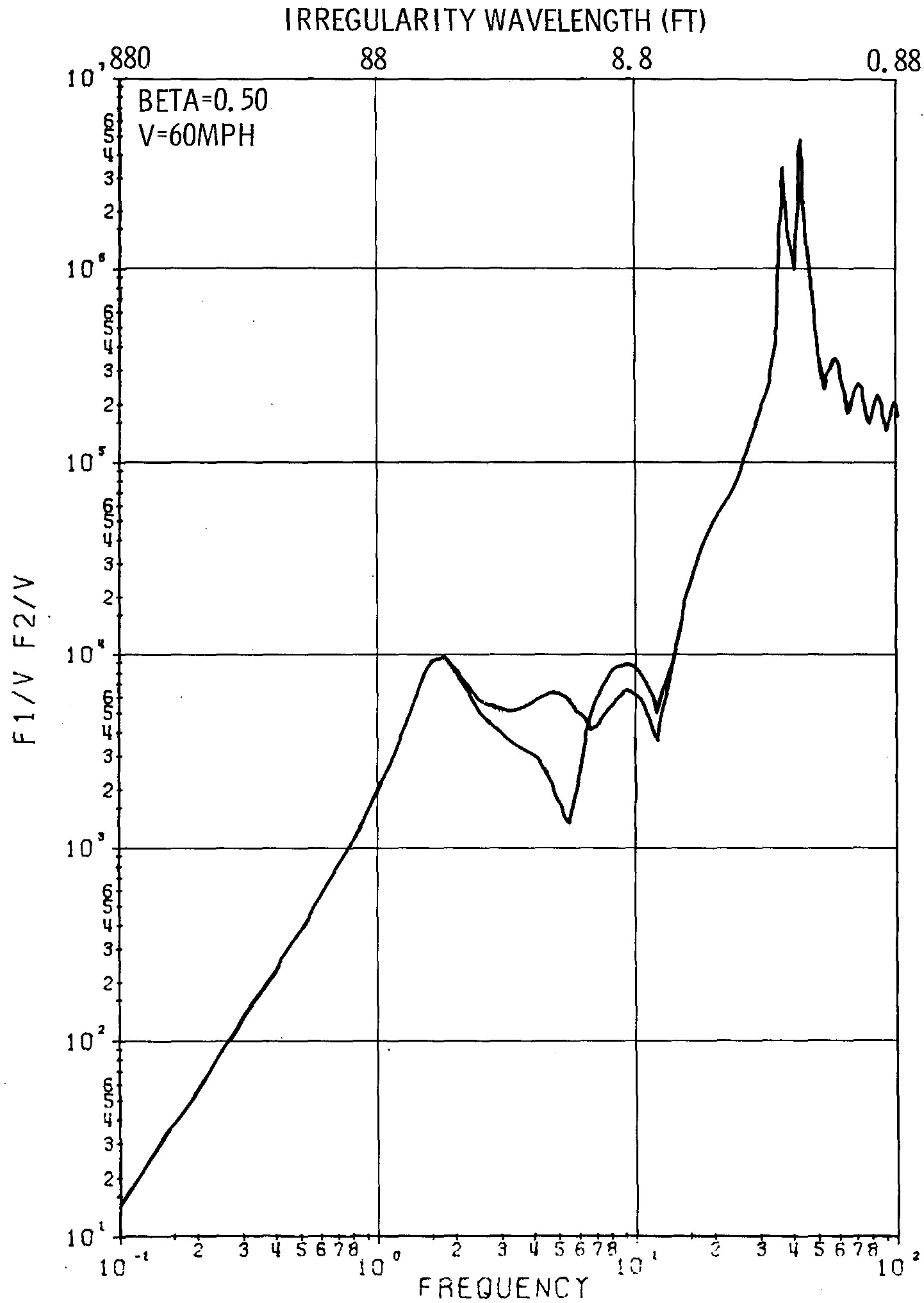

Figure 3-5. Force (lbs) at Wheel/Rail Interface Due to 1" Rail Irregularity vs Frequency (Hz) and Irregularity Wavelength

3.5 SUSPENSION SYSTEM NON-LINEARITIES

Figure 3-6 schematically indicates the assembly of typical transit vehicle trucks. For small longitudinal lateral and yaw motions the clearance between the journal boxes and the truck frame permit the wheelsets to move relative to the truck frame to compensate for track misalignments. However, as the motions become large the journal boxes will come into contact with the truck frame resulting in a sudden stiffening of the effective primary suspension. Large acceleration on braking forces will produce a similar effect. When the relative motions between the car body and truck are large, sliding will occur on rubbing surfaces. There will also be impacts with mechanical stops and snubbers which have been designed to prevent excessive relative motions.

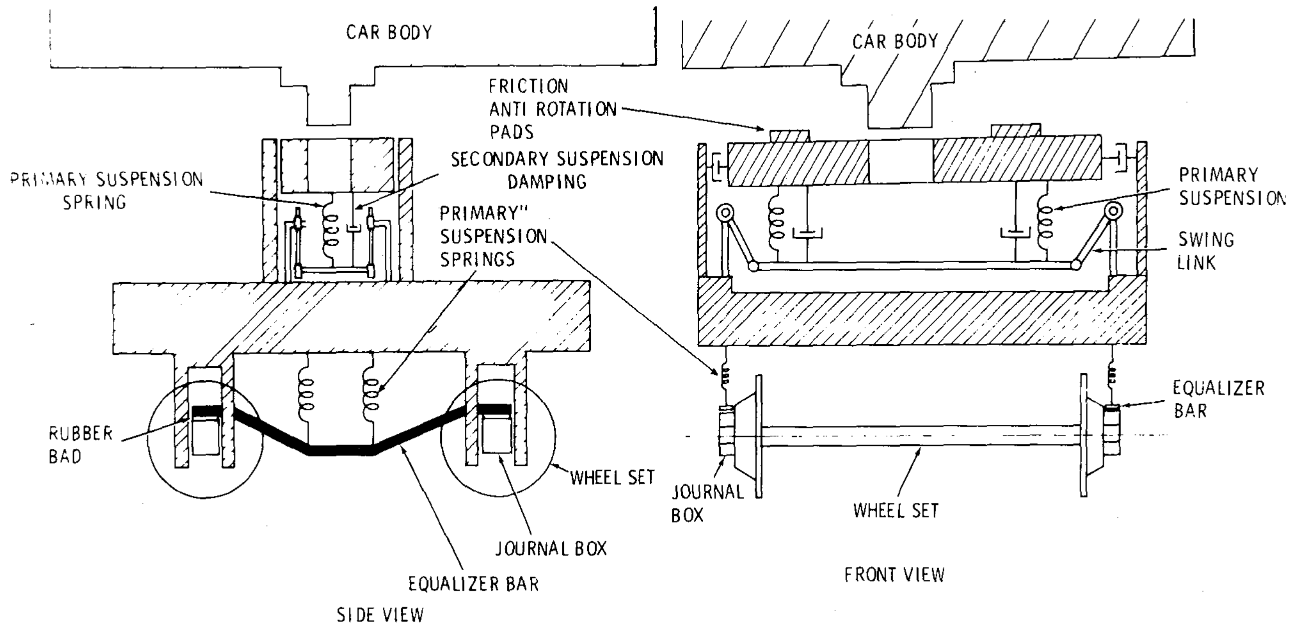

Figure 3-6. Typical Truck Assembly

REFERENCES

1. Wickens, A. H., The Dynamics of Railway Vehicles on Straight Track: Fundamental Considerations of Lateral Stability. Proceedings of the Institution of Mechanical Engineers, London, 1965-66.
2. Matsudaira, T., Hunting Problem of High Speed Railway Vehicles with Special Reference to Bogie Design for the new Tokaido Line. Proceedings of the Institution of Mechanical Engineers, London, 1965-66.
3. Cooperrider, N. K., High Speed Dynamics of Conventional Railway Trucks, Phd Thesis, Dept. of Mechanical Engineering, Stanford University, 1968.
4. Mueller, C. T., Das Schlenger problem in der sicht von Vergangenheit und Gegenwart, Zeitschnift fuer Eisenbahnwesen und Verkehstechnik, Berlin, 1969
5. Langer, B. F., Dynamic Stability of Railway Trucks, Timoshenko 60th Anniversary Volume, MacMillan Company, New York, 1938.
6. Newland, D. E., The Steering of a Flexible Railway Truck on Curved Track, Department of Mechanical Engineering, Sheffield University, Sheffield, England, 1968.

APPENDIX A

COMPUTER PROGRAM FOR PREDICTING CHARACTERISTIC ROOTS DESCRIBING TRANSIENT LATERAL DYNAMICS OF TWO AXLED RAIL VEHICLES

Prepared by

Leonard Somers

Service Technology Corp.

KENTRON HAWAII, LTD
DOT-TSC ADP Support Services Project

PROGRAM "POLY552" - AN INTRODUCTION

The computer program "POLY552" described herein was developed to obtain the characteristic roots of a set of seven differential equations which define a relatively simple system, representing a four-wheeled railway vehicle such as a wagon or a bogie. This simple system contains the essential physical content of the larger systems which must be considered in investigations on stability. Further details on the equations may be found in the appendix.

POLY552 is implemented in the MAC-360 language, an algebric compiler developed at the MIT Instrumentation Laboratory for use in fields such as dynamics and control theory. MAC-360 features a three-line format corresponding to the 3 levels of an ordinary algebric equation, thus inputing equations in a form as close to the original as possible.

The resultant matrix of equations is solved by POLY552 through use of a modified MAC routine "AU232.PLOYMATRX", renamed "POLY551", which evaluates the determinant of a matrix with polynomial elements using the MAC determinant function. The output of the determinant function are the polynomial coefficients of the system polynomial.

A non-MAC routine DPRQD (from the IBM SSP library) is linked to POLY551 to provide rooting of the system polynomial.

Routine DPRQD uses a double precision ratio quotient algorithm to obtain the roots of a polynomial. The generated complex roots are then manipulated to yield the frequencies and damping ratios.

The complete set of frequencies and damping factors are stored and then plotted using the MAC routine DCGPLOT. Labelling and lettering of the plots are also included in the plot portion of the program.

POLY552 is catalogued in the MAC symbolic-program storage file at the MIT Draper Laboratory. It can be called into use by specific control cards. The control cards to summon POLY552 the necessary input, and the output and plots expected are discussed in the next few pages.

```
M018200           C00 = SQOMEG /SQOMEG
S018300                       K        L

M018400           SM =C00
S018500             2

M018600           SM =B00,SM  =B15,SM  =B15
S018700             1       41        61

R018800   END OF FIRST ROW, START OF SECOND ROW.

E018900                                                          2
M019000           SM     = SM , SM     = SM , SM     = B15 H L
S019100             161      1    162      2    201              PRIME

R019200   END OF SECOND ROW, START OF THIRD ROW.

M019300           B36 = - 2 BETA   R OMEGA /OMEGA
S019400                         TWO T     K       T

M019500           C33 = SQOMEG /SQOMEG
S019600                       K        T

M019700           SM   =C33
S019800             322

M019900           SM   =1-B36,SM   =B36
S020000             321          351

R020100   END OF THIRD ROW, START OF FOURTH ROW.

M020200           SM     = SM    , SM     = SM
S020300             481      321     482      322

R020400   END OF FOURTH ROW, START OF FIFTH ROW.

M020500           SM     = -2 BETA OMEGA /OMEGA , SM     = -SM
S020600             601            Y     K      Y   641       601

M020700           SM     = SQOMEG /SQOMEG , SM     = SM   E
S020800             642         K        Y    661      641 PRIME

R020900   END OF FIFTH ROW, START OF SIXTH ROW.

M021000           SM     = -2 BETA     OMEGA     OMEGA /(SQOMEG   H L      )
S021100             761           FIVE      FIVE      K        PSI   PRIME

M021200           SM     = -2 BETA     OMEGA     OMEGA /SQOMEG
S021300             771           FOUR      FOUR      K       PSI

M021400           SM     = 2 BETA   OMEGA /OMEGA    , SM     = SQOMEG /SQOMEG
S021500             801        PSI      K       PSI   802          K        PSI

R021600   END OF SIXTH ROW, START OF SEVENTH ROW.
```

```
M014700          A33 = SQR  - SQOMEG /SQOMEG
S014800                   T           A        T

M014900          SM    = 1, SM    = A33, SM    = -SQR
S015000            300         320          350        T

M015100          SM    = 1, SM    = A33
S015200            460        480

M015300          SM    = -1, SM    = 1, SM    = F
S015400            600          640         660    PRIME

M015500          SM    = -SQOMEG    /(SQOMEG   H L      )
S015600            760          FIVE         PSI   PRIME

M015700          SM    = -SQOMEG    /SQOMEG   , SM    = 1
S015800            770          FOUR        PSI    800

M015900          SM    = -SQOMEG     /(SQOMEG      E      )
S016000            900           THREE         THETA PRIME

M016100          SM    = -SM    , SM    = 1
S016200            940      900    960

R016300

M016400          COUNT = 0

M016500          DO TO 12 FOR V =VSTART(VINC)VMAX

M016600          PRINT HDG, TIMEOFDAY, SP2

M016700          TIME

M016800          OMEGA  = V/BETA
S016900               K         K

E017000                         2
M017100          SQOMEG  = OMEGA
S017200                K        K

M017300          PRINT HDG,V,OMEGA ,SQOMEG ,SP2
S017400                           K       K

E017500                                   2
M017600          VELOCITY  OMEGA      OMEGA
S017700                        K          K

M017800          B15 = -2 BETA   R OMEGA /OMEGA
S017900                       ONE L     K      L

R018000  START OF FIRST ROW OF MATRIX ELEMENTS.

M018100          B00 = 1 - B15
```

```
      SUBROUTINE FMAC(CALFIL)
      DOUBLE PRECISION CALFIL(1), Q(15), EE(15), POL(15)
      IC = CALFIL(1)
      CALL DPRQD(CALFIL(2),IC,Q,EE,POL,IX,IER)
      CALFIL(1) =IER
      CALFIL(2)=IX
      CALFIL(2+IX+1)=Q(IX+1)
      DO 3 I=1,IX
      CALFIL(I+2) = Q(I)
      CALFIL( I+2+IX+1)=EE(I)
    3 CALFIL(2+IX*2 +1+I) =POL(I)
      CALFIL(4+ IX*3) =POL(IX+1)
      RETURN
      END
```

```
R031300  SET TWO
M031400          MODEY,LINE,MARK,NMARK,NPOINTS,PERIOD,
M031500          VVMIN,VVMAX,VVINCH,VVTICK,VVLOC,
M031600          YAMIN,YAMAX,YAINCH,YATICK,YBLOC,
R031700  SET THREE
M031800          MODEY,LINE,MARK,NMARK,NPOINTS,PERIOD,
M031900          VVMIN,VVMAX,VVINCH,VVTICK,VVLOC,
M032000          YAMIN,YAMAX,YAINCH,YATICK,YCLOC,
R032100  SET FOUR
M032200          MODEY,LINE,MARK,NMARK,NPOINTS,PERIOD
M032300          VVMIN,VVMAX,VVINCH,VVTICK,VVLOC,
M032400          YAMIN,YAMAX,YAINCH,YATICK,YDLOC,
R032500  SET FIVE
M032600          MODEY,LINE,MARK,NMARK,NPOINTS,PERIOD,
M032700          VVMIN,VVMAX,VVINCH,VVTICK,VVLOC,
M032800          YAMIN,YAMAX,YAINCH,YATICK,YELOC,
R032900  SET SIX
M033000          MODEY,LINE,MARK,NMARK,NPOINTS,PERIOD,
M033100          VVMIN,VVMAX,VVINCH,VVTICK,VVLOC,
M033200          YAMIN,YAMAX,YAINCH,YATICK,YFLOC,
R033300  SET SEVEN
M033400          MODEY,LINE,MARK,NMARK,NPOINTS,PERIOD,
M033500          VVMIN,VVMAX,VVINCH,VVTICK,VVLOC,
M033600          YAMIN,YAMAX,YAINCH,YATICK,YGLOC
M033700          CALL DCGPLOT(LABL),
M033800          00,3100,3100,0.06
M033900          CALL DCGPLOT(LETR),
M034000          1.1,(PI/2),(-1.2),3.5,
```

```
M034100          22,41,21,40,52,21,37,19,56,60,24,21,41,51,57,28,999
M034200          CALL DCGPLOT(LETR),
M034300          1.1,0,3,(-1.2),53,21,35,38,19,25,51,56,999
R034400
R034500
R034600 START OF PLOT GENERATION OF DAMPING RATIOS
M034700          NSETS=7,LINE=0,MARK=1,NMARK=1,NPOINTS=LOOP,PERIOD=15
M034800          VVMIN=0,VVMAX=220,VVINCH=5.5,VVTICK=10,VVLOC=80000
M034900          YAMIN=-0.10,YAMAX=0.10,YAINCH=7,YATICK=0.005,YALOC=VVLOC+1
M035000          MODEX=0,MODEY=2,YBLOC=VVLOC+3,YCLOC=VVLOC+5,YDLOC=VVLOC+7
M035100          YELOC=VVLOC+9,YFLOC=VVLOC+11,YGLOC=VVLOC+13
M035200          CALL DCGPLOT(PLOT),NSETS,
  35300   SET ONE
M035400          MODEX,LINE,MARK,NMARK,NPOINTS,PERIOD,
M035500          VVMIN,VVMAX,VVINCH,VVTICK,VVLOC,
M035600          YAMIN,YAMAX,YAINCH,YATICK,YALOC,
R035700   SET TWO
M035800          MODEY,LINE,MARK,NMARK,NPOINTS,PERIOD,
M035900          VVMIN,VVMAX,VVINCH,VVTICK,VVLOC,
M036000          YAMIN,YAMAX,YAINCH,YATICK,YBLOC,
R036100   SET THREE
M036200          MODEY,LINE,MARK,NMARK,NPOINTS,PERIOD,
M036300          VVMIN,VVMAX,VVINCH,VVTICK,VVLOC,
M036400          YAMIN,YAMAX,YAINCH,YATICK,YCLOC,
R036500   SET FOUR
M036600          MODEY,LINE,MARK,NMARK,NPOINTS,PERIOD,
M036700          VVMIN,VVMAX,VVINCH,VVTICK,VVLOC,
M036800          YAMIN,YAMAX,YAINCH,YATICK,YDLOC,
R036900   SET FIVE
```

```
M037000           MODEY,LINE,MARK,NMARK,NPOINTS,PERIOD,
M037100           VVMIN,VVMAX,VVINCH,VVTICK,VVLOC,
M037200           YAMIN,YAMAX,YAINCH,YATICK,YFLOC,
R037300   SET SIX
M037400           MODEY,LINE,MARK,NMARK,NPOINTS,PERIOD,
M037500           VVMIN,VVMAX,VV INCH,VVTICK,VVLOC,
M037600           YAMIN,YAMAX,YAINCH,YATICK,YFLOC,
R037700   SET SEVEN
M037800           MODEY,LINE,MARK,NMARK,NPOINTS,PERIOD,
M037900           VVMIN,VVMAX,VVINCH,VVTICK,VVLOC,
M038000           YAMIN,YAMAX,YAINCH,YATICK,YGLOC
M038100           CALL DCGPLOT(LABL),
M038200           00,3100,3100,0.06
M038300           CALL DCGPLOT(LETR),
M038400           1.1,(PI/2),(-1.2),3.5,
M038500           20,17,36,39,25,37,23,13,22,17,19,51,38,41,999
M038600           CALL DCGPLOT(LETR),
M038700           1.1,0,3,(-1.2),53,21,35,33,19,25,51,56,999
M038800           CALL DCGPLOT,(-1)
R038900   END OF PLOT GENERATION
M039000           CALL(NONMAC)GO,(-1)
M039100           START AT BEGIN
```

```
M028300            PRINT HDG,LOOP,SP1

M028400            RUN NO.

M028500            QOUT=2000 + 50 LOOP

M028600            SET FILE READ QOUT

M028700            FILE READ V,X

M028800            PRINT HDG,V,X

M028900            VELOCITY  NO. ROOTS

M029000            FILE READ  OMGA  TO OMGA
S029100                           1         X

M029200            PRINT MSG, OMGA  TO OMGA  ,SP2
S029300                           1         X

M029400            REAL ROOTS IN HERTZ

M029500            FILE READ  BETA  TO BETA
S029600                           1         X

M029700            PRINT MSG,BETA TO BETA ,SP2
S029800                         1        X

M029900            IMAGINARY ROOTS IN HERTZ:

M030000   100      DUMMD = 0

R030100  START OF PLOT GENERATION OF REAL ROOTS
R030200

M030300            NSETS=7,LINE=0,MARK=1,NMARK=1,NPOINTS=LOOP,PERIOD=15

M030400            VVMIN=0,VVMAX=220,VVINCH=5.5,VVTICK=10,VVLOC=75000

M030500            YAMIN=0,YAMAX= 12 ,YAINCH=7 ,YATICK= 1 ,YALOC=VVLOC+1

M030600            MODEX=0,MODEY=2,YBLOC=VVLOC+3,YCLOC=VVLOC+5,YDLOC=VVLOC+7

M030700            YELOC=VVLOC+9,YFLOC=VVLOC+11,YGLOC=VVLOC+13

M030800            CALL DCGPLOT(PLOT),NSETS,

R030900  SET ONE

M031000            MODEX,LINE,MARK,NMARK,NPOINTS,PERIOD,

M031100            VVMIN,VVMAX,VVINCH,VVTICK,VVLOC,

M031200            YAMIN,YAMAX,YAINCH,YATICK,YALOC,
```

```
M025000         WORKING VECTOR IS:

M025100         PRINT MSG,Q ,SP2
S025200                    X+1

M025300         MAXIMAL RELATIVE ERROR IS:

M025400         SET FILE WRITE QB

M025500         FILE WRITE V,X

M025600         DO TO 22 FOR W=1(1)X

E025700                            2   2
M025800         OMGA =OMEGA  SQRT(C +EE )/(2 PI)
S025900             W      K       W   W

M026000      22 FILE WRITE OMGA
S026100                        W

M026200         DO TO 34 FOR W=1(1)X

M026300         BETA =-OMEGA  Q /(OMGA  2 PI)
S026400             W       K  W      W

M026500      34 FILE WRITE BETA
S026600                        W

M026700         SET FILE READ QB

M026800         FILE READ V,X,OMGA TO OMGA , BETA  TO BETA
S026900                           1       X      1         X

M027000         SET FILE WRITE QC

M027100         FILE WRITE V

M027200         FILE WRITE OMGA  TO OMGA
S027300                        1        X

M027400         QC=QC+15

M027500         SET FILE WRITE QD

M027600         FILE WRITE V, BETA  TO BETA
S027700                           1        X

M027800         QD=QD+15

M027900    12   DUMMB = 0

R028000 END OF FILE WRITE, START OF FILE READ AND PRINT.
R028100

M028200         DO TO 100 FOR LOOP = 1(1)COUNT
```

```
M021700          SM    = -2 BETA      OMEGA     OMEGA /(SQOMEG      E      )
S021800            901            THREE     THREE      K          THETA PRIME

M021900          SM    = -SM    , SM    = 2 BETA      OMEGA /OMEGA
S022000            941      901    961            THETA      K        THETA

M022100          SM    = SQOMEG /SQOMEG
S022200            962          K         THETA

R022300    END OF SEVENTH ROW.

M022400          CALL POLY551(SUB),0,1,7,2

M022500          RESUME N,GAINN,GAINDC,POLY  TO POLY
S022600                                    0        N

M022700          COUNT  = COUNT + 1

M022800          QA= 1000 + 25 COUNT, QB = 2000 + 50 COUNT

M022900          SET FILE WRITE QA

M023000          FILE WRITE V,N,POLY  TO POLY
S023100                             0       N

M023200          IC=N+1

M023300          COEF  =0
S023400              0

M023500          DO TO 11 FOR A=1(1)(N+1)

M023600       11 COEF  =POLY
S023700              A      N+1-A

M023800          PRINT MSG,COEF  TO COEF   ,SP2
S023900                        1        N+1

M024000          COEFFICIENTS IN ASCENDING ORDER ARE:

M024100          CALL(NONMAC,RESIDENT)GO,IC,COEF  TO COEF
S024200                                       1        N+1

M024300          RESUME  IER,X,Q  TO Q   , EE  TO EE , POL  TO POL
S024400                         1     X+1    1       X     1       X+1

M024500          IF IER NZ, GO TO 13, OTHERWISE GO TO 20

M024600       13 COUNT=COUNT-1

M024700          GO TO 12

M024800       20 PRINT MSG,POL TO POL   ,SP2
S024900                       1      X+1
```

```
M011000            SQOMEG       = KG/MS
S011100                  G

M011200            SQOMEG       = KA/   C
S011300                  A

M011400            SQOMEG       = K /M
S011500                  Y          Y

M011600            OMEGA        = SQRT(SQOMEG )
S011700                 Y                     Y

M011800            BETA         = C  /(2  M OMEGA   )
S011900                Y           Y              Y

M012000            E        = E/BETA
S012100             PRIME           K

M012200            L        = L/BETA
S012300             PRIME           K

M012400            R        = OMEGA    /OMEGA
S012500             L             ONE        L

E012600                       2
M012700            SQR      = R
S012800               L       L

M012900            R        = OMEGA    /OMEGA
S013000             T             TWO        T

E013100                    2
M013200            SQR   = R
S013300               T    T

M013400            QC=75000

M013500            QD=80000

R013600 MATRIX CONSTANTS
R013700

M013800            A00 = SQR   + SQOMEG /SQOMEG
S013900                     L          G        L

M014000            A15 = -SQR E
S014100                      L PRIME

M014200            SM   = A00, SM    = -1, SM    = A15, SM    = A15
S014300              0             20            40             60

E014400                                                                2
M014500            SM     = SM , SM     = -1, SM     = -SQR H L
S014600              160       0    180            200        L   PRIME
```

```
M007200        OMEGA       = SQRT(SQOMEG     )
S007300             TWO                   TWO

M007400        BETA     = SC    /(2 C OMEGA     )
S007500            TWO     PSI             TWO

M007600        SQOMEG     = K    /J
S007700             PSI     PSI

M007800        OMEGA       = SQRT(SQOMEG     )
S007900             PSI                   PSI

M008000        BETA        = C    /(2 J OMEGA     )
S008100            PSI        PSI            PSI

M008200        SQOMEG        = K       /I
S008300             THETA     THETA

M008400        OMEGA         = SQRT(SQOMEG       )
S008500             THETA                   THETA

M008600        BETA          = C       /(2 I OMEGA        )
S008700            THETA      THETA              THETA

E008800                           2
M008900        SQOMEG        = K   E /I
S009000             THREE       Y

M009100        OMEGA         = SQRT(SQOMEG       )
S009200             THREE                   THREE

E009300                           2
M009400        BETA          = C   E /(2 I OMEGA        )
S009500            THREE        Y                THREE

M009600        SQOMEG        = 2 SK    /J
S009700             FOUR           PSI

M009800        OMEGA         = SQRT(SQOMEG      )
S009900             FOUR                   FOUR

M010000        BETA          = C    /( J OMEGA      )
S010100            FOUR        PSI            FOUR

E010200                          2 2
M010300        SQOMEG        = K   H L /J
S010400             FIVE        Y

M010500        OMEGA         = SQRT(SQOMEG      )
S010600             FIVE                   FIVE

E010700                          2 2
M010800        BETA          = C   H L /(2 J OMEGA       )
S010900            FIVE         Y                 FIVE
```

```
M000100          COMMON(POLY551),SM
S000200                              2249

M0CC300          INDEX N,W,A,X

M000400          RESERVE POLY   ,COEF   ,Q  ,EE   ,POL   ,OMGA   ,BETA
S00C500                      15      16  16    16     16      16      16

M000600  BEGIN   READ VSTART,VINC,VMAX

M000700          READ ALPHA,B,C,E,FL,FT

M000800          READ H,I,J,KA,KG,L

M000900          READ M,MS,RO

M001000          READ C1,C2,C3,K1,K2,K3

M001100          PRINT HDG, VSTART,VINC,VMAX,SP2

M001200          V START   INCR      V END

M001300          PRINT HDG,ALPHA,B,C,E,FL,FT,SP2

M001400          ALPHA      B         C         E         FL        FT

M001500          PRINT HDG,H,I,J,KA,KG,L,SP2

M001600          H          I         J         KA        KG        L

M001700          PRINT HDG,M,MS,RO,SP2

M001800          M          MS        RO

M001900          PRINT HDG,C1,C2,C3,K1,K2,K3,SP2

M002000          C1         C2        C3        K1        K2        K3

M002100          K  = 4 K2
S002200           Y

E002300                        2
M002400          SK     = 2 K1 B
S002500            PSI

E002600                     2 2
M002700          K      = K  H L + 2 SK
S002800           PSI       Y           PSI

E002900                     2          2
M003000          K      = K  E + 4 K3 B
S003100           THETA     Y

M003200          C      = 4 C2
S003300           Y
```

```
              2
SC    = 2 C1 B
  PSI

            2 2
C     = C  H L + 2 SC
 PSI     Y           PSI

            2        2
C     = C  E + 4 C3 B
 THETA   Y

PRINT HDG,K ,SK    ,K    ,K      ,C ,SC   ,SP2
           Y   PSI  PSI   THETA   Y   PSI

K         SK        K         K         C         SC
 Y          PSI      PSI       THETA     Y          PSI

PRINT HDG,C   ,C     ,SP2
           PSI  THETA

C         C
 PSI       THETA

SQBETA  = RO L/ALPHA
      K

BETA    = SQRT(SQBETA )
    K                K

SQOMEG  = 2 FL/(MS BETA )
      L                K

OMEGA   = SQRT(SQOMEG )
     L               L

SQOMEG    = K /(2 MS)
      ONE  Y

OMEGA     = SQRT(SQOMEG    )
     ONE               ONE

BETA    = C  /(4 MS OMEGA    )
    ONE  Y               ONE

                2
SQOMEG  = 2 FT L /(C BETA )
      T                  K

OMEGA   = SQRT(SQOMEG )
     T               T

SQOMEG    = SK    /C
      TWO     PSI
```

CONTROL CARDS

The following control cards are required to invoke POLY552 from storage:

1) // JOB

This card enables job accounting and has the form:

Col 1-2:	//
Col 3-8:	job name
Col 14-16:	JOB
Col 18-21:	job charge number [to be obtained from Data Services]
Col 23-28:	User's name

The following parameters may also be inserted:

a) Region
b) Time estimate in minutes

Example JOB card

Card Column 1 b≡blank

2)//PGPOLY552bbJOB4379,SOMERS,REGION=220K,TIME=6

2) //bbbbbbbEXECbMACOMPIL

Indicates that the MAC compile-time monitor is to process a compilation.

3) //SYSINbDDb*

This card informs the Operating System that the following cards will be processed by the program being executed.

4) *bbbbbbbMAC*POLY552

Compilation Control Card

5) /*

Last card of a job step.

6) //bbbbbbbbEXECbFORTGCL

Causes compilation and linking of Fortran subroutines

7) //LKED.SYSLINbDDbDSN=MAC.MAC4TRAN,DISP=SHR
//bbbbbbbbbbDDbDSn=AAAALIN,DISP=(OLD,DELETE)

causes new linking routine to be included in the load module into which the Fortran subroutines have

8) //dddddddEXECbMACRUN

This card indicates that the MAC monitor is to process the run steps in the job.

9) //R.EXTLIBbbDDbDSN=&AAAAMOD,DISP=OLD,DELETE)
//bbbbbbbbbbDDbDSNAME=SYS1.MACEXT,DISP=SHR

Defines data set in which non-MACload modules are located at MACRUN collection time.

10) //R.FT06F001bDDbSYSOUT=A

Messages produced by the Fortran error monitor are written in the data set described on the DD card corresponding to Fortran unit 6.

11) //R.CATLGbbDDbbDSN=SYSPLOT.CATLGB,DISP=SHR

This card alerts the plotter and should be used only if a plot is desired.

12) *bbbbbbbbRUNPOLY552

Triggers POLY552 from storage and transfers control to it.

This card is followed by the data cards.

INPUT

The input parameters, which are outlined below, are projected into the deck in the order indicated. The comma-delimited format is utilized; this format dispenses with the need of parameter definition by separate format statements, but does require the parameters to be separated from one another on a data card by commas. No comma should follow the last parameter on a data card. Parameters may be punched on any of the 80 columns.

FIRST DATA CARD [3 Parameters]

Order of Parameter	Name	Description	Units
1st	VSTART	Initial Velocity	ft/sec
2nd	VINC	Incremental Value of Velocity	ft/sec
3rd	VMAX	Final Velocity	ft/sec

SECOND DATA CARD [6 Parameters]

Order of Parameter	Name	Description	Units
1st	ALPHA	Effective conicity of a wheel, of a wheel-set in question	ft/ft
2nd	B	Half length of contact area in direction transverse to the direction of rolling	ft

3rd	C	Moment of Inertial of a wheel-set in yaw	slug ft^2
4th	E	Height of body centre of gravity above wheel-set axle center-line	ft
5th	FL	Longitudinal creep ccefficient	lbs
6th	FT	Transverse creep coefficient	lbs

THIRD DATA CARD [6 Parameters]

Order of Parameter	Name	Description	Units
1st	H	Constant which when multiplied by "L" gives "HL", the semi-wheel base	-
2nd	I	Moment of Inertia of body in roll	slug ft^2
3rd	J	Moment of Inertia of body in yaw	slug ft^2
4th	KA		ft-lbs/rad
5th	KG		lbs/ft
6th	L	Half-distance between contact points in a lateral direction	ft

FOURTH DATA CARD [3 Parameters]

Order of Parameter	Name	Description	Units
1st	M	Mass of body	slugs
2nd	MS	Mass of wheel-set	slugs
3rd	RO	Wheel-tread circle radius, wheel-set in central position	ft

FIFTH DATA CARD [6 Parameters]

Order of Parameter	Name	Description	Units
1st	C1	Longitudinal suspension damping coefficient	lbs/fps
2nd	C2	Lateral suspension damping coefficient	lbs/fps
3rd	C3	Vertical suspension damping coefficient	lbs/fps
4th	K1	Longitudinal suspension stiffness	lbs/ft
5th	K2	Lateral suspension stiffness	lbs/ft
6th	K3	Vertical suspension stiffness	lbs/ft

The significance of the various parameters and their diagrammatic representation is given in the Appendix.

DECK STRUCTURE

```
//JOB
// EXEC MACOMPIL
// SYSIN DD*

  POLY552
MAC PROGRAM

/*
// EXEC FORTGCL
// FORT. SYSIN DD*

  FMAC
FORTRAN SUBROUTINE

/*
// LKED.SYSLIN DD DSN=MAC.MAC4 TRAN, DISP=SHR
//            DD DSN=&AAAALIN, DISP = (OLD, DELETE)
//RUN   EXEC MACRUN
//R.EXTLIB DD DSN=&AAAAMOD, DISP=(OLD,DELETE)
            DD DSNAME=SYS1. MACEXT, DISP=SHR
//R.FT06F001 DD SYSOUT = A
//R.CATLG DD DSN=SYSPLOT.CATLGB,DISP=SHR
//SYSIN DD*
* RUN POLY 552

  DATA
```

Sample Data

```
Card   Col 1    Col 9
                  5, 20, 220
                  0.4, 3,25, 360, 4, 3E6, 3E6
                  2, 4E3, 12E3, 1787, 949E2, 2.5
                  4E2, 90, 1.75
                  0.0, 0.0, 0.0, 5E3, 5E3, 5E4
```

PLOTTING

The Plot Control Card should be used if a plot is required; otherwise remove this card.

POLY552 will provide 2 framed "7.5 x 9" plots for

1) System Frequency (on the ordinate axis) against velocity.

2) Damping Constant (on the ordinate axis) against velocity.

Points are marked by small dots.

The program in its present form will only provide for plot values of velocity in ft/sec from 0 to 220 against corresponding values of frequency in hertz from 0 to 12, and Damping Constant from -0.10 to +0.10.

For the sample data, the following plots were produced.

OUTPUT

For each velocity value POLY552 will supply system frequencies and corresponding damping ratios.

The two identical sets of values observed is due to the fact that complex roots of the system, on which computation is performed, occur in pairs.

For the sample data, the following is the output. Only one data set, of the identical two, is listed.

A later modification will be to remove the second set of identical values from the print format

Appendix

This computer simulation model is based upon seven sets of second-order differential equations. From the definition of the externally-applied forces and moments Equations 1-4 defined below and the use of Figure 1 showing the vehicle geometry, the seven equations of motions of the vehicles Equations 5-11 can be written.

Externally-applied forces and moments

$$Q_1 = -2f_L\ (\dot{y}_1/V - \psi_1) - k_g\ (y_1 - \delta_1) \tag{1}$$

$$Q_2 = -2f_T\ [\frac{\alpha\ell}{r_o}\ (y_1 - \delta_1) + \frac{\ell^2}{V}\dot{\psi}_1] + k_a\ \psi_1 \tag{2}$$

$$Q_6 = -2f_L\ (\dot{y}_2/V - \psi_2) - k_g\ (y_2 - \delta_2) \tag{3}$$

$$Q_7 = -2f_T\ [\frac{\alpha\ell}{r_o}\ (y_2 - \delta_2) + \frac{\ell^2}{V}\psi_2] + k_a\ \psi_2 \tag{4}$$

lateral motion, fwd wheelset:

$$m\ddot{y}_1 + \frac{C_Y}{2}\ (\dot{y}_1 - \dot{y}_a - h\ell\ \dot{\psi}_a - e\dot{\Theta}) + \frac{K_Y}{2}\ (y_1 - y_a - h\ell\ \psi_a - e\Theta)$$
$$+ 2f_L\ (y_1/V - \psi_1) + k_g\ y_1 = k_g\ \delta_1 \tag{5}$$

yaw motion, fwd wheelset:

$$C\ddot{\psi}_1 + c\psi\ (\dot{\psi}_1 - \dot{\psi}_a) + k_\psi\ (\psi_1 - \psi_a) + 2f_T\left(\frac{\alpha\ell}{r_o}\ y_1 + \frac{\ell^2}{V}\ \dot{\psi}_1\right)$$
$$- k_a\ \psi_1 = 2f_T\ \frac{\alpha\ell}{r_o}\ \delta_1 \tag{6}$$

body lateral motion:

$$M\ddot{y}_a + \frac{C_Y}{2}\ (2\dot{y}_a - \dot{y}_1 - \dot{y}_2 + 2e\dot{\Theta}) + \frac{K_Y}{2}\ (2y_a - y_1 - y_2 + 2e\Theta = 0 \tag{7}$$

body yaw motion:

$$J\ddot{\psi}_a + C_\psi \dot{\psi}_a - c_\psi (\dot{\psi}_1 + \dot{\psi}_2) - \frac{C_y}{2} h\ell (\dot{y}_1 - \dot{y}_2)$$
$$+ K_\psi \psi_a - k_\psi (\psi_1 + \psi_2) - \frac{K_y}{2} h\ell (y_1 - y_2) = 0 \tag{8}$$

body roll motion:

$$I\ddot{\theta} + C_\theta \dot{\theta} + K_\theta \theta - \frac{C_y}{2} e (\dot{y}_1 + \dot{y}_2 - 2\dot{y}_a) - \frac{K_y}{2} e (y_1 - y_2 - 2y_a) = 0 \tag{9}$$

lateral motion, aft wheelset:

$$m\ddot{y}_2 + \frac{C_y}{2} (\dot{y}_2 - \dot{y}_a + h\ell \dot{\psi}_a - e\dot{\theta}) + \frac{K_y}{2} (y_2 - y_a + h\ell \psi_a - e\theta)$$
$$+ 2f_L (\dot{y}_2/V + \psi_2) + k_g y_2 = k_g \delta_2 \tag{10}$$

yaw motion, aft wheelset:

$$C\ddot{\psi}_2 + c_\psi (\dot{\psi}_2 - \dot{\psi}_a) + k_\psi (\psi_2 - \psi_a) + 2f_T \left(\frac{\alpha\ell}{r_o} y_2 + \frac{\ell^2}{V} \dot{\psi}_2 \right)$$
$$- k_a \psi_2 = 2f_T \frac{\alpha\ell}{r_o} \delta_2 \tag{11}$$

where

$$C_\psi = C_y h^2 \ell^2 + 2 c_\psi$$
$$K_\psi = K_y h^2 \ell^2 + 2 k_\psi$$
$$C_\theta = C_\theta' + C_y e^2$$
$$K_\theta = K_\theta' + K_y e^2$$

The seven equations of motion are transformed (non-dimensionalized in time and amplitude) by the following substitutions

$$\beta_K^2 = \frac{v_o \ell}{\alpha} \ , \ \omega_K = \frac{V}{\beta_K} \ , \ \tau \ \omega_K \ t \tag{12}$$

$$\omega_L^2 = \frac{2f_L}{m\beta_K} \ , \ \omega_T^2 = \frac{2f_T \ell^2}{C\beta_K} \tag{13}$$

$$\omega_1^2 = \frac{K_y}{2m}, \ \beta_1 = \frac{C_y}{4m\omega_1} \tag{14}$$

$$\omega_2^2 = \frac{k_\psi}{C} \ , \ \beta_2 = \frac{c_\psi}{2C\omega_2} \tag{15}$$

$$\omega_3^2 = \frac{K_y e^2}{I} \ , \ \beta_3 = \frac{C_y e^2}{2I\omega_3} \tag{16}$$

$$\omega_4^2 = \frac{2k_\psi}{J} \ , \ \beta_4 = \frac{c_\psi}{J\omega_4} \tag{17}$$

$$\omega_5^2 = \frac{K_y h^2 \ell^2}{J} \ , \ \beta 5 = \frac{C_y h^2 \ell^2}{2J\omega 5} \tag{18}$$

$$\omega_\psi^2 = \frac{K_\psi}{J} \ , \ \beta_\psi = \frac{C_\psi}{2J\omega_\psi} \tag{19}$$

$$\omega_\Theta^2 = \frac{K_\Theta}{I} \ , \ \beta_\Theta = \frac{C_\Theta}{2I\omega_\Theta} \tag{20}$$

$$\omega_y^2 = \frac{K_y}{M} \ , \ \beta_y = \frac{C_y}{2M\omega_y} \tag{21}$$

$$\omega_g^2 = \frac{k_g}{m} \ , \ \omega_a^2 = \frac{k_a}{C} \tag{22}$$

$$e^1 = \frac{e}{\beta_K} \ , \ \ell' = \frac{\ell}{\beta_K} \ , \ \gamma_a = \frac{y_a}{\beta_K} \tag{23}$$

$$\bar{\gamma} = \frac{y_1 + y_2}{2\beta_K} \ , \ \gamma_\Delta = \frac{y_1 - y_2}{2\beta_K} \tag{24}$$

$$R_L^2 = \frac{\omega_1^2}{\omega_L^2} = \frac{K_y \ \beta_K}{4f_L} \tag{25}$$

$$R_T^2 = \frac{\omega_2^2}{\omega_T^2} = \left(\frac{\beta_K}{\ell}\right)^2 \left(\frac{k_\psi}{2f_T \ \beta_K}\right) \tag{26}$$

$$\bar{\psi} = \frac{\psi_1 - \psi_2}{2} \ , \ \psi_\Delta = \frac{\psi_1 - \psi_2}{2} \tag{27}$$

$$\bar{\delta}_1 = \delta_1, \ \bar{\delta}_2 = \delta_2 \tag{28}$$

$$\psi_a = \psi_a, \ \Theta = \Theta \tag{29}$$

using the above substitutions, the final set of equations become:

$$\frac{\omega_K^2}{\omega_L^2} \ \ddot{\bar{\gamma}} + [1 + 2\beta_1 \ R_L \frac{\omega_K}{\omega_L}] \ \dot{\bar{\gamma}} + \left(R_L^2 + (\frac{\omega_g}{\omega_L})^2 \right) \bar{\gamma}$$

$$- R_L^2 \ (\gamma_a + e' \ \Theta) - 2\beta_1 \ R_L \frac{\omega_K}{\omega_L} \ (\dot{\gamma}_a + e' \ \dot{\Theta}) \tag{30}$$

$$- \bar{\psi} = \frac{\omega_g^2}{\omega_L^2} \ \frac{\bar{\delta}_1 + \bar{\delta}_2}{2 \ \beta_K}$$

$$\frac{\omega_K^2}{\omega_L^2} \ \ddot{\gamma}_\Delta + [1 + 2\beta_1 \ R_L \frac{\omega_K}{\omega_L}] \ \dot{\gamma}_\Delta + \left(R_L^2 + (\frac{\omega_g}{\omega_L})^2 \right) \gamma_\Delta$$

$$- \psi_\Delta - R_L^2 \ h \ \ell' \ \psi_a - 2 \ \beta_1 \ R_L \frac{\omega_K}{\omega_L} \ h \ \ell' \ \dot{\psi}_a = \tag{31}$$

$$\frac{\omega_g^2}{\omega_L^2} \left(\frac{\bar{\delta}_1 - \bar{\delta}_2}{2 \ \beta_K} \right)$$

$$\frac{\omega_K^2}{\omega_T^2} \ddot{\bar{\psi}} + [1 + 2\ \beta_2\ R_T \frac{\omega_K}{\omega_T}]\ \dot{\bar{\psi}} + \left(R_T^2 - \frac{\omega_a^2}{\omega_T^2} \right) \bar{\psi}$$

$$= 2\ \beta_2\ R_T \frac{\omega_K}{\omega_T}\ \dot{\psi}_a - R_T^2\ \psi_a + \bar{r} = \frac{\bar{\delta}_1 + \bar{\delta}_2}{2\ \beta_K} \qquad (32)$$

$$\frac{\omega_K^2}{\omega_T^2} \ddot{\psi}_\Delta + [1 + 2\ \beta_2\ R_T \frac{\omega_K}{\omega_T}]\ \dot{\psi}_\Delta + \left(R_T^2 - \frac{\omega_a^2}{\omega_T^2} \right) \psi_\Delta + r_\Delta =$$

$$\frac{\bar{\delta}_1 - \bar{\delta}_2}{2\ \beta_K} \qquad (33)$$

$$\frac{\omega_K^2}{\omega_y^2} \ddot{r}_a + 2\ \beta_y \frac{\omega_K}{\omega_y}\ \dot{r}_a + r_a - (\bar{r} - e'\ \Theta)$$

$$- 2\ \beta_y \frac{\omega_K}{\omega_y}\ (\dot{\bar{r}} - e'\ \dot{\Theta}) = 0 \qquad (34)$$

$$\frac{\omega_K^2}{\omega_\psi^2} \ddot{\psi}_a + 2\ \beta_{\psi_a} \frac{\omega_K}{\omega_\psi}\ \dot{\psi}_a + \psi_a - \frac{\omega_4^2}{\omega_\psi^2} \bar{\psi} - 2\ \beta_4 \frac{\omega_K}{\omega_\psi} \left(\frac{\omega_4}{\omega_\psi}\right) \dot{\bar{\psi}}$$

$$- \frac{\omega_5^2}{\omega_\psi^2} \left(\frac{r_\Delta}{h\ell'}\right) - 2\ \beta_5 \left(\frac{\omega_r}{\omega_\psi}\right) \left(\frac{\omega_K}{\omega_\psi}\right) \left(\frac{\dot{r}_\Delta}{h\ell'}\right) = 0 \qquad (35)$$

$$\frac{\omega_K^2}{\omega_\Theta^2}\ddot{\Theta} + 2\ \beta_\Theta \frac{\omega_K}{\omega_\Theta}\dot{\Theta} + \Theta - \frac{\omega_3^2}{\omega_\Theta^2}\left(\frac{\bar{r}}{e'}\right) - 2\ \rho_3 \left(\frac{\omega_3}{\omega_\Theta}\right)\left(\frac{\omega_K}{\omega_\Theta}\right)\left(\frac{\dot{\bar{r}}}{e'}\right)$$

$$+ \frac{\omega_3^2}{\omega_\Theta^2}\left(\frac{r_a}{e'}\right) + 2\ \beta_3 \left(\frac{\omega_3}{\omega_2}\right)\left(\frac{\omega_K}{\omega_\Theta}\right)\frac{\dot{r}_a}{e'} = 0 \qquad (36)$$

where the dot represents differentiation with respect to dimensionless time (τ).

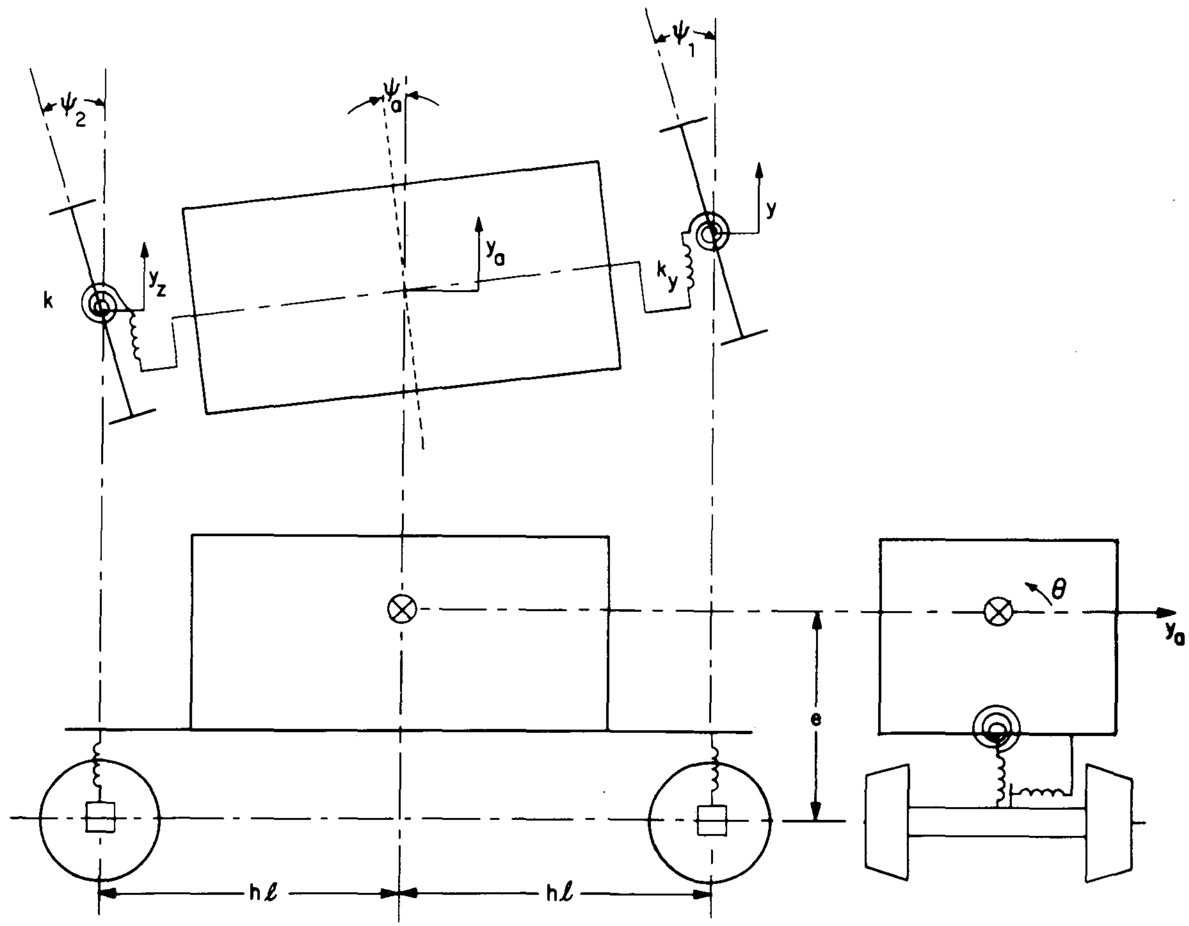

Figure A-1. Lateral Dynamics Model for Two Axled Vehicle

APPENDIX B

COMPUTER PROGRAM TO PREDICT TRACK DEFLECTION DUE TO RESPONSE OF RAIL VEHICLES TO VERTICAL TRACK IRREGULARITIES

"HALF CAR MODEL"

Prepared by

B. Mackenzie

Service Technology Corp.

PURPOSE

The program computes the response of the dynamic model shown in Figure 1, consisting of a table of values of ten functions. It then plots the magnitude of each function against frequency.

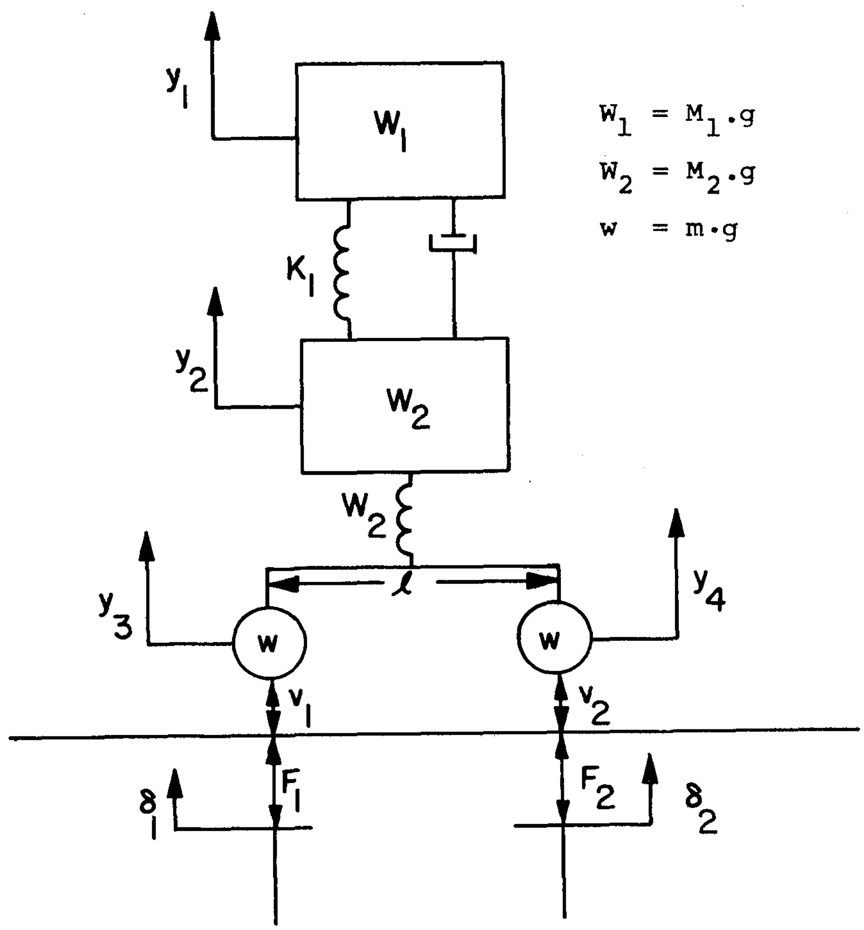

Figure B-1. The Half Car Model

EQUATIONS

The following system of equations was solved for F_1/v_1, F_2/v_1, y_1/v_1, y_2/v_1, y_3/v_1, y_4/v_1, δ_1/v_1, and δ_2/v_1, as functions of frequency. Refer to Figure 1.

1. $y_3 = v_1 + \delta_1$

2. $y_4 = v_2 + \delta_2$

3. $\delta_1 = G_{11}F_1 + G_{12}F_2$

4. $\delta_2 = G_{11}F_2 + G_{12}F_1$

5. $F_1 = m\ddot{y}_4 = F_2 - m\ddot{y}_3$

6. $$\frac{y_1}{y_2} = \frac{1 + 2j\beta \dfrac{\omega}{\omega_1}}{\left(1 - \left(\dfrac{\omega}{\omega_1}\right)^2\right) + 2j\beta \dfrac{\omega}{\omega_1}}$$

7. $F_1 + F_2 = m\left(\ddot{y}_3 + \ddot{y}_4\right) + M_2 \ddot{y}_2 + M_1\ddot{y}_1$

8. $K_2 \left(y_2 - \dfrac{y_3 + y_4}{2}\right) + M_2\ddot{y}_2 + M_1\ddot{y}_1 = 0$

where

$$v_1 = v_o \sin \frac{2\pi x}{\lambda}, \quad v_2 = v_o \sin 2\pi \left(\frac{\lambda+\ell}{\lambda}\right)$$

$$\ddot{y}_i = -\omega^2 y_i \,, \quad i = 1, 2, 3, 4,$$

$$x = Vt$$

$$\omega = \frac{2\pi V}{\lambda}, \quad f = \frac{V}{\lambda} = \frac{\omega}{2\pi}$$

The functions G_{11} and G_{12} are the dynamic compliance coefficients of a beam on a visco-elastic foundation and are given by:

let

$$\omega_a = \sqrt{\frac{kg}{W}} \quad \text{, then for } \omega < \omega_a$$

$$G_{11} = \frac{\pi}{k\, \lambda_o \left(1 - \frac{\omega^2}{\omega_a^2}\right)^{3/4}} \qquad \text{where} \quad \lambda_o = 2\pi \sqrt[4]{\frac{4Er}{k}}$$

and

$$G_{12} = G_{11}\, e^{-\frac{2\pi\ell}{\lambda_1}} \left(\sin \frac{2\pi\ell}{\lambda_1} + \cos \frac{2\pi\ell}{\lambda_1}\right)$$

$$\text{where} \quad \lambda_1 = \frac{\lambda_o}{\left(1 - \frac{\omega^2}{\omega_a^2}\right)^{1/4}}$$

for $\omega > \omega_a$

$$G_{11} = \frac{-\pi(1 + j)}{\sqrt{2}\, k\, \lambda_o \left(\frac{\omega^2}{\omega_a^2} - 1\right)^{3/4}}$$

and

$$G_{12} = \frac{-\pi\left(e^{-\sqrt{2}\,\beta_1 \ell} + je^{-j\sqrt{2}\,\beta_1 \ell}\right)}{\sqrt{2}\, k\, \lambda_o \left(\frac{\omega^2}{\omega_a^2} - 1\right)^{3/4}}$$

$$\text{where} \quad \beta = \frac{2\pi}{\lambda_o}\left(\frac{\omega^2}{\omega_a^2} - 1\right)^{1/4}$$

INPUT

The program calculations are in units of inches, pounds and seconds. The input variables are given below.

Card	Variable	Units of Input	Format
1	k	lb/in^2	F10.2
2	K_1	lb/in	F10.2
3	K_2	lb/in	F10.2
4	W_1	lb	F10.2
5	W_2	lb	F10.2
6	w	lb	F10.2
7	W	lb/yd	F10.2
8	I	in^4	F10.2
9	E	lb/in^2	E10.7
10	λ	in	F10.2, 1 in col 15
	V	in/sec	F10.2, 2 in col 15
11	l	in	F10.2
12	β	-	F10.2

Either λ or V can be an input variable and the other value is then calculated. This requires a code number in column 15 of the data card. For λ input the code is 1, for V the code is 2.

The values of w, W_1, W_2 are read in units of pounds; conversion to mass units is done in the program. The program also converts W from lb/yd to lb/in.

Information about the desired frequency range must also be read in. The program can accept up to 5 consecutive intervals of frequencies with a different increment in each interval. To do this the following cards are read:

Card	Description	Format
13	Number of intervals	I2
14	Increments for each of the intervals (in order)	5F10.4
15	Boundaries of the intervals	6F10.4

Figure 2 shows a sample list of data cards. The last three cards give a frequency range that goes from 0.1 to 1.0 in increments of 0.1, from 1.0 to 2.0 in increments of 0.2, from 2.0 to 5.0 in increments of 0.5, from 5.0 to 10.0 in increments of 1.0, and from 10.0 to 100.0 in increments of 10.0.

The table of frequencies can contain a maximum of 100 values.

```
$DATA
   1500.0k'
  14193.00
  39856.00
  18600.00
   7000.00
   1000.00
    119.00
    312.5
 .3000E+08
   1760.00     2
     82.00
       .10
05
        .1       0.2       0.5       1.0      10.0
        .1       1.0       2.0       5.0      10.0      100.0
```

Figure 2

OUTPUT

A list of input variables precedes the tables of functional values. The values printed are converted values, i.e., M_1, M_2, and m are in mass units, W is in lb/in. The printed value of each of the other variables is the same as the value read in.

Two computed constants β_o and k* are also printed out:

$$\beta_o = \sqrt[4]{\frac{k}{4EI}} \text{ and } k^* = \frac{2k}{\beta_o}$$

The values of the ten functions (G_{11} and G_{12} are printed and plotted along with the eight functions solved for in equations (1) - (8)) are printed out in magnitude-phase form. The magnitudes are in exponential format; the phases are in floating-point format.

All functions except G_{11} and G_{12} are normalized by v_1. This normalization leaves the output for y_i (i=1,2,3,4), δ_1 and δ_2 unitless. F_1/v_1 and F_2/v_1 have units of lb/in; G_{11} and G_{12} are in in/lb.

OPERATING INSTRUCTIONS

This program is written in FORTRAN for the IBM 7094 computer. The deck is set up to run on the DOT/TSC computer.

SAMPLE OUTPUT

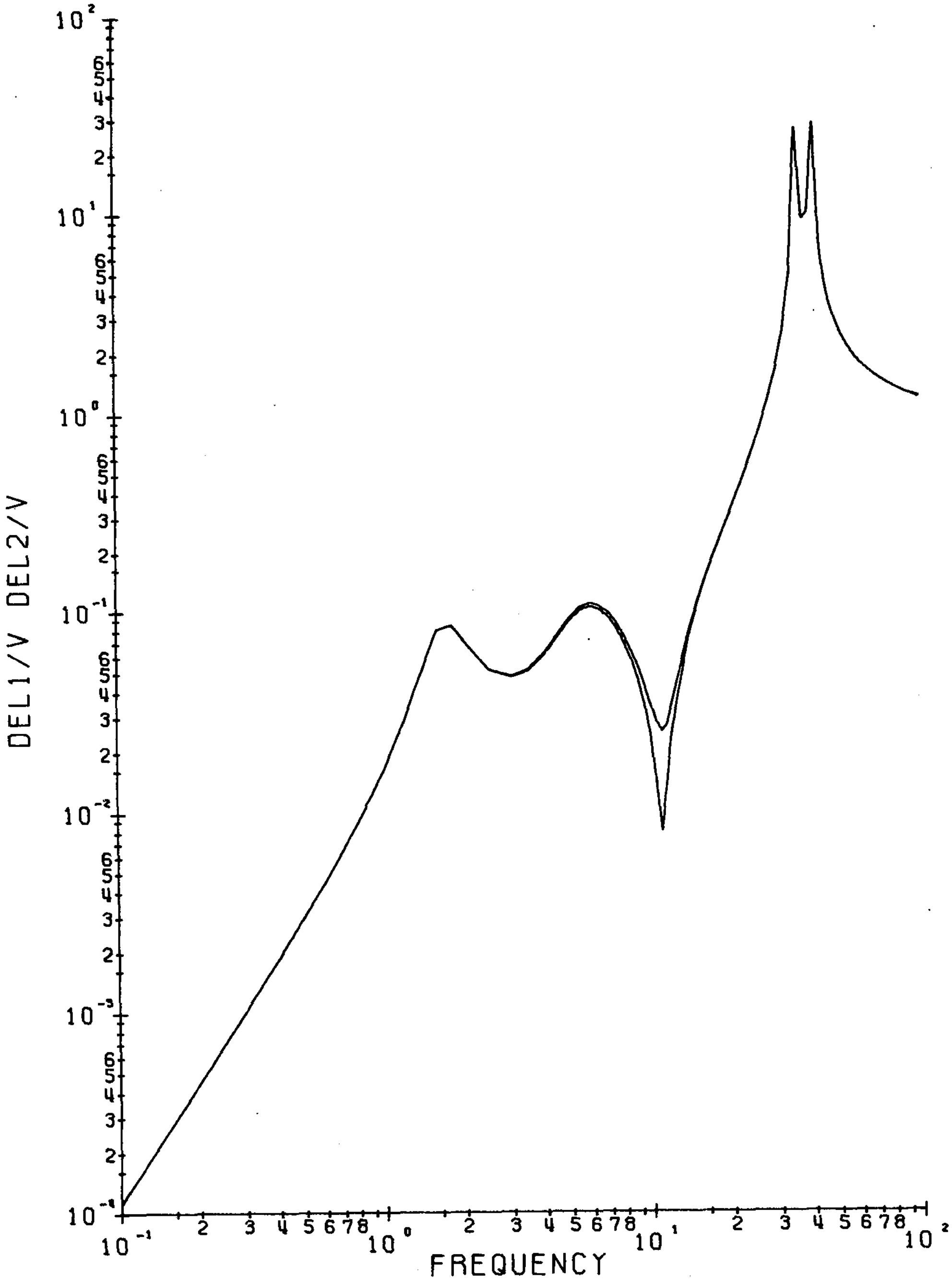

Figure B-2. Track Deflection Amplitude Ratio

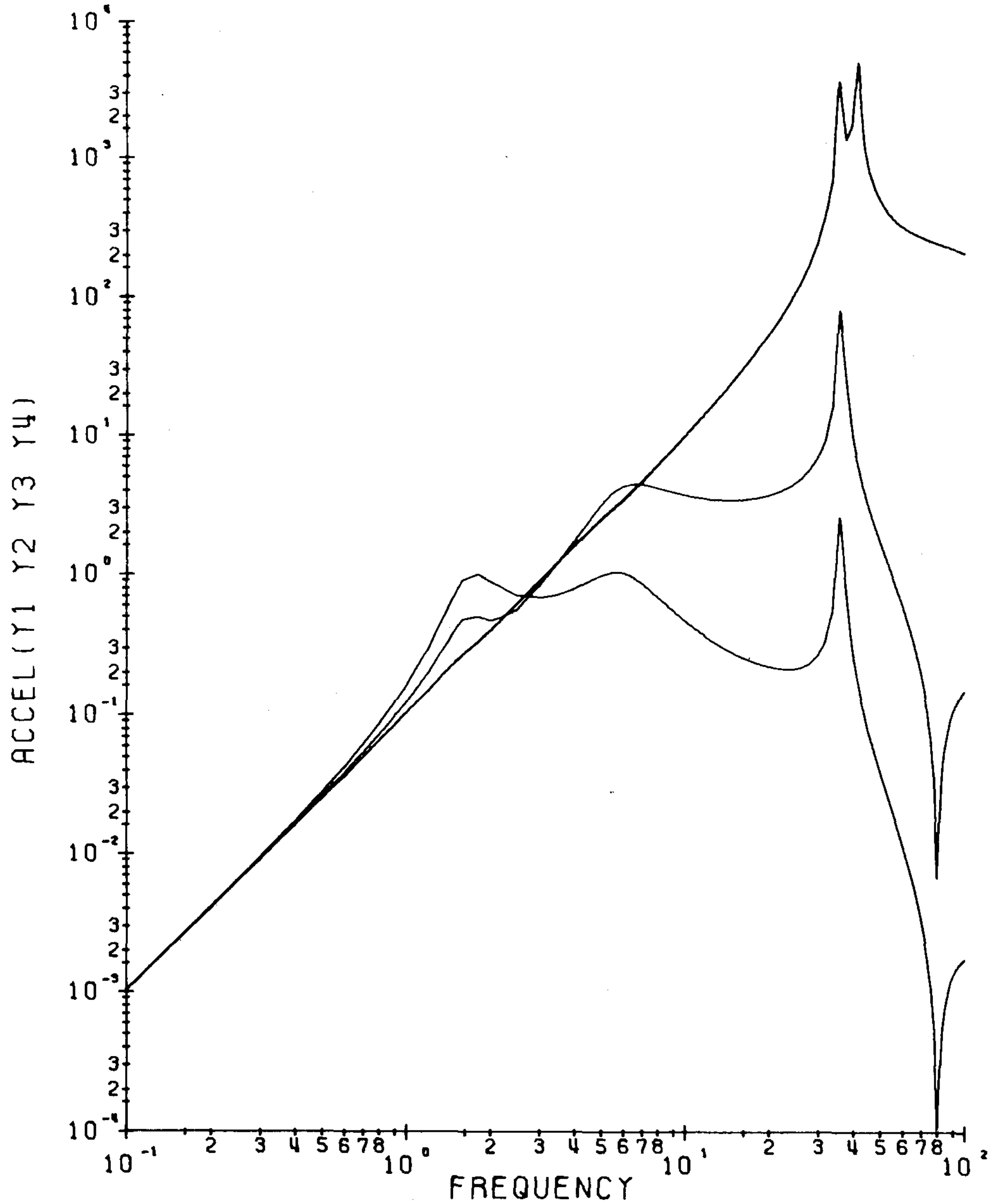

Figure B-3. Car Body and Truck Accelerations Due to 1-Inch Amplitude Track Irregularity

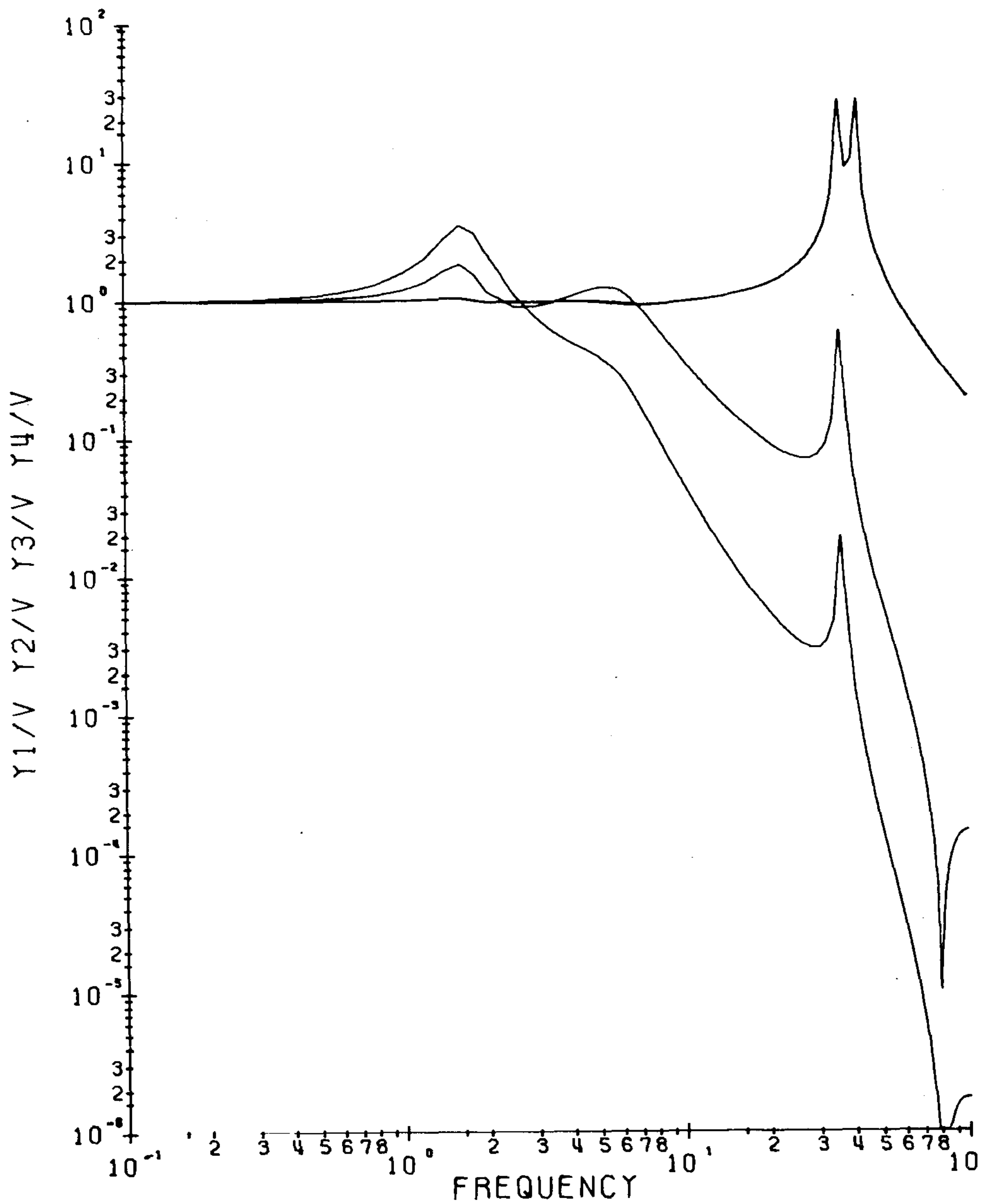

Figure B-4. Car Body and Truck Displacement Amplitude Ratio

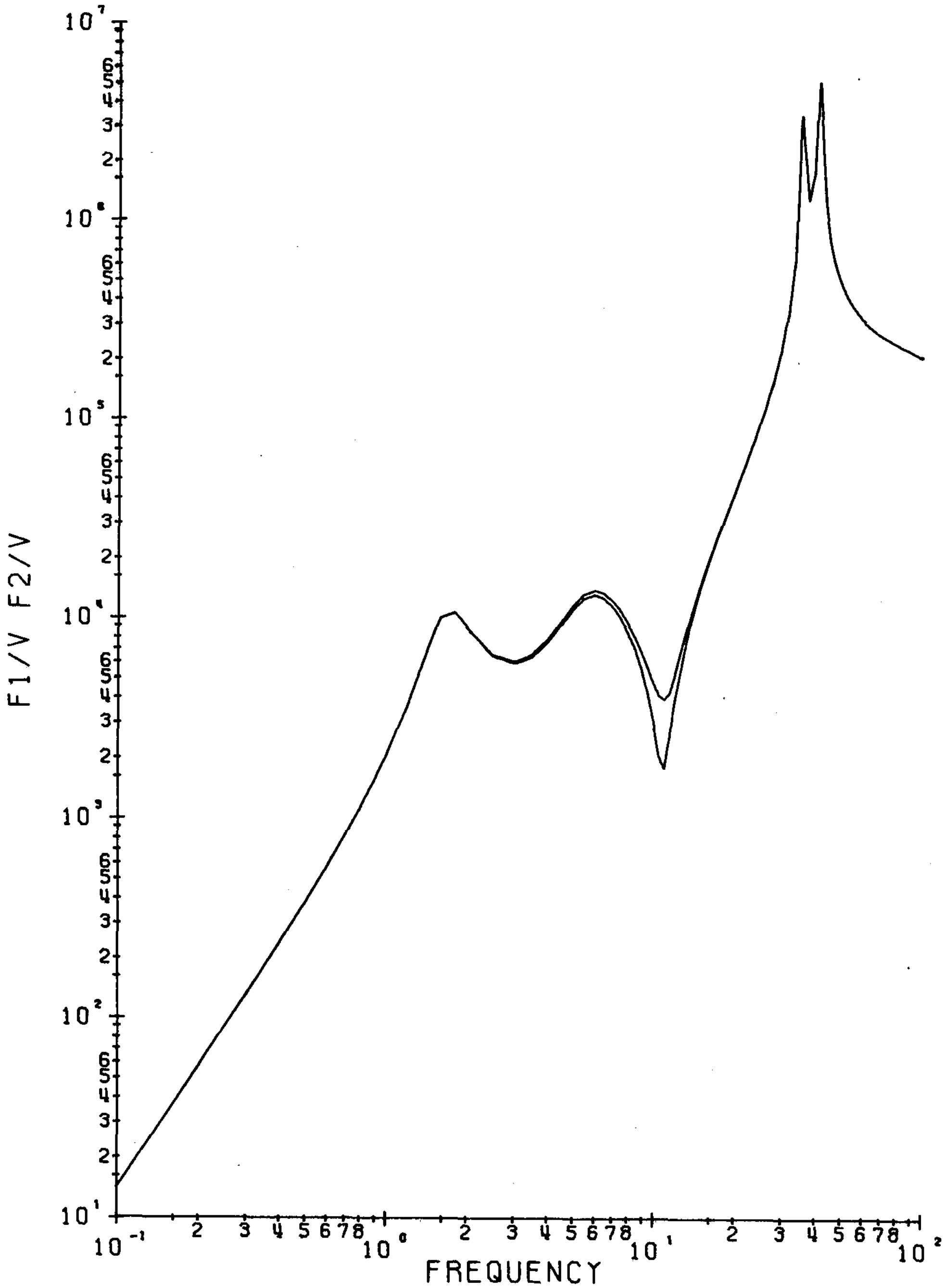

Figure B-5. Wheel Rail Forces Produced by Unit Track Irregularity (lb/in)

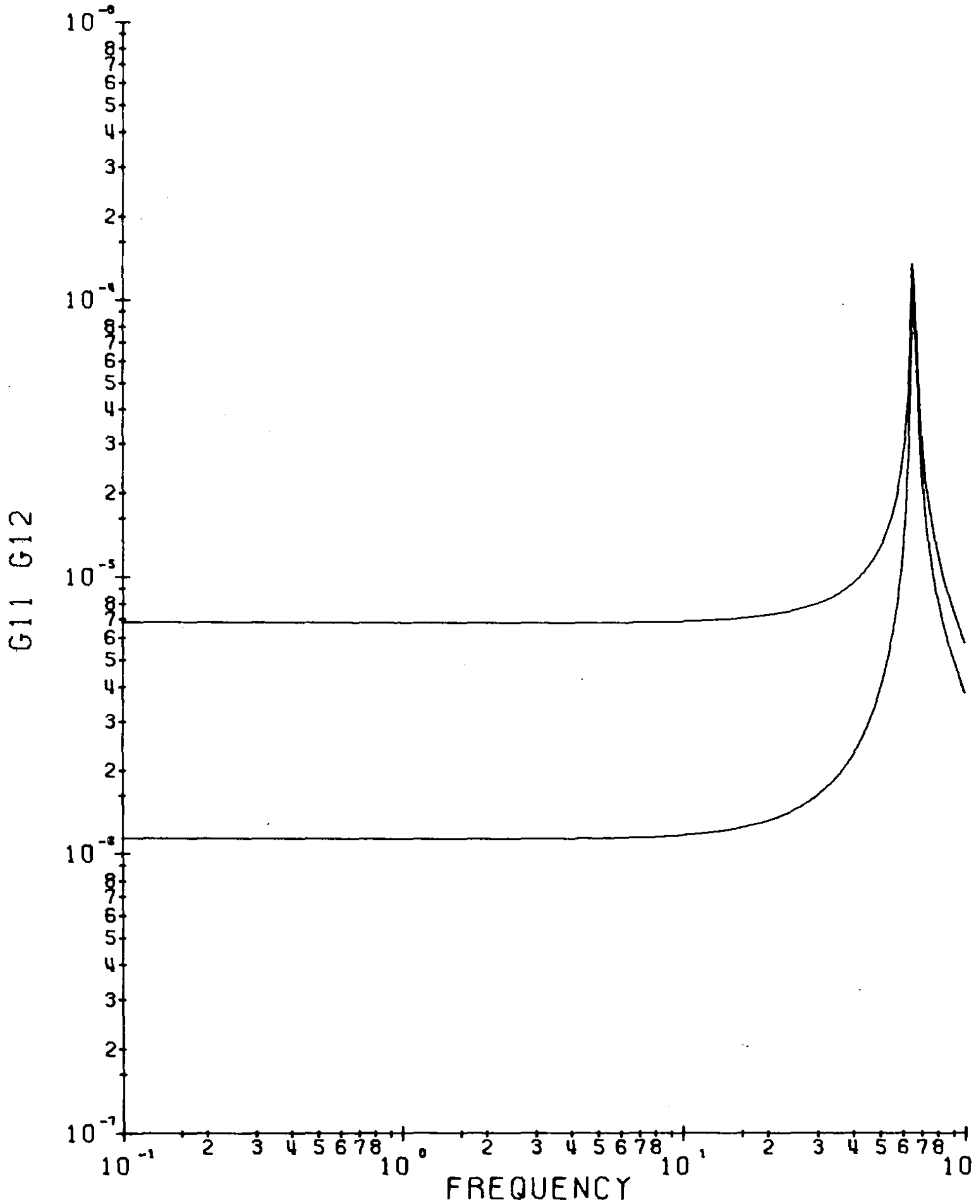

Figure B-6. Track Compliance Function

PROGRAM LISTING

```
      DIMENSION IBUF(1024)
      CALL PLOTS(IBUF,1024)                                          2
      CALL PLOT(0.,-11.,-3)                                          4
      CALL PLOT(0.,.5,-3)                                            6
      COMPLEX GA,GB,GC,GD
      DIMENSION ACCY1(100),ACCY2(100),ACCY3(100),ACCY4(100)
      DIMENSION AF1(100),TF1(100),AF2(100),TF2(100)
      DIMENSION ADEL1(100),TDEL1(100),ADEL2(100),TDEL2(100)
      DIMENSION AY1(100),TY1(100),AY2(100),TY2(100)
      DIMENSION AY3(100),TY3(100),AY4(100),TY4(100)
      DIMENSION AG1(100),TG1(100),AG2(100),TG2(100)
      COMPLEX F1(100),F2(100),DEL1(100),DEL2(100)
      COMPLEX Y1(100),Y2(100),Y3(100),Y4(100)
      COMPLEX B1,B2,B3,B6,B7
      COMPLEX A1,A2,A3,A4
      COMPLEX A5
      COMPLEX G1(100),G2(100)
      DIMENSION DF(5)
      DIMENSION FL(6)
      DIMENSION F(100)
      COMPLEX BL1,BL2,BL3,BL4,BL5
      G=386.
      PI=3.14159265
      EPSW=.01
C    READ INPUT VARIABLES
      READ (5,9) XK                                                  8
      READ (5,9) XK1                                                 9
      READ (5,9) XK2                                                10
      READ (5,9) XM1                                                11
      READ (5,9) XM2                                                12
      READ (5,9) XM                                                 13
      READ (5,9) WT                                                 14
      READ (5,9) XI                                                 15
      READ (5,7) E                                                  16
      READ (5,11) XX,JA                                             17
      READ (5,9) XL                                                 19
      READ (5,9) BET                                                20
      READ (5,9) ZETA                                               21
    7 FORMAT (E10.7)
    9 FORMAT (F10.2)
   11 FORMAT (F10.2,4X,I1)
C   CONVERSIONS AND COMPUTEDCONSTANTS
      XM1=XM1/386.
      XM2=XM2/386.
      XM=XM/386.
      WT=WT/36.
      WA=SQRT(XK*G/WT)                                              22
      XLAMN=2.*PI*(4.*E*XI/XK)**.25                                 23
      W1=SQRT(XK1/XM1)                                              24
      XLL=XL
      RT2=SQRT(2.)
C     WRITE INPUT VARIABLES                                         25
      WRITE (6,10)                                                  26
   10 FORMAT (1H0,15HINPUT VARIABLES)
      WRITE (6,12) XK                                               27
```

```
 12 FORMAT (1H0,5X,4HK = ,E15.8)
    WRITE (6,13) XK1                                   28
 13 FORMAT (1H0,4X,5HK1 = ,E15.8)
    WRITE (6,14) XK2                                   29
 14 FORMAT (1H0,4X,5HK2 = ,E15.8)
    WRITE (6,15) XM1                                   30
 15 FORMAT (1H0,4X,5HM1 = ,E15.8)
    WRITE (6,16) XM2                                   31
 16 FORMAT (1H0,4X,5HM2 = ,E15.8)
    WRITE (6,17) XM                                    32
 17 FORMAT (1H0,5X,4HM = ,E15.8)
    WRITE (6,18) WT                                    33
 18 FORMAT (1H0,5X,4HW = ,E15.8)
    WRITE (6,22) E                                     34
 22 FORMAT (1H0 5X,4HE = ,E15.8)
    WRITE (6,23) XI                                    35
 23 FORMAT (1H0,5X,4HI = ,E15.8)
    WRITE (6,24) BET                                   36
 24 FORMAT (1H0,2X,7HBETA = ,E15.8)
    WRITE(6,122) ZETA                                  37
122 FORMAT(1H0,2X,7HZETA = ,E15.8)
    WRITE (6,27) XL                                    38
 27 FORMAT (1H0,5X,4HL = ,E15.8)
    IF(JA.EQ.1) GO TO 31
    IF(JA.EQ.2) GO TO 32
    IF((JA.NE.1).AND.(JA.NE.2))GO TO 6
 32 WRITE (6,21) XX                                    48
 21 FORMAT (1H0,5X,4HV = ,E15.8)
    GO TO 34
 31 WRITE (6,19) XX                                    50
 19 FORMAT (1H0,9HLAMBDA = ,E15.8)
    GO TO 34
  6 WRITE (6,8)                                        52
  8 FORMAT (2X,32HERROR ON V/LAMBDA IDENTIFICATION)
 34 CONTINUE
C   GENERATE FREQUENCY TABLE
    READ(5,20) NDF                                     53
 20 FORMAT (I2)
    READ (5,30) (DF(I1),I1=1,NDF)                      55
 30 FORMAT (5F10.4)
    NFL=NDF+1
    READ (5,40) (FL(L),L=1,NFL)                        62
 40 FORMAT (6F10.4)
    L=0
    N=0
    DO 50 I1=1,NDF
    N1=1
    L=L+1
 70 N=N+1
    XF1=N1-1
    XFN=FL(L)+XF1*DF(I1)
    XF2=XFN-FL(L+1)
    XF2=ABS(XF2)
    IF(XF2.GT..002)GO TO 60
    GO TC 49
 60 F(N)=XFN
```

```
      N1=N1+1
      GO TO 70
   49 N=N-1
   50 CONTINUE
      N=N+1
      F(N)=FL(NFL)
      NF=N
C     DO LOOP TO COMPUTE FUNCTIONAL VALUES
      DO 80 I=1,NF
      IF(JA.EQ.1)XLAM=XX
      IF(JA.EQ.2)XLAM=XX/F(I)
    5 V=XLAM*F(I)
      W=2.*PI*F(I)
      WW=W-WA
      AWW=ABS(WW)
      IF (AWW.LT.EPSW) GO TO 25
      IF(WW.GT.0.0) GO TO 3
      GO TO 2
   25 WRITE (6,26)                                          113
   26 FORMAT(3X,5HERROR,5X,4HW=WA)
C COMPUTE G11 AND G12 FOR W LESS THAN WA
    2 WB=W/WA
      DA=(1.-WB**2)
      DB=2.*ZETA*WB
      PHI=DB/DA
      PHI=ATAN(PHI)                                         115
      DC=(DA**2+DB**2)**.125                                116
      BETA1=2.*PI*DC/XLAMN
      ZA=PI/(XK*XLAMN*DC**3)
      ZB=COS(3.*PHI/4.)                                     117
      ZB=ZB*ZA
      ZC=SIN(3.*PHI/4.)                                     118
      ZC=(-1.)*ZC*ZA
      G1(I)=CMPLX(ZB,ZC)
      G1(I)=-G1(I)
      PHIN=(3.*PI+PHI)/4.
      DELTA=RT2*BETA1*XLL
      CALL DBLEXP(DELTA,PHIN,GA)                            122
      PHI3=(5.*PI+PHI)/4.
      CALL DBLEXP(DELTA,PHI3,GB)                            124
      DE=AIMAG(GB)
      DF=REAL(GB)
      GB=CMPLX(-DE,DF)
      PHI2=PI/4.
      DE=COS(PHI2)                                          126
      DF=SIN(PHI2)                                          127
      DF=-DF
      GC=CMPLX(DE,DF)
      G2(I)=G1(I)*GC*(GA+GB)/RT2
      GO TO 4
C COMPUTE G11 AND G12 FOR W GREATER THAN WA
    3 WB=W/WA
      DA=WB**2-1.
      DB=2.*ZETA*WB
      PHI=DB/DA
      PHI=ATAN(PHI)                                         132
```

```
      DC=(DA**2+DB**2)**.125                                               133
      BETA1=2.*PI*DC/XLAMN
      GA=(-1.)*PI/(RT2*XK*XLAMN*DC**3)
      PHIN=3.*PHI/4.
      DE=COS(PHIN)                                                         134
      DF=SIN(PHIN)                                                         135
      GB=CMPLX(DE,DF)
      DF=-DF
      GC=CMPLX(DF,DE)
      G1(I)=GA*(GB+GC)
      G1(I)=-G1(I)
      DELTA=RT2*BETA1*XLL
      PHI2=PI-PHI/4.
      PHI3=(6.*PI-PHI)/4.
      CALL DBLEXP(DELTA,PHI2,GC)                                           139
      CALL DBLEXP(DELTA,PHI3,GD)                                           141
      DE=-AIMAG(GD)
      DF=REAL(GD)
      GD=CMPLX(DF,DE)
      G2(I)=GA*GB*(GC+GD)
      G2(I)=-G2(I)
    4 D7=2.*BET*W/W1
      D8=1.-(W/W1)**2
      C1=(D8+D7**2)/(D8**2+D7**2)
      C2=(D7*D8-D7)/(D8**2+D7**2)
      B1=CMPLX(C1,C2)
      B2=XK2/(2.*XK2-2.*XM2*W**2-2.*XM1*B1*W**2)
      B3=(-1.)*(W**2)*(XM+XM2*B2+XM1*B1*B2)
      B6=(B3-XM*W**2)/2.
      B7=(B3+XM*W**2)/2.
      A1=G1*B7+G2*B6
      A2=G1*B6+G2*B7-1.
      CS1=COS(2.*PI*XL/XLAM)                                               147
      CS2=SIN(2.*PI*XL/XLAM)                                               148
      A5=CMPLX(CS1,CS2)
      Y3(I)=(A2-A1*A5)/(A1*A1-A2*A2)
      Y4(I)=(A2*A5-A1)/(A1*A1-A2*A2)
      F1(I)=B6*Y3(I)+B7*Y4(I)
      F2(I)=B7*Y3(I)+B6*Y4(I)
      Y2(I)=B2*(Y3(I)+Y4(I))
      Y1(I)=B1*Y2(I)
      DEL1(I)=Y3(I)-1.
      DEL2(I)=Y4(I)-A5
      WRITE(6,2001) I,A5,Y3(I),Y4(I),F1(I),F2(I),Y1(I),Y2(I),DEL1(I),
     X              DEL2(I)                                                166
 2001 FORMAT(5X,I3, (5X,2E20.8)/8X,
     1              2(5X,2E20.8)/8X,
     2              2(5X,2E20.8)/8X,
     3              2(5X,2E20.8)/8X,
     4              2(5X,2E20.8))
      BL1 = Y3(I)-DEL1(I)-1.
      BL2 = Y4(I)-DEL2(I)-A5
      BL3 = F1(I)+F2(I)+(XM*(Y3(I)+Y4(I))+XM2*Y2(I)+XM1*Y1(I))*W**2
      BL4 = F1(I)-F2(I)-XM*(Y4(I)-Y3(I))*W**2
      BL5 = XK2*(Y2(I)-(Y3(I)+Y4(I))/2.)-(XM2*Y2(I)+XM1*Y1(I))*W**2
      WBL=REAL(BL1)
```

```
      WBM=AIMAG(BL1)
      BL11=WBL**2+WBM**2
      BL11=SQRT(BL11)                                                   194
      WBL=REAL(BL2)
      WBM=AIMAG(BL2)
      BL22=WBL**2+WBM**2
      BL22=SQRT(BL22)                                                   195
      WBL=REAL(BL3)
      WBM=AIMAG(BL3)
      BL33=WBL**2+WBM**2
      BL33=SQRT(BL33)                                                   196
      WBL=REAL(BL4)
      WBM=AIMAG(BL4)
      BL44=WBL**2+WBM**2
      BL44=SQRT(BL44)                                                   197
      WBL=REAL(BL5)
      WBM=AIMAG(BL5)
      BL55=WBL**2+WBM**2
      BL55=SQRT(BL55)                                                   198
      WRITE(6,2000) I,BL11,BL22,BL33,BL44,BL55                          199
 2000 FORMAT (5X,I3,5(5X,E17.8))
   80 CONTINUE
C     CONVERT COMPLEX NOS. TO MAGNITUDE-PHASE FORM
      DO 150 I=1,NF
      CALL POLAR(F1(I),AF1(I),TF1(I))                                   209
      CALL POLAR(F2(I),AF2(I),TF2(I))                                   214
      CALL POLAR(DEL1(I),ADEL1(I),TDEL1(I))                             219
      CALL POLAR(DEL2(I),ADEL2(I),TDEL2(I))                             224
      CALL POLAR(Y1(I),AY1(I),TY1(I))                                   229
      CALL POLAR(Y2(I),AY2(I),TY2(I))                                   234
      CALL POLAR(Y3(I),AY3(I),TY3(I))                                   239
      CALL POLAR(Y4(I),AY4(I),TY4(I))                                   244
      CALL POLAR(G1(I),AG1(I),TG1(I))                                   249
      CALL POLAR(G2(I),AG2(I),TG2(I))                                   254
  150 CONTINUE
C     PRINTED OUTPUT
  105 FORMAT (1H0,F6.2,3X,2(E13.6,3X,F7.4,5X))
      WRITE (6,102)                                                     257
  102 FORMAT(1H0,2X,4HFREQ,5X,9HMAGN F1/V,5X,8HPHS F1/V,5X,9HMAGN F2/V,5
     1X,8HPHS F2/V)
      DO 110 I=1,NF
      WRITE (6,105) F(I),AF1(I),TF1(I),AF2(I),TF2(I)                    260
  110 CONTINUE
      WRITE (6,103)                                                     268
  103 FORMAT (1H0,2X,4HFREQ,5X,11HMAGN DEL1/V,3X,10HPHS DEL1/V,3X,11HMAG
     1N DEL2/V,3X,10HPHS DEL2/V)
      DO 111 I=1,NF
      WRITE (6,105) F(I),ADEL1(I),TDEL1(I),ADEL2(I),TDEL2(I)            271
  111 CONTINUE
      WRITE (6,107)                                                     279
  107 FORMAT (1H0,2X,4HFREQ,5X,9HMAGN Y1/V,5X,8HPHS Y1/V,5X,9HMAGN Y2/V,
     15X,8HPHS Y1/V)
      DO 112 I=1,NF
      WRITE (6,105) F(I),AY1(I),TY1(I),AY2(I),TY2(I)                    282
  112 CONTINUE
      WRITE (6,108)                                                     290
```

```
 108 FORMAT (1H0,2X,4HFREQ,5X,9HMAGN Y3/V,5X,8HPHS Y3/V,5X,9HMAGN Y4/V,
    15X,8HPHS Y4/V)
     DO 113 I=1,NF
     WRITE (6,105) F(I),AY3(I),TY3(I),AY4(I),TY4(I)                    293
 113 CONTINUE
     WRITE (6,109)                                                     301
 109 FORMAT (1H0,2X,4HFREQ,5X,8HMAGN G11,6X,7HPHS G11,6X,8HMAGN G12,6X,
    17HPHS G11)
     DO 114 I=1,NF
     WRITE (6,105) F(I),AG1(I),TG1(I),AG2(I),TG2(I)                    304
 114 CONTINUE
     WRITE(6,116)                                                      312
 116 FORMAT (1H0,4HFREQ,6X,10HACCEL Y1/V,7X,10HACCEL Y2/V,7X,10HACCEL Y
    13/V,7X,10HACCEL Y4/V)
     DO 200 I=1,NF
     W=2.*PI*F(I)
     ACCY1(I)=W**2*AY1(I)/G
     ACCY2(I)=W**2*AY2(I)/G
     ACCY3(I)=W**2*AY3(I)/G
     ACCY4(I)=W**2*AY4(I)/G
     WRITE(6,115)F(I),ACCY1(I),ACCY2(I),ACCY3(I),ACCY4(I)              325
 115 FORMAT (1H0,F6.2,3X,4(E13.6,4X))
 200 CONTINUE
C    SCALING FOR PLOT ROUTINE
     DO 155 I=1,NF
     F(I)=(ALOG10(F(I))+1.)*2.                                         338
      AF1(I)=(ALOG10(AF1(I))-1.)*1.5                                   341
     AF2(I)=(ALOG10(AF2(I))-1.)*1.5                                    344
     ADEL1(I)=(ALOG10(ADEL1(I))+4.)*1.5                                347
     ADEL2(I)=(ALOG10(ADEL2(I))+4.)*1.5                                350
     AY1(I)=(ALOG10(AY1(I))+6.)                                        353
     AY2(I)=(ALOG10(AY2(I))+6.)                                        356
     AY3(I)=(ALOG10(AY3(I))+6.)                                        359
     AY4(I)=(ALOG10(AY4(I))+6.)                                        362
     AG1(I)=(ALOG10(AG1(I))+7.)*2.                                     365
     AG2(I)=(ALOG10(AG2(I))+7.)*2.                                     368
     IF(AF1(I).LT.0.)AF1(I)=0.
     IF(AF2(I).LT.0.)AF2(I)=0.
     IF(AY1(I).LT.0.)AY1(I)=0.
     IF(AY2(I).LT.0.)AY2(I)=0.
     IF(AY3(I).LT.0.)AY3(I)=0.
     IF(AY4(I).LT.0.)AY4(I)=0.
     IF(ADEL1(I).LT.0.)ADEL1(I)=0.
     IF(ADEL2(I).LT.0.)ADEL2(I)=0.
     IF(AG1(I).LT.0.)AG1(I)=0.
     IF(AG2(I).LT.0.)AG2(I)=0.
     IF(AF1(I).GT.9.)AF1(I)=9.
     IF(AF2(I).GT.9.)AF2(I)=9.
     IF(ADEL1(I).GT.9.)ADEL1(I)=9.
     IF(ADEL2(I).GT.9.)ADEL2(I)=9.
     IF(AG1(I).GT.8.)AG1(I)=8.
     IF(AG2(I).GT.8.)AG2(I)=8.
     ACCY1(I)=(ALOG10(ACCY1(I))+4.)                                    435
     ACCY2(I)=(ALOG10(ACCY2(I))+4.)                                    438
     ACCY3(I)=(ALOG10(ACCY3(I))+4.)                                    441
     ACCY4(I)=(ALOG10(ACCY4(I))+4.)                                    444
```

```
      IF(ACCY1(I).LT.0.)ACCY1(I)=0.
      IF(ACCY2(I).LT.0.)ACCY2(I)=0.
      IF(ACCY3(I).LT.0.)ACCY3(I)=0.
      IF(ACCY4(I).LT.0.)ACCY4(I)=0.
  155 CONTINUE
C     PLOT ROUTINE
      CALL LAXIS(0.,0.,3,9HFREQUENCY,9,6.,-1,2)
      CALL LAXIS(0.,0.,8,19HY1/V Y2/V Y3/V Y4/V,19,8.,-6,1)
      CALL LLINE(F,AY1,NF)
      CALL LLINE(F,AY2,NF)
      CALL LLINE(F,AY3,NF)
      CALL LLINE(F,AY4,NF)
      CALL PLOT(12.,0.,-3)
      CALL LAXIS(0.,0.,3,9HFREQUENCY,9,6.,-1,2)
      CALL LAXIS(0.,0.,6,9HF1/V F2/V,9,9.,+1,1)
      CALL LLINE(F,AF1,NF)
      CALL LLINE(F,AF2,NF)
      CALL PLOT(12.,0.,-3)
      CALL LAXIS(0.,0.,3,9HFREQUENCY,9,6.,-1,2)
      CALL LAXIS(0.,0.,6,13HDEL1/V DEL2/V,13,9.,-4,1)
      CALL LLINE(F,ADEL1,NF)
      CALL LLINE(F,ADEL2,NF)
      CALL PLOT(12.,0.,-3)
      CALL LAXIS(0.,0.,3,9HFREQUENCY,9,6.,-1,2)
      CALL LAXIS(0.,0.,4,7HG11 G12,7,8.,-7,1)
      CALL LLINE(F,AG1,NF)
      CALL LLINE(F,AG2,NF)
      CALL PLOT(12.,0.,-3)
      CALL LAXIS(0.,0.,3,9HFREQUENCY,9,6.,-1,2)
      CALL LAXIS(0.,0.,8,18HACCEL(Y1 Y2 Y3 Y4),18,8.,-4,1)
      CALL LLINE(F,ACCY1,NV)
      CALL LLINE(F,ACCY1,NF)
      CALL LLINE(F,ACCY2,NF)
      CALL LLINE(F,ACCY3,NF)
      CALL LLINE(F,ACCY4,NF)
      CALL PLOT(12.,0.,-3)
      CALL PLOT(0.,0.,999)
   33 STOP
      END
```

INPUT VARIABLES

```
   K =  0.15000C00E C4
  K1 =  0.70965000E 04
  K2 =  C.19928000E C5
  M1 =  0.48186528E 02
  M2 =  C.18134715E 02
   M =  0.25906736E 01
   W =  C.33055556E 01
   E =  0.30000000E 08
   I =  C.71400000E 02
BETA =  0.30000000E 00
ZETA =  C.00000000E-38
   L =  C.82000000E 02
   V =  0.13200000E 05
```

FREQ	MAGN F1/V	PHS F1/V	MAGN F2/V	PHS F2/V
0.10	0.141584E 02	-3.1398	0.141584E 02	-3.1396
0.20	0.571735E 02	-3.1384	0.571735E 02	-3.1379
0.30	0.130718E 03	-3.1377	0.130718E 03	-3.1369
0.40	0.237769E 03	-3.1382	0.237768E 03	-3.1371
0.50	0.382922E 03	-3.1403	0.382918E 03	-3.1390
0.60	0.572913E 03	3.1384	0.572901E 03	3.1399
0.70	0.817442E 03	3.1306	0.817410E 03	3.1322
0.80	0.113046E 04	3.1181	0.113038E 04	3.1199
0.90	0.153220E 04	3.0990	0.153203E 04	3.1009
1.00	0.205227E 04	3.0705	0.205192E 04	3.0724
1.20	0.364173E 04	2.9648	0.364036E 04	2.9667
1.40	0.646893E 04	2.7266	0.646425E 04	2.7281
1.60	0.102595E 05	2.2310	0.102462E 05	2.2320
1.80	0.108162E 05	1.6425	0.107929E 05	1.6426
2.00	0.899598E 04	1.3204	0.896532E 04	1.3194
2.50	0.647065E 04	1.1745	0.641422E 04	1.1703
3.00	0.602190E 04	1.2809	0.592023E 04	1.2746
3.50	0.657180E 04	1.4127	0.640406E 04	1.4067
4.00	0.785128E 04	1.4921	0.759692E 04	1.4868
4.50	0.967767E 04	1.4899	0.931545E 04	1.4833
5.00	0.117057E 05	1.4047	0.112184E 05	1.3930
5.50	0.133211E 05	1.2559	0.127086E 05	1.2341
6.00	0.139263E 05	1.0831	0.132129E 05	1.0453
6.50	0.134557E 05	0.9286	0.126743E 05	0.8670
7.00	0.123134E 05	0.8152	0.114837E 05	0.7198
7.50	0.109108E 05	0.7468	0.100333E 05	0.6037
8.00	0.947643E 04	0.7201	0.853531E 04	0.5092
8.50	0.810434E 04	0.7332	0.706984E 04	0.4244

9.00	0.683249E 04	0.7891	0.565783E 04	0.3345
9.50	0.569284E 04	0.8987	0.430697E 04	0.2164
10.00	0.474584E 04	1.0812	0.304923E 04	0.0185
10.50	0.410849E 04	1.3553	0.203465E 04	-0.3973
11.00	0.394026E 04	1.7031	0.177478E 04	-1.1724
11.50	0.432228E 04	2.0437	0.256331E 04	-1.7739
12.00	0.516970E 04	2.3078	0.384638E 04	-2.0412
14.00	0.109647E 05	2.7700	0.104106E 05	-2.2981
16.00	0.189614E 05	2.9118	0.186276E 05	-2.3178
18.00	0.291330E 05	2.9798	0.288918E 05	-2.2923
20.00	0.420899E 05	3.0236	0.418950E 05	-2.2513
22.00	0.588329E 05	3.0583	0.586617E 05	-2.2048
24.00	0.809629E 05	3.0910	0.808012E 05	-2.1577
26.00	0.111201E 06	3.1262	0.111036E 06	-2.1139
28.00	0.154629E 06	-3.1147	0.154448E 06	-2.0776
30.00	0.222181E 06	-3.0584	0.221959E 06	-2.0556
32.00	0.343427E 06	-2.9749	0.343106E 06	-2.0612
34.00	0.642524E 06	-2.8328	0.641896E 06	-2.1260
36.00	0.345347E 07	-2.5457	0.344947E 07	-2.3438
38.00	0.125329E 07	1.2631	0.125192E 07	0.2220
40.00	0.173213E 07	2.0616	0.173174E 07	-0.5003
42.00	0.508210E 07	-0.6864	0.508223E 07	2.3258
44.00	0.121489E 07	-0.5060	0.121494E 07	2.2234
46.00	0.760389E 06	-0.4057	0.760416E 06	2.2012
48.00	0.583090E 06	-0.3409	0.583104E 06	2.2145
50.00	0.488198E 06	-0.2945	0.488206E 06	2.2461
52.00	0.428978E 06	-0.2585	0.428983E 06	2.2882
54.00	0.388480E 06	-0.2290	0.388483E 06	2.3367

56.00	0.359041E 06	-0.2037	0.359043E 06	2.3895
58.00	0.336675E 06	-0.1814	0.336676E 06	2.4452
60.00	0.319097E 06	-0.1611	0.319098E 06	2.5030
62.00	0.304902E 06	-0.1422	0.304903E 06	2.5622
64.00	0.293177E 06	-0.1245	0.293177E 06	2.6226
66.00	0.283298E 06	-0.1077	0.283299E 06	2.6838
68.00	0.274830E 06	-0.0915	0.274830E 06	2.7456
70.00	0.267455E 06	-0.0758	0.267455E 06	2.8081
72.00	0.260937E 06	-0.0606	0.260937E 06	2.8709
74.00	0.255099E 06	-0.0458	0.255099E 06	2.9342
76.00	0.249802E 06	-0.0313	0.249802E 06	2.9978
78.00	0.244940E 06	-0.0172	0.244940E 06	3.0617
80.00	0.240425E 06	-0.0033	0.240425E 06	3.1259
82.00	0.236191E 06	0.0102	0.236191E 06	-3.0928
84.00	0.232182E 06	0.0235	0.232182E 06	-3.0280
86.00	0.228353E 06	0.0364	0.228353E 06	-2.9628
88.00	0.224668E 06	0.0490	0.224668E 06	-2.8974
90.00	0.221096E 06	0.0612	0.221096E 06	-2.8316
92.00	0.217614E 06	0.0731	0.217614E 06	-2.7654
94.00	0.214202E 06	0.0846	0.214202E 06	-2.6988
96.00	0.210844E 06	0.0957	0.210844E 06	-2.6318
98.00	0.207526E 06	0.1063	0.207526E 06	-2.5643
100.00	0.204240E 06	0.1164	0.204240E 06	-2.4964
FREQ	MAGN DEL1/V	PHS DEL1/V	MAGN DEL2/V	PHS DEL2/V
0.10	0.112564E-03	0.0018	0.112549E-03	0.0020
0.20	0.454533E-03	0.0032	0.454518E-03	0.0036
0.30	0.103920E-02	0.0040	0.103920E-02	0.0046
0.40	0.189024E-02	0.0036	0.189022E-02	0.0044

0.50	0.304419E-02	0.0015	0.304416E-02	0.0024
0.60	0.455457E-02	-0.0030	0.455451E-02	-0.0019
0.70	0.649852E-02	-0.0108	0.649832E-02	-0.0096
0.80	0.898695E-02	-0.0232	0.898649E-02	-0.0220
0.90	0.121806E-01	-0.0423	0.121796E-01	-0.0409
1.00	0.163149E-01	-0.0708	0.163129E-01	-0.0694
1.20	0.289497E-01	-0.1765	0.289419E-01	-0.1752
1.40	0.514219E-01	-0.4148	0.513953E-01	-0.4137
1.60	0.815464E-01	-0.9104	0.814711E-01	-0.9098
1.80	0.859611E-01	-1.4991	0.858286E-01	-1.4990
2.00	0.714823E-01	-1.8213	0.713079E-01	-1.8220
2.50	0.513769E-01	-1.9677	0.510561E-01	-1.9707
3.00	0.477582E-01	-1.8616	0.471801E-01	-1.8661
3.50	0.520551E-01	-1.7297	0.511012E-01	-1.7340
4.00	0.621288E-01	-1.6503	0.606823E-01	-1.6540
4.50	0.765262E-01	-1.6526	0.744664E-01	-1.6573
5.00	0.925069E-01	-1.7385	0.897356E-01	-1.7469
5.50	0.105205E 00	-1.8887	0.101722E 00	-1.9043
6.00	0.109896E 00	-2.0636	0.105839E 00	-2.0907
6.50	0.106064E 00	-2.2214	0.101619E 00	-2.2654
7.00	0.968998E-01	-2.3392	0.921787E-01	-2.4074
7.50	0.856461E-01	-2.4137	0.806491E-01	-2.5161
8.00	0.740852E-01	-2.4488	0.687186E-01	-2.5997
8.50	0.629267E-01	-2.4471	0.570093E-01	-2.6683
9.00	0.524136E-01	-2.4061	0.456494E-01	-2.7326
9.50	0.427090E-01	-2.3149	0.346050E-01	-2.8075
10.00	0.341710E-01	-2.1487	0.238692E-01	-2.9252
10.50	0.276897E-01	-1.8681	0.138109E-01	3.0817

11.00	0.249344E-01	-1.4597	0.788732E-02	2.1183
11.50	0.272689E-01	-1.0313	0.140008E-01	1.1474
12.00	0.339470E-01	-0.7136	0.247587E-01	0.8777
14.00	0.796339E-01	-0.2325	0.761972E-01	0.6903
16.00	0.140903E 00	-0.0994	0.138875E 00	0.6891
18.00	0.217766E 00	-0.0342	0.216308E 00	0.7198
20.00	0.314830E 00	0.0097	0.313653E 00	0.7615
22.00	0.439536E 00	0.0458	0.438501E 00	0.8070
24.00	0.603891E 00	0.0799	0.602911E 00	0.8529
26.00	0.828610E 00	0.1159	0.827614E 00	0.8960
28.00	0.115307E 01	0.1577	0.115198E 01	0.9329
30.00	0.166354E 01	0.2108	0.166220E 01	0.9581
32.00	0.259701E 01	0.2854	0.259509E 01	0.9616
34.00	0.495579E 01	0.4041	0.495210E 01	0.9201
36.00	0.273821E 02	0.6245	0.273592E 02	0.7692
38.00	0.934146E 01	-2.0097	0.933314E 01	-2.7881
40.00	0.102275E 02	-1.1851	0.102245E 02	2.7465
42.00	0.289589E 02	2.4808	0.289599E 02	-0.8414
44.00	0.704563E 01	2.7139	0.704606E 01	-0.9965
46.00	0.446593E 01	2.8342	0.446613E 01	-1.0388
48.00	0.344550E 01	2.9068	0.344561E 01	-1.0332
50.00	0.289008E 01	2.9554	0.289014E 01	-1.0038
52.00	0.253758E 01	2.9905	0.253762E 01	-0.9609
54.00	0.229268E 01	3.0172	0.229271E 01	-0.9095
56.00	0.211204E 01	3.0383	0.211205E 01	-0.8525
58.00	0.197299E 01	3.0555	0.197300E 01	-0.7916
60.00	0.186248E 01	3.0698	0.186249E 01	-0.7278

62.00	0.177243E 01	3.0819	0.177243E 01	-0.6619
64.00	0.169755E 01	3.0923	0.169755E 01	-0.5942
66.00	0.163425E 01	3.1013	0.163425E 01	-0.5252
68.00	0.157999E 01	3.1092	0.157999E 01	-0.4550
70.00	0.153293E 01	3.1161	0.153293E 01	-0.3839
72.00	0.149169E 01	3.1223	0.149169E 01	-0.3120
74.00	0.145523E 01	3.1277	0.145523E 01	-0.2394
76.00	0.142275E 01	3.1326	0.142275E 01	-0.1661
78.00	0.139361E 01	3.1369	0.139361E 01	-0.0924
80.00	0.136730E 01	3.1407	0.136730E 01	-0.0182
82.00	0.134344E 01	-3.1391	0.134344E 01	0.0565
84.00	0.132168E 01	-3.1360	0.132168E 01	0.1315
86.00	0.130176E 01	-3.1334	0.130176E 01	0.2069
88.00	0.128345E 01	-3.1310	0.128345E 01	0.2827
90.00	0.126656E 01	-3.1290	0.126656E 01	0.3587
92.00	0.125094E 01	-3.1273	0.125094E 01	0.4350
94.00	0.123646E 01	-3.1258	0.123646E 01	0.5116
96.00	0.122299E 01	-3.1245	0.122299E 01	0.5884
98.00	0.121045E 01	-3.1235	0.121045E 01	0.6654
100.00	0.119875E 01	-3.1226	0.119875E 01	0.7427
FREQ	MAGN Y1/V	PHS Y1/V	MAGN Y2/V	PHS Y1/V
0.10	0.100412E 01	0.0019	0.100143E 01	0.0020
0.20	0.101663E 01	0.0032	0.100577E 01	0.0039
0.30	0.103804E 01	0.0035	0.101322E 01	0.0058
0.40	0.106922E 01	0.0022	0.102408E 01	0.0077
0.50	0.111153E 01	-0.0014	0.103885E 01	0.0094

0.60	0.116690E 01	-0.0083	0.105827E 01	0.0109
0.70	0.123812E 01	-0.0195	0.108336E 01	0.0117
0.80	0.132909E 01	-0.0364	0.111561E 01	0.0114
0.90	0.144534E 01	-0.0613	0.115713E 01	0.0091
1.00	0.159471E 01	-0.0971	0.121092E 01	0.0031
1.20	0.204043E 01	-0.2222	0.137331E 01	-0.0334
1.40	0.277696E 01	-0.4876	0.163928E 01	-0.1560
1.60	0.352670E 01	-1.0189	0.185628E 01	-0.4724
1.80	0.307635E 01	-1.6527	0.154236E 01	-0.8226
2.00	0.216849E 01	-2.0300	0.115211E 01	-0.8994
2.50	0.109657E 01	-2.3564	0.891386E 00	-0.7301
3.00	0.737069E 00	-2.4716	0.912515E 00	-0.6634
3.50	0.575007E 00	-2.5614	0.984575E 00	-0.6913
4.00	0.488337E 00	-2.6695	0.107646E 01	-0.7823
4.50	0.434033E 00	-2.8161	0.117266E 01	-0.9301
5.00	0.389356E 00	-3.0098	0.124552E 01	-1.1330
5.50	0.339820E 00	3.0412	0.125502E 01	-1.3775
6.00	0.281920E 00	2.8010	0.117940E 01	-1.6312
6.50	0.223413E 00	2.5878	0.104319E 01	-1.8579
7.00	0.173074E 00	2.4189	0.891486E 00	-2.0398
7.50	0.133876E 00	2.2929	0.753499E 00	-2.1781
8.00	0.104636E 00	2.2009	0.638487E 00	-2.2815
8.50	0.830261E-01	2.1341	0.545655E 00	-2.3591
9.00	0.669429E-01	2.0853	0.471216E 00	-2.4178
9.50	0.548087E-01	2.0494	0.411240E 00	-2.4628
10.00	0.455087E-01	2.0230	0.362466E 00	-2.4977
10.50	0.382682E-01	2.0037	0.322371E 00	-2.5249

11.00	0.325468E-01	1.9897	0.289054E 00	-2.5463
11.50	0.279636E-01	1.9798	0.261082E 00	-2.5630
12.00	0.242464E-01	1.9730	0.237374E 00	-2.5761
14.00	0.147767E-01	1.9667	0.171271E 00	-2.6038
16.00	0.938810E-02	1.9791	0.132245E 00	-2.6081
18.00	0.709998E-02	2.0009	0.107536E 00	-2.5996
20.00	0.539856E-02	2.0279	0.912842E-01	-2.5833
22.00	0.431569E-02	2.0582	0.805551E-01	-2.5619
24.00	0.361725E-02	2.0905	0.738546E-01	-2.5371
26.00	0.318361E-02	2.1242	0.705654E-01	-2.5098
28.00	0.296334E-02	2.1590	0.708535E-01	-2.4805
30.00	0.296762E-02	2.1944	0.761265E-01	-2.4499
32.00	0.333040E-02	2.2303	0.912286E-01	-2.4182
34.00	0.473009E-02	2.2664	0.137794E 00	-2.3858
36.00	0.199763E-01	2.2989	0.616641E 00	-2.3566
38.00	0.476828E-02	-0.7986	0.155468E 00	0.8262
40.00	0.166419E-02	-0.7621	0.571479E-01	0.8599
42.00	0.858047E-03	-0.7248	0.309531E-01	0.8948
44.00	0.511001E-03	-0.6872	0.193196E-01	0.9302
46.00	0.328501E-03	-0.6495	0.129890E-01	0.9660
48.00	0.221449E-03	-0.6115	0.913972E-02	1.0020
50.00	0.154151E-03	-0.5735	0.662912E-02	1.0384
52.00	0.109766E-03	-0.5354	0.491044E-02	1.0749
54.00	0.794454E-04	-0.4972	0.369152E-02	1.1117
56.00	0.581675E-04	-0.4589	0.280348E-02	1.1486
58.00	0.429174E-04	-0.4206	0.214273E-02	1.1856

60.00	0.318014E-04	-0.3822	0.164276E-02	1.2228
62.00	0.235876E-04	-0.3438	0.125926E-02	1.2602
64.00	0.174508E-04	-0.3053	0.961813E-03	1.2976
66.00	0.128247E-04	-0.2668	0.729019E-03	1.3351
68.00	0.931270E-05	-0.2283	0.545482E-03	1.3727
70.00	0.663210E-05	-0.1897	0.399934E-03	1.4104
72.00	0.457821E-05	-0.1511	0.283993E-03	1.4482
74.00	0.300093E-05	-0.1125	0.191339E-03	1.4861
76.00	0.178883E-05	-0.0739	0.117147E-03	1.5240
78.00	0.858363E-06	-0.0352	0.576962E-04	1.5620
80.00	0.146288E-06	0.0035	0.100858E-04	1.6000
82.00	0.395663E-06	-3.0994	0.279625E-04	-1.5035
84.00	0.804593E-06	-3.0607	0.582530E-04	-1.4654
86.00	0.110922E-05	-3.0220	0.822246E-04	-1.4272
88.00	0.133190E-05	-2.9832	0.101032E-03	-1.3890
90.00	0.149011E-05	-2.9445	0.115608E-03	-1.3508
92.00	0.159762E-05	-2.9057	0.126709E-03	-1.3125
94.00	0.166527E-05	-2.8669	0.134951E-03	-1.2742
96.00	0.170167E-05	-2.8281	0.140840E-03	-1.2359
98.00	0.171364E-05	-2.7893	0.144791E-03	-1.1975
100.00	0.170662E-05	-2.7505	0.147146E-03	-1.1591

FREQ	MAGN Y3/V	PHS Y3/V	MAGN Y4/V	PHS Y4/V
0.10	0.100011E 01	0.0000	0.100011E 01	0.0039
0.20	0.100045E 01	0.0000	0.100045E 01	0.0078
0.30	0.100104E 01	0.0000	0.100104E 01	0.0117
0.40	0.100189E 01	0.0000	0.100189E 01	0.0156

0.50	0.100304E 01	0.0000	0.100304E 01	0.0195
0.60	0.100455E 01	-0.0000	0.100455E 01	0.0233
0.70	0.100650E 01	-0.0001	0.100649E 01	0.0271
0.80	0.100898E 01	-0.0002	0.100897E 01	0.0308
0.90	0.101217E 01	-0.0005	0.101214E 01	0.0342
1.00	0.101627E 01	-0.0011	0.101622E 01	0.0373
1.20	0.102851E 01	-0.0049	0.102825E 01	0.0406
1.40	0.104727E 01	-0.0198	0.104612E 01	0.0325
1.60	0.105199E 01	-0.0613	0.104807E 01	-0.0018
1.80	0.100981E 01	-0.0850	0.100381E 01	-0.0154
2.00	0.984718E 00	-0.0704	0.979267E 00	0.0091
2.50	0.981283E 00	-0.0483	0.976665E 00	0.0516
3.00	0.987366E 00	-0.0464	0.982042E 00	0.0731
3.50	0.993094E 00	-0.0518	0.986116E 00	0.0871
4.00	0.996994E 00	-0.0622	0.987374E 00	0.0964
4.50	0.996672E 00	-0.0766	0.983335E 00	0.1024
5.00	0.988774E 00	-0.0924	0.971051E 00	0.1089
5.50	0.972265E 00	-0.1030	0.950964E 00	0.1233
6.00	0.952936E 00	-0.1018	0.930744E 00	0.1512
6.50	0.939563E 00	-0.0900	0.919355E 00	0.1892
7.00	0.935256E 00	-0.0746	0.918358E 00	0.2286
7.50	0.937792E 00	-0.0608	0.924150E 00	0.2642
8.00	0.944183E 00	-0.0501	0.933216E 00	0.2955
8.50	0.952502E 00	-0.0423	0.943595E 00	0.3232
9.00	0.961778E 00	-0.0366	0.954430E 00	0.3485
9.50	0.971581E 00	-0.0323	0.965419E 00	0.3721

10.00	0.981749E 00	-0.0292	0.976500E 00	0.3945
10.50	0.992241E 00	-0.0267	0.987705E 00	0.4162
11.00	0.100307E 01	-0.0247	0.999101E 00	0.4372
11.50	0.101428E 01	-0.0231	0.101076E 01	0.4578
12.00	0.102590E 01	-0.0217	0.102276E 01	0.4780
14.00	0.107765E 01	-0.0170	0.107547E 01	0.5566
16.00	0.114029E 01	-0.0123	0.113862E 01	0.6324
18.00	0.121766E 01	-0.0061	0.121628E 01	0.7056
20.00	0.131482E 01	0.0023	0.131361E 01	0.7761
22.00	0.143922E 01	0.0140	0.143809E 01	0.8430
24.00	0.160269E 01	0.0301	0.160159E 01	0.9052
26.00	0.182557E 01	0.0525	0.182442E 01	0.9610
28.00	0.214642E 01	0.0845	0.214512E 01	1.0072
30.00	0.264959E 01	0.1317	0.264807E 01	1.0380
32.00	0.356770E 01	0.2064	0.356535E 01	1.0412
34.00	0.588838E 01	0.3373	0.588376E 01	0.9875
36.00	0.281994E 02	0.6037	0.281700E 02	0.7903
38.00	0.895235E 01	-1.9085	0.895202E 01	-2.8893
40.00	0.106441E 02	-1.0980	0.106410E 02	2.6593
42.00	0.281761E 02	2.4590	0.281771E 02	-0.8196
44.00	0.614972E 01	2.6464	0.615015E 01	-0.9290
46.00	0.352579E 01	2.7483	0.352600E 01	-0.9529
48.00	0.248386E 01	2.8130	0.248397E 01	-0.9394
50.00	0.191631E 01	2.8587	0.191638E 01	-0.9071
52.00	0.155627E 01	2.8937	0.155631E 01	-0.8640
54.00	0.130631E 01	2.9221	0.130634E 01	-0.8144
56.00	0.112212E 01	2.9463	0.112213E 01	-0.7605

58.00	0.980480E 00	2.9676	0.980490E 00	-0.7038
60.00	0.868033E 00	2.9870	0.868040E 00	-0.6451
62.00	0.776507E 00	3.0049	0.776512E 00	-0.5849
64.00	0.700503E 00	3.0218	0.700507E 00	-0.5237
66.00	0.636341E 00	3.0379	0.636343E 00	-0.4618
68.00	0.581422E 00	3.0534	0.581424E 00	-0.3992
70.00	0.533862E 00	3.0684	0.533863E 00	-0.3361
72.00	0.492256E 00	3.0830	0.492257E 00	-0.2727
74.00	0.455538E 00	3.0973	0.455538E 00	-0.2089
76.00	0.422883E 00	3.1112	0.422884E 00	-0.1448
78.00	0.393645E 00	3.1249	0.393645E 00	-0.0804
80.00	0.367306E 00	3.1384	0.367306E 00	-0.0158
82.00	0.343452E 00	-3.1317	0.343452E 00	0.0491
84.00	0.321744E 00	-3.1188	0.321744E 00	0.1143
86.00	0.301903E 00	-3.1062	0.301903E 00	0.1797
88.00	0.283698E 00	-3.0938	0.283698E 00	0.2455
90.00	0.266936E 00	-3.0819	0.266936E 00	0.3115
92.00	0.251453E 00	-3.0702	0.251452E 00	0.3780
94.00	0.237110E 00	-3.0589	0.237110E 00	0.4448
96.00	0.223791E 00	-3.0481	0.223791E 00	0.5120
98.00	0.211394E 00	-3.0377	0.211394E 00	0.5796
100.00	0.199831E 00	-3.0277	0.199830E 00	0.6477
FREQ	MAGN G11	PHS G11	MAGN G12	PHS G11
0.10	0.681840E-05	3.1416	0.113148E-05	-3.1416
0.20	0.681843E-05	3.1416	0.113149E-05	-3.1416
0.30	0.681849E-05	3.1416	0.113151E-05	-3.1416
0.40	0.681857E-05	3.1416	0.113154E-05	-3.1416
0.50	0.681868E-05	3.1416	0.113158E-05	-3.1416
0.60	0.681880E-05	3.1416	0.113163E-05	-3.1416

0.70	0.681895E-05	3.1416	0.113169E-05	-3.1416
0.80	0.681913E-05	3.1416	0.113175E-05	-3.1416
0.90	0.681932E-05	3.1416	0.113182E-05	-3.1416
1.00	0.681954E-05	3.1416	0.113191E-05	-3.1416
1.20	0.682005E-05	3.1416	0.113210E-05	-3.1416
1.40	0.682065E-05	3.1416	0.113232E-05	-3.1416
1.60	0.682134E-05	3.1416	0.113258E-05	-3.1416
1.80	0.682212E-05	3.1416	0.113287E-05	-3.1416
2.00	0.682300E-05	3.1416	0.113320E-05	-3.1416
2.50	0.682560E-05	3.1416	0.113417E-05	-3.1416
3.00	0.682878E-05	3.1416	0.113536E-05	-3.1416
3.50	0.683254E-05	3.1416	0.113677E-05	-3.1416
4.00	0.683689E-05	3.1416	0.113840E-05	-3.1416
4.50	0.684182E-05	3.1416	0.114024E-05	-3.1416
5.00	0.684735E-05	3.1416	0.114231E-05	-3.1416
5.50	0.685346E-05	3.1416	0.114461E-05	-3.1416
6.00	0.686018E-05	3.1416	0.114713E-05	-3.1416
6.50	0.686749E-05	3.1416	0.114987E-05	-3.1416
7.00	0.687542E-05	3.1416	0.115285E-05	-3.1416
7.50	0.688395E-05	3.1416	0.115606E-05	-3.1416
8.00	0.689310E-05	3.1416	0.115950E-05	-3.1416
8.50	0.690287E-05	3.1416	0.116319E-05	-3.1416
9.00	0.691326E-05	3.1416	0.116711E-05	-3.1416
9.50	0.692429E-05	3.1416	0.117127E-05	-3.1416
10.00	0.693597E-05	3.1416	0.117569E-05	-3.1416
10.50	0.694829E-05	3.1416	0.118035E-05	-3.1416
11.00	0.696126E-05	3.1416	0.118527E-05	-3.1416
11.50	0.697490E-05	3.1416	0.119044E-05	-3.1416

12.00	0.698922E-05	3.1416	0.119588E-05	-3.1416
14.00	0.705339E-05	3.1416	0.122037E-05	-3.1416
16.00	0.712918E-05	3.1416	0.124949E-05	-3.1416
18.00	0.721740E-05	3.1416	0.128365E-05	-3.1416
20.00	0.731907E-05	3.1416	0.132337E-05	-3.1416
22.00	0.743541E-05	3.1416	0.136929E-05	-3.1416
24.00	0.756790E-05	3.1416	0.142216E-05	-3.1416
26.00	0.771833E-05	3.1416	0.148293E-05	-3.1416
28.00	0.788885E-05	3.1416	0.155275E-05	-3.1416
30.00	0.808212E-05	3.1416	0.163305E-05	-3.1416
32.00	0.830137E-05	3.1416	0.172559E-05	-3.1416
34.00	0.855063E-05	3.1416	0.183262E-05	-3.1416
36.00	0.883492E-05	3.1416	0.195698E-05	-3.1416
38.00	0.916061E-05	3.1416	0.210232E-05	-3.1416
40.00	0.953588E-05	3.1416	0.227342E-05	-3.1416
42.00	0.997142E-05	3.1416	0.247666E-05	-3.1416
44.00	0.104815E-04	3.1416	0.272067E-05	-3.1416
46.00	0.110854E-04	3.1416	0.301749E-05	-3.1416
48.00	0.118105E-04	3.1416	0.338432E-05	-3.1416
50.00	0.126960E-04	3.1416	0.384663E-05	-3.1416
52.00	0.138012E-04	3.1416	0.444378E-05	-3.1416
54.00	0.152203E-04	3.1416	0.523976E-05	-3.1416
56.00	0.171127E-04	3.1416	0.634601E-05	-3.1416
58.00	0.197735E-04	3.1416	0.797509E-05	-3.1416
60.00	0.238234E-04	3.1416	0.105886E-04	-3.1416
62.00	0.308518E-04	3.1416	0.154140E-04	-3.1416
64.00	0.467271E-04	3.1416	0.271959E-04	-3.1416
66.00	0.137481E-03	3.1416	0.103485E-03	-3.1416

68.00	0.732552E-04	0.7854	0.621851E-04	0.8223
70.00	0.371273E-04	0.7854	0.285424E-04	1.1132
72.00	0.259376E-04	0.7854	0.189743E-04	1.3067
74.00	0.202525E-04	0.7854	0.143665E-04	1.4582
76.00	0.167442E-04	0.7854	0.116338E-04	1.5850
78.00	0.143363E-04	0.7854	0.981609E-05	1.6952
80.00	0.125682E-04	0.7854	0.851507E-05	1.7933
82.00	0.112077E-04	0.7854	0.753508E-05	1.8821
84.00	0.101243E-04	0.7854	0.676857E-05	1.9635
86.00	0.923872E-05	0.7854	0.615142E-05	2.0388
88.00	0.849956E-05	0.7854	0.564299E-05	2.1092
90.00	0.787220E-05	0.7854	0.521623E-05	2.1753
92.00	0.733228E-05	0.7854	0.485245E-05	2.2377
94.00	0.686216E-05	0.7854	0.453828E-05	2.2969
96.00	0.644873E-05	0.7854	0.426395E-05	2.3533
98.00	0.608204E-05	0.7854	0.402209E-05	2.4072
100.00	0.575436E-05	0.7854	0.380707E-05	2.4588

FREQ	ACCEL Y1/V	ACCEL Y2/V	ACCEL Y3/V	ACCEL Y4/V
0.10	0.102697E-02	0.102422E-02	0.102287E-02	0.102287E-02
0.20	0.415907E-02	0.411465E-02	0.409289E-02	0.409289E-02
0.30	0.955498E-02	0.932647E-02	0.921438E-02	0.921438E-02
0.40	0.174969E-01	0.167581E-01	0.163950E-01	0.163950E-01
0.50	0.284205E-01	0.265623E-01	0.256468E-01	0.256467E-01
0.60	0.429644E-01	0.389646E-01	0.369869E-01	0.369869E-01
0.70	0.620484E-01	0.542926E-01	0.504407E-01	0.504405E-01
0.80	0.869974E-01	0.730238E-01	0.660445E-01	0.660438E-01
0.90	0.119737E 00	0.958603E-01	0.838515E-01	0.838494E-01
1.00	0.163100E 00	0.123847E 00	0.103940E 00	0.103934E 00

1.20	0.300509E 00	0.202257E 00	0.151476E 00	0.151438E 00
1.40	0.556670E 00	0.328610E 00	0.209935E 00	0.209705E 00
1.60	0.923381E 00	0.486023E 00	0.275439E 00	0.274412E 00
1.80	0.101942E 01	0.511097E 00	0.334623E 00	0.332635E 00
2.00	0.887134E 00	0.471330E 00	0.402851E 00	0.400621E 00
2.50	0.700955E 00	0.569795E 00	0.627259E 00	0.624307E 00
3.00	0.678458E 00	0.839953E 00	0.908852E 00	0.903951E 00
3.50	0.720413E 00	0.123355E 01	0.124423E 01	0.123548E 01
4.00	0.799120E 00	0.176154E 01	0.163149E 01	0.161575E 01
4.50	0.898918E 00	0.242867E 01	0.206419E 01	0.203657E 01
5.00	0.995541E 00	0.318465E 01	0.252819E 01	0.248287E 01
5.50	0.105135E 01	0.388282E 01	0.300803E 01	0.294213E 01
6.00	0.103801E 01	0.434246E 01	0.350864E 01	0.342693E 01
6.50	0.965401E 00	0.450779E 01	0.405999E 01	0.397267E 01
7.00	0.867360E 00	0.446769E 01	0.468704E 01	0.460236E 01
7.50	0.770189E 00	0.433489E 01	0.539512E 01	0.531664E 01
8.00	0.684912E 00	0.417931E 01	0.618028E 01	0.610850E 01
8.50	0.613515E 00	0.403208E 01	0.703844E 01	0.697262E 01
9.00	0.554577E 00	0.390371E 01	0.796769E 01	0.790682E 01
9.50	0.505905E 00	0.379590E 01	0.896807E 01	0.891119E 01
10.00	0.465444E 00	0.370714E 01	0.100409E 02	0.998722E 01
10.50	0.431508E 00	0.363503E 01	0.111884E 02	0.111373E 02
11.00	0.402778E 00	0.357714E 01	0.124134E 02	0.123642E 02
11.50	0.378235E 00	0.353138E 01	0.137191E 02	0.136715E 02
12.00	0.357094E 00	0.349597E 01	0.151092E 02	0.150629E 02
14.00	0.296214E 00	0.343330E 01	0.216026E 02	0.215588E 02
16.00	0.258896E 00	0.346252E 01	0.298558E 02	0.298120E 02
18.00	0.235274E 00	0.356345E 01	0.403500E 02	0.403043E 02

20.00	C.220857E 00	0.373446E 01	0.537896E 02	0.537401E 02
22.00	0.213633E 00	0.398760E 01	0.712433E 02	0.711877E 02
24.00	C.213095E 00	0.435083E 01	0.944157E 02	0.943508E 02
26.00	C.220110E 00	0.487878E 01	0.126217E 03	0.126137E 03
28.00	0.237613E 00	0.568132E 01	0.172109E 03	0.172005E 03
30.00	0.273164E 00	0.700730E 01	0.243899E 03	0.243750E 03
32.00	0.348794E 00	0.955440E 01	0.373646E 03	0.373400E 03
34.00	C.559242E 00	0.162915E 02	0.696187E 03	0.695642E 03
36.00	0.264785E 01	0.817354E 02	0.373781E 04	0.373391E 04
38.00	0.704208E 00	0.229605E 02	0.132361E 04	0.132209E 04
40.00	0.272330E 00	0.935174E 01	0.174182E 04	0.174131E 04
42.00	C.154804E 00	0.558439E 01	0.508337E 04	0.508356E 04
44.00	0.101181E 00	0.382539E 01	0.121768E 04	0.121776E 04
46.00	C.710926E-01	0.281101E 01	0.763036E 03	0.763081E 03
48.00	0.521829E-01	0.215371E 01	0.585304E 03	0.585331E 03
50.00	0.394147E-01	0.169499E 01	0.489981E 03	0.489998E 03
52.00	0.303563E-01	0.135800E 01	0.430391E 03	C.430402E 03
54.00	C.236935E-01	0.110095E 01	0.389589E 03	0.389597E 03
56.00	0.186565E-01	0.899179E 00	0.359904E 03	0.359909E 03
58.00	0.147660E-01	0.737218E 00	0.337339E 03	0.337343E 03
60.00	0.117090E-01	0.604851E 00	0.319603E 03	0.319606E 03
62.00	C.927341E-02	0.495074E 00	0.305282E 03	0.305284E 03
64.00	0.731049E-02	0.402924E 00	0.293456E 03	0.293457E 03
66.00	0.571356E-02	0.324787E 00	0.283498E 03	0.283499E 03
68.00	0.440419E-02	0.257971E 00	0.274968E 03	0.274969E 03
70.00	C.332368E-02	0.200427E 00	0.267545E 03	0.267546E 03
72.00	0.242735E-02	0.150572E 00	0.260993E 03	C.260993E 03
74.00	0.168070E-02	0.107162E 00	0.255129E 03	0.255130E 03

76.00	0.105674E-02	0.692041E-01	0.249816E 03	0.249816E 03
78.00	0.534113E-03	0.359012E-01	0.244944E 03	0.244944E 03
80.00	0.957548E-04	0.660178E-02	0.240426E 03	0.240426E 03
82.00	0.272098E-03	0.192299E-01	0.236193E 03	0.236193E 03
84.00	0.580641E-03	0.420387E-01	0.232189E 03	0.232189E 03
86.00	0.839049E-03	0.621973E-01	0.228369E 03	0.228369E 03
88.00	0.105489E-02	0.800199E-01	0.224695E 03	0.224695E 03
90.00	0.123446E-02	0.957738E-01	0.221138E 03	0.221138E 03
92.00	0.138300E-02	0.109687E 00	0.217673E 03	0.217673E 03
94.00	0.150492E-02	0.121957E 00	0.214279E 03	0.214279E 03
96.00	0.160394E-02	0.132752E 00	0.210940E 03	0.210940E 03
98.00	0.168323E-02	0.142222E 00	0.207643E 03	0.207643E 03
100.00	0.174546E-02	0.150495E 00	0.204378E 03	0.204378E 03

APPENDIX C

COMPUTER PROGRAM TO PREDICT VEHICLE RESPONSE TO VERTICAL TRACK IRREGULARITIES "FULL CAR MODEL"

EQUATIONS OF MOTION FOR VERTICAL DYNAMICS

For an evaluation of the vertical response to track profile irregularities, the model in Figure C-1 which includes damping in the secondary suspension can be used to describe the vehicle. Since the parameters of interest are the motion of the car body and displacements of the wheels, a convenient set of coordinates to describe the system is y_2 and θ_2, the vertical and angular displacements of the car body, and v_1, v_2, v_3, v_4, the displacements of the trucks at their connections to the equalizer springs. Since the motion described by this model is not coupled to roll or lateral response of the vehicle, the wheel inputs, v_{10}, v_{20}, v_{30}, v_{40} represent the average of the two rail profiles.

$$m_2\ddot{y}_2 + 2c_2\left[\dot{y}_2 - \frac{1}{4}\left(\dot{v}_1+\dot{v}_2+\dot{v}_3+\dot{v}_4\right)\right] + 2k_2\left[y_2 - \frac{1}{4}\left(v_1+v_2+v_3+v_4\right)\right] = 0 \tag{C-1}$$

$$I_2\ddot{\theta}_2 + 2ac_2\left[a\dot{\theta}_2 + \frac{1}{4}\left(\dot{v}_1+\dot{v}_2-\dot{v}_3-\dot{v}_4\right)\right] + 2ak_2\left[a\dot{\theta}_2 + \frac{1}{4}\left(v_1+v_2-v_3-v_4\right)\right] = 0 \tag{C-2}$$

$$\frac{m_1}{4}\left(\ddot{v}_1+\ddot{v}_2\right) + \frac{I_1}{L^2}\left(\ddot{v}_1-\ddot{v}_2\right) + \frac{c_2}{2}\left[a\dot{\theta}_2-\dot{y}_2 + \frac{1}{2}\left(\dot{v}_1+\dot{v}_2\right)\right] + \frac{k_1}{2}v_1 + \frac{k_2}{2}\left[a\theta_2 - y_2 + \frac{1}{2}\left(v_1+v_2\right)\right] = 0 \tag{C-3}$$

$$\frac{m_1}{4}\left(\ddot{v}_1+\ddot{v}_2\right) - \frac{I_1}{L^2}\left(\ddot{v}_1-\ddot{v}_2\right) + \frac{c_2}{2}\left[a\dot{\theta}_2 - \dot{y}_2 + \frac{1}{2}\left(\dot{v}_1+\dot{v}_2\right)\right] + \frac{k_1}{2} v_2$$

$$+ \frac{k_2}{2}\left[a\theta_2 - y_2 + \frac{1}{2}\left(v_1+v_2\right)\right] = 0 \qquad \text{(C-4)}$$

$$\frac{m_1}{4}\left(\ddot{v}_3+\ddot{v}_4\right) - \frac{I_1}{L^2}\left(\ddot{v}_3-\ddot{v}_4\right) + \frac{c_2}{2}\left[\frac{1}{2}\left(\dot{v}_3+\dot{v}_4\right) - a\dot{\theta}_2 - \dot{y}_2\right] + \frac{k_1}{2} v_3$$

$$+ \frac{k_2}{2}\left[\frac{1}{2}\left(v_3+v_4\right) - a\theta_2 - y_2\right] = 0 \qquad \text{(C-5)}$$

$$\frac{m_1}{4}\left(\ddot{v}_3+\ddot{v}_4\right) - \frac{I_1}{L^2}\left(\ddot{v}_3-\ddot{v}_4\right) + \frac{c_2}{2}\left[\frac{1}{2}\left(\dot{v}_3+\dot{v}_4\right) - a\dot{\theta}_2 - \dot{y}_2\right] + \frac{k_1}{2} v_4$$

$$+ \frac{k_2}{2}\left[\frac{1}{2}\left(v_3+v_4\right) - a\theta_2 - y_2\right] = 0 \qquad \text{(C-6)}$$

As discussed previously, the normal modes containing pitch and bounch motions of the car body can be decoupled from the pitch motion of the trucks. In addition, the bounce can be uncoupled from unsymmetric translation of the trucks (Figures C-2d and A-2e) and the pitch from symmetric translation (Figures C-2b and A-2c) so that the dynamics of the car can be interpreted in terms of two simpler equivalent two degrees of freedom systems.

Symmetric translation of the trucks can be represented by $v_1=v_2=v_3=v_4=y_1$. Substitution in the equations of motion reduces the six equations to,

$$m_1\ddot{y}_1 + c_2\left(\dot{y}_1-\dot{y}_2\right) + k_1y_1 + k_2\left(y_1-y_2\right) = 0 \qquad \text{(C-7)}$$

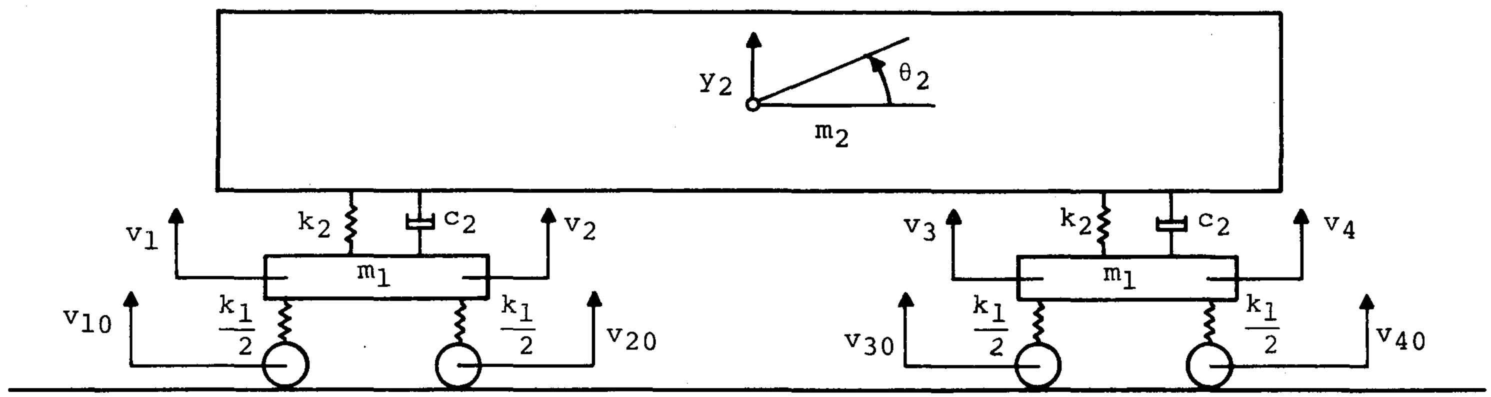

Figure C-1. Full Car Dynamic Model

$$m_2\ddot{y}_2 + 2c_2\left(\dot{y}_2-\dot{y}_1\right) + 2k_2\left(y_2-y_1\right) = 0 \qquad \text{(C-8)}$$

Thus the vertical motion of the car body can be interpreted in terms of the equivalent system of Figure C-2a which also is described by Equations C-7 and C-8. Similarly, the unsymmetric translation of the trucks can be represented by $v_1=v_2=y_3=-v_3=-v_4$. In this case, the six equations of motion reduce to,

$$m_1\ddot{y}_3 + c_2\left(\dot{y}_3+a\dot{\theta}_2\right) + k_1y_3 + k_2\left(y_3+a\theta_2\right) = 0 \qquad \text{(C-9)}$$

$$I_2\ddot{\theta} + 2a\ c_2\left(\dot{y}_3+a\dot{\theta}_2\right) + 2a\ k_2\left(y_3+a\theta_2\right) = 0 \qquad \text{(C-10)}$$

which describe the equivalent system of Figure C-2b.

These equivalent descriptions provide a description of inputs at the vehicle wheels in terms of simple base motions of the equivalent systems. For example, a unit movement of each of the wheel displacements, v_{10}, v_{20}, v_{30}, v_{40}, is equivalent to a unit base displacement y_{10}, where, $\bar{v} = 1/4\ (v_{10}+v_{20}+v_{30}+v_{40})$. Similarly, angular body motion is excited by an equivalent base motion,

$$v_\Delta = \frac{1}{4}\left(v_{10}+v_{20}-v_{30}-v_{40}\right) .$$

Figures C-2a and C-2b indicate that these base motions are inputs to the system represented by forcing functions $k(y_{10})$ and $k(y_{30})$ on the right hand sides of Equations C-7 and C-9, respectively.

The transfer functions for these inputs are,

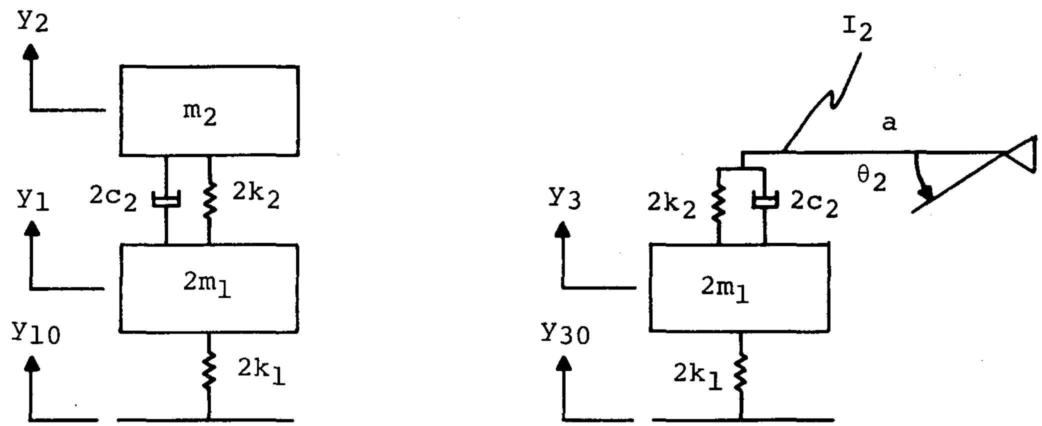

(a) (b)

Figure C-2. Simplified Models for Vertical Dynamics

$$\frac{\bar{y}_2}{\bar{v}} = H_1(s) = \frac{\left(1 + \frac{2\beta s}{\omega_2}\right)}{\left[1 + \frac{2\beta s}{\omega_2} + \frac{\omega_1^2 + (2+\mu)\omega_2^2}{2\omega_1^2\omega_2^2} s^2 + \frac{(2+\mu)\beta}{\omega_2\omega_1^2} s^3 + \frac{s^4}{2\omega_1^2\omega_2^2}\right]}$$

$$\frac{\bar{\theta}_2}{v\Delta} = H_2(s) =$$

$$\frac{-\left(1 + \frac{2G\beta s}{\omega_2}\right)}{a\left[1 + \frac{2G\beta s}{\omega_2} + \frac{\omega_1^2 + (2G+\mu)\omega_2^2}{2G\omega_1^2\omega_2^2} s^2 + \frac{(2G^2+\mu)\xi}{G\omega_2\omega_1^2} s^3 + \frac{s^4}{2G\omega_1^2\omega_2^2}\right]}$$

where,

$$\omega_1^2 = \frac{k_1}{m_1},\ \omega_2^2 = \frac{k_2}{m_2},\ \mu = \frac{m_2}{m_1},\ G = \frac{a^2}{\rho^2},\ \beta = \frac{c_2}{2m_2\omega_2}$$

The vertical response of any point in the car is a linear combination of the y_2 and θ_2 responses.

A program to solve the above equations for a sinusoidal irregularity has been prepared. The program solves the following equations:

$$\left|\frac{z_2}{\bar{v}}\right| = \left|\frac{\left(1 + \frac{2\beta s}{\omega_{2z}}\right)}{\left[1 + \frac{2\beta s}{\omega_{2z}} + \frac{\left(\omega_{1z}^2 + (2+\mu)\omega_{2z}^2\right)}{2\omega_{1z}^2\ \omega_{2z}^2} s^2 + \frac{(2+\mu)\beta}{\omega_{2z}\omega_{1z}^2} s^3 + \frac{s^4}{2\omega_{1z}^2\ \omega_{2z}^2}\right]}\right.$$

$$\left|\frac{a\phi}{v_\Delta}\right| = - \frac{\left(1 + \frac{2G\beta s}{\omega_{2z}}\right)}{\left[1 + \frac{2G\beta s}{\omega_{2z}} + \frac{\omega_{1z}^2 + (2G+\mu)\omega_{2z}^2}{2G\omega_{1z}^2\ \omega_{2z}} s^2 + \frac{2G^2+\mu\ \beta}{G\omega_2\omega_{1z}^2} s^3 + \frac{s^4}{2G\omega_{1z}^2\omega_{2z}^2}\right]}$$

given that

$$\bar{v} = 1/4\ \left(v_1+v_2+v_3+v_4\right)$$

$$v_1 = v_o \sin \frac{2\pi x}{\lambda}$$

$$v_2 = v_1(x+\ell)$$

$$v_3 = v_1(x+L)$$

$$v_4 = v_2(x+L)$$

as functions of ω with β as a field variable and to plot the curves of these values against given frequencies on a log-log axis. The method by which the program solves the equations, as well as the required input and sample output are discussed on the following pages.

INPUT

The input quantities for the program are described below in the order and units they must be put into the data deck. Column 4 shows the equivalent in Figure 1 for the input quantity.

Data Card	Quantity	Format	Description	Units
1	V	F7.3	Velocity	MPH
2	XL	F7.3	L in Fig. 1	feet
3	XLL	F7.3	LL in Fig. 1	feet
4	K1	F12.4	Spring Constant K1 in Fig. 1	lb./in.
5	W1	F12.4	M1 in Fig. 1	lb.
6	K2	F12.4	Spring Constant K2 in Fig. 1	lb./in.
7	W2	F12.4	M2 in Fig. 1	lb.
8	NDF	I2	No. of F's	See discussion of Input frequencies, P.
9	DF	6 F10.4	No. of Δ F's	
10	FL	7 F10.4	No. of F limits	
11	N1	I2	No. of β values input	
12	B	7 F10.4	β values (field variable) more than 7 values may be input, but only 7 are allowed per data card.	
13	G	F12.4	$\frac{M_2 a^2}{I_2}$ in Fig. 1	

Sample Input Data, found on page 14, is a list of the data cards in the order and format they should appear in the program.

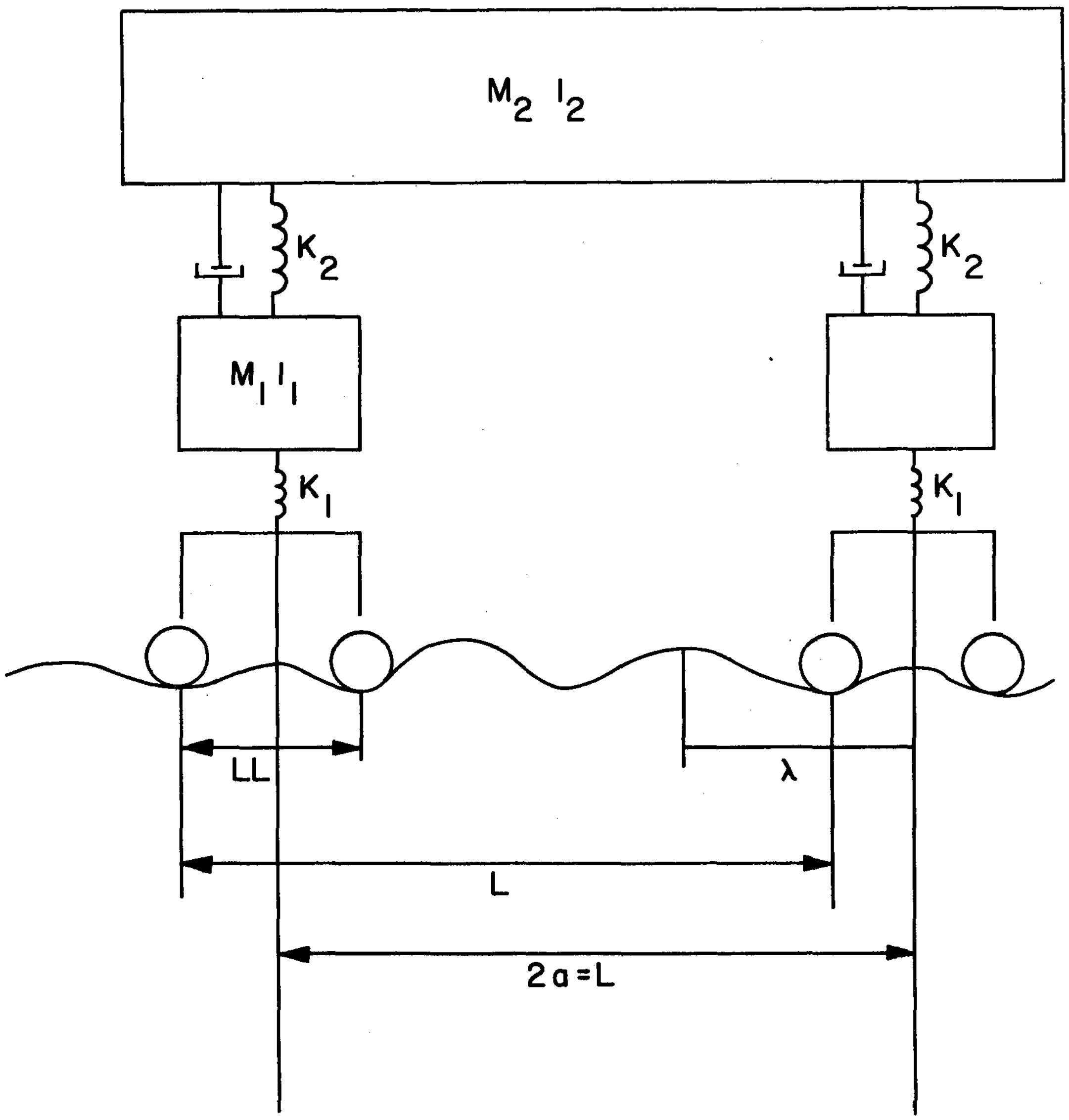

Figure C-3. Full Car Model Assumed in Program

INPUT FREQUENCIES

The user may determine the frequency values against which he wants the equations plotted and input these himself, the only restriction being that the plot routine is equipped to handle a range of 0 to 100.

The actual frequencies are computed within the program from the information input on the 9th and 10 data cards.

The smallest frequency value computed in the first frequency limit (FL) and is punched beginning in column 1 of the 10th data card. This quantity is repeatedly incremented by the first ΔF (DF) on the 9th data card, until it reaches the second F limit, or the second value on the 10th data card. Upon reaching the second limit, the program increments this value by the second ΔF or the second quantity on the 9th data card until it reaches the next limit. This process continues until it arrives at the last limit.

As there will always be one more F limit than ΔF, there will always be one more quantity entered on the 10th data card than on the 9th.

The first equation solved by the program is:

$$\left|\frac{z_2}{\bar{v}}\right| = \frac{\left(1 + \frac{2\beta s}{\omega_{2z}}\right)}{\left[1 + \frac{2\beta s}{\omega_{2z}} + \frac{\omega_{1z}^2 + (2+\mu)\omega_{2z}^2}{2\omega_{1z}^2\ \omega_{2z}^2}\ s^2 + \frac{(2+\mu)\beta}{\omega_{2z}\omega_{1z}^2}\ s^3 + \frac{s^4}{2\omega_{1z}^2\ \omega_{2z}^2}\right]}$$

The value for $z_2/\bar{v}$ is computed for all ω, which are functions of the input frequency values - $\omega = 2\pi f$.

In the above equation and the one which follows:

$s = j\omega$ where $j = \sqrt{-1}$

$\omega_{1z} = \frac{K_1}{M_1}$, referring to Figure 1

$\omega_{2z} = \frac{K_2}{M_2}$, referring to Figure 1

$\mu = \frac{M_2}{M_1}$, referring to Figure 1

Let

$C_1 = \frac{2\beta}{\omega_{2f}}$, $C_2 = \omega_{1z}^2 + (2+\mu)\omega_{2z}^2$

$C_3 = (2+\mu)\beta$, $C_4 = 2_{\omega 1z}^{\ 2}\ \omega_{2z}^2$

$C_5 = \omega_{2z}\ \omega_{1z}^2$

Then let

$A_1 = \frac{C_2}{C_4}$

$$A_2 = \frac{C_3}{C_5}$$

$$A_3 = \frac{1}{C_4}$$

The denominator can now be separated into its real and imaginary part. Since $s^2\left((j\omega)^2\right)$ and $s^4\left((j\omega)^4\right)$ are real numbers, the real terms in the denominator are

$$DR = 1 - \left(A_1 s^2\right) + \left(A_3 s^4\right)$$

$s(j\omega)$ and $s^3\left((j\omega)^3\right)$ are imaginary, the imaginary terms are written

$$DI = C_1 s - \left(A_2 s^3\right)$$

The denominator may be expressed as DR + DI and both numerator and denominator may be multiplied by DR - DI.

$$\frac{(1 + C_1 s)}{(DR + DI)} \times \frac{(DR - DI)}{(DR - DI)}$$

The terms resulting from this multiplication may be grouped by real and imaginary, so that the real terms are written as

$$z2vR = \frac{DR + (C_1 s)(DI)}{DR^2 + DI^2}$$

and the imaginary part is

$$z2vI = -\frac{DI + (C_1 s)(DR)}{DR^2 + DI^2}$$

$$\left|\frac{z_2}{v}\right| = \sqrt{z2vR^2 + z2vI^2}$$

This equation is solved for every value of s for all β's.

The same approach is used in solving the equation

$$\frac{a_\phi}{v_\Delta} = - \frac{\left(1 + \frac{2G\beta s}{\omega_{2z}}\right)}{\left[1 + \frac{2G\beta s}{\omega_{2z}} + \frac{\omega_{1z}^2 + (2G+\mu)\omega_{2z}^2}{2G\omega_{1z}^2\ \omega_{2z}^2} s^2 + \frac{\left(2G^2+\mu\right)\beta}{G\omega_{2z}\ \omega_{1z}^2} s^3 + \frac{s^4}{2\omega_{1z}^2}\right]}$$

Where

$$G = \frac{M_2 a^2}{I_2}$$

Let

$$x_1 = 2G\beta$$

$$x_2 = \omega_{1z}^2 +$$

$$x_3 = 2G\omega_{1z}^2\ \omega_{2z}^2$$

$$x_4 = \left(2G^2 + \mu\right)\beta$$

$$x_5 = G\omega_{2z}\ \omega_{1z}^2$$

Then

$$y_1 = \frac{x_1}{\omega_{2z}}$$

$$y_2 = \frac{x_2}{x_3}$$

$$y_3 = \frac{x_4}{x_5}$$

$$1/4 = \frac{1}{x_3}$$

The next step is separating the real from the imaginary terms in the denominator, since s^2 and s^4 are real

$$yR = 1 - \left(y_2 s^2\right) + \left(y_4 s^4\right)$$

s and s^3 are imaginary, so

$$yI = y_1 s - y_3 s^3$$

Both numerator and denominator are multiplied by YR - yI

$$- \frac{(1 + 2G\beta s)}{(yR + yI)} \times \frac{(yR - yI)}{(yR - yI}$$

After multiplication, the real part is written as

$$APVR = - \frac{yR - \left(yI \times y_{1s}\right)}{yR^2 + yI^2}$$

and the imaginary part is

$$APVI = \frac{yI - (yR \times s)}{yR^2 + yI^2}$$

Therefore,

$$\left|\frac{a_\phi}{v_\Delta}\right| = \sqrt{APVR^2 + APVI^2}$$

The next step in the program is to solve for z_2/v_o for every lambda ($\lambda = \frac{v}{f}$), where v is velocity in mph and f is frequency.

Given that

$$\bar{v} = \frac{1}{4} (v_1 + v_2 + v_3 + v_4)$$

$$v_1 = v_o \sin \frac{2\pi x}{\lambda}$$

$$v_2 = v_1 (x + \ell)$$

$v_3 = v_1(x+L)$

$v_4 = v_2(x+L)$

Where x - vt, L = L in feet (see Figure 1) and 1 = LL in feet (see Figure 1)

Let

$$\bar{f} = \frac{2\pi}{\lambda}$$

$$\frac{\bar{v}}{v_o} = \frac{1}{4}\Big[\sin(\bar{f}x)\big[1 + \cos(\bar{f}\ell) + \cos(\bar{f}L) + \cos(\bar{f}L)\cos(\bar{f}\ell)$$

$$- \sin(\bar{f}\ell)\sin(fL)\cos(fx)\big[\sin(f\ell) + \sin(fL)$$

$$+ \sin(\bar{f}\ell)\cos(fL) + \cos(f\ell)\sin(fL)\big]$$

If

$$A_1 = 1 + \cos(\bar{f}\ell) + \cos(\bar{f}L) + \cos(\bar{f}\ell)\cos(\bar{f}L)$$
$$- \sin(\bar{f}\ell)\sin(\bar{f}L)$$

and

$$B_1 = \sin(\bar{f}\ell) + \sin(\bar{f}L) + \sin(\bar{f}\ell)\cos(\bar{f}L) + \cos(\bar{f}\ell)\sin(\bar{f}L)$$

then

$$\left|\frac{\bar{v}}{v_o}\right| = \left(\frac{1}{4}\left[A_1^2 + B_1^2\right]\right)^{\frac{1}{2}}$$

$\frac{z_2}{v_o}$ may be written as $\frac{z_2}{\bar{v}} \times \frac{\bar{v}}{v_o}$, so

$$\left|\frac{z_2}{v_o}\right| = \left(\frac{1}{4}\left[A_1^2 + B_1^2\right]^{\frac{1}{2}}\right)\left|\frac{z_2}{\bar{v}}\right|$$

Likewise $\frac{a\phi}{v_o}$ may be written as $\frac{a\phi}{v_o} \times \frac{v_o}{v_o}$ so in order to compute

$\frac{a\phi}{v_o}$ for all small λ the program solves first for $\frac{v_\Delta}{v_o}$

$$v_\Delta = \frac{1}{4}\left(v_1+v_2-v_3-v_4\right)$$

so

$$\frac{v_o}{v_o} = \frac{1}{4}\Big[\sin(\bar{f}x)\ 1 + \cos(\bar{f}\ell) - \cos(\bar{f}L) - \cos(\bar{f}\ell)\cos(\bar{f}L)$$
$$+ \sin(\bar{f}\ell)\ \sin + \cos(\bar{f}x)\big[\sin(\bar{f}\ell) - \sin(\bar{f}L)$$
$$- \sin(\bar{f}\ell)\cos(\bar{f}L) - \cos(\bar{f}\ell)\sin(\bar{f}L)\big]$$

Let

$$A_2 = 1 + \cos(\bar{f}\ell) - \cos(\bar{f}L) - \cos(\bar{f}\ell)\cos(\bar{f}L)$$
$$+ \sin(\bar{f}\ell)\sin(\bar{f}L)$$

and

$$B_2 = \sin(\bar{f}\ell) - \sin(\bar{f}L) - \sin(\bar{f}\ell)\cos(\bar{f}L) - \cos(\bar{f}\ell)\sin(\bar{f}L)$$

then

$$\left|\frac{v_\Delta}{v_o}\right| = \frac{1}{4}\left[A_2^2 + B_2^2\right]^{\frac{1}{2}}$$

so

$$\left|\frac{a\phi}{v_o}\right| = \left(\frac{1}{4}\left[A_2^2 + B_2^2\right]^{\frac{1}{2}}\right)\left|\frac{a\phi}{v_\Delta}\right|$$

OUTPUT

The output for this program consists of a list of the input variables and one set of tables for each value of β. Each of these tables contains a list of all frequencies and the corresponding ω and λ, as well as the values of $z_2/\bar{v}$, $a\phi/v_o$, z_2/v_o, and $a\phi/v_o$ for that frequency.

In addition, all curves for each of the above four values are plotted by the CALCOMP plotter against the frequency on a log-log axis.

The following pages contain a listing of the program, followed by sample data cards and sample output. The subroutine which draws the log axes (LAXIS) is listed in binary.

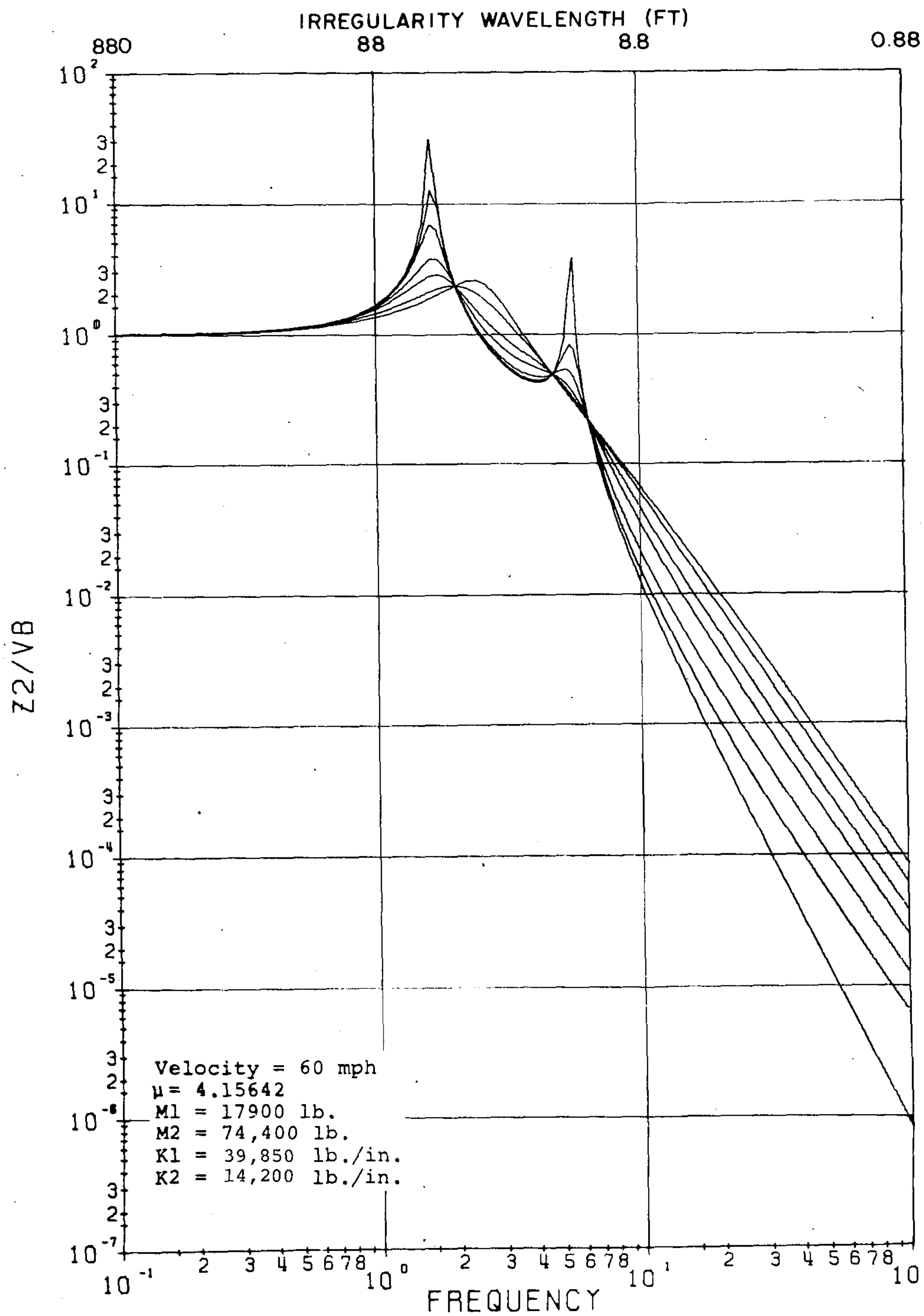

Figure C-4. Car Body Response Characteristics to Track Irregularity for Different Damping Ratios

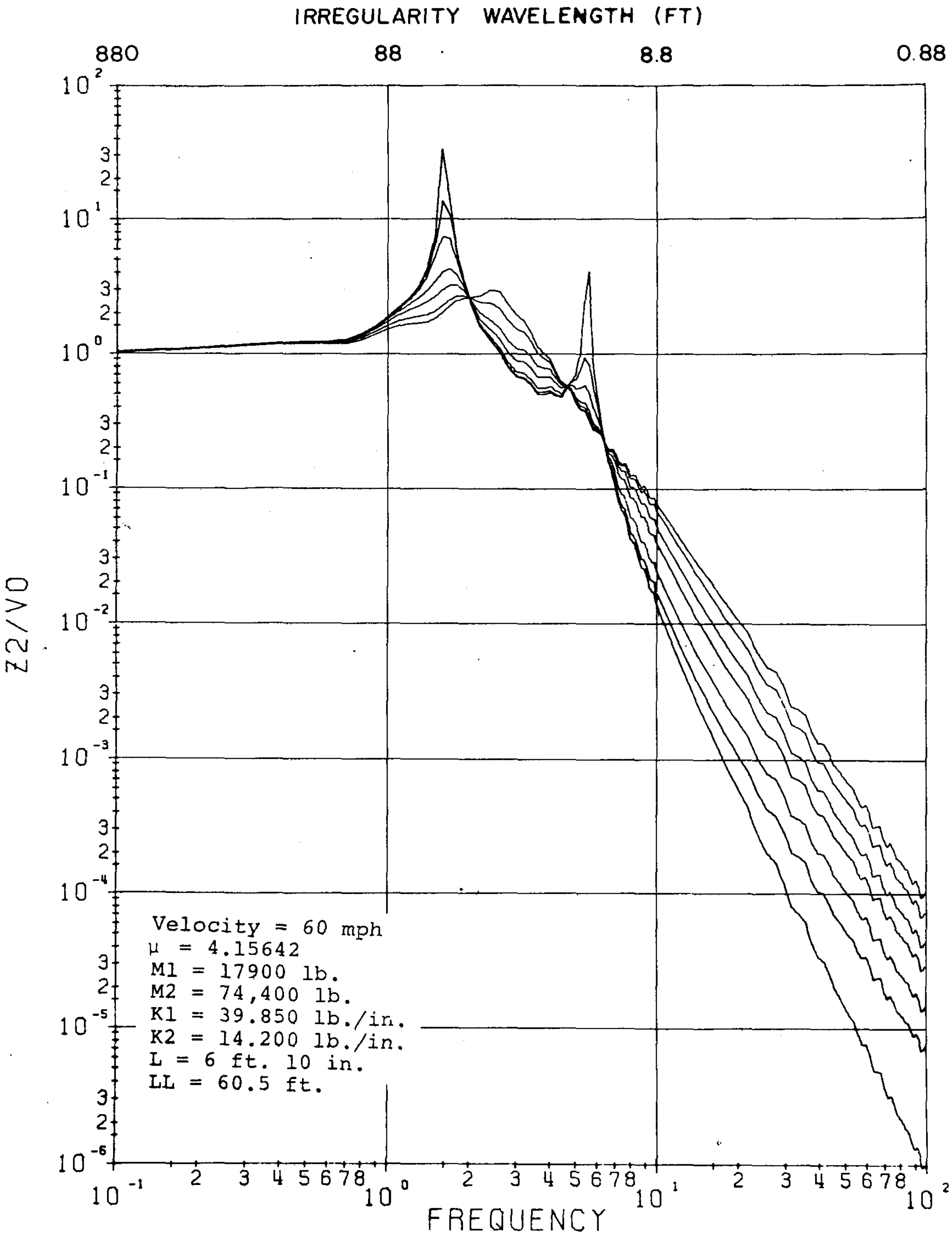

Figure C-5. Car Body Response to Sinusoidal Track Irregularity

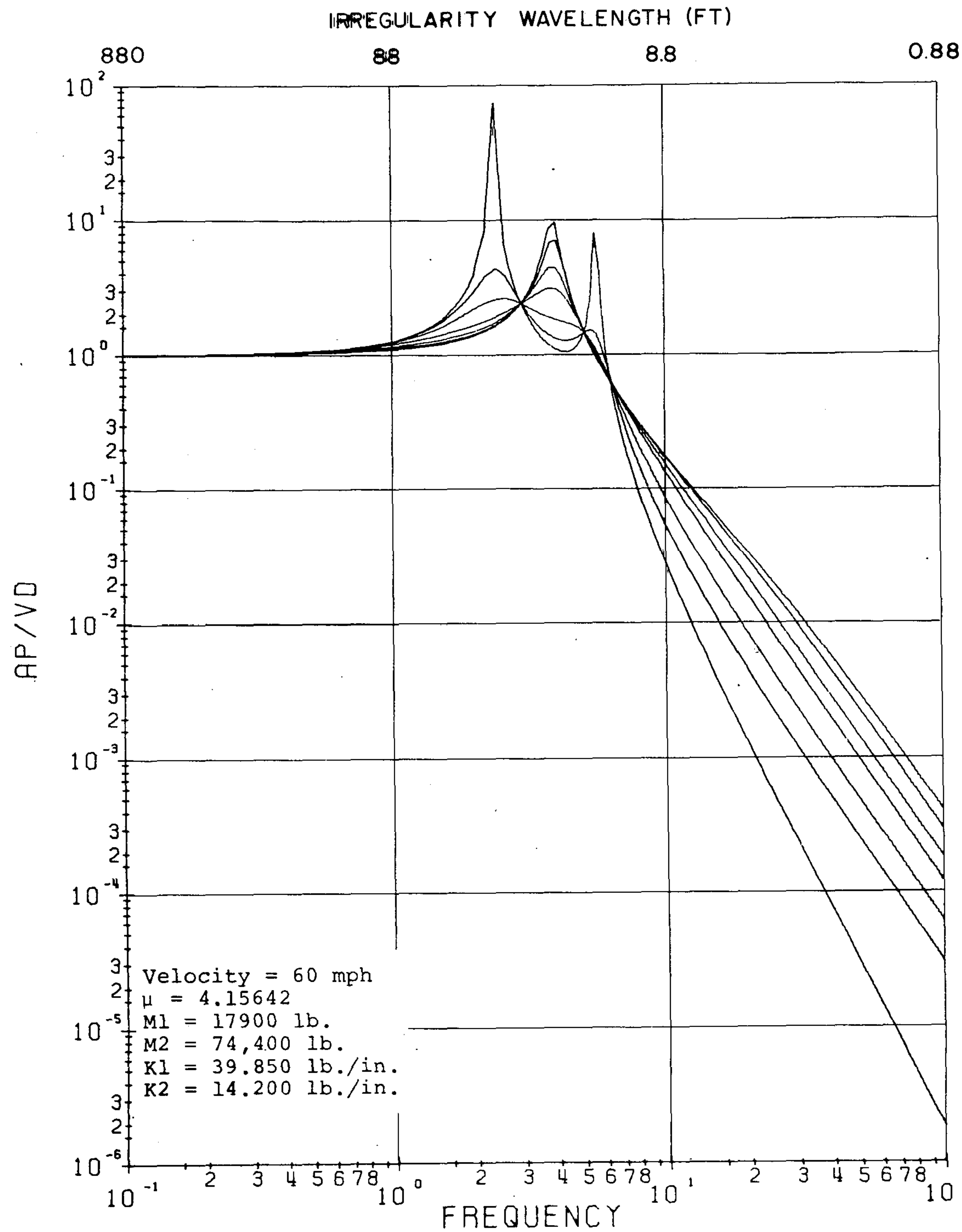

Figure C-6. Car Body Pitch Response Function

```
11/15/69  TIME... 0781.24 MIN
            $EXECUTE        IBJOB
IBJOB VERSICN 5 HAS CONTROL.
$IBJOB          FIOCS
$IBFTC MAIN
```

```
      DIMENSION B(10)
      DIMENSION F(150)
      DIMENSION PF(150)
      DIMENSION LAM(150)
      DIMENSION DF(10)
      DIMENSION FL(10)
      DIMENSION Z2DDV(150,10)
      DIMENSION S(150)
      DIMENSION APDDV(150,10)
      DIMENSION Z2A(150,10)
      DIMENSION APA(150,10)
      DIMENSION IBUF(1024)
      DIMENSION ZADDV(150,10),Z2APA(150,10)
      REAL M
      REAL LAM
      REAL K1, K2
      CALL PLOTS(IBUF,1024)
      CALL PLOT(0.,-11.,-3)
      CALL PLOT(0.,.5,-3)
      PI=3.14159265
C FIRST DATA CARD IS VELOCITY IN MPH
      READ(5,1) V1
    1 FORMAT(F7.3)
      V=V1*5280.0/3600.0
C SECOND DATA CARD IS L IN FEET
      READ(5,2) XL
    2 FORMAT(F7.3)
C THIRD DATA CARD IS LL IN FEET
      READ(5,3) XLL
    3 FORMAT(F7.3)
C FOURTH DATA CARD IS K1
      READ(5,4) K1
C FIFTH DATA CARD IS W1
      READ(5,4) W1
C SIXTH DATA CARD IS K2
      READ(5,4) K2
C SEVENTH DATA CARD IS W2
      READ(5,4) W2
    4 FORMAT(F12.4)
      W1Z=SQRT(K1*386./W1)
      W2Z=SQRT(K2*386./W2)
      M=W2/W1
C EIGHTH DATA CARD IS NUMBER OF DELTA FS
      READ(5,10) NDF
   10 FORMAT(I2)
C NINTH DATA CARD IS DELTA FS
      READ(5,20) (DF(I1),I1=1,NDF)
   20 FORMAT(6F10.4)
      NFL=NDF+1
C TENTH DATA CARD IS F LIMITS
      READ(5,30) (FL(L),L=1,NFL)
   30 FORMAT(7F10.4)
C ELEVENTH DATA CARD IS NUMBER OF BETAS
      READ(5,35) N1
   35 FORMAT(I2)
```

```
C TWELFTH DATA CARD IS VALUES FOR BETA
      READ(5,40) (B(J),J=1,N1)                                35
   40 FORMAT (7F10.4)
C THIRTEENTH DATA CARD IS G
      READ(5,4) G                                             42
      WRITE(6,41) V                                           43
   41 FORMAT(1H1,5X,4HV = ,F7.3)
      WRITE(6,42) XL                                          44
   42 FORMAT(1H0,5X,5HXL = ,F7.3)
      WRITE(6,43) XLL                                         45
   43 FORMAT(1H0,5X,6HXLL = ,F7.3)
      WRITE(6,44) M                                           46
   44 FORMAT(1H0,5X,4HM = ,F10.5)
      WRITE(6,45) W1Z                                         47
   45 FORMAT(1H0,5X,6HW1Z = ,F10.5)
      WRITE(6,46) W2Z                                         48
   46 FORMAT(1H0,5X,6HW2Z = ,F10.5)
      WRITE(6,47) N1                                          49
   47 FORMAT(1H0,5X,18HNUMBER OF BETAS = ,I2)
C COMPUTE FREQUENCIES
      DO 55 J=1,N1
      WRITE(6,48) B(J)                                        52
   48 FORMAT(1H0,5X,7HBETA = ,F10.4)
   55 CONTINUE
      L=0
      N=0
      DO 50 I1=1,NDF
      N2=1
      L=L+1
   70 N=N+1
      XF1=N2-1
      XFN=FL(L)+XF1*DF(I1)
      XF2=XFN-FL(L+1)
      XF2=ABS(XF2)
      IF(XF2.GT..002)GO TO 60
      GO TO 49
   60 F(N)=XFN
      N2=N2+1
      GO TO 70
   49 N=N-1
   50 CONTINUE
      N=N+1
      L=NFL
      F(N)=FL(L)
      NF=N
C COMPUTE LAMBCAS
      DO 80 N=1,NF
      I=N
      LAM(I)=V/F(N)
   80 CONTINUE
C COMPUTE Z2/VM FOR EVERY S FOR ALL BETAS
      DO 100 J=1,N1
      DO 100 I=1,NF
C COMPUTE S FOR EVERY LAMBDA
      S(I)=2.0*PI*F(I)
      C1=2.0*B(J)/W2Z
```

```
      C2=W1Z**2+(2.0+M)*W2Z**2
      C3=(2.0+M)*B(J)
      C4=2.0*(W1Z**2)*(W2Z**2)
      C5=W2Z*W1Z**2
      A1=C2/C4
      A2=C3/C5
      A3=1.0/C4
C REAL TERMS IN DENOMINATOR
      DR=1.0-(A1*S(I)**2)+A3*S(I)**4
C IMAGINARY TERMS IN DENOMINATOR
      DI=C1*S(I)-(A2*S(I)**3)
      DM=DR**2+DI**2
C REAL TERMS
      Z2VR=(DR+C1*S(I)*DI)/DM
C IMAGINARY TERMS
      Z2VI=(-DI+C1*S(I)*DR)/DM
C Z2/VM EQUALS
      Z2VM=SQRT(Z2VR**2+Z2VI**2)
C COMPUTE APHI/V DELTA FOR EVERY S FOR ALL BETAS
      X1=2.0*G*B(J)                                        111
      X2=W1Z**2+((2.0*G+M)*W2Z**2)
      X3=2.0*G*(W1Z**2)*(W2Z**2)
      X4=(2.0*G**2+M)*B(J)
      X5=G*W2Z*(W1Z**2)
      Y1=X1/W2Z
      Y2=X2/X3
      Y3=X4/X5
      Y4=1.0/X3
C REAL TERMS IN DENOMINATOR
      YR=1.0-(Y2*S(I)**2)+(Y4*S(I)**4)
C IMAGINARY TERMS IN DENOMINATOR
      YI=(Y1*S(I))-(Y3*S(I)**3)
      YM=(YR**2)+(YI**2)
C REAL TERMS
      APVR=(-YR-(YI*Y1*S(I)))/YM
C IMAGINARY TERMS
      APVI=(YI-YR*(Y1*S(I)))/YM
C APHI/V DELTA EQUALS
      APVD=SQRT(APVR**2+APVI**2)
      FB=2.0*PI/LAM(I)                                     122
C COMPUTE Z2/VO FOR EVERY LAMBDA FOR ALL BETAS
      FBLL=FB*XLL
      FBL=FB*XL
      CFBLL=COS(FBXLL)
      CFBL=COS(FBXL)                                       124
      SFBLL=SIN(FBLL)                                      125
      SFBL=SIN(FBL)                                        126
      A1=1.0+CFBLL+CFBL+CFBLL*CFBL-SFBLL*SFBL              127
      B1=SFBLL+SFBL+SFBLL*CFBL+CFBLL*SFBL
C Z2/VO EQUALS
      Z2VN=(SQRT(A1**2+B1**2)*Z2VM)/4.0
C COMPUTE APHI/VO FOR EVERY LAMBDA FOR ALL BETAS
      A2=1.0+CFBLL-CFBL-CFBLL*CFBL+SFBLL*SFBL              128
      B2=SFBLL-SFBL-SFBLL*CFBL-CFBLL*SFBL
C APHI/VO EQUALS
      APVN=(SQRT(A2**2+B2**2)*APVD)/4.0
```

```
C COMPUTE Z2/VO + A PHI/VO                                                    129
      P1=Z2VR*A1
      P2=Z2VI*B1
      P3=Z2VI*A1
      P4=Z2VR*B1
      ZAR1=P1-P2
      ZAI1=P3+P4
      P5=APVR*A2
      P6=APVI*B2
      P7=APVR*B2
      P8=APVI*A2
      ZAR2=P5-P6
      ZAI2=P7+P8
      ZAR3=ZAR1+ZAR2
      ZAI3=ZAI1+ZAI2
      ZAVN=SQRT(ZAR3**2+ZAI3**2)/4.0                                          130
      PF(I)=((2.0*PI*F(I))**2)/386.
      Z2DDV(I,J)=PF(I)*Z2VN
      APDDV(I,J)=PF(I)*APVN
      ZADDV(I,J)=ZAVN*PF(I)
      Z2A(I,J)=Z2DDV(I,J)*LAM(I)
      APA(I,J)=APDDV(I,J)*LAM(I)
      Z2APA(I,J)=ZADDV(I,J)*LAM(I)
  100 CONTINUE
      DO 120 J=1,N1
   94 FORMAT(1H1,3X,5HBETA=,F6.4)
      WRITE(6,94) B(J)                                                        154
      WRITE(6,110)                                                            156
  110 FORMAT(1H0,5X,4HFREQ,14X,5HZDDVO,11X,6HAPDDVO,11X,4HZ2/A,14X,4HAP/
     1A)
      DO 119 I=1,NF
      WRITE (6,112) F(I),Z2DDV(I,J),APDDV(I,J),Z2A(I,J),APA(I,J)              158
  112 FORMAT(1H0,5(2X,E13.6,2X))
  119 CONTINUE
  120 CONTINUE
      DO 140 J=1,N1
      WRITE(6,94) B(J)                                                        171
      WRITE(6,125)                                                            173
  125 FORMAT(1H0,5X,4HFREQ,14X,7HZ+ADD/V,11X,7HZ2+AP/A)
      DO 130 I=1,NF
      WRITE(6,126) F(I),ZADDV(I,J),Z2APA(I,J)                                 175
  126 FORMAT(1H0,3(2X,E13.6,2X))
  130 CONTINUE
  140 CONTINUE
      DO 200 I=1,NF
      F(I)=ALOG10(F(I))                                                       188
      DO 300 J=1,N1
      Z2DDV(I,J)=ALOG10(Z2DDV(I,J))                                           193
      IF(APDDV(I,J).LT..0000001)APDDV(I,J)=.0000001
      APDDV(I,J)=ALOG10(APDDV(I,J))                                           200
      Z2A(I,J)=ALOG10(Z2A(I,J))                                               203
      IF(APA(I,J).LT..000001)APA(I,J)=.000001
      APA(I,J)=ALOG10(APA(I,J))                                               210
      Z2APA(I,J)=ALOG10(Z2APA(I,J))                                           213
      ZADDV(I,J)=ALOG10(ZADDV(I,J))                                           216
  300 CONTINUE
```

```
 200 CONTINUE
     F(NF+1)=-1.
     F(NF+2)=.5
     DO 500 J=1,N1
     Z2DDV(NF+1,J)=-5.
     Z2DDV(NF+2,J)=1.
     APDDV(NF+1,J)=-7.
     APDDV(NF+2,J)=1.
     Z2A(NF+1,J)=-5.
     Z2A(NF+2,J)=1.
     APA(NF+1,J)=-6.
     APA(NF+2,J)=1.
     Z2APA(NF+1,J)=-4.
     Z2APA(NF+2,J)=1.
     ZADDV(NF+1,J)=-5.
     ZADDV(NF+2,J)=1.
 500 CONTINUE
     CALL LAXIS(0.,0.,3,9HFREQUENCY,9,6.,-1,2)                243
     CALL LAXIS(0.,0.,7,6HZDD/V0,6,7.,-5,1)                   245
     CALL SYMBOL(1.,3.,.14,3HV =,0.,3)                        247
     CALL NUMBER(999.,999.,14,V1,0,0.,0)                      249
     CALL SYMBOL(999.,999.,.14,3HMPH,0.,3)                    251
     CALL SYMBOL(1.0,2.5,.14,3HG =,0.,3)                      253
     CALL NUMBER(999.,999.,.14,G,0.,2)                        255
     DO 1010 I=1,N1
     CALL LINE(F,Z2DDV(1,I),NF,1,0)                           261
     XP=(F(NF)-F(NF+1))/F(NF+2)
     YP=(Z2DDV(NF,I)-Z2DDV(NF+1,I))/Z2DDV(NF+2,I)
     CALL SYMBOL(XP,YP,.07,3HB =,0.,3)                        269
     CALL NUMBER(999.,999.,.07,B(I),0.,2)                     272
1010 CONTINUE
     CALL PLOT(12.,0.,-3)                                     276
     CALL LAXIS(0.,0.,3,9HFREQUENCY,9,6.,-1,2)                278
     CALL LAXIS(0.,0.,9,7HAPDD/V0,7,9.,-7,1)                  280
     CALL SYMBOL(1.,3.,.14,3HV =,0.,3)                        282
     CALL NUMBER(999.,999.,.14,V1,0,0.,0)                     284
     CALL SYMBOL(999.,999.,.14,3HMPH,0.,3)                    286
     CALL SYMBOL(1.0,2.5,.14,3HG =,0.,3)                      288
     CALL NUMBER(999.,999.,.14,G,0.,2)                        290
     DO 1020 I=1,N1
     CALL LINE(F,APDDV(1,I),NF,1,0)                           296
     XP=(F(NF)-F(NF+1))/F(NF+2)
     YP=(APDDV(NF,I)-APDDV(NF+1,I))/APDDV(NF+2,I)
     CALL SYMBOL(XP,YP,.07,3HB =,0.,3)                        304
     CALL NUMBER(999.,999.,.07,B(I),0.,2)                     307
1020 CONTINUE
     CALL PLOT(12.,0.,-3)                                     311
     CALL LAXIS(0.,0.,3,9HFREQUENCY,9,6.,-1,2)                313
     CALL LAXIS(0.,0.,7,4HZ2/A,4,7.,-5,1)                     315
     CALL SYMBOL(1.,3.,.14,3HV =,0.,3)                        317
     CALL NUMBER(999.,999.,.14,V1,0,0.,0)                     319
     CALL SYMBOL(999.,999.,.14,3HMPH,0.,3)                    321
     CALL SYMBOL(1.0,2.5,.14,3HG =,0.,3)                      323
     CALL NUMBER(999.,999.,.14,G,0.,2)                        325
     DO 1030 I=1,N1
     XP=(F(NF)-F(NF+1))/F(NF+2)
```

```
      YP=(Z2A(NF,I)-Z2A(NF+1,I))/Z2A(NF+2,I)
      CALL SYMBOL(XP,YP,.07,3HB =,0.,3)                              336
      CALL NUMBER(999.,999.,.07,B(I),0.,2)                           339
      CALL LINE(F,Z2A(1,I),NF,1,0)                                   342
 1030 CONTINUE
      CALL PLOT(12.,0.,-3)                                           346
      CALL LAXIS(0.,0.,3,9HFREQUENCY,9,6.,-1,2)                      348
      CALL LAXIS(0.,0.,9,6HAPHI/A,6,9.,-6,1)                         350
      CALL SYMBOL(1.,3.,.14,3HV =,0.,3)                              352
      CALL NUMBER(999.,999.,.14,V1,0,0.,0)                           354
      CALL SYMBOL(999.,999.,.14,3HMPH,0.,3)                          356
      CALL SYMBOL(1.0,2.5,.14,3HG =,0.,3)                            358
      CALL NUMBER(999.,999.,.14,G,0.,2)                              360
      DO 1040 I=1,N1
      XP=(F(NF)-F(NF+1))/F(NF+2)
      YP=(APA(NF,I)-APA(NF+1,I))/APA(NF+2,I)
      CALL SYMBOL(XP,YP,.07,3HB =,0.,3)                              371
      CALL NUMBER(999.,999.,.07,B(I),0.,2)                           374
      CALL LINE(F,APA(1,I),NF,1,0)                                   377
 1040 CONTINUE
      CALL PLOT(12.,0.,-3)                                           381
      CALL LAXIS(0.,0.,3,9HFREQUENCY,9,6.,-1,2)                      383
      CALL LAXIS(0.,0.,6,10HZ2+APDD/V0,10,6.,-5,1)                   385
      CALL SYMBOL(1.,3.,.14,3HV =,0.,3)                              387
      CALL NUMBER(999.,999.,.14,V1,0,0.,0)                           389
      CALL SYMBOL(999.,999.,.14,3HMPH,0.,3)                          391
      CALL SYMBOL(1.0,2.5,.14,3HG =,0.,3)                            393
      CALL NUMBER(999.,999.,.14,G,0.,2)                              395
      DO 1050 I=1,N1
      XP=(F(NF)-F(NF+1))/F(NF+2)
      YP=(ZADDV(NF,I)-ZADDV(NF+1,I))/ZADDV(NF+2,I)
      CALL SYMBOL(XP,YP,.07,3HB =,0.,3)                              406
      CALL NUMBER(999.,999.,.07,B(I),0.,2)                           409
      CALL LINE(F,ZADDV(1,I),NF,1,0)                                 412
 1050 CONTINUE
      CALL PLOT(12.,0.,-3)                                           416
      CALL LAXIS(0.,0.,3,9HFREQUENCY,9,6.,-1,2)                      418
      CALL LAXIS(0.,0.,7,7HZ2+AP/A,7,7.,-4,1)                        420
      CALL SYMBOL(1.0,3.0,.14,3HV =,0.,3)                            422
      CALL NUMBER(999.,999.,.14,V1,0,0.,0)                           424
      CALL SYMBOL(999.,999.,.14,3HMPH,0.,3)                          426
      CALL SYMBOL(1.0,2.5,.14,3HG =,0.,3)                            428
      CALL NUMBER(999.,999.,.14,G,0.,2)                              430
      DO 1060 I=1,N1
      CALL LINE(F,Z2APA(1,I),NF,1,0)                                 436
      XP=(F(NF)-F(NF+1))/F(NF+2)
      YP=(Z2APA(NF,I)-Z2APA(NF+1,I))/Z2APA(NF+2,I)
      CALL SYMBOL(XP,YP,.07,3HB =,0.,3)                              444
      CALL NUMBER(999.,999.,.07,B(I),0.,2)                           447
 1060 CONTINUE
      CALL PLOT(0.,0.,999)                                           451
      STOP
      END
```

```
V =  88.000

XL =  60.500

XLL =   6.833

M =    4.15642

W1Z =   29.31442

W2Z =    8.58324

NUMBER OF BETAS =  7

BETA =      0.0000

BETA =      0.0500

BETA =      0.1000

BETA =      0.2000

BETA =      0.3000

BETA =      0.5000

BETA =      0.7000
```

BETA=0.0000

FREQ	ZDDVO	APDDVO	Z2/A	AP/A
0.100000E 00	0.104953E-02	0.214602E-03	0.923587E 00	0.188850E 00
0.200000E 00	0.445478E-02	0.157028E-02	0.196010E 01	0.690924E 00
0.300000E 00	0.106330E-01	0.452567E-02	0.311901E 01	0.132753E 01
0.400000E 00	0.196149E-01	0.839675E-02	0.431528E 01	0.184729E 01
0.500000E 00	0.310449E-01	0.112887E-01	0.546389E 01	0.198682E 01
0.600000E 00	0.450102E-01	0.104950E-01	0.660149E 01	0.153926E 01
0.700000E 00	0.634374E-01	0.331926E-02	0.797499E 01	0.417279E 00
0.800000E 00	0.907343E-01	0.118405E-01	0.998078E 01	0.130245E 01
0.900000E 00	0.132208E 00	0.344027E-01	0.129270E 02	0.336382E 01
0.100000E 01	0.191909E 00	0.608077E-01	0.168880E 02	0.535108E 01
0.110000E 01	0.273169E 00	0.843042E-01	0.218535E 02	0.674434E 01
0.120000E 01	0.383596E 00	0.955231E-01	0.281304E 02	0.700503E 01
0.130000E 01	0.549609E 00	0.839109E-01	0.372043E 02	0.568013E 01
0.140000E 01	0.863934E 00	0.399342E-01	0.543044E 02	0.251015E 01
0.150000E 01	0.172548E 01	0.421928E-01	0.101228E 03	0.247531E 01
0.160000E 01	0.883727E 01	0.161605E 00	0.486050E 03	0.888827E 01
0.170000E 01	0.428502E 01	0.308044E 00	0.221813E 03	0.159458E 02
0.180000E 01	0.201307E 01	0.459367E 00	0.984166E 02	0.224579E 02
0.190000E 01	0.138409E 01	0.578610E 00	0.641051E 02	0.267988E 02
0.200000E 01	0.106629E 01	0.607460E 00	0.469166E 02	0.267282E 02
0.220000E 01	0.780933E 00	0.170960E 00	0.312373E 02	0.683840E 01
0.240000E 01	0.736875E 00	0.195232E 02	0.270188E 02	0.715850E 03
0.260000E 01	0.707107E 00	0.244402E 01	0.239328E 02	0.827207E 02
0.280000E 01	0.630191E 00	0.698352E 00	0.198060E 02	0.219482E 02
0.300000E 01	0.620352E 00	0.463922E 00	0.181970E 02	0.136084E 02
0.320000E 01	0.682027E 00	0.101108E 01	0.187557E 02	0.278047E 02
0.340000E 01	0.687947E 00	0.844081E 00	0.178057E 02	0.218468E 02

0.360000E 01	0.662018E 00	0.150072E 00	0.161827E 02	0.366842E 01
0.380000E 01	0.734712E 00	0.622237E 00	0.170144E 02	0.144097E 02
0.400000E 01	0.840986E 00	0.981795E 00	0.185017E 02	0.215995E 02

BETA=0.5000

FREQ	ZDDVO	APDDVO	Z2/A	AP/A
0.100000E 00	0.104952E-02	0.214594E-03	0.923573E 00	0.188843E 00
0.200000E 00	0.445376E-02	0.156940E-02	0.195965E 01	0.690535E 00
0.300000E 00	0.106207E-01	0.451406E-02	0.311539E 01	0.132412E 01
0.400000E 00	0.195432E-01	0.833707E-02	0.429950E 01	0.183416E 01
0.500000E 00	0.307683E-01	0.111196E-01	0.541523E 01	0.195704E 01
0.600000E 00	0.441805E-01	0.102152E-01	0.647981E 01	0.149823E 01
0.700000E 00	0.612744E-01	0.317879E-02	0.770307E 01	0.399620E 00
0.800000E 00	0.854611E-01	0.111060E-01	0.940073E 01	0.122166E 01
0.900000E 00	0.119900E 00	0.314509E-01	0.117235E 02	0.307520E 01
0.100000E 01	0.164649E 00	0.538986E-01	0.144891E 02	0.474308E 01
0.110000E 01	0.216245E 00	0.720370E-01	0.172996E 02	0.576296E 01
0.120000E 01	0.270090E 00	0.781837E-01	0.198066E 02	0.573347E 01
0.130000E 01	0.325032E 00	0.653047E-01	0.220022E 02	0.442063E 01
0.140000E 01	0.388387E 00	0.293000E-01	0.244129E 02	0.184172E 01
0.150000E 01	0.475203E 00	0.288870E-01	0.278786E 02	0.169471E 01
0.160000E 01	0.595686E 00	0.101947E 00	0.327627E 02	0.560707E 01
0.170000E 01	0.741284E 00	0.176207E 00	0.383723E 02	0.912128E 01
0.180000E 01	0.886061E 00	0.233279E 00	0.433185E 02	0.114048E 02
0.190000E 01	0.100168E 01	0.253341E 00	0.463936E 02	0.117337E 02
0.200000E 01	0.107645E 01	0.219625E 00	0.473636E 02	0.966348E 01
0.220000E 01	0.119375E 01	0.320187E-01	0.477501E 02	0.128075E 01
0.240000E 01	0.140897E 01	0.431778E 00	0.516622E 02	0.158318E 02
0.260000E 01	0.151661E 01	0.679284E 00	0.513313E 02	0.229911E 02
0.280000E 01	0.142061E 01	0.418093E 00	0.446478E 02	0.131401E 02
0.300000E 01	0.141068E 01	0.471581E 00	0.413799E 02	0.138330E 02
0.320000E 01	0.152072E 01	0.160867E 01	0.418199E 02	0.442383E 02
0.340000E 01	0.147130E 01	0.205938E 01	0.380807E 02	0.533015E 02
0.360000E 01	0.133226E 01	0.568158E 00	0.325663E 02	0.138883E 02
0.380000E 01	0.136575E 01	0.356840E 01	0.316279E 02	0.826367E 02
0.400000E 01	0.141619E 01	0.632592E 01	0.311563E 02	0.139170E 03

BETA=0.1000

FREQ	ZDDVO	APDDVO	Z2/A	AP/A
0.100000E 00	0.104953E-02	0.214602E-03	0.923586E 00	0.188850E 00
0.200000E 00	0.445474E-02	0.157024E-02	0.196009E 01	0.690907E 00
0.300000E 00	0.106325E-01	0.452509E-02	0.311886E 01	0.132736E 01
0.400000E 00	0.196118E-01	0.839335E-02	0.431459E 01	0.184654E 01
0.500000E 00	0.310322E-01	0.112774E-01	0.546167E 01	0.198483E 01
0.600000E 00	0.449698E-01	0.104729E-01	0.659558E 01	0.153602E 01
0.700000E 00	0.633238E-01	0.330608E-02	0.796071E 01	0.415621E 00
0.800000E 00	0.904300E-01	0.117586E-01	0.994731E 01	0.129344E 01
0.900000E 00	0.131411E 00	0.340121E-01	0.128491E 02	0.332562E 01
0.100000E 01	0.189873E 00	0.597260E-01	0.167088E 02	0.525589E 01
0.110000E 01	0.268085E 00	0.820399E-01	0.214468E 02	0.656320E 01
0.120000E 01	0.370850E 00	0.917628E-01	0.271957E 02	0.672927E 01
0.130000E 01	0.515487E 00	0.791863E-01	0.348945E 02	0.536030E 01
0.140000E 01	0.754612E 00	0.367827E-01	0.474328E 02	0.231205E 01
0.150000E 01	0.121238E 01	0.376054E-01	0.711263E 02	0.220618E 01
0.160000E 01	0.194216E 01	0.137755E 00	0.106819E 03	0.757651E 01
0.170000E 01	0.211318E 01	0.247148E 00	0.109388E 03	0.127935E 02
0.180000E 01	0.168582E 01	0.339230E 00	0.824181E 02	0.165846E 02
0.190000E 01	0.132024E 01	0.380868E 00	0.611478E 02	0.176402E 02
0.200000E 01	0.106745E 01	0.339668E 00	0.469677E 02	0.149454E 02
0.220000E 01	0.811755E 00	0.510974E-01	0.324702E 02	0.204390E 01
0.240000E 01	0.779208E 00	0.674708E 00	0.285709E 02	0.247393E 02
0.260000E 01	0.756531E 00	0.971396E 00	0.256056E 02	0.328780E 02
0.280000E 01	0.680766E 00	0.511850E 00	0.213955E 02	0.160867E 02
0.300000E 01	0.675850E 00	0.467814E 00	0.198249E 02	0.137225E 02
0.320000E 01	0.748615E 00	0.123511E 01	0.205869E 02	0.339656E 02
0.340000E 01	0.759809E 00	0.116796E 01	0.196656E 02	0.302296E 02

0.360000E 01	0.734349E 00	0.226015E 00	0.179508E 02	0.552482E 01
0.380000E 01	0.816177E 00	0.992538E 00	0.189009E 02	0.229851E 02

BETA=0.2000

FREQ	ZDDVO	APDDVO	Z2/A	AP/A
0.100000E 00	0.104953E-02	0.214601E-03	0.923585E 00	0.188849E 00
0.200000E 00	0.445462E-02	0.157013E-02	0.196003E 01	0.690856E 00
0.300000E 00	0.106309E-01	0.452344E-02	0.311841E 01	0.132688E 01
0.400000E 00	0.196026E-01	0.838384E-02	0.431256E 01	0.184444E 01
0.500000E 00	0.309952E-01	0.112471E-01	0.545515E 01	0.197948E 01
0.600000E 00	0.448531E-01	0.104162E-01	0.657845E 01	0.152771E 01
0.700000E 00	0.630002E-01	0.327413E-02	0.792002E 01	0.411605E 00
0.800000E 00	0.895811E-01	0.115727E-01	0.985392E 01	0.127300E 01
0.900000E 00	0.129249E 00	0.331904E-01	0.126377E 02	0.324529E 01
0.100000E 01	0.184566E 00	0.576380E-01	0.162418E 02	0.507215E 01
0.110000E 01	0.255581E 00	0.780717E-01	0.204465E 02	0.624573E 01
0.120000E 01	0.342193E 00	0.858502E-01	0.250941E 02	0.629568E 01
0.130000E 01	0.449482E 00	0.726085E-01	0.304265E 02	0.491504E 01
0.140000E 01	0.594925E 00	0.329555E-01	0.373953E 02	0.207149E 01
0.150000E 01	0.804103E 00	0.328298E-01	0.471740E 02	0.192601E 01
0.160000E 01	0.106251E 01	0.116906E 00	0.584380E 02	0.642982E 01
0.170000E 01	0.125849E 01	0.203559E 00	0.651452E 02	0.105372E 02
0.180000E 01	0.129249E 01	0.271009E 00	0.631882E 02	0.132493E 02
0.190000E 01	0.120196E 01	0.295404E 00	0.556697E 02	0.136819E 02
0.200000E 01	0.107006E 01	0.256501E 00	0.470825E 02	0.112860E 02
0.220000E 01	0.891375E 00	0.372561E-01	0.356550E 02	0.149025E 01
0.240000E 01	0.892268E 00	0.495241E 00	0.327165E 02	0.181589E 02
0.260000E 01	0.888361E 00	0.758051E 00	0.300676E 02	0.256571E 02
0.280000E 01	0.813391E 00	0.446298E 00	0.255637E 02	0.140265E 02
0.300000E 01	0.817507E 00	0.470242E 00	0.239802E 02	0.137938E 02
0.320000E 01	0.912648E 00	0.144681E 01	0.250978E 02	0.397872E 02
0.340000E 01	0.929094E 00	0.158352E 01	0.240471E 02	0.409851E 02

0.360000E 01	0.895469E 00	0.346383E 00	0.218892E 02	0.846713E 01
0.380000E 01	0.985235E 00	0.164851E 01	0.228160E 02	0.381760E 02
0.400000E 01	0.110246E 01	0.275206E 01	0.242540E 02	0.605453E 02

BETA=0.3000

FREQ	ZDDVO	APDDVO	Z2/A	AP/A
0.100000E 00	0.104952E-02	0.214599E-03	0.923582E 00	0.188847E 00
0.200000E 00	0.445441E-02	0.156994E-02	0.195994E 01	0.690774E 00
0.300000E 00	0.106284E-01	0.452088E-02	0.311767E 01	0.132612E 01
0.400000E 00	0.195876E-01	0.836995E-02	0.430927E 01	0.184139E 01
0.500000E 00	0.309363E-01	0.112056E-01	0.544478E 01	0.197219E 01
0.600000E 00	0.446714E-01	0.103449E-01	0.655181E 01	0.151725E 01
0.700000E 00	0.625117E-01	0.323737E-02	0.785862E 01	0.406984E 00
0.800000E 00	0.883483E-01	0.113786E-01	0.971831E 01	0.125165E 01
0.900000E 00	0.126264E 00	0.324165E-01	0.123458E 02	0.316961E 01
0.100000E 01	0.177710E 00	0.558722E-01	0.156385E 02	0.491675E 01
0.110000E 01	0.240826E 00	0.750695E-01	0.192661E 02	0.600556E 01
0.120000E 01	0.312406E 00	0.818595E-01	0.229098E 02	0.600303E 01
0.130000E 01	0.392388E 00	0.686548E-01	0.265616E 02	0.464740E 01
0.140000E 01	0.489535E 00	0.309088E-01	0.307708E 02	0.194284E 01
0.150000E 01	0.619944E 00	0.305574E-01	0.363700E 02	0.179270E 01
0.160000E 01	0.786577E 00	0.108068E 00	0.432617E 02	0.594376E 01
0.170000E 01	0.955889E 00	0.187057E 00	0.494813E 02	0.968295E 01
0.180000E 01	0.107257E 01	0.247841E 00	0.524365E 02	0.121167E 02
0.190000E 01	0.110595E 01	0.269193E 00	0.512228E 02	0.124679E 02
0.200000E 01	0.107274E 01	0.233246E 00	0.472006E 02	0.102628E 02
0.220000E 01	0.993963E 00	0.338986E-01	0.397585E 02	0.135594E 01
0.240000E 01	0.104867E 01	0.454264E 00	0.384514E 02	0.166564E 02
0.260000E 01	0.107240E 01	0.707313E 00	0.362966E 02	0.239398E 02
0.280000E 01	0.994691E 00	0.428376E 00	0.312617E 02	0.134632E 02
0.300000E 01	0.100364E 01	0.471068E 00	0.294401E 02	0.138180E 02
0.320000E 01	0.111677E 01	0.154146E 01	0.307111E 02	0.423902E 02
0.340000E 01	0.112574E 01	0.183616E 01	0.291369E 02	0.475242E 02

0.360000E 01	0.106746E 01	0.445724E 00	0.260935E 02	0.108955E 02
0.380000E 01	0.114809E 01	0.232711E 01	0.265872E 02	0.538910E 02
0.400000E 01	0.124810E 01	0.395401E 01	0.274582E 02	0.869883E 02

BETA=0.0500

FREQ	ZDDVO	APDDVO	Z2/A	AP/A
0.100000E 00	0.104953E-02	0.214602E-03	0.923587E 00	0.188850E 00
0.200000E 00	0.445477E-02	0.157027E-02	0.196010E 01	0.690920E 00
0.300000E 00	0.106329E-01	0.452552E-02	0.311897E 01	0.132749E 01
0.400000E 00	0.196141E-01	0.839589E-02	0.431511E 01	0.184710E 01
0.500000E 00	0.310417E-01	0.112859E-01	0.546334E 01	0.198631E 01
0.600000E 00	0.450000E-01	0.104893E-01	0.660001E 01	0.153843E 01
0.700000E 00	0.634087E-01	0.331582E-02	0.797138E 01	0.416846E 00
0.800000E 00	0.906572E-01	0.118188E-01	0.997229E 01	0.130007E 01
0.900000E 00	0.132005E 00	0.342974E-01	0.129071E 02	0.335353E 01
0.100000E 01	0.191386E 00	0.605101E-01	0.168419E 02	0.532489E 01
0.110000E 01	0.271846E 00	0.836656E-01	0.217477E 02	0.669325E 01
0.120000E 01	0.380212E 00	0.944309E-01	0.278822E 02	0.692493E 01
0.130000E 01	0.540207E 00	0.824894E-01	0.365679E 02	0.558390E 01
0.140000E 01	0.831280E 00	0.389450E-01	0.522519E 02	0.244797E 01
0.150000E 01	0.153380E 01	0.406777E-01	0.899832E 02	0.238642E 01
0.160000E 01	0.357047E 01	0.153224E 00	0.196376E 03	0.842732E 01
0.170000E 01	0.318192E 01	0.284963E 00	0.164711E 03	0.147510E 02
0.180000E 01	0.190906E 01	0.409407E 00	0.933319E 02	0.200155E 02
0.190000E 01	0.136632E 01	0.486505E 00	0.632822E 02	0.225328E 02
0.200000E 01	0.106659E 01	0.464403E 00	0.469301E 02	0.204337E 02
0.220000E 01	0.788876E 00	0.811715E-01	0.315550E 02	0.324686E 01
0.240000E 01	0.747721E 00	0.113701E 01	0.274164E 02	0.416903E 02
0.260000E 01	0.719783E 00	0.142247E 01	0.243619E 02	0.481451E 02
0.280000E 01	0.643216E 00	0.605845E 00	0.202154E 02	0.190408E 02
0.300000E 01	0.634735E 00	0.465456E 00	0.186189E 02	0.136534E 02
0.320000E 01	0.699424E 00	0.108791E 01	0.192342E 02	0.299175E 02
0.340000E 01	0.706912E 00	0.946652E 00	0.182966E 02	0.245016E 02

0.360000E 01	0.681351E 00	0.173156E 00	0.166552E 02	0.423271E 01
0.380000E 01	0.756845E 00	0.733252E 00	0.175269E 02	0.169806E 02
0.400000E 01	0.866068E 00	0.117531E 01	0.190535E 02	0.258568E 02

BETA=0.7000

FREQ	ZDDVO	APDDVO	Z2/A	AP/A
0.100000E 00	0.104950E-02	0.214587E-03	0.923561E 00	0.188836E 00
0.200000E 00	0.445282E-02	0.156870E-02	0.195924E 01	0.690227E 00
0.300000E 00	0.106099E-01	0.450657E-02	0.311223E 01	0.132193E 01
0.400000E 00	0.194848E-01	0.830661E-02	0.428666E 01	0.182745E 01
0.500000E 00	0.305629E-01	0.110520E-01	0.537908E 01	0.194515E 01
0.600000E 00	0.436290E-01	0.101278E-01	0.639891E 01	0.148542E 01
0.700000E 00	0.600129E-01	0.314430E-02	0.754448E 01	0.395284E 00
0.800000E 00	0.828203E-01	0.109632E-01	0.911023E 01	0.120596E 01
0.900000E 00	0.114733E 00	0.309938E-01	0.112184E 02	0.303051E 01
0.100000E 01	0.155331E 00	0.530417E-01	0.136691E 02	0.466767E 01
0.110000E 01	0.200966E 00	0.708137E-01	0.160773E 02	0.566509E 01
0.120000E 01	0.247314E 00	0.767908E-01	0.181364E 02	0.563132E 01
0.130000E 01	0.293674E 00	0.641011E-01	0.198795E 02	0.433915E 01
0.140000E 01	0.347324E 00	0.287476E-01	0.218318E 02	0.180699E 01
0.150000E 01	0.422708E 00	0.283350E-01	0.247989E 02	0.166232E 01
0.160000E 01	0.530875E 00	0.999885E-01	0.291981E 02	0.549937E 01
0.170000E 01	0.668182E 00	0.172829E 00	0.345882E 02	0.894646E 01
0.180000E 01	0.817143E 00	0.228850E 00	0.399492E 02	0.111882E 02
0.190000E 01	0.957060E 00	0.248610E 00	0.443270E 02	0.115146E 02
0.200000E 01	0.107835E 01	0.215622E 00	0.474475E 02	0.948735E 01
0.220000E 01	0.134387E 01	0.314780E-01	0.537550E 02	0.125912E 01
0.240000E 01	0.176355E 01	0.425373E 00	0.646634E 02	0.155970E 02
0.260000E 01	0.200299E 01	0.671283E 00	0.677934E 02	0.227204E 02
0.280000E 01	0.187236E 01	0.415109E 00	0.588455E 02	0.130463E 02
0.300000E 01	0.179603E 01	0.471735E 00	0.526835E 02	0.138376E 02
0.320000E 01	0.185007E 01	0.163043E 01	0.508770E 02	0.448367E 02
0.340000E 01	0.171160E 01	0.214253E 01	0.443004E 02	0.554536E 02
0.360000E 01	0.148986E 01	0.628610E 00	0.364187E 02	0.153660E 02
0.380000E 01	0.147773E 01	0.458233E 01	0.342211E 02	0.106117E 03
0.400000E 01	0.149195E 01	0.854440E 01	0.328230E 02	0.187977E 03

BETA=0.0000

FREQ	Z+ADD/V	Z2+AP/A
0.100000E 00	0.111349E-02	0.979872E 00
0.200000E 00	0.522330E-02	0.229825E 01
0.300000E 00	0.132392E-01	0.388349E 01
0.400000E 00	0.245175E-01	0.539385E 01
0.500000E 00	0.368821E-01	0.649124E 01
0.600000E 00	0.487326E-01	0.714745E 01
0.700000E 00	0.637183E-01	0.801031E 01
0.800000E 00	0.932792E-01	0.102607E 02
0.900000E 00	0.146922E 00	0.143657E 02
0.100000E 01	0.224308E 00	0.197391E 02
0.110000E 01	0.319865E 00	0.255892E 02
0.120000E 01	0.431386E 00	0.316350E 02
0.130000E 01	0.579988E 00	0.392607E 02
0.140000E 01	0.869469E 00	0.546523E 02
0.150000E 01	0.173009E 01	0.101498E 03
0.160000E 01	0.888419E 01	0.488630E 03
0.170000E 01	0.417141E 01	0.215932E 03
0.180000E 01	0.185429E 01	0.906541E 02
0.190000E 01	0.125310E 01	0.580384E 02
0.200000E 01	0.103641E 01	0.456023E 02
0.220000E 01	0.792853E 00	0.317141E 02
0.240000E 01	0.198113E 02	0.726414E 03
0.260000E 01	0.282569E 01	0.956387E 02
0.280000E 01	0.103908E 01	0.326567E 02
0.300000E 01	0.841565E 00	0.246859E 02
0.320000E 01	0.144212E 01	0.396584E 02
0.340000E 01	0.128109E 01	0.331577E 02

BETA=0.0500

FREQ	Z+ADD/V	Z2+AP/A
0.100000E 00	0.111349E-02	0.979873E 00
0.200000E 00	0.522332E-02	0.229826E 01
0.300000E 00	0.132393E-01	0.388352E 01
0.400000E 00	0.245174E-01	0.539382E 01
0.500000E 00	0.368803E-01	0.649093E 01
0.600000E 00	0.487246E-01	0.714628E 01
0.700000E 00	0.636910E-01	0.800686E 01
0.800000E 00	0.931947E-01	0.102514E 02
0.900000E 00	0.146694E 00	0.143434E 02
0.100000E 01	0.223771E 00	0.196918E 02
0.110000E 01	0.318728E 00	0.254982E 02
0.120000E 01	0.428975E 00	0.314582E 02
0.130000E 01	0.573377E 00	0.388132E 02
0.140000E 01	0.840554E 00	0.528348E 02
0.150000E 01	0.152773E 01	0.896268E 02
0.160000E 01	0.348594E 01	0.191726E 03
0.170000E 01	0.289836E 01	0.150033E 03
0.180000E 01	0.153485E 01	0.750370E 02
0.190000E 01	0.951007E 00	0.440466E 02
0.200000E 01	0.696415E 00	0.306423E 02
0.220000E 01	0.856383E 00	0.342553E 02
0.240000E 01	0.182903E 01	0.670643E 02
0.260000E 01	0.213998E 01	0.724300E 02
0.280000E 01	0.121916E 01	0.383163E 02
0.300000E 01	0.561289E 00	0.164645E 02
0.320000E 01	0.118475E 01	0.325807E 02
0.340000E 01	0.109555E 01	0.283553E 02
0.360000E 01	0.630875E 00	0.154214E 02
0.380000E 01	0.137284E 01	0.317920E 02

0.360000E 01	0.690133E 00	0.168699E 02
0.380000E 01	0.109971E 01	0.254671E 02
0.400000E 01	0.155232E 01	0.341510E 02

BETA=0.1000

FREQ	Z+ADD/V	Z2+AP/A
0.100000E 00	0.111349E-02	0.979873E 00
0.200000E 00	0.522331E-02	0.229826E 01
0.300000E 00	0.132389E-01	0.388341E 01
0.400000E 00	0.245144E-01	0.539318E 01
0.500000E 00	0.368681E-01	0.648879E 01
0.600000E 00	0.486899E-01	0.714118E 01
0.700000E 00	0.636049E-01	0.799604E 01
0.800000E 00	0.929630E-01	0.102259E 02
0.900000E 00	0.146046E 00	0.142801E 02
0.100000E 01	0.222114E 00	0.195461E 02
0.110000E 01	0.314867E 00	0.251893E 02
0.120000E 01	0.420164E 00	0.308120E 02
0.130000E 01	0.550848E 00	0.372882E 02
0.140000E 01	0.766634E 00	0.481884E 02
0.150000E 01	0.120127E 01	0.704742E 02
0.160000E 01	0.186693E 01	0.102681E 03
0.170000E 01	0.189264E 01	0.979721E 02
0.180000E 01	0.134983E 01	0.659917E 02
0.190000E 01	0.939715E 00	0.435236E 02
0.200000E 01	0.734320E 00	0.323101E 02
0.220000E 01	0.857979E 00	0.343192E 02
0.240000E 01	0.138502E 01	0.507840E 02
0.260000E 01	0.167938E 01	0.568576E 02
0.280000E 01	0.119237E 01	0.374745E 02
0.300000E 01	0.370571E 00	0.108701E 02
0.320000E 01	0.101179E 01	0.278242E 02

0.340000E 01	0.102484E 01	0.265252E 02
0.360000E 01	0.604854E 00	0.147853E 02
0.380000E 01	0.174584E 01	0.404299E 02
0.400000E 01	0.248841E 01	0.547450E 02

BETA=0.2000

FREQ	Z+ADD/V	Z2+AP/A
0.100000E 00	0.111349E-02	0.979872E 00
0.200000E 00	0.522318E-02	0.229820E 01
0.300000E 00	0.132367E-01	0.388276E 01
0.400000E 00	0.244998E-01	0.538996E 01
0.500000E 00	0.368124E-01	0.647898E 01
0.600000E 00	0.485407E-01	0.711931E 01
0.700000E 00	0.632681E-01	0.795371E 01
0.800000E 00	0.921484E-01	0.101363E 02
0.900000E 00	0.143903E 00	0.140705E 02
0.100000E 01	0.216759E 00	0.190748E 02
0.110000E 01	0.302534E 00	0.242027E 02
0.120000E 01	0.392795E 00	0.288050E 02
0.130000E 01	0.487986E 00	0.330329E 02
0.140000E 01	0.609492E 00	0.383109E 02
0.150000E 01	0.791465E 00	0.464326E 02
0.160000E 01	0.101170E 01	0.556433E 02
0.170000E 01	0.113969E 01	0.589959E 02
0.180000E 01	0.108991E 01	0.532844E 02
0.190000E 01	0.942241E 00	0.436406E 02
0.200000E 01	0.821187E 00	0.361322E 02
0.220000E 01	0.927311E 00	0.370924E 02
0.240000E 01	0.132521E 01	0.485911E 02
0.260000E 01	0.155831E 01	0.527429E 02
0.280000E 01	0.124084E 01	0.389978E 02
0.300000E 01	0.358183E 00	0.105067E 02
0.320000E 01	0.789646E 00	0.217153E 02
0.340000E 01	0.980905E 00	0.253881E 02

0.360000E 01	0.604160E 00	0.147684E 02
0.380000E 01	0.261304E 01	0.605125E 02
0.400000E 01	0.381540E 01	0.839389E 02

BETA=0.3000

FREQ	Z+ADD/V	Z2+AP/A
0.100000E 00	0.111349E-02	0.979870E 00
0.200000E 00	0.522292E-02	0.229808E 01
0.300000E 00	0.132326E-01	0.388155E 01
0.400000E 00	0.244743E-01	0.538435E 01
0.500000E 00	0.367195E-01	0.646263E 01
0.600000E 00	0.483015E-01	0.708422E 01
0.700000E 00	0.627543E-01	0.788912E 01
0.800000E 00	0.910071E-01	0.100108E 02
0.900000E 00	0.141135E 00	0.137998E 02
0.100000E 01	0.210240E 00	0.185012E 02
0.110000E 01	0.288368E 00	0.230694E 02
0.120000E 01	0.364068E 00	0.266983E 02
0.130000E 01	0.432178E 00	0.292552E 02
0.140000E 01	0.504465E 00	0.317093E 02
0.150000E 01	0.608415E 00	0.356937E 02
0.160000E 01	0.751004E 00	0.413052E 02
0.170000E 01	0.885792E 00	0.458527E 02
0.180000E 01	0.948845E 00	0.463880E 02
0.190000E 01	0.925677E 00	0.428734E 02
0.200000E 01	0.874926E 00	0.384968E 02
0.220000E 01	0.102776E 01	0.411104E 02
0.240000E 01	0.145842E 01	0.534753E 02
0.260000E 01	0.168956E 01	0.571850E 02
0.280000E 01	0.139414E 01	0.438160E 02
0.300000E 01	0.532659E 00	0.156247E 02
0.320000E 01	0.568855E 00	0.156435E 02

0.340000E 01	0.865280E 00	0.223955E 02
0.360000E 01	0.635323E 00	0.155301E 02
0.380000E 01	0.347363E 01	0.804420E 02
0.400000E 01	0.517299E 01	0.113806E 03

BETA=0.5000

FREQ	Z+ADD/V	Z2+AP/A
0.100000E 00	0.111348E-02	0.979862E 00
0.200000E 00	0.522197E-02	0.229767E 01
0.300000E 00	0.132193E-01	0.387765E 01
0.400000E 00	0.243985E-01	0.536767E 01
0.500000E 00	0.364621E-01	0.641732E 01
0.600000E 00	0.476717E-01	0.699185E 01
0.700000E 00	0.614587E-01	0.772623E 01
0.800000E 00	0.883316E-01	0.971648E 01
0.900000E 00	0.135270E 00	0.132264E 02
0.100000E 01	0.197812E 00	0.174074E 02
0.110000E 01	0.264347E 00	0.211477E 02
0.120000E 01	0.321967E 00	0.236109E 02
0.130000E 01	0.364262E 00	0.246577E 02
0.140000E 01	0.402177E 00	0.252797E 02
0.150000E 01	0.466640E 00	0.273762E 02
0.160000E 01	0.579958E 00	0.318977E 02
0.170000E 01	0.722732E 00	0.374120E 02
0.180000E 01	0.848409E 00	0.414778E 02
0.190000E 01	0.921381E 00	0.426745E 02
0.200000E 01	0.954596E 00	0.420022E 02
0.220000E 01	0.122474E 01	0.489898E 02
0.240000E 01	0.182409E 01	0.668834E 02
0.260000E 01	0.211932E 01	0.717307E 02
0.280000E 01	0.180052E 01	0.565877E 02
0.300000E 01	0.950061E 00	0.278684E 02
0.320000E 01	0.959448E-01	0.263848E 01
0.340000E 01	0.588202E 00	0.152240E 02

0.360000E 01	0.785995E 00	0.192132E 02
0.380000E 01	0.490072E 01	0.113490E 03

BETA=0.7000

FREQ	Z+ADD/V	Z2+AP/A
0.100000E 00	0.111346E-02	0.979849E 00
0.200000E 00	0.522052E-02	0.229703E 01
0.300000E 00	0.132010E-01	0.387230E 01
0.400000E 00	0.243052E-01	0.534714E 01
0.500000E 00	0.361725E-01	0.636635E 01
0.600000E 00	0.470077E-01	0.689446E 01
0.700000E 00	0.601558E-01	0.756245E 01
0.800000E 00	0.858194E-01	0.944014E 01
0.900000E 00	0.130327E 00	0.127431E 02
0.100000E 01	0.188571E 00	0.165942E 02
0.110000E 01	0.248717E 00	0.198974E 02
0.120000E 01	0.298177E 00	0.218663E 02
0.130000E 01	0.331212E 00	0.224205E 02
0.140000E 01	0.359679E 00	0.226084E 02
0.150000E 01	0.416557E 00	0.244380E 02
0.160000E 01	0.527478E 00	0.290113E 02
0.170000E 01	0.677218E 00	0.350560E 02
0.180000E 01	0.824140E 00	0.402913E 02
0.190000E 01	0.932711E 00	0.431992E 02
0.200000E 01	0.100661E 01	0.442907E 02
0.220000E 01	0.137157E 01	0.548627E 02
0.240000E 01	0.218556E 01	0.801373E 02
0.260000E 01	0.261101E 01	0.883725E 02
0.280000E 01	0.224119E 01	0.704375E 02
0.300000E 01	0.135203E 01	0.396597E 02
0.320000E 01	0.350139E 00	0.962883E 01

0.340000E 01	0.625137E 00	0.161800E 02
0.360000E 01	0.977902E 00	0.239043E 02
0.380000E 01	0.591590E 01	0.137000E 03
0.400000E 01	0.100128E 02	0.220281E 03

APPENDIX D

PRELIMINARY ESTIMATES OF THE ACCURACIES REQUIRED FOR SIMULATION OF LATERAL DYNAMICS AND TRACTION

SUMMARY

In order to accurately simulate the behavior of a rail vehicle operating on a track, it is necessary for the wheel/rail simulator modules to maintain an accurate geometric interrelationship between the roller motions.

To provide a good simulation of lateral dynamics, the calculations given below indicate that it is desirable to control the actuator motions to the following accuracies:

Roller	-	0.1 milliradian (20 arc seconds)
Lateral Vibration	-	0.01% of forward velocity
Longitudinal Vibration	-	0.01% of forward velocity (0.025 inch/second at 15 mph)

A deterioration of performance by a factor of ten would tend to invalidate the simulation.

Stray longitudinal vibrations may be theoretically compensated for by changes in roller speed to maintain the relation:

$$V = r_a \Lambda_a = \dot{x}_a$$

to within 0.01% of the simulated forward velocity (see page D-3 for definitions).

The evaluation testing of the prototype module should therefore include accurate measurements of the stray lateral and longitudinal vibrations to an accuracy of 0.025 inch per second under the full range of loads, amplitudes and frequencies contemplated for the machine. The measurements in the tests should also include measurements of the controlled yaw angle of the roller to an accuracy of 20 arc seconds.

Evaluation testing should also demonstrate decrowning of less than 0.5 inch.

DISCUSSION

The actuator modules of the wheel rail simulator are intended to provide motions and forces on a wheel of a rail vehicle that are identical to those that would be experienced by a rail vehicle operating on a real track. As shown in the following paragraphs, a simulation of the forces requires that the roller a gular velocity, horizontal motions and yaw angle satisfy the following relations

$$e_1 = \left(r_a \Lambda_a - \dot{x}_a\right) - V = 0 \qquad (1)$$

$$e_2 = \left(r_a \Lambda_a \psi_a - \dot{\delta}_1\right) = 0 \qquad (2)$$

$$e_3 = \left(x - \ell\psi - x_a\right) = 0 \qquad (3)$$

where:

V = Simulated forward velocity

Λ_a = Roller angular velocity

r_a = Roller radius

ψ_a = Actuator yaw angle

ψ = Wheelset yaw angle

δ_1 = Actuator lateral position

x_a = Actuator longitudinal position

x = Wheelset longitudinal displacement.

If these relations are not satisfied, forces will be exerted on the wheel which will not exist in practice. Equation 1 requires that the apparent forward velocity of the roller be equal to the apparent velocity of the rail as seen by an observer travelling on a vehicle having velocity V.

Equation 2 requires that the instantaneous lateral velocity of the roller be zero since the rail will not have an instantaneous lateral velocity except for the effects of rail compliance.

Equation 3 requires that the roller center must remain directly below the axle center to avoid destabilizing forces and moments.

The error in satisfying Equation 1 will result in a longitudinal creep force:

$$F_T = - f \frac{e_1}{V} = - f \left[\frac{\left(r_a \Lambda_a - \dot{x}_a \right)}{V} - 1 \right]$$

For most vehicles of interest the creep coefficient, f, will be about 150 times the normal force.

$$F_T = 150 \; N \left[1 - \frac{\left(r_a \Lambda_a - \dot{x}_a \right)}{V} \right]$$

A stray longitudinal vibration of 0.1% of the forward velocity would result in a creep force of 15% of the normal force. Since the available adhesion is typically 15% to 30% of the normal force, this could result in a total loss of adhesion or a reduction in the apparent braking or acceleration capability of the vehicle of 50 to 100%. It is therefore desirable that the velocity associated with stray longitudinal vibrations be limited to less than 0.01% of the forward velocity. At a forward velocity of 15 mph this represents a velocity of about 0.025

inch per second. At 1 Hz this would limit stray longitudinal vibrations to an acceleration of 4.05×10^{-4}g. At 10 Hz this requirement would be relaxed to 4.05×10^{-3}g.

Similarly an error in satisfying Equation 2 would result in a lateral creep force of

$$F_L = 150\ N \quad \frac{\dot{\delta}_1}{V} - \frac{r_a \Lambda_a}{V}\, \psi_a$$

Therefore an error in ψ_a of 10^{-3} radian would result in a creep force of 15% of the normal force resulting in a loss of lateral adhesion of 50 to 100%. Therefore, it is desired that the yaw angle be controlled to better than 0.1 milliradian at all frequencies. Similarly the stray lateral vibrations should be controlled to better than 0.01% of the simulated forward velocity. At 15 mph this implied 0.025 inch per second.

$$v_{aT} = \left(V - \ell\dot{\psi}\right) - \frac{V}{r_o}\left(r_o + \alpha\left(y-\delta_1\right)\right)$$

$$v_{bT} = \left(V + \ell\dot{\psi}\right) - \frac{V}{r_o}\left(r_o - \alpha\left(y-\delta_2\right)\right)$$

$$v_{aL} = \dot{y} - \frac{V}{r_o}\left(r_o + \alpha\left(y-\delta_1\right)\right)\ \psi \approx \dot{y} - V\psi$$

$$v_{bL} = \dot{y} - \frac{V}{r_o}\left(r_o - \alpha\left(y-\delta_2\right)\right)\ \psi \approx \dot{y} - \quad \psi$$

Referring to Figures 3 and 4 the corresponding creep velocities on the simulator are:

$$v_{AT} = r_a\Lambda_a - \dot{x}_a - \ell\psi - \frac{V}{r_o}\left(r_o + \alpha\left(y-\delta_1\right)\right)$$

$$v_{bT} = r_b\Lambda_b - \dot{x}_b - \ell\psi - \frac{V}{r_o}\left(r_o - \alpha\left(y-\delta_2\right)\right)$$

$$v_{aL} = r_a \Lambda_a \psi_a - \dot{\delta}_1 + (\dot{y} - V\psi)$$

$$v_{bL} = r_b \Lambda_b \psi_b - \delta + (y - V\psi)$$

For the creep velocities to be equal in both cases we require:

$$e_1 = V - (r_a \Lambda_a - \dot{x}_a) = 0$$

$$e_2 = (r_a \Lambda_a \psi_a - \dot{\delta}_1) = 0$$

$$e_1' = V - (r_b \Lambda_b - \dot{x}_b) = 0$$

$$e_2' = (r_b \Lambda_b \psi_b - \dot{\delta}_2) = 0$$

Creep coefficients used by British Rail (PB 192718) for analysis of stability of the LIM test vehicle range from 100 to 200 times the normal force. If the above requirements are not satisfied there will be undesired forces on wheel "a" of (Figure 1).

$$F_T = f \frac{e_1}{V} = 150 \text{ N} \left[1 - \frac{r_a \Lambda_a - \dot{x}_a}{V} \right]$$

$$F_L = f \frac{e_2}{V} = 150 \text{ N} \left[\frac{r_a \Lambda_a \psi_a - \dot{\delta}_1}{V} \right]$$

The existence of these forces will reduce the observed adhesion and because of the non-linearity of the creep phenomenon produce a change in the apparent creep coefficient.

In addition to the above creep force errors, the curvature of the roller produces a destabilizing force on the wheel as shown in Figure 5. The destabilizing forces on the two rollers corresponding to a wheelset are:

$$F_{aTN} = \left(\frac{x - \ell\psi - x_a}{r_o + r_o}\right) N$$

$$F_{bTN} = \left(\frac{x + \ell\psi - x_b}{r_o + r_o}\right) N$$

for a 40 inch diameter roller and 30 inch diameter wheel an error of 0.35 inch would produce a force of 1% of the normal force. An error of 3.5 inches would produce a force of 10% of the normal force. A positioning accuracy of 0.51 inches would produce a force error of 1.5% which would represent 5% of the available adhesion with an adhesion coefficient of 0.3.

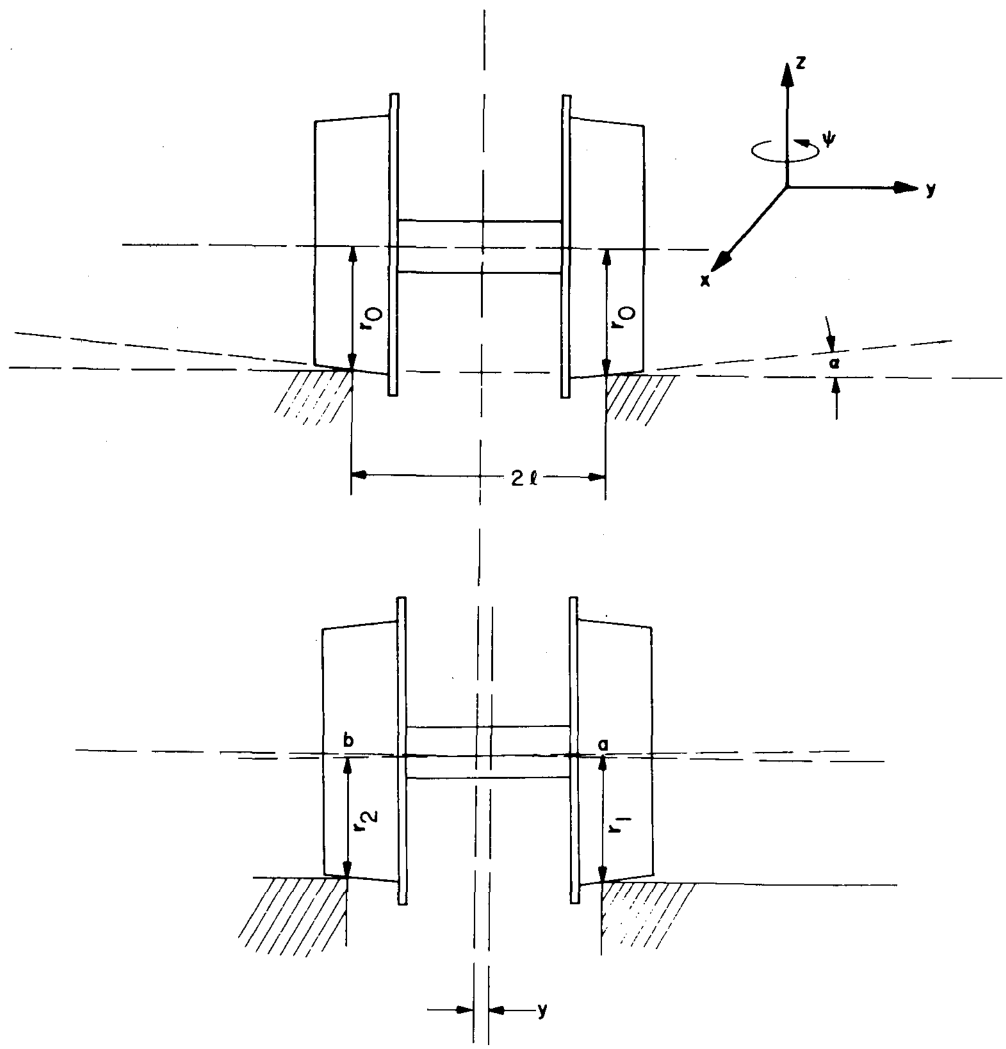

Figure D-1. Wheelset Travelling on Nominally Straight Track

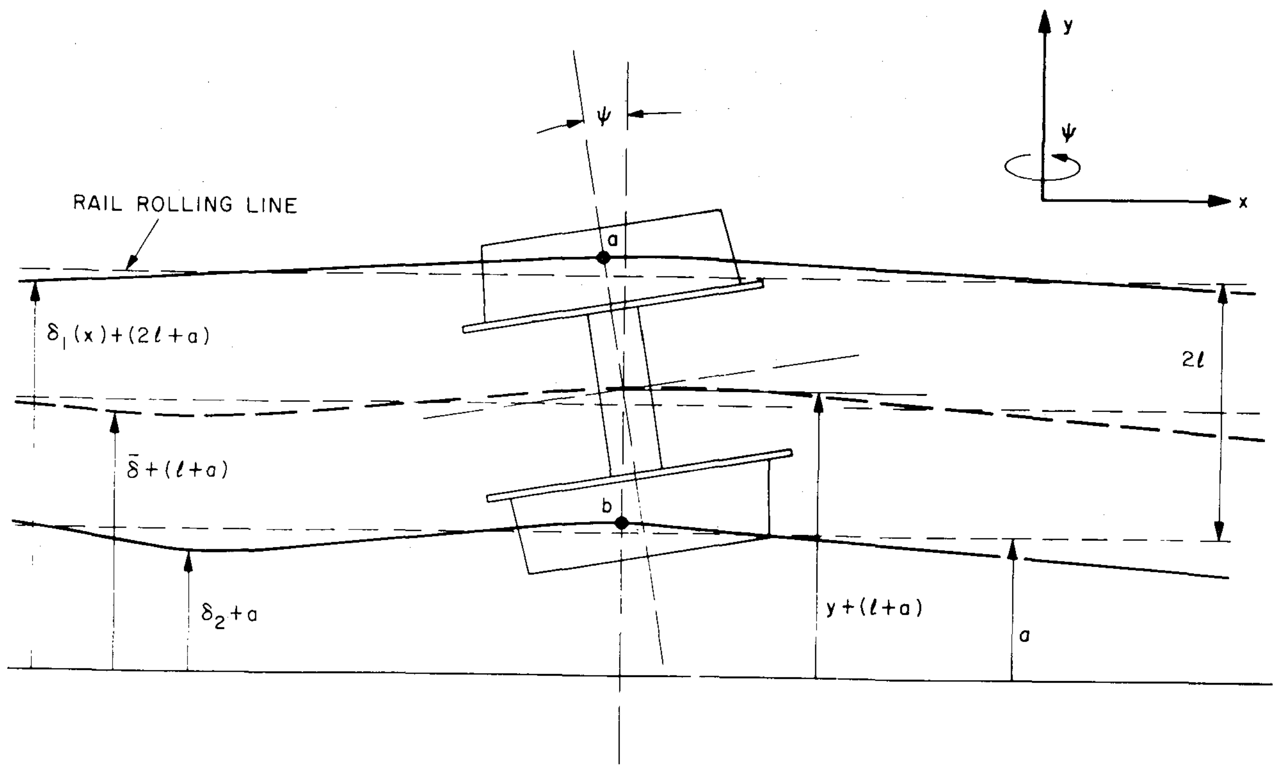

Figure D-2. Wheelset Travelling on Nominally Straight Track

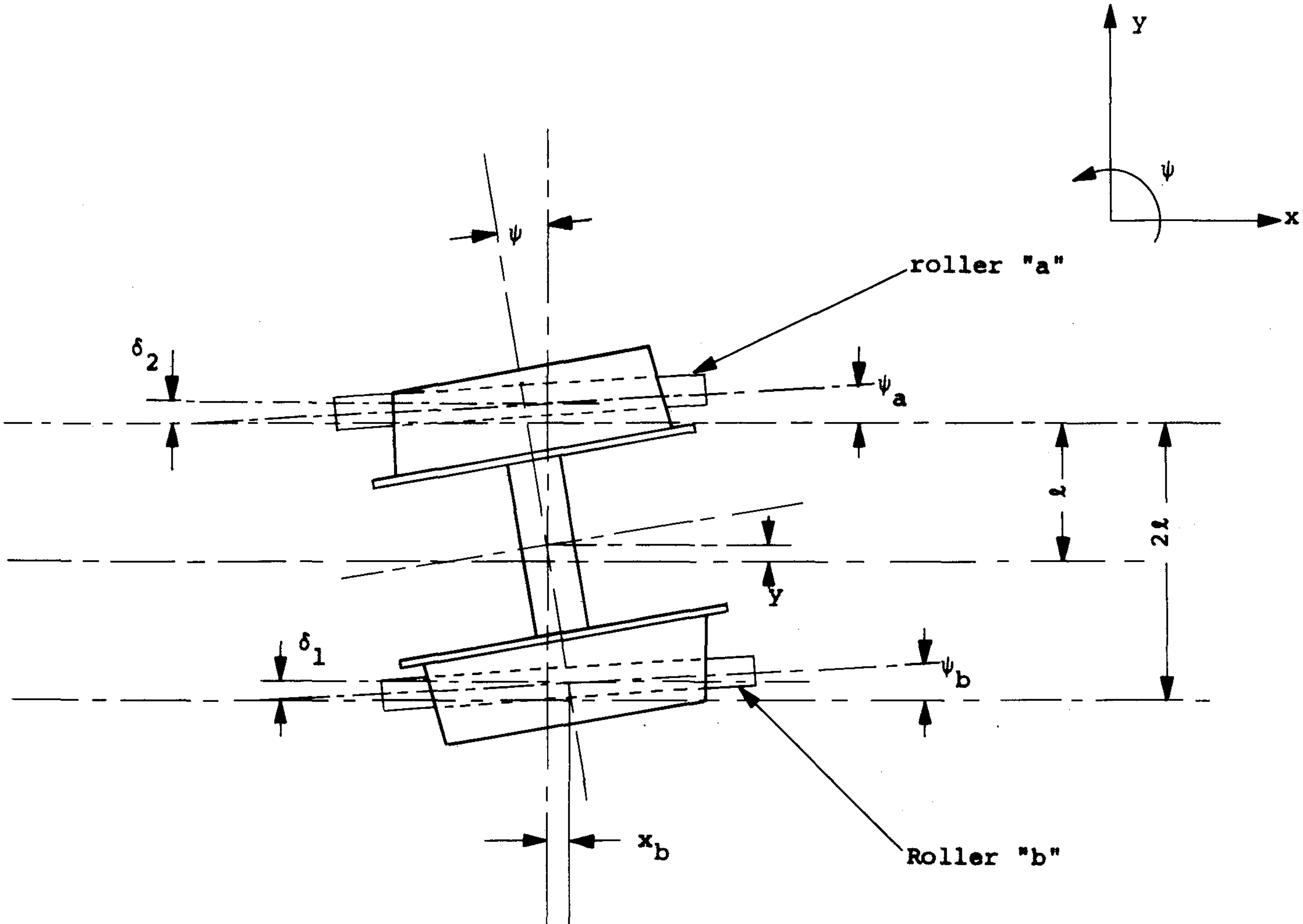

Figure D-3. Wheelset Rolling on Track Simulated by Rollers

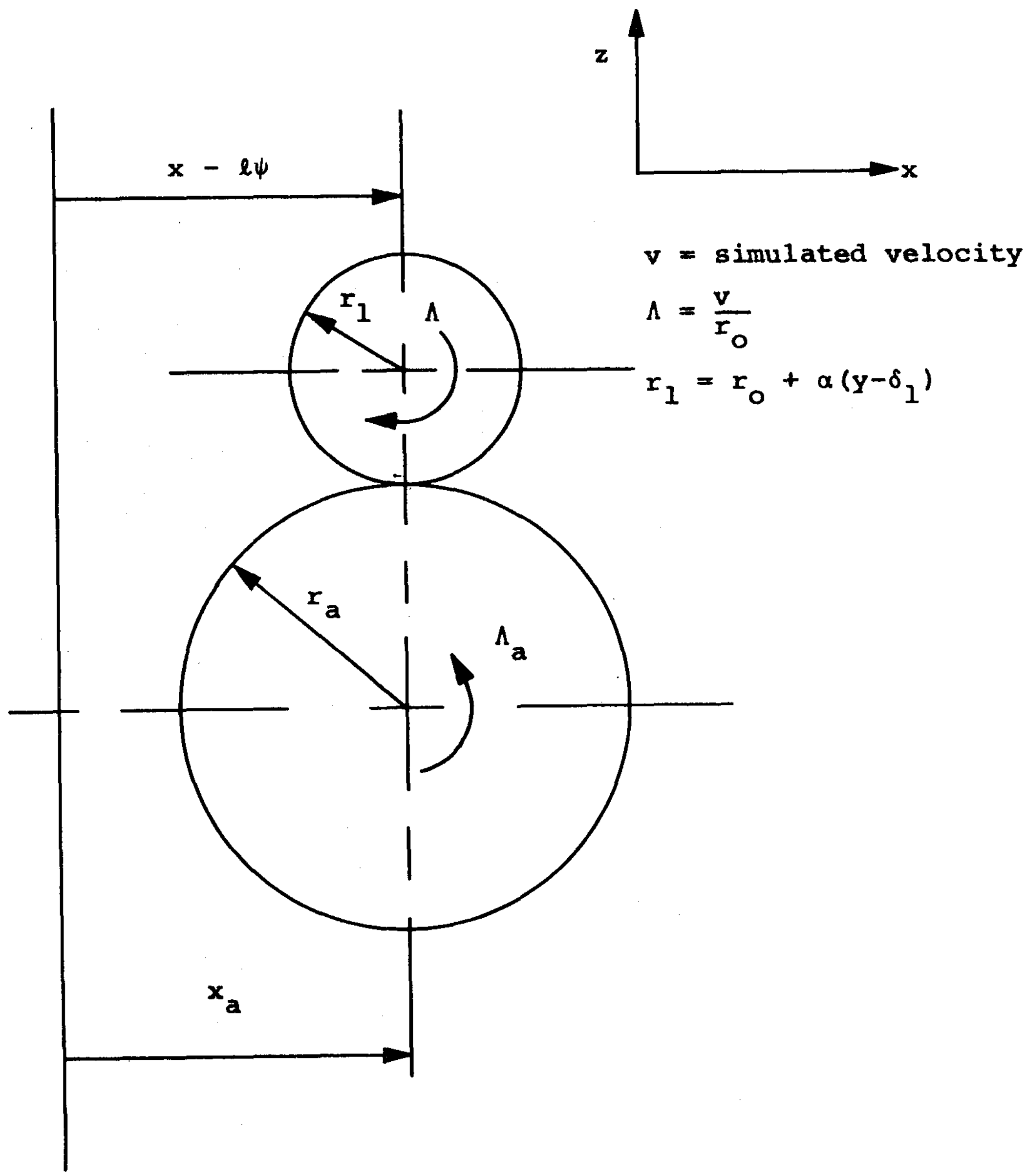

$$v_a = -\ell\dot{\psi} - \frac{v}{r_o}\left(r_o + \alpha(y-\delta_1)\right) + \Lambda_a r_a - \dot{x}_a$$

Figure D-4. Wheelset rolling on Track Simulated by Rollers

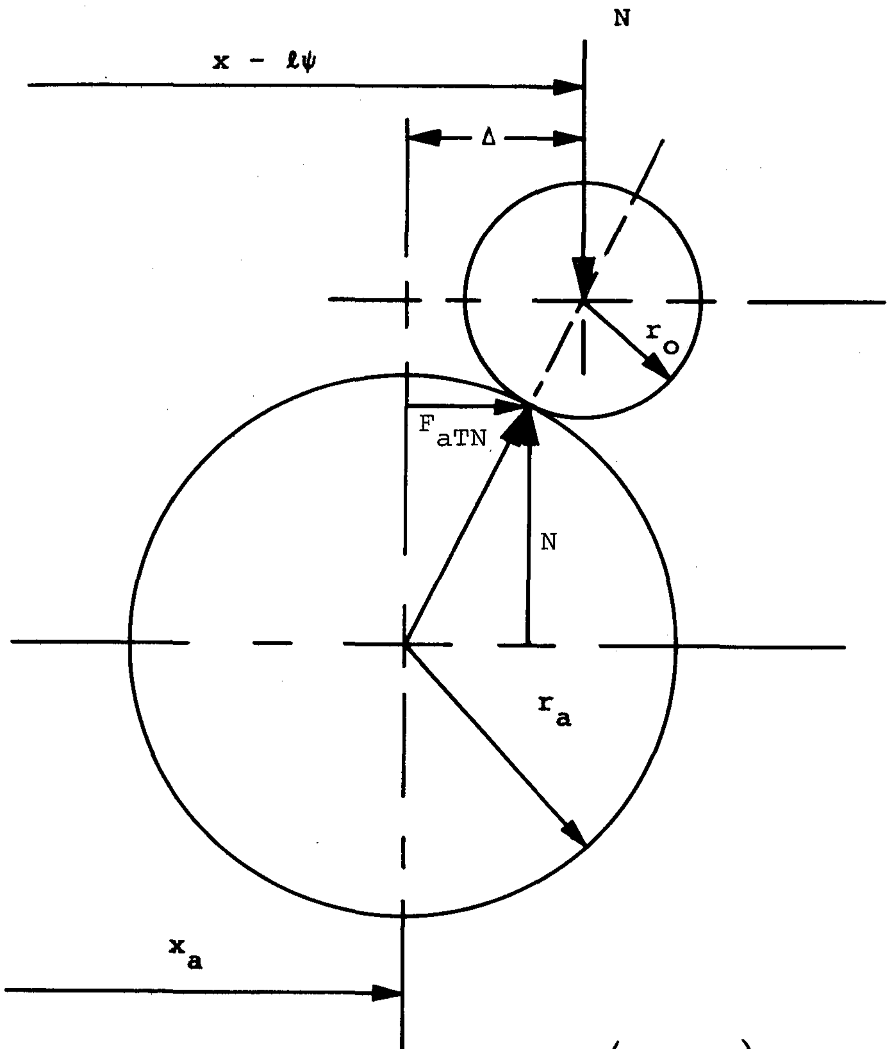

$$\text{Horizontal Force Reaction} \approx \left(\frac{\Delta}{r_a + r_o}\right) N$$

$$F_{aTN} = \frac{(x - \ell\psi - x_a)}{r_a + r_o} N$$

Figure D-5. Force Produced by "Decrowning"